Book of Abstracts

ELSEVIER

ITMO UNIVERSITY

department of PHYSICS

Michael Mischenko's Scientific Legacy

ELSEVIER

ITMO UNIVERSITY

department of PHYSICS

Scattering and absorption properties of spheroidal soot-sulfate aerosols

Janna. M. Dlugach*

Main Astronomical Observatory of the National Academy of Sciences of Ukraine,
27 Akad. Zabolotny Str., 03143, Kyiv, Ukraine
**corresponding author's e-mail:* *dl@mao.kiev.ua, zhanna.dlugach@gmail.com*

It is widely recognized that carbonaceous particles represent an important type of tropospheric aerosols affecting cloud formation, causing a direct radiative forcing on climate. Freshly emitted soot particles mix with other atmospheric aerosol constituents, and, in particular, tend to become internally mixed as they age in the atmosphere. The aging process includes, in particular, condensation of sulfates on soot particle's surface. By now, numerical modeling of optical properties has been carried out for various models of soot particles coated in various ways with spherical shell (see, e.g., [1–2]). Besides in [3], it was demonstrated that the concentric core-mantle particle composed of spheroidal soot core enveloped by spheroidal sulfate shell can reproduce the observed spectral dependences of the linear depolarization ratios.

Here, given the practical importance of the clarification of potential effect of shell shape on the optical properties of soot particles coated with sulfate, we analyze the results of computations of the absorption cross section (C_{abs}), absorption Ångström component (AAE), backscattering linear depolarization ratio (LDR), and scattering matrix elements of spheroidal soot particles covered by spheroidal *nonabsorbing* sulfate shell. In our computations, we applied the random-orientation *T*-matrix code by Quirantes [4]. Computations were performed for polydispersed particles with core volume-equivalent effective radius $R_{core,eff}$ = 0.1, 0.15, 0.2 μm, soot volume fraction f = 7 % and 15 %, and corresponding values of the shell volume-equivalent effective radius $R_{shell,eff}$ in the range $0.1882 \le R_{shell,eff} \le 0.4853$ μm. The aspect ratio of the core-mantle spheroidal particle E (the ratio of the larger and the smaller spheroid axis) was assumed to be the same for both the soot core and the sulfate shell, and $1 \le E \le 1.5$. We used the standard power-law size distribution with effective variance v = 0.1. Our computations were carried out for three wavelengths λ = 0.355, 0.532, and 1.064 μm according to the spectral channels used in LDR measurements with backscattering lidars. The spectrally dependent refractive indices for the particle components were taken from [1]. The results of our computations demonstrate, in particular, that: (i) in the considered range of particle sizes, the C_{abs} and AAE depend weakly on aerosol-particle aspect ratio E, but their dependences on particle size and the amount of coating material are quite noticeable; the AAE decreases significantly with increasing aerosol-particle size and soot volume fraction; ii) the LDR significantly increases with increasing particle nonsphericity and size, and decreases with increasing wavelength; iii) the first scattering matrix element (phase function) shows noticeable dependence on aerosol-particle nonsphericity only in the range of backscattering, which increases with increasing particle size; the degree of linear polarization for unpolarized incident radiation is strongly dependent on particle shape at scattering angles larger than 70°, the depth of the negative polarization branch at backscattering angles decreases with increasing aerosol-particle nonsphericity, E-dependence of the degree of linear polarization becomes less pronounced with increasing the amount of soot volume fraction.

Acknowledgement

A few years ago, we discussed this problem with Michael Mishchenko, but postponed this work for the future. Life has made its tragic changes.

References

[1] L. Liu, and M. I. Mishchenko. *Scatterinhg and radiative properties of morphologically complex carbonaceous aerosols: A systematic modeling study.* Remote Sens., 10:1634, 2018.

[2] M. Kahnert, and F. Kanngießer. *Aerosol optics model for black carbon applicable to remote sensing, chemical data assimilation, and climate modelling*. Opt. Express, 29:10639–10658, 2021.

[3] M. I. Mishchenko, J. M. Dlugach, and L. Liu. *Linear depolarization of lidar returns by aged smoke particles.* Appl. Opt, 55:9968–9973, 2016.

[4] A. Quirantes. A T-matrix method and computer code for randomly oriented, axially symmetric coated scatters. J. Quant. Spectrosc. Radiat. Transf,, 92:373–381, 2005.

Electromagnetic scattering by discrete random media. An overview of a valuable collaboration.

Adrian Doicu

Remote Sensing Technology Institute, German Aerospace Centre,
Oberpfaffenhofen, Wessling, Germany.
E-mail: adrian.doicu@dlr.de

This presentation is dedicated to the memory of Michael I. Mishchenko, a beautiful mind and a brilliant scientist. I will summarize our common results related to the electromagnetic scattering by discrete random media. These include (i) an overview of methods for deriving the radiative transfer equation for sparse media, (ii) an analysis of the electromagnetic scattering by dense random media with the focus on the derivation of the dispersion equation, coherent field, radiative transfer equation, and coherent backscattering, (iii) the derivation of the radiative transfer equation for a discrete random medium adjacent to a half-space with a rough interface, and (iv) the description of the electromagnetic scattering by discrete random media illuminated by a Gaussian beam.

References

[1,2,3] A. Doicu, and M. I. Mishchenko. *An Overview of methods for deriving the radiative transfer theory from the Maxwell equations. I: Approach based on the far-field Foldy equations*. J. Quant. Spectrosc. Radiat. Transfer, 220:123–139, 2018; *II: Approach based on the Dyson and Bethe–Salpeter equations*. J. Quant. Spectrosc. Radiat. Transfer, 224:25–36, 2019; *III: Effects of random rough boundaries and packing density*. J. Quant. Spectrosc. Radiat. Transfer, 224:154–170, 2019.

[4,5,6,7] A. Doicu, and M. I. Mishchenko. *Electromagnetic scattering by discrete random media. I: The dispersion equation and the configuration-averaged exciting field*. J. Quant. Spectrosc. Radiat. Transfer, 230:282–303, 2019; *II: The coherent field.* J. Quant. Spectrosc. Radiat. Transfer, 230:86–105, 2019; *III: The vector radiative transfer equation*. J. Quant. Spectrosc. Radiat. Transfer, 236:106564, 2019; *IV: Coherent backscattering*. J. Quant. Spectrosc. Radiat. Transfer, 236:106565, 2019.

[8] A. Doicu, and M. I. Mishchenko. *Radiative transfer in a discrete random medium adjacent to a half-space with a rough interface*. J. Quant. Spectrosc. Radiat. Transfer, 218:194–202, 2018.

[9,10] A. Doicu, M. I. Mishchenko, and T. Trautmann. *Electromagnetic scattering by discrete random media illuminated by a Gaussian beam I: Derivation of the radiative transfer equation*. J. Quant. Spectrosc. Radiat. Transfer, 256:107301, 2020; *II: Solution of the radiative transfer equation*. J. Quant. Spectrosc. Radiat. Transfer, 256:107297, 2020.

Accounting for particle non-sphericity in aerosol remote sensing

Oleg Dubovik[1], Michael Mishchenko[2] and Ping Yang[3]

[1]*Univ. Lille, CNRS, UMR 8518 - LOA - Laboratoire d'Optique Atmosphérique, F-59000 Lille, France*
[2]*NASA Goddard Institute for Space Studies, New York, NY, USA*
[3]*College of Geosciences Texas A&M University, College Station, TX 77843, USA*
E-mail: oleg.dubovik@univ-lille.fr

Adequate modeling of light scattering by nonspherical particles is widely recognized as one of the major difficulties in remote sensing of tropospheric aerosols in general and desert dust in particular. There are various in situ and laboratory measurements that reveal significant deviations of light scattering of desert dust aerosols from scattering properties of homogeneous spheres. As a result, there have been numerous efforts to account for particle nonsphericity in aerosol retrieval algorithms. Nevertheless, the development of such a model appears to be difficult both methodologically and technically.

The presentation discusses the development and evolution of "spheroid kernels" - a look-up-tables simulated for quadrature coefficients of randomly oriented spheroids developed by Dubovik et al. (2006). The look-up-tables were arranged into a software package, which allows fast, accurate, and flexible modeling of scattering by randomly oriented spheroids with different size and shape distributions. The software has been designed for easy integration into inversion algorithms. This allowed the researchers both to evaluate spheroid model and explore the possibility of using the spheroidal approximation of particle shape in diverse retrievals of aerosol properties from light scattering sensing measurements. At present, the "spheroid kernels" has become one of most accepted and popular approach for modeling light scattering by non-spherical applications. The "spheroid kernels" software is now employed in numerous approaches developed for aerosol retrieval from laboratory and various remote sensing measurements.

The earlier studies by Mishchenko et al., (2000) was a fundamental base for the development of "spheroid kernels" approach and Michael has made a major contribution into development of the approach and software. In the presentation we will share the precious the memories of working and collaborating with Michael on this software and generally on aerosol remote sensing.

Scattering by small oblate spheroidal drops of water in the rainbow region: T-matrix results and geometric interpretation

Philip L. Marston[1,*] and Michael I. Mishchenko[2]

[1]*Physics and Astronomy Department, Washington State University Pullman, WA 99164-2814, USA*
[2]*NASA Goddard Institute for Space Studies, 2880 Broadway, New York, NY 10025, USA*
[*]*corresponding author's e-mail: marston@wsu.edu*

Late in 1999 Michael Mishchenko carried out T-matrix calculations of light scattered by oblate spheroidal drops of water at Philip Marston's request. The purpose of the investigation was to determine if the caustic features, known by that time to be visible in the far-field scattering near the primary rainbow region for horizontally illuminated relatively large drops [1-5], would also be present in T-matrix calculations [6] of the scattering by small drops. The drop's axis of rotational symmetry was taken to be vertical and the illumination was taken to be horizontal. Scattering into the relevant angular region was evaluated for drop aspect ratios D/H = 1, 1.23, 1.311, and 1.37 where D denotes the equatorial diameter. The results currently available are limited to monochromatic illumination with ka = 140 where a = D/2 and $k = 2\pi/\lambda$ with λ being the wavelength of the illumination. As expected from geometrical analysis [2-5] a horizontal "Vee" shaped caustic is visible for D/H = 1.311. The T-matrix results are preserved in printed gray-tone intensity displays provided by Mishchenko in 1999 with parameters described in email correspondence of that period. The results remain instructive along with subsequent related computational developments [7, 8]. (Preparation of this Abstract was supported in part by the US Office of Naval Research.)

References

[1] P. L. Marston and E. H. Trinh. *Hyperbolic umbilic diffraction catastrophe and rainbow scattering from spheroidal drops.* Nature (London) 312: 529–531, 1984.

[2] J. F. Nye. *Rainbow scattering from spheroidal drops—an explanation of the hyperbolic umbilic foci.* Nature (London) 312: 531–532, 1984.

[3] P. L. Marston. *Cusp diffraction catastrophe from spheroids: generalized rainbows and inverse scattering.* Optics Letters 10: 588-590, 1985.

[4] P. L. Marston. *Geometrical and catastrophe optics methods in scattering*. Physical Acoustics 21: 1–234, 1992.

[5] P. L. Marston. *Catastrophe optics of spheroidal drops and generalized rainbows.* J. Quant. Spectrosc. Radiat. Transfer 63: 341–351, 1999.

[6] M. I. Mishchenko and L. D. Travis. *Capabilities and limitations of a current FORTRAN implementation of the T-matrix method for randomly oriented, rotationally symmetric scatterers.* J. Quant. Spectrosc. Radiat. Transfer 60:309-324, 1998.

[7] J. A. Lock and F. Xu. *Optical caustics observed in light scattered by an oblate spheroid*. Applied optics 49: 1288-1304, 2010.

[8] M. I. Mishchenko, N. T. Zakharova, N. G. Khlebtsov, G. Videen, and T. Wriedt. *Comprehensive thematic T-matrix reference database: a 2015-2017 update*. J. Quant. Spectrosc. Radiat. Transfer, 202:240-246, 2017.

This Abstract is intended for the Michael Mishchenko memorial session.

Dr. Michael I. Mishchenko's contributions to Electromagnetic Scattering, Radiative Transfer, and Remote Sensing

P. Yang[1,*], B. Cairns[2], A. Marshak[3], O. Dubovik[4], and L. Kolokolova[5], A. Lacis[2] and L. Travis[2]

[1]*Department of Atmospheric Sciences, Texas A&M University, College Station, TX 77843, USA*
[2]*NASA Godard Institute for Space Studies, 2880 Broadway, New York, NY 10025, USA*
[3]*NASA Godard Space Fight Center, Greenbelt, MD 20771, USA*
[4]*Laboratorie d'Optique Atmosphérique, CNRS/Université de Lille, 59655 Villeneuve d'Ascq CEDEX, France*
[5]*Department of Astronomy, University of Maryland, College Park, MD 20742, USA*

[*]*corresponding author's e-mail: pyang@tamu.edu*

Dr. Michael I. Mishchenko's scientific accomplishments

Dr. Michael I. Mishchenko who was a scientist at NASA Goddard Institute for Space Studies passed away on July 21, 2020. Dr. Mishchenko's seminal research on the theory and applications of electromagnetic scattering, radiative transfer, and remote sensing has largely defined the progress of these disciplines over the past three decades. His pioneering studies have resulted in more than 310 peer-reviewed journal papers (note that Michael first-authored 158 of them) and four state-of-the-art first-authored monographs. As of 11 May 2020, the number of Google Scholar citations of Michael's publications exceeds 33,661, while his *h*-index is 88 (https://scholar.google.com/citations?user=Q5-7dVYAAAAJ&hl=en).

In addition to his highest-rated scientific accomplishments, Michael made sustained contributions to the well-being of the international applied optics, radiative transfer, and remote sensing communities. He served as Topical Editor of *Applied Optics* for 6 years and, since 2006, he was Editor-in-Chief of the *Journal of Quantitative Spectroscopy and Radiative Transfer*. Furthermore, Michael organized 10 major remote-sensing conferences, including six *Electromagnetic and Light Scattering Conferences* and two *NATO Advanced Study Institutes*.

As tribute to Dr. Mishchenko, this presentation will summarize his groundbreaking scientific accomplishments and voluminous service to the international light scattering, remote-sensing, and radiative transfer community.

Additional information

Figure 1: Dr. Michael I. Mishchenko, 1959-2020.

On the feasibility of measuring extinction of single particles

M. A. Yurkin[1,2,*]

[1]*Voevodsky Institute of Chemical Kinetics and Combustion, SB RAS, Institutskaya str. 3, 630090, Novosibirsk, Russia*
[2]*Novosibirsk State University, Pirogova 2, 630090 Novosibirsk, Russia*
[*]*corresponding author's e-mail: yurkin@gmail.com*

The extinction of a single particle is often considered as a total power extracted from the beam as a result of the scattering and absorption, which is the essence of the optical theorem. On the one hand, when a collection of particles (e.g., a cloud or suspension) is involved the extinction is reliably measured by the detector in the forward direction, subtracting the results with and without the sample present. On the other hand, the extinction is described by the interference of the scattered and incident fields in the far-field zone, which happens not only in the forward direction but for a wide range of scattering angles. This interference was described in details by Berg *et al.* [1], who suggested that a detector covering up to 60° may be required for single-particle extinction measurement. Inspired by this alarming suggestion, Mishchenko *et al.* [2] explicitly calculated the reading of a circular and square detectors placed around the forward direction (for a simplified case of isotropic scalar scattering). The reading of a perfectly centered circular detector indeed oscillate with a detector size and have no limit. However, for a square detector these oscillations decrease with detector size, converging to the expected result proportional to the extinction cross section. Still, a relatively large detector size R is required ($R^2 \gg \lambda z$, z is the distance to the detector and λ is the wavelength), which has already been mentioned in classical textbooks [3,4]. It has also been recently discussed in [5], which showed that use of collimated beam improves convergence of measured power with increasing detector size.

In this work I analyze the extinction measurements for a single particle illuminated by a plane wave using a detector of arbitrary shape, described by a function $\rho(\theta)$ in polar coordinates. Using the stationary-phase arguments, it is shown that the error scales as $\sqrt{\lambda z/\Delta(\rho^2)}$, where $\Delta(\dots)$ denotes the difference between the maximum and minimum values of a function (or its variation). This general result is further applied to a non-centered circular detector and, next, extended to a random movement of a particle during the measurement time (which was previously analyzed only qualitatively). The latter decreases (averages out) the error, but the diffusion shifts should be smaller than the size of the detector, so that the geometrical shadow of the particle always falls inside the detector. Finally, the feasibility of the extinction measurement is analyzed in terms of the dynamic range of the detector (since the reference signal increases proportionally to the detector area). Measuring extinction of a fixed particle with 1% accuracy requires the dynamic range of 10^8, while 10^4 can be sufficient for a randomly moving one.

References

[1] Berg MJ, Sorensen CM, Chakrabarti A. Extinction and the optical theorem. Part I. Single particles. J Opt Soc Am A, JOSAA 2008;25:1504–13.
[2] Mishchenko MI, Berg MJ, Sorensen CM, van der Mee CVM. On definition and measurement of extinction cross section. J Quant Spectrosc Radiat Transfer 2009;110:323–7.
[3] van de Hulst HC. Light Scattering by Small Particles. New York: Dover; 1981.
[4] Bohren CF, Huffman DR. Absorption and Scattering of Light by Small Particles. New York: Wiley; 1983.
[5] Markel VA. What is extinction? Operational definition of the extinguished power for plane waves and collimated beams. J Quant Spectrosc Radiat Transfer 2020;246:106933.

Abstracts

ELSEVIER

ITMO UNIVERSITY

department of PHYSICS

Scattering and absorption in discrete random media of densely-packed particles

Karri Muinonen[a,b]*

[a]*Department of Physics, University of Helsinki, Finland*
[b]*Finnish Geospatial Research Institute FGI, National Land Survey, Masala, Finland*

[*]*Presenting author (karri.muinonen@helsinki.fi)*

Theoretical, numerical, and experimental methods are presented for scattering and absorption of light in large discrete random media of densely-packed small particles. The theoretical and numerical methods are based on the framework of Radiative Transfer with Reciprocal Transactions (R^2T^2; e.g., [1-3] and references therein). Monte Carlo order-of-scattering tracing of interactions is carried out in the frequency space, assuming that the fundamental scatterers and absorbers are wavelength-scale volume elements composed of statistically significant numbers of randomly distributed particles. For spherical and nonspherical particles, the interactions within the volume elements are computed exactly using the Superposition *T*-Matrix Method (STMM) and the Volume Integral Equation Method (VIEM), respectively. For both types of particles, the interactions between different volume elements are computed using the STMM. As the tracing takes place within the discrete random media, incoherent electromagnetic fields are utilized, that is, the coherent field of the volume elements is removed from the interactions. The R^2T^2 is validated using experimental measurements for a macroscopic sample of densely-packed spherical silica particles [4,5].

References

[1] Muinonen, K., Markkanen, J., Väisänen, T., Peltoniemi, J., and Penttilä, A., 2018: Multiple scattering of light in discrete random media using incoherent interactions. *Opt. Lett.* **43**, 683-686.
[2] Markkanen, J., Väisänen, T., Penttilä, A., and Muinonen, K., 2018: Scattering and absorption in dense discrete random media of irregular particles. *Opt. Lett.* **43**, 2925-2928.
[3] Väisänen, T., Martikainen, J., and Muinonen, K., 2020: Scattering of light by dense particulate media in the geometric optics regime. *JQSRT* **241**, 106719, 1-11.
[4] Maconi, G., Helander, P., Gritsevich, M., Salmi, A., Penttilä, A., Kassamakov, I., Haeggström, E., and Muinonen, K., 2020. 4π Scatterometer: A new technique for understanding the general and complete scattering properties of particulate media. *JQSRT* **246**, 106910, 1-7.
[5] Väisänen, T., Markkanen, J., Hadamcik, E., Renard, J.-B., Lasue, J., Levasseur-Regourd, A.-C., Blum, J., and Muinonen, K., 2020: Scattering of light by a large, densely-packed agglomerate of small silica spheres. *Opt. Lett.* **45**, *1679-1682*.

Recent progress in polarization lidar applications to aerosols and clouds

Albert Ansmann[a,*]

[a]*Leibniz Institute for Tropospheric Research, Permoserstrasse 15, 04318 Leipzig, Germany*

[*]*Presenting author (albert@tropos.de)*

The polarization lidar technique has been significantly developed towards detailed aerosol and cloud monitoring since 2012. Traditionally, the measured linear depolarization ratio was used to separate non-spherical mineral dust particles from spherical marine and continental haze particles and to distinguish cloud layers containing mainly spherical cloud droplets and layers with dominating ice crystal backscattering. Meanwhile, this lidar technique permits the separation of fine-mode dust particles (with diameters < 1µm) and coarse-mode dust [1] and to retrieve height profiles of mass concentration, cloud condensation nucleus, and ice-nucleating particle concentrations separately for dust particles, marine aerosol, and continental fine-mode particles [2,3]. Examples of measurements performed with our polarization lidar Polly at Dushanbe, Tajikistan, will illustrate the new potential of advanced polarization lidars. Another highlight is the approach to characterize aerosols by means of triple-wavelength depolarization ratio observations [4,5,6,7].

In a second approach, the polarization lidar is used for profiling of microphysical properties of liquid-water clouds such as droplet number concentration, effective radius, extinction coefficient, and liquid water concentration by using the recently introduced so-called dual-receiver-field-of-view technique [8]. Now, we are able to investigate aerosol-cloud interaction in the case of liquid-water clouds in large detail. We will show recent studies of aerosol-cloud interaction performed in pristine marine conditions at Punta Arenas, Chile, at the southernmost tip of South America.

References

[1] Mamouri, R.-E., and A. Ansmann, 2014: Fine and coarse dust separation with polarization lidar, *Atmos. Meas. Tech.*, **7**, *3717-3735.*

[2] Mamouri, R.-E., and A. Ansmann, 2016: Potential of polarization lidar to provide profiles of CCN- and INP-relevant aerosol parameters, *Atmos. Chem. Phys.*, **16**, *5905-5931*.

[3] Mamouri, R.-E., and A. Ansmann, 2017: Potential of polarization/Raman lidar to separate fine dust, coarse dust, maritime, and anthropogenic aerosol profiles, *Atmos. Meas. Tech.*, **10**, *3403-3427*.

[4] Burton, S. P., J. W. Hair, M. Kahnert, *et al.*, 2015: Observations of the spectral dependence of linear particle depolarization ratio of aerosols …, *Atmos. Chem. Phys.*, **15**, 13453-13473.

[5] Haarig, M., Ansmann, A., Althausen, D., *et al.*, 2017: Triple-wavelength depolarization-ratio profiling of Saharan dust over Barbados during SALTRACE …, Atmos. Chem. Phys., 17, 10767–10794, 2017.

[6] Haarig, M., Ansmann, A., Gasteiger, *et al.*, 2017: Dry versus wet marine particle optical properties: RH dependence of depolarization ratio, backscatter, …, Atmos. Chem. Phys., 17, 14199–14217.

[7] Hu, Q., P. Goloub, I. Veselovskii, *et al.*, 2019: Long-range-transported Canadian smoke plumes in the lower stratosphere over northern France, *Atmos. Chem. Phys.*, **19**, *1173-1193.*

[8] Jimenez, C., A. Ansmann, R. Engelmann, *et al.*, 2020: The dual-field-of-view polarization lidar technique: A new concept in monitoring aerosol-cloud effects, *Atmos. Chem. Phys. Discuss.*

The Rayleigh hypothesis: from single particle to multiple scattering

Eric C. Le Ru[a,*], B. Auguié[a], W.R.C. Somerville[a], D. Schebarchov[a], J. Grand[a.b], M. Majic[a]

[a]*The MacDiarmid Institute for Advanced Materials and Nanotechnology, School of Chemical and Physical Sciences, Victoria University of Wellington, P.O. Box 600, Wellington 6140, New Zealand*.
[a]*Université Paris Diderot, Sorbonne Paris Cité, ITODYS, UMR CNRS 7086, 15 rue J-A de Baïf, 75205 Paris Cedex 13, France*
[*]*Presenting author (eric.leru@vuw.ac.nz)*

In this talk, we will summarize some recent developments in our understanding of the Rayleigh hypothesis (RH) in the context of the T-matrix method for electromagnetic scattering by particles. Within this framework, it has been shown that the scattered field expansion into a series of vector spherical wave functions converges outside the circumscribed sphere. The Rayleigh hypothesis states that this expansion is also valid for the rest of the outside region (the RH region), all the way down to the particle surface. The RH has been much debated over the years [1]. The T-matrix framework and extended-boundary condition method (EBCM) do not rely on the validity of the RH, but it remains important from a fundamental point of view and for applications where the near fields are required. The more general question of the domain of validity of series expansions also has implications for the applicability of the T-matrix method to multiple scatterers, especially where the circumbscribed spheres of neighbouring particles overlap.

We will show how recent developments in the accuracy of T-matrix calculations for spheroids [2,3] allow us to numerically test the validity of the RH [4]. A complementary approach is to consider the long-wavelength limit, for which analytic results can be obtained, giving further insight into the RH [5,6]. Finally, we will discuss extensions of these investigations to the case of multiple particles [7]. From these studies, a unified picture of the RH emerges, which allows us to understand its relevance to T-matrix and electromagnetic scattering calculations in general.

References

[1] Rother, T., and Kahnert, M., 2009: *Electromagnetic Wave Scattering on Nonspherical Particles*. Springer, Berlin.
[2] Somerville, W. R. C., Auguié, B., and Le Ru, E. C., 2015: Accurate and convergent T-matrix calculations of light scattering by spheroids. *J. Quant. Spectrosc. Rad. Trans.* **160**, 29– 35.
[3] Somerville, W.R.C., Auguié, B., and Le Ru, E. C., 2016: SMARTIES: User-friendly codes for fast and accurate calculations of light scattering by spheroids. *J. Quant. Spectrosc. Rad. Trans.* **174**, 39– 55.
[4] Auguié, B., Somerville, W. R. C., Roache, S., and Le Ru, E. C., 2016: Numerical investigation of the Rayleigh hypothesis for electromagnetic scattering by a particle. *J. Opt.* **18**, 075007.
[5] Majic, M. R. A., Gray, F., Auguié, B., and Le Ru, E. C., 2017: Electrostatic limit of the T -matrix for electromagnetic scattering: Exact results for spheroidal particles. *J. Quant. Spectrosc. Rad. Trans.* **200**, 50-58.
[6] Majic, M., Pratley, L., Schebarchov, D., Somerville, W. R. C., Auguié, B., and Le Ru, E. C., 2019: Approximate T-matrix and optical properties of spheroidal particles to third order with respect to size parameter. *Phys. Rev. A* **99**, 013853.
[7] Schebarchov, D., Le Ru, E. C., Grand, J., and Auguié, B., 2019: Mind the gap: testing the Rayleigh hypothesis in T-matrix calculations with adjacent spheroids. *Opt. Express* **27**,35750.

Single Particle Extinction and Scattering: a new approach for multiparametric optical characterization of nano- and microparticles

Marco Potenza[a]*

[a]*Instrumental Optics Laboratory, University of MiIlan, Italy*

[*]*Presenting author (marco.potenza@unimi.it)*

In this talk I will introduce the SPES method, giving an overview of some results and focusing on recent applications in characterizing the optical properties of particles in view of feeding radiative transfer models.

Electromagnetic wave scattering by superspheroids

Lei Bi

[1]*Department of Atmospheric Sciences, Zhejiang University*
[*]*corresponding author's e-mail: bilei@zju.edu.cn*

Atmosphere contains various aerosols (e.g., dust, sea salt, etc.) and cloud and precipitation particles. The optical properties of these particles fundamentally impact atmospheric radiative transfer, which should be accurately quantified in remote sensing, numerical weather data assimilation and climate modeling studies. However, it is challenging to characterize these particle morphologies for optical property computations. In this talk, we review our persistent research efforts in the past few years on studying the optical properties of superspheroids [1-8] and report a comprehensive optical property database of super-spheroidal models computed by using the invariant imbedding T-matrix method. The database contains the optical properties of superspheroids at 273 refractive indices and 110 particle shapes. In addition, we will highlight relevant applications in remote sensing, atmospheric radiative transfer and climate studies and discuss in depth why one additional freedom of superspheroids matters in applications.

Additional information

The superspheroidal equation is given by [9,10]

$$\left(\frac{x}{a}\right)^{2/n} + \left(\frac{y}{a}\right)^{2/n} + \left(\frac{z}{c}\right)^{2/n} = \mathbf{1}, \tag{1}$$

where n is referred to roundness parameter, and a and c are horizontal and vertical semi-axis, respectively. Figure 1 shows a shape space of superspheroids constructed by the roundness and aspect ratio parameters. Note, the superspheroids of roundness unity are traditional spheroids and the particles are concave when the roundness parameter (n) is larger than 2.

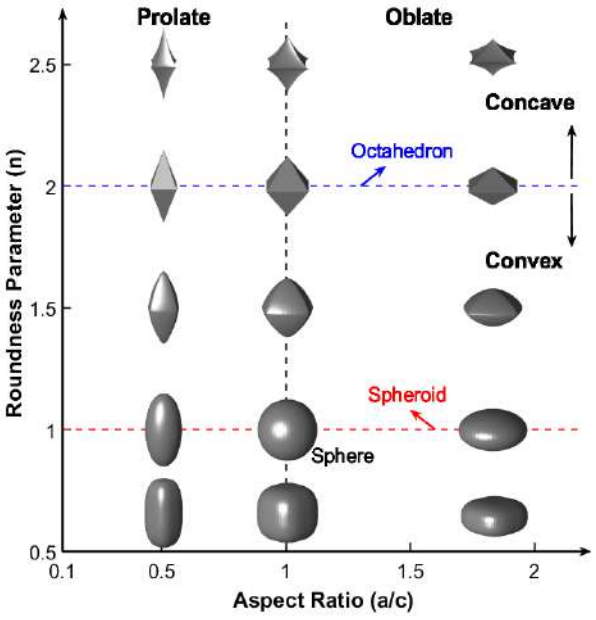

Figure 1: Morphology of superspheroids

References

[1] L. Bi, W. Lin, D. Liu, and K. Zhang *Assessing the depolarization capabilities of nonspherical particles in a super-ellipsoidal shape space.* Optics Express, 26(2):1726-1742, 2018.

[2] L. Bi, W. Lin, Z. Wang, X. Tang, X. Zhang, and B. Yi *Optical modeling of sea salt aerosols: the effects of nonsphericity and inhomogeneity.* Journal of Geophysical Research: Atmospheres, 123:543-558, 2018.

[3] W. Lin, L. Bi, and O. Dubovik *Assessing super-spheroids in modelling the scattering matrices of dust aerosols.* Journal of Geophysical Research: Atmospheres, 123:13917-13943, 2018.

[4] X. Tang, L. Bi, W. Lin, D. Liu, K. Zhang, and W. Li *Backscattering ratios of soot-contaminated dusts at triple LiDAR wavelengths: T-matrix results.* Optics Express, 27(4):A92-A116, 2019.

[5] W. Lin, L. Bi, F. Weng, Z. Li, and O. Dubovik, *Capability of superspheroids for modeling PARASOL observations under dusty-sky conditions*. Journal of Geophysical Research: Atmospheres, 126, 2021.

[6] Z. Wang, L. Bi, B. Yi, and X. Zhang *How the inhomogeneity of wet sea salt aerosols affects direct radiative forcing.* Geophysical Research Letters, 46:1805-1813, 2019.

[7] Z. Wang, L. Bi, X. Jia, B. Yi, X. Lin, F. Zhang *Impact of Dust Shortwave Absorbability on the East Asian Summer Monsoon.* Geophysical Research Letters, 47, e2020GL089585, 2020

[8] L. Sun, L. Bi, and B. Yi. *The use of superspheroids as surrogates for modeling electromagnetic wave scattering by ice crystals.* Remote Sensing, 13: 1733, 2021.

[9] A. H. Barr, *Superquadrics and Angle-Preserving Transformations* IEEE Comput. Graph. Appl., vol. 1, no. 1, pp. 11–23, 1981, doi: 10.1109/MCG.1981.1673799.

[10] T. Wriedt *Using the T-matrix method for light scattering computations by non-axisymmetric particles: Superellipsoids and realistically shaped particles*. Particle and Particle Systems Characterization, 19:256–268, 2002.

The discrete dipole approximation: from Maxwell's equations to practical applications

M. A. Yurkin[1,2,*]

[1]*Voevodsky Institute of Chemical Kinetics and Combustion, SB RAS, Institutskaya str. 3, 630090, Novosibirsk, Russia*
[2]*Novosibirsk State University, Pirogova 2, 630090 Novosibirsk, Russia*
[*]*corresponding author's e-mail: yurkin@gmail.com*

Light scattering is widely used in remote sensing of various objects ranging from metal nanoparticles and macromolecules to atmospheric aerosols and interstellar dust. Moreover, the structure of electromagnetic fields near a particle is of major importance for other phenomena, such as the surface-enhanced Raman scattering (SERS) or the electron energy-loss spectroscopy (EELS). All these applications require accurate simulations of interaction of electromagnetic fields with particles of arbitrary shape and internal structure. The discrete dipole approximation (DDA) is one of the general methods to handle such problems [1].

The DDA is a numerically exact method derived from the volume-integral form of the frequency-domain Maxwell's equation for the electric field [2], and is a special case of method of moments. It commonly employs a regular rectangular grid of dipoles, leading to the computational complexity (and required memory) linear in the number of dipoles. This allows one to solve the problems with up to 1 billion dipoles using modern supercomputers [3]. Overall, the DDA is widely used for light-scattering and near-field simulations, thanks to the availability of robust and easy-to-used open-source codes, such as DDSCAT [4] and ADDA [3].

Importantly, the DDA can be applied to a broad range of electromagnetic applications apart from the standard problem of far-field scattering by single isolated particles. This includes complicated environments (e.g., particles on substrate) and unusual incident fields (leading to the SERS and EELS). The DDA can even be applied to simulate fluctuation phenomena, i.e. the near-field radiative transfer and Casimir forces, which are related to the Green's tensor in the presence of a particle. The only drawback is that the latter applications require much larger computational resources.

References

[1] Yurkin MA, Hoekstra AG. The discrete dipole approximation: an overview and recent developments. J Quant Spectrosc Radiat Transfer 2007;106:558–89.
[2] Yurkin MA, Mishchenko MI. Volume integral equation for electromagnetic scattering: Rigorous derivation and analysis for a set of multilayered particles with piecewise-smooth boundaries in a passive host medium. Phys Rev A 2018;97:043824.
[3] Yurkin MA, Hoekstra AG. The discrete-dipole-approximation code ADDA: capabilities and known limitations. J Quant Spectrosc Radiat Transfer 2011;112:2234–47.
[4] Draine BT, Flatau PJ. Discrete-dipole approximation for scattering calculations. J Opt Soc Am A 1994;11:1491–9.

Optical Excitations with Free Electrons: Challenges and Opportunities

F. Javier García de Abajo[a,b]*

[a] *ICFO-Institut de Ciencies Fotoniques, The Barcelona Institute of Science and Technology, 08860 Castelldefels (Barcelona), Spain*
[b] *ICREA-Institució Catalana de Recerca i Estudis Avançats, Passeig Lluís Companys 23, 08010 Barcelona, Spain*

[*] *Presenting author (javier.garciadeabajo@nanophotonics.es)*

Electron beams have evolved into powerful tools to investigate photonic nanostructures with an unrivaled combination of spatial and spectral precision through the analysis of electron energy losses and cathodoluminescence light emission. Combined with ultrafast optics, the emerging field of ultrafast electron microscopy relies on synchronized femtosecond electron and light pulses that are aimed at the sampled structures, holding the promise to bring simultaneous sub-Angstrom--sub-fs--sub-meV space-time-energy resolution to the study of material and optical-field dynamics. In this talk, we will overview the potential of free electrons to probe and manipulate photonic fields. We will also discuss exciting possibilities that include disruptive approaches to non-invasive spectroscopy and microscopy, the possibility of sampling the nonlinear optical response at the nanoscale, the manipulation of the density matrices associated with free electrons and optical sample modes, and applications in optical modulation of electron beams.

Inverse problem of light scattering: applications in remote sensing

Oleg Dubovik [1,*]

[1]*Univ. Lille, CNRS, UMR 8518 - LOA - Laboratoire d'Optique Atmosphérique, F-59000 Lille, France*

[*]*corresponding author's e-mail: oleg.dubovik@univ-lille.fr*

Remote sensing is a major tool for studying the interactions of solar radiation with the atmosphere and surface and their influence on the Earth radiation balance. One of the challenges in remote sensing is the development of a reliable inversion procedure. The inversion is particularly crucial and demanding for interpreting high complexity polarimetric measurements where many unknowns should be derived simultaneously. Numerous publications offer a wide diversity of inversion methodologies suggesting somewhat different inversion methods. Such uncertainty in methodological guidance leads to excessive dependence of inversion algorithms on the personalized input and preferences of the developer. The reviews of inversion methods can be found in various textbooks, however, the textbook often do not provide the reader with sufficient explanations of existing alternatives and as to which method and why it should be chosen for a particular application.

We describe an approach to the Multi-term Least Square Method (LSM) that has been used to develop complex aerosol inversion algorithms for a number of years and applied to retrievals of laboratory and ground-based measurements. Theoretically, it was shown to unite the advantages of a variety of approaches and provides transparency and flexibility in development of practically efficient retrievals. The LSM concept suggests a generalized Least Square type formulation that allows for uniting the advantages of a variety of approaches, such as Phillips-Tikhonov-Twomey constrained inversion, Optimal Estimation approach, Kalman filters, Newton-Gauss and Levenberg-Marquardt iterations, etc. In addition the concept is convenient for the development of innovative and practically efficient retrieval procedures. One of recent examples is the multi-pixel retrieval concept by Dubovik et al. (2011) - a simultaneous optimized fitting of a large group of image pixels with additional constraints limiting the time variability of surface properties and spatial variability of aerosol properties. From practical viewpoint, this approach provides a methodology for using multiple a priori constraints to atmospheric problems where rather different groups of parameters should be retrieved simultaneously. For example, Dubovik and King (2000) used multi-term LSM for designing the algorithm that retrieves aerosol size distribution and spectrally dependent complex index of refraction from Sun/sky-radiometer ground-based observations. Furthermore, the significant potential the approach was demonstrated with the development of the GRASP (Generalized Retrieval of Aerosol and Surface Properties) algorithm.

The illustrations of methodology are provided for GRASP aerosol retrieval from diverse light scattering observations. The proposed methodology has resulted from the multi-year efforts of developing inversion algorithms from remote sensing observations (Dubovik and King, 2000; Dubovik 2004, Dubovik et al. 2008, 2011, 2021).

Studying comets by means of polarimetry: Current status and further development

E. Zubko[1,*]

[1]*Humanitas College, Kyung Hee University, South Korea*

[*]*corresponding author's e-mail: evgenij.s.zubko@gmail.com*

Current status

When initially unpolarized solar radiation is scattered from a comet, it acquires a partial linear polarization. Its quantity is described in terms of the degree of linear polarization $P = (F_{\perp} - F_{||})/(F_{\perp} + F_{||})$ 100%, where $F_{\perp}$ and $F_{||}$ are the flux components of the scattered light that are polarized perpendicularly to the scattering plane and within the scattering plane, respectively. P is a function of phase angle α that is complementary to the scattering angle θ = 180° – α. All comets reveal a branch of the negative polarization (i.e., $F_{\perp} < F_{||}$) at small phase angles α < 30° and branch of the positive polarization (i.e., $F_{\perp} > F_{||}$) at larger phase angles, α > 30°. The strength of the polarimetric response varies greatly from one comet to another. The location of the positive polarization maximum P_{max} occurs at different locations within the phase angles α ~ 80° – 100°. In practice, P_{max} spans the range from only ~6% in comet C/2018 V1 (Machholz-Fujikawa-Iwamoto) [1] to up to ~50% in a freshly split comet C/2019 Y4 (ATLAS) [2]; whereas, in the same comet before disintegration, the polarization maximum was about 34%, similar to comet C/1995 O1 (Hale-Bopp). Dispersion of P_{max} initially was interpreted as a result of the depolarizing effect of gaseous molecules whose emission lines indeed appear in the spectra of comets [3]; however, a thorough analysis of the entire set of data (spectra, mid-IR thermal emission, and polarization) unambiguously suggests a dusty origin of the dispersion of P_{max} [4]. Furthermore, a highly realistic model of the *agglomerated debris particles* was demonstrated to be capable of fitting the positive polarization in comets with different P_{max} [1,2,4] as well as the negative polarization [5].

Further development

Comets are known for their activity. Apparent brightness, photometric color, relative strength of the gaseous-emission lines, and/or mid-IR thermal emission in a comet could change significantly within only a day or two. Surprisingly, this is hardly reflected in databases of polarimetric observations of comets, such as [3]. It is of a great interest, therefore, to investigate possible temporal variations of polarization in comets. However, rare examples of such monitoring do suggest that the polarization of comets could be subject of significant temporal variations [2, 6].

References

[1] E. Zubko, E. Chornaya, M. Zheltobryukhov, A. Matkin, O.V. Ivanova, D. Bodewits, A. Kochergin, et al. *Extremely low linear polarization of comet C/2018 V1 (Machholz–Fujikawa–Iwamoto)*. Icarus, 336:113453, 2020.

[2] E. Zubko, M. Zheltobryukhov, E. Chornaya, A. Kochergin, G. Videen, G. Kornienko, and S.S. Kim. *Polarization of disintegrating Comet C/2019 Y4 (ATLAS)*. Mon. Not. Roy. Astron. Soc., 497:1536–1542, 2020.

[3] G.P. Chernova, N.N. Kiselev, and K. Jockers. *Polarimetric characteristics of dust particles as observed in 13 comets – Comparisons with asteroids*. Icarus 103:144–158, 1993.

[4] E. Zubko, G. Videen, D.C. Hines, and Yu. Shkuratov. *The positive-polarization of cometary comae*. Planet. Space Sci., 123:63–76, 2016.

[5] E. Zubko and G. Videen. *Dust in Comet 67P/Churyumov–Gerasimenko: Interrelation between in situ Findings by Rosetta and Ground-based Polarimetry*. Research Notes of the AAS, 5:68, 2021.

[6] E. Chornaya, E. Zubko, I. Luk'yanyk, A. Kochergin, M. Zheltobryukhov, O.V. Ivanova, G. Kornienko, et al. *Imaging polarimetry and photometry of comet 21P/Giacobini-Zinner*. Icarus, 337:113471, 2020.

Surface-enhanced Raman scattering from gold nanorods as a function of their aspect ratio and morphology: a reexamination study

N. Khlebtsov[1,2*], B. Khlebtsov[1], V. Khanadeev[1], A. Burov[1] and E. Le Ru[3]

[1]*Institute of Biochemistry and Physiology of Plants and Microorganisms, Russian Academy of Sciences, Saratov, Russia*
[2]*Saratov State University, Saratov, Russia*
[3]*Victoria University of Wellington, Wellington, New Zealand*
[*]*khlebtsov@ibppm.ru*

Introduction

The on-resonance excitation of plasmonic nanoparticles is assumed to be necessary for increasing the Raman signal intensity of nearby molecules [1]. That is why researchers seek to fabricate rationally designed nanoparticles for surface-enhanced Raman scattering (SERS) applications with the plasmon resonance (PR) close to the excitation wavelength. The crucial role of hot-spot generation and the electromagnetic (EM) contribution to the overall SERS enhancement factor (EF) has been established for a long time [2]. Still, there remain some gaps in the current understanding of the interplay between the near-field (SERS) and the far-field optical response. Indeed, the SERS EF scales like the fourth power of the local field [3]. As a result, even a tiny detuning of the longitudinal PR from the excitation wavelength could substantially decrease the theoretical EF. However, the existing experimental data for Au nanorod (AuNR) colloids do not confirm such theoretical predictions [2]. The random orientation of AuNRs in suspensions is a complicating factor. However, the recently published single-particle data for the simple long-axis excitation of AuNRs [4] also do not show any substantial variations in the EF as a function of the aspect ratio, in contradiction with current EM models. Most previous studies have used samples of AuNRs with different diameters, particle concentrations, amounts of impurities, and probably some variations in the nanorod shape. Here, we discuss a reexamination study [2] using a well-defined experimental model obtained by controllable nanorod etching.

Results and Discussion

We used the controllable etching method [2] to prepare a set of AuNR samples of equal number concentrations by keeping the AuNR width and shape morphology. At the same time, the plasmon resonance was incrementally decreased from 925 to 650 nm through the finely tuned aspect ratio (Fig. 1). The AuNRs were functionalized with 1,4-nitrobenzenethiol (NBT), and SERS spectra of the colloids were measured under 785-nm laser excitation. The nanorod concentration (~7×10^{10} 1/mL) was quantified by atomic absorption spectroscopy and spectrophotometry combined with TEM statistical data and T-matrix simulations. The number of adsorbed NBT molecules per one nanorod (~10^4) corresponded to the effective footprint ~0.55 nm^2 and was close to the monolayer packing density with the topological polar surface area of NBT 0.468 nm^2. SERS spectra of colloids and drop samples were measured under 785-nm laser excitation with a fiber-optic spectrometer and a Renishaw inVia Raman microscope. For PR wavelengths between 800 nm and 900 nm, both simulated and experimental EFs then show minimal variations and are in remarkable agreement (Fig. 2). However, for PR wavelengths between 650 nm and 800 nm, EM simulations still predict substantial variations in the SERS intensity within one order of magnitude, in stark contrast to the experimental EFs. The exact reasons for such disagreement between measurements and EM simulations are unclear, and further work is needed to clarify the point. By contrast to weak plasmonic dependence of SERS signals from the aspect ratio of AuNRs, minor variations in shape morphology lead to notable changes in SERS response. Specifically, when the initial AuNRs were further overgrown to have dumbbell morphology, their SERS intensity increased fivefold. Thus the rational design of the nanoparticle shape morphology is a more critical factor towards the highest SERS response compared to the tuning of the plasmonic peak

for on-resonance excitation. Finally, we demonstrate that the dependence of the SERS background spectra on the particle aspect ratio is consistent with both the photoluminescence from AuNRs and the elastic light scattering of a weak laser background by AuNRs.

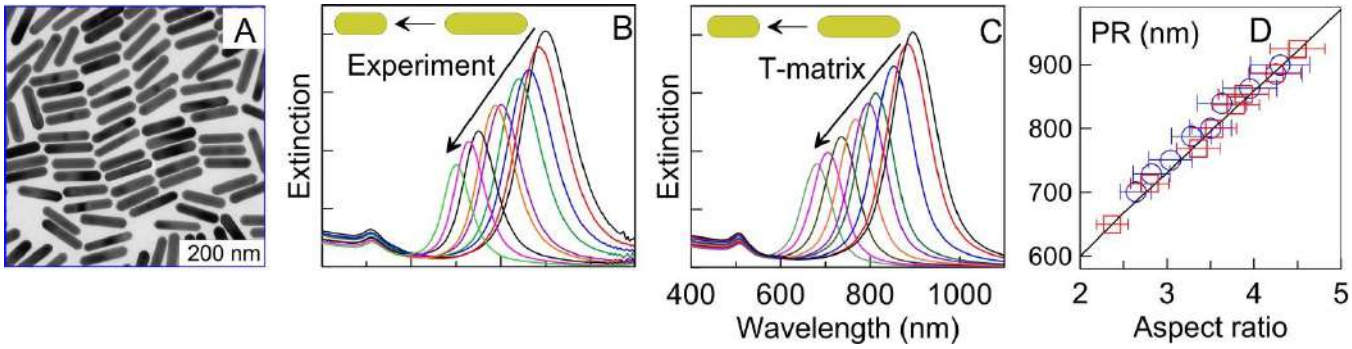

Figure 1. TEM images of the initial AuNRs (A), experimental (B), and simulated (C) extinction spectra of nine etched samples. (D) Dependence of the longitudinal PR on the TEM-measured aspect ratio of two independent nanorod sets. The black plot shows T-matrix simulations for polydisperse AuNR ensembles derived from TEM images.

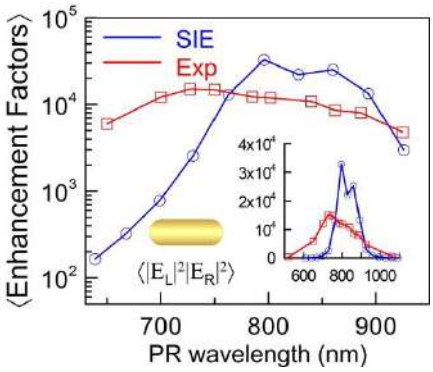

Figure 2. Experimental and simulated (SIE) dependences of the surface- and orientation-averaged SERS EFs on the PR wavelength. The inset shows an enlarged spectral range that includes spheres and long AuNRs.

Acknowledgments

This research was supported by the Russian Scientific Foundation (project no. 18-14-00016-П).

References

[1] N. Pazos-Perez, L. Guerrini, and R. A. Alvarez-Puebla. *Plasmon tunability of gold nanostars at the tip apexes*. ACS Omega, 3:17173−17179, 2018.

[2] B. Khlebtsov, V. Khanadeev, A. Burov, E. Le Ru, and N. Khlebtsov. *Reexamination of surface-enhanced Raman scattering from gold nanorods as a function of aspect ratio and shape*. J. Phys. Chem. C. 124:10647-10658, 2020.

[3] E. C. Le Ru and P. G. Etchegoin. *Principles of Surface Enhanced Raman Spectroscopy and Related Plasmonic Effects,* Amsterdam: Elsevier, 2009.

[4] K.-Q. Lin, J. Yi, J.-H. Zhong, S. Hu, B.-J. Liu, J.-Y. Liu, C. Zong, Z.-C. Lei, X. Wang, J. Aizpurua, R. Esteban, and B. Ren, *Plasmonic photoluminescence for recovering native chemical information from surface-enhanced Raman scattering*. Nat. Commun. 8:14891-14897, 2017.

Professor Kuo-Nan Liou's contributions to Light Scattering, Radiative Transfer, and Remote Sensing

P. Yang[1,*], Y. Gu[2], and Q. Fu[3]

[1]*Department of Atmospheric Sciences, Texas A&M University, College Station, TX 77843, USA*
[2]*Joint Institute for Regional Earth System Science and Engineering/Department of Atmospheric and Oceanic Sciences, University of California, Los Angeles; Los Angeles, CA 90095 USA*
[3]*Department of Atmospheric Sciences, University of Washington, Seattle, WA 98195, USA*

[*]*corresponding author's e-mail: pyang@tamu.edu*

Prof. Kuo-Nan Liou's scientific accomplishments and Services to the Science Conmmunity

Prof. Kuo-Nan Liou, one of the greatest atmospheric physicists of the last half century, passed away on 20 March 2021. He was a *Distinguished Professor* in the Department of Atmospheric and Oceanic Sciences at the University of California, Los Angeles (UCLA), and the founding director of UCLA's Joint Institute for Regional Earth System Science and Engineering (JIFRESSE). Before joining UCLA, he was a professor at the University of Utah for 22 years.

Prof. Liou made seminal contributions to atmospheric and climate science in many areas, particularly in atmospheric radiation and light scattering. He moved the field of atmospheric radiation forward with a quantum leap through his work on the theory of radiative transfer and light scattering, the investigation of radiative forcing effects of clouds and aerosols, and the development of methods for inferring atmospheric and surface parameters by means of remote sensing. Prof. Liou was actively engaged in services to the science community throughout his career. He served on numerous national and international committees. To list a few, he served as Chair of Section 12, Special Fields and Interdisciplinary Engineering, National Academy of Engineering (2008-2010), Chair of the AGU Atmospheric Sciences Section Fellows Committee (2013-2014), Chair of the AGU Roger Revelle Medal Committee (2017-2020), Chair of the 1986 International Radiation Symposium, Chair of the AMS Committee on Atmospheric Radiation (1982-1984), and Chair-Elect of the AMS Atmospheric Research Awards Committee (2021-2022). Although Prof. Liou always had a very busy schedule, he often reviewed manuscripts for a number of journals and research proposals for funding agencies. Moreover, he served as an editor for the *Journal of the Atmospheric Sciences* (1999-2005), a Guest Editor for Special Volume on Clouds and Radiation, *Journal of Geophysical Research* (1987), a Review Editor for the Intergovernmental Panel on Climate Change (IPCC) Report (1998-1999), and an Associate Editor for *Journal of Quantitative Spectroscopy and Radiative Transfer* (2011-2021). As tribute to Prof. Liou, this presentation will summarize his groundbreaking scientific accomplishments, contributions to education, and voluminous service to the science community.

Additional information

Figure 1: Professor Kuo-Nan Liou, 1943-2021.

Light Scattering by Fire Smoke Aerosols in Visible Wavelength

Qixing Zhang*, Jia Liu, Jie Luo and Yongming Zhang

State Key Laboratory of Fire Science, University of Science and Technology of China, Hefei 230026, China

**corresponding author's e-mail: qixing@ustc.edu.cn*

Abstract

Smoke aerosols produced by fire, including soot, brown carbon, and the internal mixed aerosol, are an important component of the global aerosol cycle. With climate change, both the number and intensity of global wildfires seem to have been increasing in recent years. Large amount of smoke aerosols are injected into the atmosphere, which seriously affect air quality, as well as the regional and global climate. Optical properties of smoke aerosols are of high interest in both passive and active remote sensing and climate modelling studies.

On the other hand, for building fire protection, smoke sensor using the principle of light scattering is the most common and widely used fire detector. However, it suffers by the high false alarm rate caused by non-fire aerosols, such as dust, steam, etc. A better knowledge of the optical properties of the aerosols from fire and nuisances will therefore help to improve the performance of existing detectors, reduce the amount of false alarms, and serve as guideline in the development of the next generation smoke detector.

Aiming to fill the fundamental research needs in the above two aspects, the research group in State Key Laboratory of Fire Science have studied the scattering properties of smoke and typical nuisance aerosols for more than ten years. The morphology of smoke particles from smoldering and flaming fires were analyzed by SEM and AFM imaging. Morphology of smoke from smoldering fires is found to be different from of that of smoke from flaming fires. Different morphological models were developed for numerical simulation of optical properties of smoke aerosols, especially for the morphologically complex internal mixed soot aerosols. An experimental platform using polarization modulation were designed to measure light scattering matrices in 532nm and 405nm wavelength, from 5° to 175°. The angular distributions of non-zero elements of scattering matrix for several fire smoke particles and typical dust particles as well as the feasibility of identifying particle types based on matrix elements were investigated. In this presentation, we will give an overview of the study on experimental and simulation study of light scattering by fire smoke aerosols in visible wavelength, summarize the main findings in current stage and discuss the requirements for future light scattering measurement study of fire smoke particles.

Analysis and Modelling of TTL ice crystals based on in-situ measurement of scattering patterns

E R Mathen[1,*], E Hesse[1], A J Baran[1,2]

[1]*University of Hertfordshire, AL10 9AB, UK.*

[2]*Met Office, Exeter, EX13PB, UK.*

**em14abz@herts.ac.uk*

Abstract

The primary objective of this research is to analyse the scattering patterns of Tropical Tropopause Layer (TTL) ice crystals and find their characteristics like shape and size distributions. As cirrus is a high cloud, it plays a crucial role in the Earth-atmosphere radiation balance and by knowing the scattering properties of ice crystals, their impact on the radiative balance can be estimated [1].

The in-situ data presented here was taken during the NERC and NASA Co-ordinated Airborne Studies in the Tropics and Airborne Tropical Tropopause Experiment (known as the CAST-ATTREX campaign) on 5th March 2015 at an altitude between 15-16km over the Eastern Pacific. During this flight, the 2D scattering patterns were captured by the Aerosol Ice Interface Transition Spectrometer (AIITS) [2] at the wavelength of 532nm.

Since manual analysis of scattering patterns is time-consuming, a Deep Learning code has been implemented to classify the scattering patterns (like rough, pristine and rounded hexagonal prisms). To speed up the process, the Deep Learning Network has been created using Transfer Learning (based on a pre-trained network called GoogLeNet). After the analysis phase, the model crystals of specific types and sizes are generated using appropriate codes for light scattering computations (example: for rough crystals [3]). The scattering data of the model crystals are then simulated using a Beam Tracing Model (BTM) [4] [5] based on physical optics. By successive testing and further analysis, the crystal sizes can be estimated.

This research further helps to broaden the understanding of the general scattering properties of TTL ice crystals, to support climate modelling and contribute towards more accurate climate prediction.

Acknowledgment: E R M acknowledges the Met Office CASE Award.

References

[1] A. J. Baran. *A review of the light scattering properties of cirrus.* J. Quant. Spectrosc. Radiat. Transfer, 110:1239-1260, 2009.
[2] E. Hirst, C Stopford, P. H. Kaye, R. S. Greenaway and J D Dorsey. *The Aerosol Ice Interface Transition Spectrometer – A new particle phase.* ATTREX Science Meeting. Boulder, United States. 30 September 2013.
[3] C. T. Collier. *Experimental and Computational Investigation into Light Scattering by Atmospheric Ice Crystals,* PhD thesis, University of Hertfordshire, 2014.
[4] L. C. Taylor. *A Beam Tracing Model for Electromagnetic Scattering by Atmospheric Ice Crystals*, PhD thesis, University of Hertfordshire, 2016.
[5] E. Hesse, L. Taylor, C. Collier, A. Penttilä, T. Nousiainen and Z. Ulanowski. *Discussion of a physical optics method and its application to absorbing smooth and slightly rough hexagonal prisms.* J. Quant. Spectrosc. Radiat. Transfer, 218:54-67, 2018.

Solving the problem of wave diffraction on a body of revolution with a rough boundary

A. G. Kyurkchan[1,2,3]and S.A. Manenkov[1*]

[1]*Moscow Technical University of Communications and Informatics, Aviamotornaya str. 8a,111024, Moscow, Russia*
[2]*Kotel'nikov Institute of Radio Engineering and Electronics, Fryazino Branch, Russian Academy of Sciences, pl. Vvedenskogo 1, Fryazino, Moscow Oblast, 141190 Russian Federation*
[3]*Central Research Institute of Communication, 8 1st Perova Polya Drive, Moscow 111141, Russian Federation*
[*]*corresponding author's e-mail: mail44471@mail.ru*

The literature contains a large number of publications devoted to the diffraction of waves on bodies and surfaces with rough boundary (including those described by a random function of coordinates) [1,2]. In this paper, we study a three-dimensional problem of wave diffraction by an dielectric body of revolution with a rough boundary. As you know, there are many methods for solving such a problem. A large group of methods is based on the use of one or another small parameter [1,2]. The presence of such a parameter imposes rather stringent conditions on the degree of "roughness" of the scatterer boundary. In this work, based on the modified method of discrete sources (MMDS) [3,4], an effective rigorous approach to solving the problem of diffraction on statistically rough body of revolution is proposed. In this case, the roughness of the boundary were modeled using the sinusoidal function with the random amplitude. As an example, diffraction of the plane wave by the rough Chebyshev particles which contour equation is stated in spherical and spheroidal coordinates is considered [4]. Note that, on the one hand, MMDS has an advantage, for example, over the method of current integral equations, since it does not require calculating integrals when finding the matrix elements of the corresponding algebraic system. This fact is very important when averaging the scattering pattern in the case of statistically rough body boundary. On the other hand, the method allows one to solve the problem of diffraction on the body with an analytical boundary with high accuracy.

Earlier in [5], an attempt was made to explain the phenomenon of recognition of mirror-like objects, i.e. scatterers with a perfectly smooth border. In short, we recognize mirrored objects due to the image of nearby objects in them. Obviously, perfectly mirrored objects do not exist in the nature. All of them are "rough" to one degree or another. Of interest is the question of how the shape of the axial section of an "unperturbed" body (provided that the roughness of the boundary is small in comparison with the wavelength) affects the fact that a rough scatterer is perceived as ideally reflecting or specular. As is known, the field scattered by any object is generated by sources located on the surface and (or) inside the scatterer. If the object belongs to the category of "specular", then the sources of the field scattered by it are located inside the scatterer [3]. In this work, an attempt is made to determine under what condition on the sectional shape the object can be classified as mirror-like. In this case, the dependence of the geometry of the set of singularities of the analytical continuation of the diffraction field into the region occupied by the body and the scattering pattern on the shape of the scatterer axial section was chosen as a criterion.

References

[1] *Muinonen K., Nousiainen T., Fast P., Lumme K., & Peltoniemi J. I.* Light scattering by gaussian random particles: ray optics approximation. J. Quant. Spectrosc. Radiat. Transfer. 1996. V. 55. P. 577.
[2] *Kahnert M, Rother T.* Modeling optical properties of particles with small-scale surface roughness: combination of group theory with a perturbation approach. Opt Express. 2011. V.19. P. 11138.

[3] *Kyurkchan A. G., Smirnova N. I.* Mathematical Modelling in Diffraction Theory Based on A Priori Information on the Analytical Properties of the Solution. Elsevier, Amsterdam, 2017.
[4] *Kyurkchan A.G, Manenkov S.A.* Application of different orthogonal coordinates using modified method of discrete sources for solving a problem of wave diffraction on a body of revolution. J. Quant. Spectrosc. Radiat. Transfer. 2012. V.113. P. 2368.
[5] *Kyurkchan A. G.* About recognition of mirror-like objects. Physics - Uspekhi. 2017. V. 60. № 10. P. 1018.

Investigating the impact of aerosol vertical distribution on aerosol radiative forcing and satellite AOD retrieval

Jing Li[1,*], Lu Zhang[1], Chong Li[1]

[1]*Department of Atmospheric and Oceanic Sciences, School of Physics, Peking University*
[*]*corresponding author's e-mail: jing-li@pku.edu.cn*

Abstract

Aerosols remain the largest source of uncertainty in anthropogenic forcing of climate change. Even for their direct radiative effect, the multi-model spread is of comparable magnitude to the ensemble mean. To constrain aerosol forcing within a column, one needs to know aerosol loading, their optical properties and vertical profiles. In this study, we mainly focus on the vertical distribution whose knowledge is still limited.

First, we explore the impact of aerosol vertical distribution on their radiative forcing using radiative transfer models and CMIP6 simulation results. Sensitivity studies show that the magnitude of radiative forcing from both scattering and absorbing aerosols increases with altitude, with higher sensitivity for absorbing aerosols. We also noticed a non-linear effect when absorbing and scattering aerosols coexist in the same column, i.e., the absorption by absorbing aerosols may be enhanced (reduced) when scattering aerosols are located below (above) absorbing aerosols. Using simulated aerosol mass density fields from 7 CMIP6 models, we find that the difference in the aerosol vertical distribution accounts for ~25% of the uncertainty in aerosol radiative forcing, and the non-linear interaction between absorbing aerosols and scattering aerosols can be significant for some regions. We also evaluated the model aerosol vertical distribution with CALIPSO and found an overall low bias of ~1 km in aerosol layer height over land. This bias will cause ~0.5 W m-2 aerosol forcing uncertainty globally.

Second, incorrect assumption of aerosol vertical distribution also causes uncertainties in aerosol optical depth (AOD) retrieval from passive satellite sensors. Typically, the retrieval algorithm assumes an exponential decreasing aerosol profile and uses the scale height to represent the height of aerosols. Sensitivity experiments using radiative transfer models show that AOD retrieval is the most sensitive to the vertical distribution of absorbing aerosols: -1km error in aerosol scale height can lead to ~30% AOD retrieval error. Ignoring the existence of the boundary layer can further result in ~10% error. The differences in the vertical distribution of scattering and absorbing aerosols within the same column may also cause ~15% error at low AOD but grows sharply as AOD increases. Surface reflectance also plays an important role in affecting the AOD error. An improved retrieval algorithm by replacing the default exponential profile with the observed aerosol vertical profile by a micro-pulse lidar at the Beijing-PKU site is developed, which produced much better agreement with surface observations, with correlation coefficients increased from 0.63 to 0.83 and bias decreased from 0.15 to 0.03.

Overall, this study highlights the importance of aerosol vertical distribution. Better constraint of this information likely requires the joint observation from multi-angle, polarized satellite sensors and space lidars.

References

[1] C. Li, J. Li, O. Dubovik, Z.-C. Zeng and Y. L. Yung: Impact of aerosol vertical distribution of aerosol optical depth retrieval from passive satellite sensors, Remote Sensing, 12(9), 1524, 2020.

1D Neutron Transport in a 1D Half-Space by the LN0 Method

B. D. Ganapol[1,*]

[1]*University of Arizona, Department of Aerospace and Mechanical Engineering*
Tucson AZ 85712, *USA*
[*]*Ganapol@cowboy.ame.arizona.edu*

Abstract

A new, highly precise, numerical solution, based on Case's analytical solution to the 1D neutron transport equation [1], is presented. Case's analytical solution for unknown reasons, generally resists straightforward numerical evaluation. One cannot simply apply Gauss quadrature to cover the entire range [0.1,1] of c, the number of scattering secondaries [2]. For c below 0.1, it is well-known that the solution requires extended arithmetic precision primarily due to the necessary precision of the eigenvalue of the transport operator and will not be considered here. In response to the inability of the Lagrange interpolation to deliver for $c < 0.4$, a novel, rather speculative method is proposed, again based on Lagrange interpolation, called the LN0 method. We show that LN0 is more than competitive with FN [3], considered one of the most accurate 1D transport methods.

Motivation and Brief Description

For any transport problem other than in an infinite medium, half- range orthogonality, requiring deep knowledge of complex variable theory for complete comprehension, is necessary when applying Case's method. As a result, numerical evaluation to find the flux is complicated because of the necessity to solve a non-linear integral equation to determine the Case X-function (or Chandrasekhar H-function) central to the solution. For this reason, the numerical solution is notoriously difficult to find. Therefore, Siewert [3] cleverly devised the FN method, based on full-range orthogonality, to construct a spectral expansion through collocation.

The FN method is one of the most successful methods of solving the neutral particle transfer equations on the planet. Therefore, why should we consider another method? Aside from the challenge and the accompanying intellectual satisfaction if successful, there is a downside to the FN method. The FN method (as well as the proposed LN0 method) for a half-space, requires determination of the eigenvalues of the transport operator. This is particularly troublesome since they are entirely dependent upon the scattering kernel and seem to have no regularity. It is for this reason, other methods such as the response matrix method, method of doubling and the DPN method have been perfected by the author [4,5,6]. However, the challenge of developing a method comparable to or even surpassing the performance of FN remains and is therefore my main objective.

The method to be proposed is based on the singular integral equation for the exiting flux from a half-space. Rather than formulate the scattering integral in terms of Gauss quadrature, the solution is expanded in terms of Lagrange polynomials. The advantage is that the principal value integration can be performed analytically in terms of Legendre functions of the second kind. Also included is the eigenvalue of the transport operator.

References

[1] K. Case, *Elementary Solutions of the Transport Equation and Their Applications*", *Ann. Phy*. **9**, pp 9-23,1960.
[2] B.D. Ganapol, submitted to ANS Math&Comp 2021.
[3] C. E. Siewert, *The F_N Method for Solving Radiative-Transfer Problems in Plane Geometry*, *Astrophysics and Space Science*, **58,** pp 131-137 1978.
[4] B.D. Ganapol, *The response matrix discrete ordinates solution to the 1D radiative transfer equation*, JQSRT, **154**, pp. 72–90, 2015.
[5] B.D. Ganapol, *An Extreme Benchmark for Monoenergetic Scattering in Hydrogen*, ANS Winter Meeting, Orlando FL., 2018.
[6] B.D. Ganapol, and Patel, K.J., *DPN Solution of the 1D Monoenergetic Neutron Transport Equation with Benchmarking*, ANS Winter Meeting Wash. DC, 2017.

Water vapor variability near clouds from ground-based spectroradiometer observed zenith radiance

G. Wen[1,2*] and A. Marshak[1]

[1]*NASA/Goddard Space Flight Center*
[2]*GESTAR/Morgan State University*
[*]*corresponding author's e-mail: Guoyong.Wen@nasa.gov*

Abstract

The transition zone between cloudy and cloud free areas is a special region in the atmosphere, where particle sizes and associated optical properties are neither cloud-like nor clear-like. The size of the transition zone ranges from a few hundred meters up to several kilometers (e.g., [1], [2]). In the transition zones, cloud droplets evaporate and shrink, aerosol particles are humidified and swollen, water vapor dilutes as relative humidity decreases from 100% in clouds to environment values away from clouds (e.g., [3], [4]). It was shown [5] that about 50% of clear areas are within 5 km from conventionally identified low-level water clouds. Thus, the transition zone has strong impact on climate forcing. It is necessary to better understand the variations of cloud and aerosol properties in the transition zone for improving the estimates of aerosol radiative forcing and reduce the uncertainties in cloud models of entrainment and mixing processes.

We have developed a new technique to retrieve precipitable water vapor (PWV) amount in the clear-cloud transition zone using ground-based spectroradiometer observations [6]. The method utilizes zenith radiances at the water vapor absorbing band at 720 nm and adjacent non-absorbing band at 750 nm. Radiative transfer calculations show that the relative difference in zenith radiance between the two bands mainly depends on PWV and the variations in cloud optical depth introduce a small change in the relative difference which is independent of PWV amount. This allows us to retrieve PWV variations in the cloud-clear transition zone for clouds over dark ocean surface. We applied this method to a Cu cloud case with zenith radiance observations by the Shortwave Array Spectroradiometer-Zenith (SASZe) during the Marine ARM GPCI Investigation of Clouds (MAGIC) field campaign. Our analysis shown that there is about 10% change in PWV amount from known-cloudy region to known-clear sky in cloud edges.

References

[1] T. Várnai, and A. Marshak. *Global CALIPSO observations of aerosol changes near clouds*, IEEE Geoscience and Remote Sensing Letters, vol. 8, no. 1, pp. 19–23, Jan. 2011. https://doi.org/10.1109/LGRS.2010.2049982

[2] I. Koren, L. A. Remer, Y. J. Kaufman, Y. Rudich, and J. V. Martins. *On the twilight zone between clouds and aerosols*, Geophysical Research Letters, vol. 34, no. L08805, Apr. 2007. https://doi.org/10.1029/2007GL029253

[3] I. Koren, G. Feingold, H. Jiang, H., and O. Altaratz, "Aerosol effects on the inter-cloud of a small cumulus cloud field," *Geophysical Research Letters*, vol. 36, no. L14805, Jul. 2009. https://doi.org/10.1029/2009GL037424

[4] D. Chand, R. Wood, S. J. Ghan, M. Wang, M. Ovchinnikov, P. J. Rasch, et al. *Aerosol optical depth increase in partly cloudy conditions*, Journal of Geophysical Research, vol. 117, no. D17207, Sept. 2012. https://doi.org/10.1029/2012JD017894

[5] T. Várnai, and A. Marshak. *Satellite Observations of Cloud-Related Variations in Aerosol Properties*, Atmosphere, vol. 9, no. 430, Nov. 2018. [10.3390/atmos9110430]

[6] G. Wen, and A. Marshak. *Precipitable Water Vapor Variation in the Clear-cloud Transition Zone from the ARM Shortwave Spectrometer*, IEEE Geoscience and Remote Sensing Letters, 2021, doi: 10.1109/LGRS2021.3064334

Blurring the cosmic microwave background with charged dust particles

Miroslav Kocifaj[1,2*], František Kundracik[1], Peter Markoš[1] and Gorden Videen[3,4]

[1]*Fmph, Comenius University, Mlynská dolina, 842 48 Bratislava, Slovakia.*
[2]*ICA, Slovak Academy of Sciences, Dúbravská cesta 9, 845 03 Bratislava, Slovakia.*
[3]*US Army Research Laboratory, 2800 Powder Mill Road, Adelphi, MD 20783-1197, United States*
[4]*Space Science Institute, 4750 Walnut Street, Boulder Suite 205, CO 80301, United States*

[*]*corresponding author's e-mail: kocifaj@savba.sk*

Dust particles in space carry surface charges that are either positive or negative. Positively charged grains tend to show electromagnetic signatures similar to those of uncharged grains. Due to their high mass the positive ions cannot respond quickly to an applied electromagnetic field and thus cannot alter the surface conductivity of the charged cosmic dust particles (CDPs). However, it has been shown that dust grains will have negative charges in a cold gas [1] with some tens of thousands of excess electrons under the lower temperature regime [2]. Free, unbound, electrons can move in a surface layer in response to an external electric field, thus affecting the electromagnetic interaction within some spectral range, resulting in distortion of the scattering signal of otherwise neutral particle [3]. It is theoretically conceived that dust particles can distort the cosmic microwave background (CMB) because the optical depth along a beam path steeply increases with redshift [4]. We show that this effect is even more pronounced in charged CDPs with excess electrons imposed on their surface. Depending on the size-to-wavelength ratio, the excess charge can either amplify or reduce the extinction cross section of a dust particle [5]. Manifestation of amplification or dampening the EM intensity due to surface charges is analyzed theoretically and numerically assuming the CMB is a perfect blackbody radiation.

References

[1] J. R. Burke, and J. Silk *Dust grains in a hot gas. I. Basic physics*. Astrophys, J. 190:1-10, 1974.
[2] S. H. Margolis, and D. N. Schramm *Dust in the Universe*. Astrophys, J. 214:339-346, 1977.
[3] R. L. Heinisch, F. X. Bronold, and H. Fehske *Phys. Rev. E.* 88:023109, 2013.
[4] V. Vavryčuk *MNRAS.* 470:L44-L48, 2017.
[5] P. Markoš, M. Kocifaj, F. Kundracik, and G. Videen *JQSRT* (preliminary accepted)

Multi-Spectral Digital Holography for Microparticle Characterization.

Ramesh Giri[1 *], Matthew J. Berg[1], and Gorden Videen[2]

[1]Department of Physics, Kansas State University, 1228 N. 17th St., Manhattan, KS 66506-2601, USA*

[2]US Army Research Laboratory, 2800 Powder Mill Road, Adelphi, MD 20783-119, USA

**Presenting author (rgiri@phys.ksu.edu)*

Digital holography is now established as a useful technique to characterize the size and morphology of particles relevant to the coarse mode aerosol for size range (> 1 micron) [1]. Yet, knowledge of the material composition of particles observed with holography is limited. The understanding of material compositions is important for many local and global climate modeling for example to characterize the radiative effects of mineral dust in atmosphere. Here, we test a multiple wavelengths method in digital holography to produce the color images of micro-particles. A color analysis is then used to investigate if particles of differing material composition can be differentiated.

References

[1] M. J. Berg and G. Videen, "Digital holographic imaging of aerosol particles in flight," J. Quant. Spectrosc. Radiat. Transf. **112**(11), 1776–1783 (2011).

Preferred mode of presentation: Oral or Poster.

Imaging polarimetry of Comet C/2020 S3 (Erasmus)

E. Chornaya[1,2,*], E. Zubko[3], A. Kochergin[1,2], M. Zheltobryukhov[2], G. Kornienko[2], and G. Videen [3,4]

[1] *Far Eastern Federal University, 8 Sukhanova St., Vladivostok 690950, Russia*
[2] *Institute of Applied Astronomy of RAS, 10 Kutuzova Emb., Saint-Petersburg 191187, Russia*
[3] *Humanitas College, Kyung Hee University, 1732, Deogyeong-daero, Giheung-gu, Yongin-si, Gyeonggi-do 17104, South Korea*
[4] *Space Science Institute, 4750 Walnut Street, Boulder Suite 205, CO 80301, USA*
[*] *corresponding author's e-mail: Ekaterina.d.Chornaya@gmail.com*

Introduction and observations

The Comet C/2020 S3 (Erasmus) is a long period comet with orbital period of ~2,600 years. We were able to observe this comet on four epochs in November of 2020: 13, 20, 22, and 23. The comet was at relatively large phase angles, α = 62.7° –66.6°. Observations were conducted using the 0.22-m telescope (F = 0.503 m) of the Ussuriysk Astrophysical Observatory (code C15), that is a division of Institute of Applied Astronomy of Russian Academy of Sciences. The comet was imaged through the broadband R filter of the Cousins photometric system and a dichroic polarization filter (analyzer) at three orientations evenly distributed around optical axis. This makes it possible to fully characterize the degree of linear polarization of light scattered by the comet (e.g., [1]). Every night, we repeated the polarimetric measurements for several full cycles of the analyzer positions. All images were processed using the *Image Reduction and Analysis Facility* (IRAF) [1,2].

Results and discussion

The comet was bright enough to make observations in the imaging-polarimetry mode. On all nights, we found qualitatively the same spatial distribution of the polarization in Comet C/2020 S3 (Erasmus). Namely, its inner coma revealed a noticeably lower positive polarization ($P \sim 10\%$) compared to the outer part of coma ($P \sim 25\%$). A similar distribution of polarization was observed previously in other comets. For instance, this was reported for short-period comets 46P/Wirtanen [2] and 2P/Encke [3] at other phase angles and spatial scale. It is worth noting that the opposite trend in spatial distribution of the polarization has also been observed (e.g., [1]). A heterogeneous distribution of polarization in comets reveals the presence in their coma of at least two types of dust population: Mg-rich silicate particles producing low positive polarization and carbonaceous particles with high positive polarization [4]. It is significant that the same two components can reproduce the phase-angle dependence of both the positive polarization [5] and negative polarization in comets [6], as demonstrated for comet Erasmus.

References

[1] E. Chornaya, E. Zubko, I. Luk'yanyk, et al. *Imaging polarimetry and photometry of comet 21P/Giacobini Zinner*. Icarus, 337:113471, 2020.
[2] M. Zheltobryukhov, E. Zubko, E. Chornaya, et al. *Monitoring polarization in comet 46P/Wirtanen*. Mon. Not. Roy. Astron. Soc., 498:1814–1825, 2020.
[3] D. Jewitt. *Looking through the HIPPO: Nucleus and Dust in Comet 2P/Encke*. Astron. J., 128:3061–3069, 2004.
[4] E. Zubko, K. Muinonen, Yu. Shkuratov, Go Videen. *Characteristics of cometary dust in the innermost coma derived from polarimetry by Giotto*. Mon. Not. Roy. Astron. Soc., 430:1118–1124, 2013.
[5] Zubko E., G. Videen, D.C. Hines, and Yu. Shkuratov. *The positive-polarization of cometary comae*. Planet. Space Sci., 123:63–76, 2016.
[6] E. Zubko, and G. Videen. *Dust in comet 67P/Churyumov–Gerasimenko: Interrelation between in situ findings by Rosetta and ground-based polarimetry*. Research Notes of the AAS, 5:68, 2021.

Optical response of polymer dispersed liquid crystal films doped with single- and multi-walled carbon nanotubes

V. Loiko[1,*], A. Konkolovich[1], A. Miskevich[1], D. Manaila-Maximean[2], O. Danila[2], V. Cîrcu[3], A. Bărar[2]

[1] *Stepanov Institute of Physics, National Academy of Sciences of Belarus, Niezalezhnastsi avenue 68-2 Minsk, 220072, Belarus*

[2] *University Politehnica of Bucharest, Department of Physics, Spl. Independentei 313, Bucharest, R-060042, Romania*

[3] *University of Bucharest, Department of Inorganic Chemistry, 23 Dumbrava Rosie St., Bucharest, Sector 2, 020484, Romania*

[*] *e-mail: loiko@ifanbel.bas-net.by*

The polymer-dispersed liquid crystal (PDLC) films [1] consist of a polymer matrix containing liquid crystal (LC) droplets, in which the orientation of the LC molecules can be changed under the electric or magnetic fields. This allows one to control the optical response of the films. They are used in displays, optoelectronic, microelectronic, and telecommunication systems, laser devices, etc. Electrically or magnetically controlled optical response of PDLC films is based on light scattering. It does not require the use of additional polaroid in comparison with the ordinary (homogeneous) LC layers.

In recent years, there is an increasing interest in studying the dielectric and optical properties of composite materials based on bulk LC and PDLC doped with carbon nanotubes (CNTs) [2,3]. Currently, studies of the electro-optical response of composite PDLC-CNTs films are mainly experimental [2]. As far as we know, there are no theoretical optical models that allow one to describe and predict electro-optical response of the PDLC-CNTs films as function of the component parameters (LC, polymer, NTs).

We suggest a model for analyzing the coefficient of coherent (directional) transmission of a PDLC-CNTs film with a homogeneous normal interface anchoring. To determine the coherent transmittance of the film, the Foldy–Twersky approximation is used. The optical characteristics of a single droplet of nematic LC are determined in the framework of the anomalous diffraction approximation and effective medium theory using the effective refractive indices of the droplets [4]. Based on the Maxwell–Garnett equations a method has been developed to determine the refractive index of the polymer matrix, the effective refractive index of the LC droplets, and the threshold field of the reorientation of the director structure of LC droplets upon doping the PDLC film with NTs. A technique has been developed for determining the volume filling factor of the film with LC droplets, volume filling factors of the LC droplets and polymer matrix doped with NTs, depending on the mass fractions of the components in the PDLC-CNTs composite. The technique is applicable to single-wall (SWCNTs) and multiwall (MWCNTs) carbon nanotubes. Experimental verification of the developed model is carried out.

References

[1] P.S. Drzaic. *Liquid Crystal Dispersions*. World Scientific, 1995.

[2] D. Mănăilă-Maximean, V.Cîrcu , P. Ganea, A. Bărar, O. Danila, T. Staicu, V.A. Loiko, A.V. Konkolovich, A.A. Miskevich. *Polymer Dispersed Liquid Crystal films doped with carbon nanotubes – preparation methods.* Proc. of SPIE 10977, 1097702(1-10). 2018.

[3] Y. Wu, H. Cao, M. Duan, E. Li, H. Wang, Z. Yang, D. Wang, and W. He. *Effects of a chemically modified multiwall carbon nanotubes on electro-optical properties of PDLC films*. Liquid Crystals, 45(7): 1023-103, 2017.

[4] V.A. Loiko, A.V. Konkolovich, V.Ya. Zyryanov, A.A. Misckevich. *Polarization of light by a polymer Film Containing Elongated Droplets of Liquid Crystal with Inhomogeneous Anchoring*. Opt. and Spectr. 122(6): 984-994, 2017.

An extinction paradox involving collimated beams and its resolution

V. A. Markel[1,*]

[1] *University of Pennsylvania*
[*] *e-mail: vmarkel@upenn.edu*

The electromagnetic power extinguished by a material particle, or the extinction cross section in the case of plane-wave illumination, are surprisingly counter-intuitive quantities. Extinction is difficult to express in terms of physical energy fluxes since the relevant formulas involve the product of the incident and the scattered fields (the "cross term") whereas only the sum of these two fields is "physical" and enters the definition of any measurable energy flux. The fundamental impossibility of separating spatially the incident and the scattered components of a wave-field, and the ensuing unavoidable interference between these two components, are at the root of all difficulties associated with extinction. Historically, these difficulties led to various paradoxes. The best known of these is the classical extinction paradox wherein the extinction cross section of an optically large particle is approximately two times larger than its geometrical cross section. Although an important insight into this paradox was made by Brillouin in 1949 [1], the complete understanding was achieved only recently [2–4]. Still, incorrect explanations of the paradox (i.e., related to edge diffraction) are quite wide-spread in the physics community.

A less known extinction-related paradox is illustrated in Fig. 1. Here a narrowly-collimated beam of light impinges on a scattering particle (shown by the red dot) whose radius is much smaller than the beam waist. Consider a spherical surface of radius L and centered on the scatterer. The field on most of this surface is given by the scattered field alone. Assuming the beam is perfectly collimated, the interference between the incident and the scattered fields occurs only within the surface regions $\mathbb{S}_{\pm}$ whose area S is much smaller than the area of the sphere, $4\pi L^2$, and is independent of L. Further, the scattered field amplitude E_s decays in the far zone as $1/L$. On the other hand, the incident field amplitude E_i is constant along the beam (as long as we disregard beam divergence due to diffraction). Therefore, the interference term in the definition of extinguished power appears to decay as $1/L$, viz, $Q_s \propto E_s E_i S \propto \alpha E_i^2 S/L$, where we have used the (rather general) linear relationship $E_s \propto \alpha E_i$. Here α can be interpreted as the dipole polarizability of the particle, but can also have a more general meaning within the T-matrix scattering formalism. In any event, as long as E_i and S do not depend on L, the extinguished power appears to decay as $1/L$. On the other hand, the scattered power Q_s can be computed by integrating the energy flux over the large sphere. Since there is no interference on most of this spherical surface, we can estimate $Q_s \propto 4\pi L^2 |E_s|^2 \propto |\alpha|^2 |E_i|^2$. As one could expect, the scattered power is independent of the radius of the sphere, L, on which the scattered energy flux is integrated. However, the *extinguished* power seems to depend on L, and goes to zero when $L \to \infty$, which clearly contradicts energy conservation.

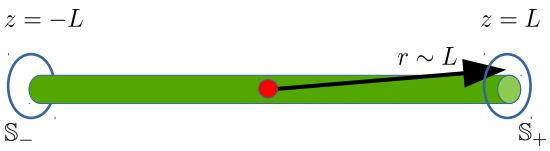

Figure 1: Illustration of the paradox involving extinction of a perfectly collimated beam by a small particle.

It is tempting to say that the reasoning above is wrong because there are no perfectly collimated beams in nature; all beams experience divergence. Therefore the interaction areas $\mathbb{S}_{\pm}$ are not independent of L; they must effectively grow with L to cancel the $1/L$ factor in the scattered field. However, this explanation is insufficient. Just like in the case of the classical extinction paradox, the resolution of the above contradiction lies not in account for diffraction but in the nature and properties of the interference term itself. In the talk, I will show the resolution of the above paradox, which will confirm the physical relevance of the extinguished power for the case of narrowly collimated beams. The talk will be based on the recent publication [5].

References

[1] L. Brillouin. The scattering cross section of spheres for electromagnetic waves. *J. Appl. Phys.*, 20:1110–1125, 1949.

[2] W. Zakowicz. On the extinction paradox. *Acta Physica Polonica A*, 101:369–385, 2002.

[3] H. M. Lai, W. Y. Wong, and W. H. Wong. Extinction paradox and actual power scattered in light beam scattering: a two-dimensional study. *J. Opt. Soc. Am. A*, 21:2324–2333, 2004.

[4] M. J. Berg, C. M. Sorensen, and A. Chakrabarti. A new explanation of the extinction paradox. *J. Quant. Spectrosc. Radiat. Transfer*, 112:1170–1181, 2011.

[5] V. A. Markel. What is extinction? operational definition of the extinguished power for plane waves and collimated beams. *J. Quant. Spectrosc. Radiat. Transfer*, 246:106933, 2020.

The coherent electromagnetic field and the effect of the pair distribution function

Magnus Gustavsson[1], Gerhard Kristensson[2,*], and Niklas Wellander[1]

[1] *Swedish Defence Research Agency, FOI, SE-581 11 Linköping, Sweden*
[2] *Department of Electrical and Information Technology, Lund University, P.O. Box 118, SE-221 00 Lund, Sweden*
[*] *corresponding author's e-mail: gerhard.kristensson@eit.lth.se*

1 Theory and results

The coherent (ensemble average) transmitted and reflected fields from a particulate slab are most commonly computed by the effective wavenumber approach, see *e.g.* [5]. The effective wave number is obtained from the roots of a determinant relation. An alternative method, presented in [1], solves the coherent transmitted and reflected fields from a particulate slab by solving a system of integral equations in the depth variable. We let a plane wave impinge at normal incidence on the slab, $z \in [0,d]$, containing spherical dielectric particles of radius a. The scattered fields (ensemble average) on either side of the slab, $[z_1,z_2]=[a,d-a]$, are

$$\boldsymbol{E}_{\mathrm{s}}^{\pm}(\boldsymbol{r}) = \frac{3f}{2(ka)^3}\sum_n \mathrm{i}^{-l+\tau-1}\boldsymbol{A}_n(\pm\hat{\boldsymbol{z}})k\int_{z_1}^{z_2}\mathrm{e}^{\pm\mathrm{i}kz'}f_n(z')\,\mathrm{d}z'\mathrm{e}^{\pm\mathrm{i}kz}, \quad \begin{cases} z>d \\ z<0 \end{cases}$$

The summation is over the multi-index $n=\{\tau,\sigma,m,l\}$, $\tau=1,2$, $\sigma=\mathrm{e},\mathrm{o}$, $m=0,1,2,\ldots,l$, and $l=1,2,3\ldots$, and $\boldsymbol{A}_n(\hat{\boldsymbol{k}}_{\mathrm{i}})$ are the vector spherical harmonics, see [3] for more details. The volume fraction of the spheres is denoted f. The coefficients $f_n(z)$ satisfies a system of linear, one-dimensional integral equations in z [1], *viz.*,

$$f_n(z) = \mathrm{e}^{\mathrm{i}kz}\sum_{n'}T_{nn'}a_{n'} + k\int_{z_1}^{z_2}\sum_{n'}K_{nn'}(z-z')f_{n'}(z')\,\mathrm{d}z', \quad z\in[z_1,z_2]$$

The entries of the kernel in this set of integral equations consist of rapidly oscillating integrals. Fortunately, for the hole correction (HC), these integrals have a closed form solution in terms of a series of spherical waves [2]. Without this analytic solution of the integrals, the integral equation approach offers challenging numerical integration. The particles are completely characterized by the transition matrix $T_{nn'}$, which for a spherical particle is diagonal in its (pairwise) indices. The expansion coefficients of the plane wave in terms of regular spherical vector waves are denoted a_n, see [3].

The hole correction — an adequate approximation for gases and other tenuous media – gives less accurate results for *e.g.*, liquids or other amorphous materials. In this paper, we analyse the effect of the Percus-Yevick (P-Y) approximation of the pair distribution function on the transmitted and reflected fields [4]. This P-Y approximation enlarges the scope of the integral equation approach considerably, and we compare the effect of the P-Y approximation on reflection and transmission from a particulate slab of finite thickness. The kernel entries now include integrals with rapidly oscillating integrands, but, due to the form of the P-Y approximation, the integration interval is accurately approximated by a finite interval, which makes numerical integration feasible.

References

[1] G. Kristensson. Coherent scattering by a collection of randomly located obstacles — an alternative integral equation formulation. *J. Quant. Spectrosc. Radiat. Transfer*, **164**, 97–108, 2015.

[2] G. Kristensson. Evaluation of some integrals relevant to multiple scattering by randomly distributed obstacles. *Journal of Mathematical Analysis and Applications*, **432**(1), 324–337, 2015.

[3] G. Kristensson. *Scattering of Electromagnetic Waves by Obstacles*. Mario Boella Series on Electromagnetism in Information and Communication. SciTech Publishing, Edison, NJ, USA, 2016.

[4] J. K. Percus and G. J. Yevick. Analysis of classical statistical mechanics by means of collective coordinates. *Phys. Rev.*, **110**(1), 1, 1958.

[5] L. Tsang and J. A. Kong. *Scattering of Electromagnetic Waves: Advanced Topics*. John Wiley & Sons, New York, NY, 2001.

Monitoring of Color in Comet 29P/Schwassmann-Wachmann 1

A. Voitko[1,*], E. Zubko[2], O. Ivanova[3,4,5], Igor Luk'yanyk[5], A. Kochergin[6,7], M. Husárik[3], G. Videen[2,8]

[1]*Department of Theoretical Physics and Astrophysics, Institute of Physics, Faculty of Sciences, P. J. Safarik University, Slovak Republic*
[2]*Humanitas College, Kyung Hee University, South Korea*
[3]*Astronomical Institute of the Slovak Academy of Sciences, Slovak Republic*
[4]*Main Astronomical Observatory of National Academy of Sciences, Ukraine*
[5]*Astronomical Observatory, Taras Shevchenko National University of Kyiv, Ukraine*
[6]*Far Eastern Federal University, Russia*
[7]*Institute of Applied Astronomy of Russian Academy of Science, Russia*
[8]*Space Science Institute, Colorado, USA*
[*]*corresponding author's e-mail: a.voitko@onu.edu.ua*

Introduction

Comet 29P/Schwassmann-Wachmann 1 (hereafter 29P/S-W) is presumably a transient object from the *Kuiper Belt* to the *Jupiter-family comets*, orbiting around the Sun between 5.7 au and 6.3 au. Comet 29P/S-W currently is also a member of the *Centaurs family*. Its relatively large nucleus, ~60 km, is almost permanently active over its entire period of observations since its discovery in 1927 (e.g., [1] for review). We present results of monitoring the photometric color in Comet 29P/S-W in August and October of 2018. These observations were aimed at improving our understanding of the microphysics of the dust population of its coma. We also were searching for possible day-to-day variations of the color in the inner coma as such variations have been reported earlier for other comets [2, 3].

Results

We measure the photometric color in the inner coma of Comet 29P/S-W on nine nights in August and October, 2018, using the 61-cm telescope at the Skalnaté Pleso (IAU Code – 056) that is equipped the *V* and *R* broadband filters from the Johnson-Cousins photometric system. We see variations in the color slope S' from $S' = (19.72 \pm 1.72)\%$ per 0.1 μm to $S' = -(6.88 \pm 1.72)\%$ per 0.1 μm. The blue color is accompanied with increasing brightness suggesting that it is caused by mild outburst activity. We model the extreme values of the color slope using *agglomerated debris particles*. The reddest color suggests a coma dominated by Fe-Mg silicate particles or organic particles obeying a power-law size distribution with power index $n \approx 2.6 \pm 0.3$. Such particles appear in good accordance with previous photometric study of 29P/S-W [4]. The bluest color is indicative of a high abundance of either water-ice having a power index is $n \leq 2$ or Mg-rich silicate particles having $n \approx 2.5 \pm 0.3$.

References

[1] R. Miles, G.A. Faillace, S. Mottola, et al. *Anatomy of outbursts and quiescent activity of Comet 29P/Schwassmann-Wachmann*. Icarus, 272:327–355, 2016.
[2] O. Ivanova, E. Zubko, G. Videen, et al. *Colour variations of Comet C/2013 UQ4 (Catalina)*. Mon. Not. Roy. Astron. Soc., 469:2695–2703, 2017.
[3] I.V. Luk'yanyk, E. Zubko, M. Husárik, et al. *Rapid variations of dust colour in comet 41P/Tuttle-Giacobini-Kresák*. Mon. Not. Roy. Astron. Soc., 485:4013–4023, 2019.
[4] E. Picazzio, I.V. Luk'yanyk, O.V. Ivanova, et al. *Comet 29P/Schwassmann-Wachmann 1 dust environment from photometric observation at the SOAR Telescope*. Icarus, 319: 58–67, 2019.

Design of a multi-angle light scattering setup covering the whole scattering angle range (0.32° to 177.6°) and interpretation of light scattering data under Q-space analysis.

Prakash Gautam[a], Justin B. Maughan, and Christopher M. Sorensen[*]

Department of Physics, Kansas State University, Manhattan, KS 66506, USA

[a] Presenting author (pgautam@ksu.edu)

We designed and built a laboratory light scattering apparatus for aerosols based on a novel optical scheme covering the scattering angle range $0.32° \leq \theta \leq 177.6°$, an extreme forward to the backscattering regime, involving 46 angles. The apparatus allows for a quick and efficient procurement of data, ensuring the elimination of the effects of possible in-homogenous of the aerosols. The experimentally observed scattered intensity is plotted in terms of scattering wave vector q on a double logarithmic scale, i.e., Q-space analysis, in addition to the conventional linear plot versus θ. Scattering data for hematite (Fe_2O_3) aggregates and molybdenum disulfide (MoS_2) particles, both having large real and imaginary part of the refractive index, were plotted under Q-space analysis that uncovered an extended Guinier regime with two Guinier crossovers for hematite and a single regime for MoS_2 particles, consistent with the microscopic pictures. The hematite showed an anomalous enhanced backscattering [1, 2]. In addition, scattering data we will be presented for irregularly shaped Al_2O_3 abrasive and Arizona road dust particles for whole scattering angle range with an emphasis on the backscattering regime.

References

[1] Gautam P, Sorensen CM. A light-scattering study of highly refractive, irregularly shaped MoS2 particles. Journal of Quantitative Spectroscopy and Radiative Transfer 2020;242:106757. https://doi.org/10.1016/j.jqsrt.2019.106757.

[2] Gautam P, Maughan JB, Ilavsky J, Sorensen CM. Light Scattering Study of Highly Absorptive, Non-fractal, Hematite Aggregates. Journal of Quantitative Spectroscopy and Radiative Transfer 2020:106919. https://doi.org/10.1016/j.jqsrt.2020.106919.

Preferred mode of presentation: Oral Presentation

Near-field radiative heat transfer between particles modeled by the discrete system Green's function method

L. Walter[1] and M. Francoeur[1,*]

[1]*University of Utah, Department of Mechanical Engineering*
[*]*mfrancoeur@mech.utah.edu*

Abstract

A novel computational method for modeling near-field radiative heat transfer, called the discrete system Green's function (DSGF) method, is presented. Based in fluctuational electrodynamics, the paradigm in which stochastic thermal source currents are inserted into Maxwell's equations, the DSGF method is a volume integral approach similar to the discrete dipole approximation for light scattering applications [1, 2]. As such, this method necessitates the discretization of thermal objects into a lattice of cubic subvolumes and may be applied to any arbitrary, three-dimensional geometry. Due to the stochastic nature of the thermal systems under study, however, previous computational techniques for near-field radiative heat transfer required explicit calculation of the inverse of a large $3N$-by-$3N$ interaction matrix, where N is the number of cubic subvolumes into which the thermal objects are discretized [3]. The DSGF method overcomes this limitation through rearrangement of system equations into a deterministic, linear form in which the system Green's function is directly computed. Here, this method is first verified against the analytical solution of near-field radiative heat transfer between perfect spheres of variable radii and separation distance and is then applied to systems of non-spherical particles of variable separation distance and geometric distortion. Regimes of applicability are determined for models which include geometric distortion, perfect spheres, and dipole approximations. This work is the first to consider geometric distortion in near-field radiative heat transfer between particles, and thus many open questions remain on the topic.

References

[1] B. T. Draine and P. J. Flatau. *Discrete-dipole approximation for scattering calculations*. J. Opt. Soc. Am. A, 11:1491–1499, 1994.

[2] M. A. Yurkin and A. G. Hoekstra. *The discrete dipole approximation: An overview and recent developments.* J. Quant. Spectrosc. Radiat. Transf., 106:558–589, 2007.

[3] S. Edalatpour, M. Čuma, T. Trueax, R. Backman, and M. Francoeur. *Convergence analysis of the thermal discrete dipole approximation*. Phys. Rev. E, 91:063307, 2015.

Deep Learning for Fast Transmittance Parameterization

P. G. Stegmann[1,2,*] and B. T. Johnson[1,2]

[1] *Joint Center for Satellite Data Assimilation, College Park MD, USA*
[2] *NOAA Center for Weather and Climate Prediction, College Park MD, USA*
[*] *corresponding author's e-mail: stegmann@ucar.edu*

Background

Applications such as satellite radiance data assimilation in operational numerical weather prediction and satellite instrument retrievals require fast radiative transfer models as a so-called *forward operator*. A crucial element of such a solver is a fast parameterization of the gaseous transmittance and its dependence on atmospheric pressure, temperature, and absorber concentrations, amongst other things. The major difficulty in this case arises from the need to accurately compute the transmittance at *instrument resolution*, making a costly convolution over a finite spectral interval necessary. In this work, deep learning neural networks [1] are investigated as a possible method for such a fast regression model.

Theory and Results

Following Rodgers [2], a simple example for the numerical solution of the clear-sky radiative transfer equation in the one-dimensional case may look like Eq. 1:

$$I_n = I_0 \cdot \mathcal{T}_0 + \sum_1^n \bar{B}_i \cdot (\mathcal{T}_i - \mathcal{T}_{i-1}) \,, \tag{1}$$

with I_n being the spectral radiance at the top of the atmospher (TOA) level n, $\mathcal{T}_i$ being the spectral level-to-TOA transmittance at level i, and $\bar{B}_i$ being the constant spectral Planck function value within each layer i. Deep learning neural networks have been shown to be universal function approximators and consequently they may also be used to approximate the $\mathcal{T}_i$ array for the solution of Eq. 1. The principal validity of the deep learning approach is demonstrated in Figure 1a, where a minimal hidden layer network is used to approximate a simple nonlinear cosine function, together with its sine derivative. The derivative is obtained via automatic differentiation of the network and accurately follows the finite difference validation result. Figure 1b demonstrates the application of a hidden-layer neural network to approximate the normalized spectral transmittance and shows the relative difference of the neural network transmittance towards the training data that was obtained from accurate line-by-line calculations.

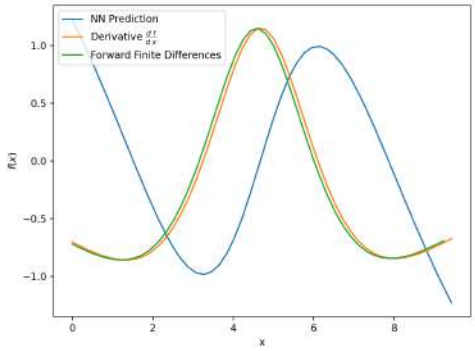

(a) Simple approximation of a cosine function and its sine derivative.

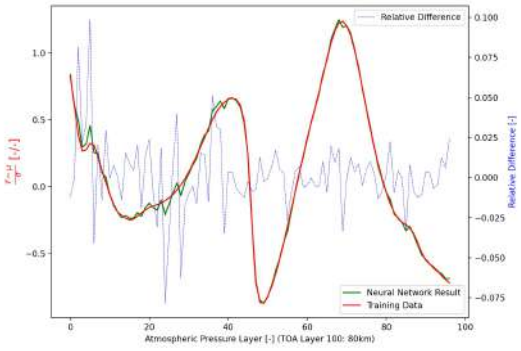

(b) Comparison between normalized transmittance from line-by-line calculations and a neural network.

Figure 1: Neural networks for approximating functional relationships by reformulating them as a statistical problem.

References

[1] Y. LeCun, Y. Bengio, and G. Hilton *Deep Learning* Nature 521:436-444, 2015.
[2] Clive D. Rodgers *Inverse Methods for Atmospheric Remote Sensing*. World Scientific Publishing, Singapore, 2000.

Active remote sensing of atmospheric dust through expansion of the Umov law

E. Zubko[1,*], K. Shmirko[2,3], A. Pavlov[3], W. Sun[1,4], G. Schuster[5], Y. Hu[5], S. Stamnes[5], A. Omar[5], R.R. Baize[5], M.P. McCormick[6], R. Loughman[6], J.A. Arnold[7], G. Videen[1,7,8]

[1]*Humanitas College, Kyung Hee University, South Korea*
[2]*Far Eastern Federal University, Russia*
[3]*Institute of Automation and Control Processes, Far Eastern Branch of Russian Academy of Science, Russia*
[4]*Science Systems and Applications Inc, Virginia, USA*
[5]*NASA Langley Research Center, Virginia, USA*
[6]*Department of Atmospheric and Planetary Sciences, Hampton University, Virginia, USA*
[7]*US Army Research Lab, Maryland, USA*
[8]*Space Science Institute, Colorado, USA*
[*]*corresponding author's e-mail: evgenij.s.zubko@gmail.com*

The Umov law in its classic form

The Umov law describes qualitatively an inverse correlation between the reflectivity of a target surface and the maximum value of the linear polarization that initially unpolarized incident light acquires when scattered from that surface. The utility of the Umov law lies in the possibility to infer the reflectance of a target whose size is insufficiently large to be resolved spatially with an optical system. It has been recently demonstrated that the Umov law holds in micron-sized irregularly shaped particles [1,2]. However, the Umov law, in its classic form, suggests illumination of a target by unpolarized radiation, like sunlight, that is suitable for passive remote sensing. We expand on the Umov law for the case of active remote sensing, which is based on scattering of fully polarized radiation initially emitted by a lidar or radar.

Expansion for the case of active remote sensing

Depolarization of fully linearly or circularly polarized light in the backscattering is characterized with the linear depolarization ratio μ_L and circular depolarization ratio μ_C; see, their definitions, e.g., in [3]. We explore different ways to describe the correlation between the depolarization ratios and geometric albedo A. The relation between μ_L or μ_C and $\log(A)$ takes on a form that is mostly linear and, hence, can be approximated with the simple equation: $\log(A) = a \times \mu - b$; see [3], for specific values of constants a and b. However, simple linear relations allow for rapidly constraining the average reflectivity of target particles based on the strength of the lidar/radar depolarization ratios of incident fully polarized electromagnetic radiation.

References

[1] E. Zubko, G. Videen, N. Zubko, and Yu. Shkuratov. *Reflectance of micron-sized dust particles retrieved with the Umov law*. J. Quant. Spectrosc. Radiat. Transfer, 190:1–6, 2017.

[2] E. Zubko, G. Videen, N. Zubko, and Yu. Shkuratov. *The Umov effect in application to an optically thin two-component cloud of cosmic dust*. Mon. Not. Roy. Astron. Soc., 477:4866–4873, 2018.

[3] E. Zubko, K. Shmirko, A. Pavlov, W. Sun, et al. *Active remote sensing of atmospheric dust using relationships between their depolarization ratios and reflectivity*. Opt. Lett., *in press*, https://doi.org/10.1364/OL.426584, 2021.

How much is enough? The convergence of finite sample scattering properties to those of infinite media

A. Penttilä[1,*], J. Markkanen[1,2], T. Väisänen[1], J. Räbinä[1,3], M.A. Yurkin[4,5], and K. Muinonen[1,6]

[1] *Department Physics, University of Helsinki, Finland.*
[2] *Max Planck Institute for Solar System Research, Göttingen, Germany.*
[3] *Faculty of Information Technology, University of Jyväskylä, Finland.*
[4] *Voevodsky Institute of Chemical Kinetics and Combustion, SB RAS, Novosibirsk, Russia.*
[5] *Novosibirsk State University, Russia.*
[6] *Finnish Geospatial Research Institute FGI, National Land Survey, Kirkkonummi, Finland.*
[*] *corresponding author's e-mail: antti.i.penttila@helsinki.fi*

Introduction

We study the scattering properties of a cloud of particles. The particles are spherical, close to the incident wavelength in size, have a high albedo, and are randomly packed to 20 % volume density. We show, using both numerically exact methods for solving the Maxwell equations and radiative-transfer-approximation methods, that the scattering properties of the cloud converge after about ten million particles in the system. After that, the backward-scattered properties of the system should estimate the properties of a macroscopic, practically infinite system.

Results

According to our results, it seems that for this particular problem, the scattering properties of the system start to converge at about 10^7 particles or at the circumscribing volume size parameter of 650, see Fig. 1. On one hand, this result is unique to this particular scattering target. On the other hand, the individual particles are close to the wavelength size ($x = 1.76$), which means that they are efficient scatterers. Furthermore, there is almost no absorption in the system, the single-scattering albedo of the single sphere in the system is $\varpi = 0.999374$. Thus, one can expect excessive multiple scattering for this system. With less multiple scattering or with smaller single-scattering albedos, the convergence might be achieved earlier. That is why we conclude that a system with 10 million particles with sizes in the wavelength range can be considered to have the scattering properties in the backward-reflected hemisphere of a macroscopic system. The full results can be found from Penttilä et al. (2021) [1].

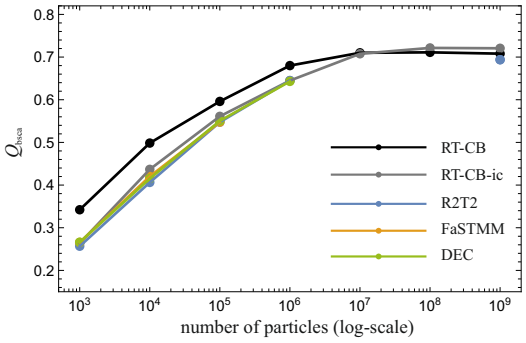

Figure 1: The backscattering hemisphere scattering efficiency Q_{bcsa} as a function of the target size, expressed as the number of the particles in the cloud. The Q_{bcsa} is shown here for five methods, of which the FaSTMM and DEC rigorously solve the macroscopic Maxwell equations, and the RT-CB, RT-CB-ic, and $\mathrm{R^2T^2}$ are based on the radiative transfer approximation.

References

[1] A. Penttilä, J. Markkanen, T. Väisänen, J. Räbinä, M. A. Yurkin, and K. Muinonen *How much is enough? The convergence of finite sample scattering properties to those of infinite media.* J. Quant. Spectrosc. Radiat. Transfer, 262, 2021.

Infrared emissions from Circumstellar core mantle dust grains

C.V.Pandya[1,*] and D.B. Vaidya[1,2]

[1] Physics Department M..G.Science Institute , Navarangpura , Ahmedabad 380 009. India.

[2] *Ex-Department of physics , Gujarat College, Ahmedabad 360 006. India.*

[*] *corresponding author's e-mail:cvpandya@gmail.com*

Abstract

As suggested by Greenberg (1989) evolution of silicate indicates that there is no separate silicate in the interstellar medium. It either exists as core mantle composition or as carbonaceous material .We studied the effects of variation in mantle thickness on the emission properties from circumstellar dust made up of host spherical silicate core and mantle of H_2O ice , in the spectral region of 5.0-25.0 μm. We calculated the absorption efficiencies of the core mantle grain using Mie-Guttler formula, for the core mantle grains of different mental thicknesses , the infrared fluxes are calculated and variations in 10 micron emission features are specifically studied at several dust temperatures . On comparing our model data and IRAS observed data , we found the change in the peak absorption wavelength at 10 μm for different mantle thicknesses , the results for core mantle grain with mantle thickness of 0.01 μm fit fairly well with the observed infrared data of the circumstellar dust . The silicate feature ratio , given by the ratio of the fluxes at 18 μm to 10 μm match very well with the observed curve. Our results clearly show the variation in peak absorption wavelengths at 10 μm with variation of mantle thickness .The theoretical model suggested here requires comparison with circumstellar dust around a few more stars.

References

[1] Greenberg JM In: IAU symposium 135. Dordrecht : Kulwer Academic publishers : 1989.

Metal-enhanced fluorescence: Stronger than we thought

Ilia L. Rasskazov[1,*], Alexander Moroz[2], and P. Scott Carney[1]

[1] *The Institute of Optics, University of Rochester, Rochester, NY 14627, USA*
[2] *Wave-scattering.com (e-mail: wavescattering@yahoo.com)*
[*] *Corresponding author: irasskaz@ur.rochester.edu*

The potential for plasmonic nanostructures to enhance fluorescence emission has been long studied. Collective electron oscillations on the surface of a plasmonic nanostructure can generate a strong local electric field, $\mathbf{E}$. The enhancement of the field boosts the excitation rate, $\gamma_{\rm exc}$ ($\propto |\mathbf{E}|^2$), of a fluorophore. At the same time, reducing the distance of a fluorophore from a metal nanostructure opens dissipative channels which diminish the quantum yield, q, and negatively affect fluorescence. An optimal *averaged* fluorescence enhancement factor,

$$\bar{F} = \frac{\gamma_{\rm exc}}{\gamma_{\rm exc;0}} \times \frac{q}{q_0} = \frac{\gamma_{\rm exc}}{\gamma_{\rm exc;0}} \times \frac{\Gamma_{\rm rad}/\Gamma_{\rm rad;0}}{\Gamma_{\rm rad}/\Gamma_{\rm rad;0} + \Gamma_{\rm nrad}/\Gamma_{\rm rad;0} + (1-q_0)/q_0} \frac{1}{q_0}, \tag{1}$$

requires a delicate balance of $\gamma_{\rm exc}$ and the radiative, $\Gamma_{\rm rad}$, and nonradiative, $\Gamma_{\rm nrad}$, decay rates. Here the subscript "0" indicates the respective quantity in the free space, and q_0 is the intrinsic quantum yield. $\Gamma_{\rm rad}$ is determined by the local density of states, whereas $\Gamma_{\rm nrad}$ is determined by metal losses. Assuming randomly oriented emitters, the decay rates in (1) are averaged over dipole orientation as $\Gamma_{\rm nrad;rad} = (\Gamma^{\perp}_{\rm nrad;rad} + 2\Gamma^{\parallel}_{\rm nrad;rad})/3$, where the superscripts "$\parallel$" and "$\perp$" denote the perpendicular (radial) and parallel (tangential) dipole orientation relative to the surface of plasmonic nanostructure. The excitation rate in (1) is *averaged* over the particle surface: $\gamma_{\rm exc} \propto \langle |\mathbf{E}|^2 \rangle$ [1].

Metal-dielectric core-shell nanoparticles offer an opportunity to engineer environments where the various competing considerations described above are in balance, or optimized for particular applications. Previous attempts to simultaneously consider all the factors in Eq. (1) were largely guided by the paradigm of *metal-enhanced fluorescence* (MEF) [2]. The usual assumption in MEF is that there is some optimal distance from a metallic surface where $\bar{F}$ attains its maximum. This arises because, by approaching a metal surface, $\Gamma_{\rm rad}$ begins to increase sooner but $\Gamma_{\rm nrad}$ increases faster. It has been assumed unproductive to decrease plasmon coupling between the metal and fluorophore by increasing emitter separation from a metal surface by more than a couple of tens of nanometers. Therefore, previous studies have limited shell thickness, t_s, to $t_s \leq 30$ nm, yielding for Au@dielectric core-shells a maximum achievable averaged $\bar{F} \approx 9$ (≈ 70 for Ag core) for shell refractive index $n_s \leq 2$ [3].

Here, we show that by extending the parameter range for the core radius, r_c, and, importantly, the shell thickness, t_s, well beyond that suggested by MEF reasoning, one can obtain $\bar{F}$ of at least two orders of magnitude larger than for the MEF range, with experimentally feasible designs using common fluorophores. By searching more than $4 \cdot 10^6$ configurations of core-shell Au@dielectric nanoparticles, we observed configurations with average fluorescence enhancement as high as $\gtrsim 3000$ on the shell surface or in its interior. Actual fluorescence enhancements can be increased further by taking advantage of hot spots. Surprisingly, the extraordinary values of $\bar{F}$ were obtained for conventional metal@dielectric core-shell nanoparticles, without any need of a fancy nontrivial shape, such as bowtie nanoantenna or a nanocube. Our results suggest a paradigm shift from the conventional metal-enhanced fluorescence, wherein the metal is becoming an auxiliary rather than determinative constituent. Our results have immediate applications in biological sensing, lasing, cell tagging, and suggest upconversion enhancements of $\gtrsim 10^6$.

References

[1] I. L. Rasskazov, A. Moroz, and P. S. Carney *Electromagnetic energy in multilayered spherical particles.* J Opt. Soc. Am. A, 36(9): 1591–1601, 2019.

[2] J. R. Lakowicz, K. Ray, M. Chowdhury, H. Szmacinski, Y. Fu, J. Zhang, and K. Nowaczyk *Plasmon-controlled fluorescence: a new paradigm in fluorescence spectroscopy.* Analyst. 133(10): 1308–1346, 2008.

[3] S. Sun, I. L. Rasskazov, P. S. Carney, T. Zhang, and A. Moroz *Critical role of shell in enhanced fluorescence of metal-dielectric core-shell nanoparticles.* J. Phys. Chem. C. 124(24): 13365–13373, 2020

Polarization of the near-Earth asteroid (52768) 1998 OR2

M. Zheltobryukhov[1,*] E. Zubko[2], E. Chornaya[1,3], A. Kochergin[1,3], G. Kornienko[1], G. Videen[2,4]

[1]*Institute of Applied Astronomy of RAS, 10 Kutuzova Emb., Saint-Petersburg 191187, Russia*
[2]*Humanitas College, Kyung Hee University, 1732, Deogyeong-daero, Giheung-gu, Yongin-do 17104, South Korea*
[3]*School of Natural Sciences, Far Eastern Federal University, 8 Sukhanova St., Vladivostok 690950, Russia*
[4]*Space Science Institute, 4750 Walnut Street, Boulder Suite 205, CO 80301, USA*
[*]*corresponding author's e-mail: maxim.s.zheltobryukhov@gmail.com*

Introduction and Observational Technique

Polarimetry is an effective method to characterize the microphysics of asteroid regolith. However, the vast majority of asteroids appear in ground-based observations at small phase angles. As a consequence, ground-based polarimetric observations predominantly address the phenomenon of negative polarization in asteroids (e.g., [1]) due to their large heliocentric distance; whereas, the branch of positive polarization at side scattering is accessible only on their close encounter with Earth. We use a rare occasion of the close approach of asteroid (52768) 1998 OR2 in April of 2020 to constrain the amplitude of its positive polarization.

Between April 10 and 27, 2020, we measured the degree of linear polarization of asteroid 1998 OR2 using a 0.5m telescope (F = 1.62 m) of the Ussuriysk Astrophysical Observatory, a division of the Institute of Applied Astronomy of RAS (code C15). This telescope was equipped with a commercially available CCD detector SBIG STX–16803 (resolution — 4096×4096, size of pixel — 9 μm), the V filter of the standard Johnson photometric system (efficient wavelength λ_{eff} = 0.551 μm and bandpass $\Delta\lambda$ = 0.088 μm), and a dichroic polarization filter (analyzer). The analyzer is rotated through three fixed position angles 0°, +60°, and +120°, which allows a complete characterization of the degree of linear polarization as described in [2]. During our observations, the phase angle of the asteroid spanned the range from α = 57.6° to 77.6°.

Results

The largest value of the degree of linear polarization P of asteroid 1998 OR2 registered in our observations was P = (14.42 ± 0.41)%. It is considerably lower compared to dark asteroids. For instance, at a similar phase angle (~77°), the F-type asteroid (3200) Phaethon reveals P in excess of 25% [3]. On the other hand, the polarization of the S-type asteroid (4179) Toutatis appears to be half lower compared to asteroid 1998 OR2 [4]. It is worth noting that the amplitude of positive polarization of regolith inversely correlates with its geometric albedo [4], suggesting that the reflectivity of asteroid 1998 OR2 is greater than in (3200) Phaethon, but somewhat lower than in (4179) Toutatis. Using the Umov effect, i.e., an inverse correlation between polarization maximum P_{max} and the geometric albedo A in asteroids [3], we estimate reflectivity of asteroid 1998 OR2.

References

[1] I.N. Belskaya et al. *Refining the asteroid taxonomy by polarimetric observations*. Icarus, 284:30–42, 2017.
[2] E. Chornaya et al. *Imaging polarimetry and photometry of comet 21P/Giacobini Zinner*. Icarus, 337:113471, 2020.
[3] M. Zheltobryukhov et al. *Umov effect in asteroid (3200) Phaethon*. Astron. Astrophys., 620:A179, 2018.
[4] M. Ishiguro et al. *Maximum visible polarization of 4179 Toutatis in the apparition of 1996*. Publ. Astron. Soc. Japan, 49:L31–L34, 1997.

Scattering of the shaped beam by a PEMC sphere

Huan Tang[1,*] and Ren Xian Li[1,2]

[1]*School of Physics and Optoelectronic Engineering, Xidian University, Xi'an 710071, China*
[2]*Collaborative Innovation Center of Information Sensing and Understanding, Xidian University, Xi'an 710071, China*
[*]*corresponding author's e-mail: htang_1@stu.xidian.edu.cn*

Abstract

Perfect electromagnetic conductor (PEMC) [1] material is a class of magneto-electric metamaterial, which has been researched in the optical scattering field. Unlike the perfect electric conductor (PEC) and the perfect magnetic conductor (PMC), PEMC highlights the rotary polarization effect and induces the cross-polarized [2] component. This rotary polarization effect also is called circular dichroism, it was observed originally in the study of rock crystals [3]. Other materials such as liquid crystals [4], plasma [5], and chiral materials [6] also have this characteristic. Because the cross-polarized component is induced, there is an interesting phenomenon that the optical scattering field is divided into two parts--co-polarized and cross-polarized components. Not only co-polarized but only cross-polarized components contribute to the scattering field when PEMC interacts with the arbitrary structural beam. There are great promising application prospects, such as in the biology [7], physical chemistry [8], and meteorology fields about the research of scattering field.

To study the scattering effect between PEMC and arbitrary structure beam, the extinction cross-section and scattering cross-section are discussed. The present investigation attains the exact mathematical expressions for scattering field, extinction cross-section, and scattering cross-section by the GLMT and series multi-pole expansion method [9]. Numerical results for the optical scattering field, extinction cross-section, and scattering cross-section illustrate the scattering features when PEMC is lighted by the Bessel beam. A summary and some perspectives of this work are presented in the end.

References

[1] I.V. Lindell, A.H. Sihvola, Perfect Electromagnetic Conductor, Journal of Electromagnetic Waves and Applications, 19 (2005) 861-869.

[2] Moreno, F. Cotera, S. Gonzlez, F. Saiz, J. Videen, G.. Multiple scattering by two-particle systems: statistics of the cross-polarized scattered intensity. Journal of Quantitative Spectroscopy and Radiative Transfer 2003;79-80.

[3] J.F.W. Herschel, On the Rotation Impressed by Plates of Rock Crystal on the Planes of Polarization of the Rays of Light as Connected with Certain Peculiarities in Its Crystallization, Transactions of the Cambridge Philosophical Society, 1 (1820) 43–51.

[4] H. Singh, S. Antony, R.M. Jha, Plasma-based Radar Cross Section Reduction, in: H. Singh, S. Antony, R.M. Jha (Eds.) Plasma-based Radar Cross Section Reduction, Springer Singapore, Singapore, 2016, pp. 1- 46.

[5] O.D. Lavrentovich, Liquid crystals, photonic crystals, metamaterials, and transformation optics, Proceedings of the National Academy of Sciences, 108 (2011) 5143-5144.

[6] C.F. Bohren, Light scattering by an optically active sphere, Chem. Phys. Lett., 29 (1974) 458-462.

[7] B. Ranjbar, P. Gill, Circular Dichroism Techniques: Biomolecular and Nanostructural Analyses- A Review, Chemical Biology & Drug Design, 74 (2009) 101-120.

[8] A.J. Miles, B.A. Wallace, Synchrotron radiation circular dichroism spectroscopy of proteins and applications in structural and functional genomics, Chemical Society Reviews, 35 (2006) 39-51.

[9] Mitri, F.G. Electromagnetic radiation force on a perfect electromagnetic conductor (pemc) circular cylinder. Journal of Quantitative Spectroscopy and Radiative Transfer 2019;233:21–28.

Visualization of light beaming and interference effects in random arrays of silicon nanowires: the inelastic scattering case.

Maria J. Lo Faro[1,2], G. Ruello[3], A.A. Leonardi [1,2,3], D. Morganti [1,3], A. Irrera [3], F. Priolo [1], S. Gigan [4], G. Volpe[3,5], and B. Fazio [3*].

[1] *Dipartimento di Fisica e Astronomia, Università di Catania, via S. Sofia, 64, 95123 Catania, Italy.*
[2] *CNR-IMM, Istituto per la Microelettronica e Microsistemi, via Santa Sofia 64, 95123, Catania, Italy.*
[3] *CNR-IPCF, viale F. Stagno d'Alcontres 37, Faro Superiore, 98158 Messina, Italy.*
[4] *Laboratoire Kastler Brossel, ENS-Université PSL, CNRS, Sorbonne Université, Collège de France, 24 rue Lhomond, 75005 Paris, France.*
[5] *Department of Chemistry, University College London, 20 Gordon Street, London WC1H 0AJ, UK.*
[*] *corresponding author's e-mail: barbara.fazio@cnr.it*

Abstract

Disordered photonics is a new research field that is attracting a large interest worldwide for its direct implications in concrete applications such as, for example, diagnostics [1], photovoltaics [2] and new light sources [3]. This is because the very multiple scattering nature and the light transport properties of random media allow optical performances often superior to those offered by ordered photonic structures [4]. On the other hand, the diffusive propagation of light through disordered materials gives rise to fascinating and sometimes unexpected interference phenomena surviving also in the inelastic scattering regime [5]. Here we will present recent experimental results where disordered arrays of silicon nanowires are used to generate and beam directional coherent Raman light [6]. We show the direct visualization of the weakly localized Raman radiation by both real- and momentum-space microscopy, that permitted us to gain insight on the mechanisms ruling the light transport through the random media. These results pave the way for the development of next generation of new light sources based on both the coherent control of directional beaming and the fine frequency tuning.

References

[1] J. Bertolotti, E.G. van Putten, C. Blum, A. Lagendijk, W.L. Vos, and A.P. Mosk. *Non-invasive imaging through opaque scattering layers*. Nature 491: 232-234, 2012.

[2] O. L. Muskens, J. G. Rivas, R. E. Algra, E. P. A. M. Bakkers, and A. Lagendijk, *Design of Light Scattering in Nanowire Materials for Photovoltaic Applications*, Nano Lett. 8: 2638–2642, 2008.

[3] D. S. Wiersma. *The physics and applications of random lasers*, Nat. Phys. 4: 359–367, 2008.

[4] B. Fazio, P. Artoni, M.A. Iatì, C. D'Andrea, M.J. Lo Faro, S. Del Sorbo, S. Pirotta, P.G. Gucciardi, P. Musumeci, C.S. Vasi, R. Saija, M. Galli, F. Priolo, and A. Irrera. *Strongly Enhanced Light Trapping in a Two-dimensional Silicon Nanowire Random Fractal Array*. Light: Science & Applications,5: e16062, 2016.

[5] B. Fazio, A. Irrera, S. Pirotta, C. D'Andrea, S. Del Sorbo, M.J. Lo Faro, P.G. Gucciardi, M.A. Iatì, R. Saija, M.Patrini, P. Musumeci, C.S. Vasi, D.S. Wiersma, M. Galli, and F. Priolo. *Coherent Backscattering of Raman Light*. Nature Photonics 11: 170-176, 2017.

[6] M.J. Lo Faro, G. Ruello, A.A. Leonardi, D. Morganti, A. Irrera, F. Priolo, S. Gigan, G. Volpe, and B. Fazio. *Visualization of directional beaming of weakly localized Raman from a random network of silicon nanowires*. Accepted in: Advanced Science, 2021.

Open-Source Implementation of the DDA for light scattering in an Absorbing Medium

Alexander E. Moskalensky [1,2,*] and Maxim A. Yurkin [1,2]

[1]*Voevodsky Institute of Chemical Kinetics and Combustion, SB RAS, Institutskaya str. 3, 630090 Novosibirsk, Russia*
[2]*Novosibirsk State University, Pirogova 2, 630090, Novosibirsk, Russia*
[*]*sunmosk@mail.ru*

Background

The theory of light scattering by single particles is well-developed, providing several computational methods which allow one to simulate the process with the desired accuracy. However, most publicly available codes for such computations are limited to non-absorbing host medium, the only exception being the Lorenz-Mie theory [1,2]. On the other hand, the case of absorbing medium is relevant for many practical applications, e.g., for particles submerged in water and droplets in oil.

Results

Technically, the extension of computational methods to the case of absorbing host medium implies the support of complex wavenumber $k = k' + \mathrm{i}k''$. We have implemented this support in the open-source popular discrete-dipole approximation code ADDA [3]. However, a more challenging task is to define scattering quantities such as the extinction, scattering and absorption cross-sections, preserving the physical sense at least for weakly absorbing medium. Here the physical sense means certain decoupling of particle's properties from far-field detector geometry (taken for granted for non-absorbing host medium), i.e. those two can be changed independently and later combined to calculate the detector response. One option is to use definitions based on far-field limit, but without the common attenuation factor $\exp(-2k''r)$. Such definitions are realized in the existing codes for spherical particles and can be computed by ADDA as well, resulting in perfect agreement. Moreover, the required far-field integration can be reduced to that over the particle's volume, which is faster and more natural for the DDA method. We will also discuss a meaningful definition of the extinction cross section in weakly absorbing medium, which can be used to predict the extinction by a diluted slab of particles.

References

[1] M.I. Mishchenko and P. Yang *Far-field Lorenz–Mie scattering in an absorbing host medium: Theoretical formalism and FORTRAN program.* J. Quant. Spectrosc. Radiat. Transfer 205:241–52, 2018
[2] M.I. Mishchenko, J.M. Dlugach, J.A. Lock and M.A. Yurkin *Far-field Lorenz–Mie scattering in an absorbing host medium. II: Improved stability of the numerical algorithm.* J. Quant. Spectrosc. Radiat. Transfer 217:274–7, 2018
[3] M.A. Yurkin and A.G. Hoekstra *The discrete-dipole-approximation code ADDA: capabilities and known limitations.* J. Quant. Spectrosc. Radiat. Transfer 112:2234–47, 2011

Optical properties of water-coated sea salt aerosol

F. Kanngießer[1,*] and M. Kahnert[1,2]

[1] *Chalmers University of Technology, SE-412 96, Gothenburg, Sweden*
[2] *Swedish Meteorological and Hydrological Institute, SE-601 76, Norrköping, Sweden*
[*] *corresponding author's e-mail: franz.kanngiesser@chalmers.se*

Introduction

Sea salt particles are an important part of marine aerosol, one of the most abundant types of atmospheric aerosol. Marine aerosol, of which sea salt aerosol is an important subset, affects the climate directly and indirectly, provides surfaces for chemical reactions and can corrode man-made structures. This warrants remote sensing observations of sea salt aerosol, which in turn require thorough studies of the links between microphysical and optical properties.

In a previous study, convex polyhedra, a randomised, cube-like class of model geometries, were found to provide a suitable tool for modelling the linear depolarisation ratio and the lidar ratio simultaneously [1]. To extend the convex polyhedral model for higher values of relative humidity a coating parametrisation was used, which is based on surface potential calculations and modifies a technique proposed and tested for coated soot particles [2]. Further, it was assumed, that the added water partially dissolves the salt crystal. The remaining salt crystal is coated by a saturated salt solution and becomes increasingly spherical.

The particle's overall non-sphericity is hypothesised to be a microphysical key property affecting the linear depolarisation ratio and the backscattering cross section. To test this hypothesis, superellipsoids, both homogeneous and inhomogeneous, and cube-sphere hybrids were used to calculate the optical properties for different model instances, covering the range between a cube and a sphere.

Optical calculations

Optical calculations were performed at a wavelength of $\lambda = 0.532\,\mu$m using the discrete approximation code ADDA (version 1.3b4) and the T-matrix code Tsym (version 6.6). Three different sizes were assumed for dry, uncoated particles, $r_0 = 0.33\,\mu$m, $0.67\,\mu$m, and $1.0\,\mu$m. For each size four different values of the salt volume fraction were considered $f_{\mathrm{vol}} = 1.0$, 0.8, 0.55, and 0.3. Convex polyhedra are created by placing N_c points randomly in a Cartesian coordinate system and constructing a complex hull around them. The value of N_c impacts the shape of the convex polyhedra, with intermediate values ($N_c \sim 100$) giving the best results for dry sea salt aerosol particles [1]. Five stochastical realisations of convex polyhedra for each $N_c = 50$, 100, and 250 were considered.

Results

The coated polyhedra model resulted in mean values, averaged over instances with different N_c and stochastical realisations, of the linear depolarisation ratio ranging from 0 to 0.35. With the help of homogeneous and inhomogeneous superellipsoids, and cube-sphere hybrids it is possible to reproduce the linear depolarisation ratio, the backscattering cross section, and the extinction cross section obtained by the coated polyhedra. This indicates, that the overall non-sphericity is indeed an important microphysical property affecting the optical properties. It further shows, that homogeneous and inhomogeneous superellipsoids, and cube-sphere hybrids are suitable candidates for modelling optical properties of water-coated sea salt aerosol.

References

[1] F. Kanngießer and M. Kahnert. *Modeling optical properties of non-cubical sea-salt particles.* J. Geophys. Res. Atmos., 126:e2020JD033674, 2021.
[2] H. Ishimoto, R. Kudo, and K. Adachi. *A shape model of internally mixed soot particles derived from artificial surface tension.* Atmos. Meas. Techn, 12:107-118, 2019.

Application of the Boundary Element Method to Complex Ice Aggregates to compute their Single-Scattering Properties at Microwave frequencies for all-sky data assimilation

A. Kleanthous[1], A. J. Baran[2,3,*], C. D. Westbrook[4], T. Betcke[1], and D. P. Hewett[1]

[1]*University College London, London, UK*
[2]*Met Office, Exeter, UK*
[3]*University of Hertfordshire, Hertfordshire, UK*
[4]*University of Reading, Reading, UK*
[*]*corresponding author's e-mail: anthony.baran@metoffice.gov.uk*

To advance the forecasting of the weather (NWP) and climate it is necessary to improve in those models the representations of atmospheric ice crystals in terms of their mass, area, and single-scattering properties (SSPs). To progress NWP models, all-sky data assimilation (i.e. cloud-affected radiances) of space-based infrared and microwave radiance data is becoming more commonplace. Eventually, this will also include wavelengths in the solar region. The demand for more precise ice crystal representations comes, in-part, from EUMETSAT's next generation of polar-orbiting and geostationary satellites that will be launched during 2022. In particular, the Ice Cloud Imager as part of that launch will remotely sense clouds between 183 and 664 GHz, inclusive of simultaneous V and H polarizations at some frequencies, hence the need for more accurate SSPs.

To prepare for this eventuality, the boundary element method (BEM) has been applied to randomly oriented complex rosette aggregates at the frequencies of 50, 183, 243, and 664 GHz, for the temperatures of 190, 230, and 270 K. The model rosette aggregates were generated by a Monte Carlo model [1], and the predicted aggregates were made to follow an observed mass-dimension relationship that is consistent with an NWP ice microphysics scheme. Existing microwave databases fail to satisfy this consistency demand. The resulting 65 differing rosette aggregates had maximum dimensions of between 10 and 10,000 μm. With the advent of recent matrix-solving acceleration techniques the memory costs and solution times of BEM have been reduced by 99 and 75%, respectively, this being especially so at the highest size parameters [2, 3]. The open-source Bempp [4] software was used for the simulations. Here, we show that our method to simulate random orientation requires only 14 incident waves, and up to 230 waves for the smallest and largest size parameters, respectively. Computational time is further reduced by distributing the incoming waves to different CPUs. Traditionally, other methods require many more orientations to simulate random orientation. We also present SSP comparisons against other methods and models. We discuss the implications of this work to generate SSPs across the electromagnetic spectrum.

References

[1] Westbrook, C. D., R. C. Ball, P. R. Field, and A. J. Heymsfield *Theory of growth by differential sedimentation, with application to snowflake formation.* Phys. Rev. E, 70:021403, 2004.

[2] Kleanthous, A., T. Betcke, D. P. Hewett, M. W. Scroggs, and A. J. Baran *Calderón preconditioning of PMCHWT boundary integral equations for scattering by multiple dielectric particles.* J. Quant. Spectrosc. Radiat. Transfer, 224:383-395, 2019.

[3] Kleanthous, A., T. Betcke, D. P. Hewett, P. Escapil-Inchauspé, C. Jerez-Hanckes, and A. J. Baran *Accelerated Calderón preconditioning* for *Maxwell transmission problems*. http://arxiv.org/abs/2008.04772, 2020.

[4] Śmigaj, W., T. Betcke, S. Arridge, J. Phillips, M. Schweiger *Solving boundary integral problems with BEM++.* ACM T Math Software, 41:1-40, 2015.

Depolarization and anisotropy parameters from Mueller polarimetry on three groups of barley leaves

S. Savenkov[1,*], R. Muttiah[2], Y. Oberemok[1], I. Kolomiets[1]

[1]*Taras Shevchenko National University of Kyiv, Volodymyrska 64/13, 01601 Kyiv*
[2]*Department of Civil Engineering, University of Texas-Arlington, 425 Nedderman Hall, 416 Yates St, Arlington, TX 76019*
[*]*corresponding author's e-mail: sns@univ.kiev.ua*

Polarization of electromagnetic radiation is rapidly gaining in popularity for studying the depolarization properties and states of various natural scatter scenes ranging from the atmosphere, smoke, aerosols to various plant leaves and soils.
In the paper [1] we reported the results of measuring Mueller matrices for three groups of leaf samples of common barley (*Hordeum vulgare*): *Chlorina* mutant, *Chlorina* etiolated mutant and *Cesaer* varieties. These samples differed in internal leaf structure from genetic mutation or by illumination during the growth.
The repeatability of the measurement results of Mueller matrix elements for such a complex and highly depolarising samples was demonstrated. It is shown that the barley leaves of these three groups can be identified both at forward scattering and backward scattering modes; the best results are obtained in the case of forward scattering. In both cases, the most informative matrix elements were identified. It was also shown that at backward scattering mode linear dichroism comes out, the magnitude of which increases with decreasing observation angle.
In this paper to examine separability and to clarify issues related to the mechanisms of depolarisation for these three groups of leaf samples we analyze their experimental Mueller matrices by calculating a number of single value depolarization metrics (degree of polarization, average degree of polarization, depolarization index, Q(**M**)-metric *etc.*). To obtain the anisotropic and depolarizing properties of the samples under study, the existing additive and multiplicative decompositions of their experimental Mueller matrices are used. The latter is of particular interest since the depolarization for the studied group of samples is anisotropic.
From the light intensity measurements (m_{11}), the Fresnels equations were solved for external ($n_1/n_2<1$) and internal ($n_1/n_2>1$) reflections and compared to the depolarization parameters. Additionally, a "spherical" model for distribution of charges on a photosynthetic membrane during light reactions is discussed for estimate ranges for refractive indices.
Obtained results contribute for a better understanding the process of penetration of light into the leaf and the evolutionary adaptation of the internal structures of the leaf to the absorption of light.

References

[1] S. N. Savenkov, R. S. Muttiah, Y.A. Oberemok, A.V. Priezzhev, I.S. Kolomiets, A.S. Klimov. *Measurement and interpretation of Mueller matrices of barley leaves*. Quantum Electronics, 50(1): 55–60, 2020.

Gap-enhanced Raman tags imaging for information security

Jian Ye*

School of Biomedical Engineering, Shanghai Jiao Tong University, Shanghai, 200030, P.R. China
**corresponding author's e-mail: yejian78@sjtu.edu.cn*

Anticounterfeiting labels based on physical unclonable functions (PUFs) are easy to generate but difficult to duplicate due to inherent randomness. Steganography, known as "invisible" information communication, refers to the technique of hiding information into another medium. We recently developed a new type of core-shell gap-enhanced Raman tags (GERTs), which show a number of advantages [1-2] for PUF labels and steganography: (1) large enhancement factor, detectable down to a single-nanoparticle level, leading to the super-fast readout speed with a good signal-to-noise ratio; (2) ultra-photostability under repeated readout due to the off-resonance excitation, leading to excellent reproducibility; (3) ultra-stable material properties in various environments (e.g., humid environment), resulting in a long shelf-life; (4) suitability for near-infrared (NIR) laser excitation, resulting in low Raman background from package materials.

Herein, we demonstrate a PUF label fabricated by drop-casting aqueous GERTs, high-speed read using a confocal Raman system, digitized through coarse-grained coding methods, and authenticated via pixel-by-pixel comparison [3-4]. A 3D encoding capacity of over 3×10^{15051} can be achieved for the labels composed of ten types of GERTs with a mapping resolution of 2500 pixels and quaternary encoding of Raman intensity levels at each pixel. Authentication experiments have ensured the robustness and security of the PUF system, and the practical viability is demonstrated. Such PUF labels could provide a potential platform to realize unbreakable anticounterfeiting. Secondly, Raman ink, fabricated by doping GERTs into commercial ink, is demonstrated as security ink for multiplexing steganography. The Raman ink generates distinct spectral profiles with low background from pure ink upon NIR laser irradiation. A multiplexing combination of seven kinds of messages extracted from the written stego-text is demonstrated, which adds enhanced safety and flexibility to information encoding. Therefore, GERTs-based imaging is promising for use in information security.

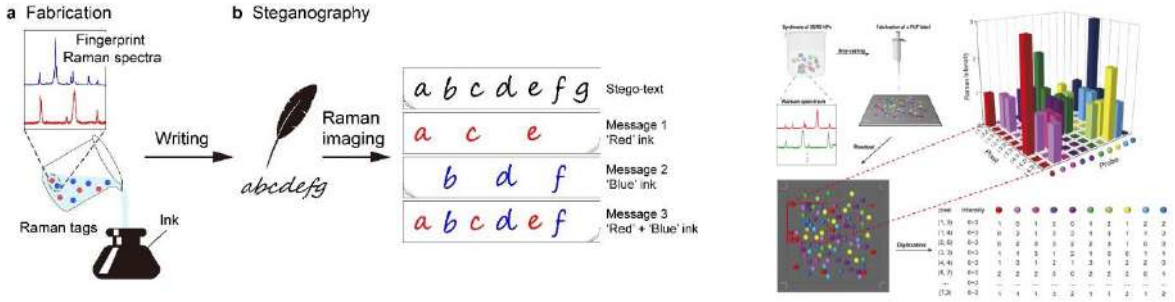

Figure 1: (Left) Schematic of Raman ink for steganography. (Right) Fabrication and encoding of Raman PUF labels.

References

[1] Lin L., et al. Ye J., 2015: *Nanooptics of plasmonic nanomatryoshkas: shrinking the size of a core–shell junction to subnanometer*. Nano Lett. 15, 6419-6428, 2015.

[2] Lin L., et al. Ye J., *Electron Transport across plasmonic molecular nanogaps interrogated with surface-enhanced Raman scattering*. ACS Nano 12, 6492-6503, 2018.

[3] Zhang Y., et al., Ye J. *Ultrabright gap-enhanced Raman tags for high-speed bioimaging*. Nat. Commun. 10, 3905, 2019.

[4] Gu Y., He C., et al., Ye J., *Gap-enhanced Raman tags for physically unclonable anticounterfeiting labels*, Nat. Commun. 11, 516, 2020.

Emission source function calculation in non-isothermal atmospheres

M. Herreras-Giralda[1,2*], P. Litivinov[1], Y. Derimian[2], O. Dubovik[2], T. Lapyonok[2], D. Fuertes[1]

[1]*GRASP-SAS, Remote sensing developments, Villeneuve d'Ascq, France*
[2]*Univ. Lille, CNRS, UMR 8518 – LOA – Laboratoire d'Optique Atmosphérique, F-59000 Lille, France*
[*]*corresponding author's e-mail: marcos.herreras@grasp-sas.com*

Thermal emission inclusion in radiative transfer equation, in general, does not represent a challenge in most of remote sensing applications. In some applications the absorption dominates over scattering and RT-equation with thermal emission is significantly simplified to be solved numerically, or sometimes analytically. For vertically inhomogeneous atmospheres in the case when both scattering and thermal absorption should be taken account, the correct vertical discretization of atmosphere can be challenging. It has to satisfy conditions for accurate calculations of both scattering and thermal emission part. The vertical discretization for scattering part depends on the extinction and phase matrix vertical profile, while the discretization for the thermal emission source function depends also on temperature vertical profile. Different methodologies to account in-layer thermal variation can be found in the literature [1][2]. This work presents an evaluation of different methodologies to obtain emission source function, its behavior under different thermal conditions and its effect on radiative transfer calculations used in atmospheric remote sensing applications. Figure 1 shows an example of the differences in source function calculations of a layer for different temperature changes through it using the exponential-in-depth [1] and linear [2] methodologies. It can be appreciated that under certain conditions the difference in radiance coming from these methodologies can reach the same level of uncertainty of the remote sensing instruments in TIR.

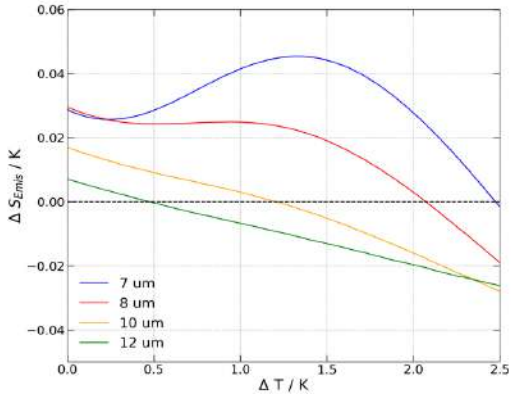

Figure 1: Difference in brightness temperature of linear and exponential-in-depth methodologies to obtain emission source function for different layer temperature variations at four wavelengths.

References

[1] Kylling, A., & Stamnes, K. (1992). Efficient yet accurate solution of the linear transport equation in the presence of internal sources: The exponential-linear-in-depth approximation. *Journal of Computational Physics*, *102*(2), 265-276, 1992.

[2] Dubuisson, P., Giraud, V., Chomette, O., Chepfer, H., & Pelon, J. (2005). Fast radiative transfer modeling for infrared imaging radiometry. *Journal of Quantitative Spectroscopy and Radiative Transfer*, *95*(2), 201-220.

Light scattering, polarization, and absorption by monolayer of spherical particles with short- and imperfect long-range spatial order

V. A. Loiko*, A. A. Miskevich, and N. A. Loiko

Stepanov Institute of Physics of the National Academy of Sciences of Belarus, Niezalezhnastsi avenue 68-2 Minsk, 220072, Belarus
* *loiko@ifanbel.bas-net.by*

A statistical method to describe coherent transmission and reflection, incoherent scattering, absorption, and polarization of light by a monolayer of homogeneous spherical particles is developed. It is based on the quasi-crystalline approximation of the theory of multiple scattering of waves and the multipole expansion of fields and the tensor Green's function in terms of the vector spherical wave functions. The method is applied to find optical characteristics of partially ordered monolayer [1] and monolayer with an imperfect lattice [2]. Spatial arrangement of particles is described by the radial distribution function [1,2]. Some calculation results for layers of SiO_2 and Ag particles are demonstrated to show the applicability of the approach [3-5].

The influence of structure parameters of a monolayer and polarization state of the incident wave on the angular distribution of light scattered by a monolayer is considered. The data for spectra of absorption, coherent transmission and reflection, and incoherent scattering coefficients are presented. The spectra of highly ordered monolayer possesses sharp resonant peaks and dips in contrast with the ones of partially ordered monolayer.

The comparison of calculated and available experimental data on spectral and angular dependences of intensity of light scattered by densely-packed monolayer with imperfect triangular lattice is fulfilled. They are in close agreement [5].

The results can be used for development and optimization of photonic crystals, metameterials, solar cells, etc.

References

[1] J. K. Percus, G. J. Yevick *Analysis of Classical Statistical Mechanics by Means of Collective Coordinates*. Phys. Rev. 110:1-13, 1958.

[2] A. A. Miskevich, V. A. Loiko *Two-dimensional planar photonic crystals: Calculation of coherent transmittance and reflectance at normal illumination under the quasicrystalline approximation*. J. Quant. Spect. Rad. Transfer, 112:1082-1089, 2011.

[3] V. A. Loiko, A. A. Miskevich *Multiple Scattering of Light in Ordered Particulate Media*. In: Kokhanovsky A (ed) Springer Series in Light Scattering Volume 1: Multiple Light Scattering, Radiative Transfer and Remote Sensing. Springer, Berlin:101-230, 2018.

[4] N. A. Loiko, A. A. Miskevich, and V. A. Loiko *Scattering of Polarized and Natural Light by a Monolayer of Spherical Homogeneous Spatially Ordered Particles under Normal Illumination*. Optics and Spectroscopy, 125:655–666, 2018.

[5] N. A. Loiko, A. A. Miskevich, and V. A. Loiko *Incoherent component of light scattered by a monolayer of spherical particles: analysis of angular distribution and absorption of light*. Journal of the Optical Society of America A. 35:108-118, 2018.

Effect of particle size on the scattering pattern of a set of forsterite samples.

O. Muñoz[1,*], E. Frattin[1,2], T. Jardiel[3], J. C. Gómez Martín[1], F. Moreno[1], J.L. Ramos[1], D. Guirado[1], M. Peiteado[3], and A.C. Caballero[3]

[1] *Instituto de Astrofísica de Andalucía, CSIC, Granada, Spain.*
[2] *Department of Physics and Astronomy G. Galilei, University of Padova, Padova, Italy.*
[3] *Instituto de Cerámica y Vidrio, CSIC, Madrid, Spain.*
[*] *corresponding author's e-mail: olga@iaa.es*

Abstract

This work is part of an experimental project devoted to disentangle size, composition and shape effects on the light scattered by clouds of randomly oriented irregular particles. In particular, we study the effect of the particles size regime on the experimental $F_{11}(\theta)$, $-F_{12}(\theta)/F_{11}(\theta)$, and $F_{22}(\theta)/F_{11}(\theta)$ curves of a set of forsterite samples. The measurements are performed at the IAA Cosmic Dust Laboratory [1] at 514 nm. The experimental curves span over the scattering angle range from 3 to 177 degrees.

The lack of control on the size distribution of top-down (grinding and sieving) approaches for synthesizing dust analogue samples has hindered a relation between photopolarimetric features and the size of the scattering grains. In this case, the size distribution production rely on processing routines from the field of functional, nano- and micro-ceramics for synthesizing well-defined narrow size distributions. A low absorbing bulk sample consisting of forsterite mm-sized pebbles has been processed to obtain five narrow size distributions spanning over a wide scattering size parameter domain, namely: Rayleigh-resonance, resonance, resonance-geometric optics, and geometric optics. The samples processing is conducted at the facilities of the Intituto de Cerámica y Vidrio that belongs to the Spanish Research Council (ICV-CSIC).

References

[1] O. Muñoz, F. Moreno, D. Guirado, J.L. Ramos, H. Volten, J.W. Hovenier. *The IAA Cosmic Dust Laboratory: experimental scattering matrices of clay particles.* Icarus, 211, 894-900: 2011.

Experimental phase function and degree of linear polarization of olivine and spinel: the effect of size.

Elisa Frattin[1,2], Olga Muñoz[1], Teresa Jardiel[3], Juan Carlos Gómez Martín[1], Fernando Moreno[1], Marco Peiteado[3], Paolo Tanga[4], Guy Libourel[4], and Alberto Cellino[5]

[1]*Instituto de Astrofísica de Andalucía, CSIC, Glorieta de la Astronomía sn, Granada 18080, Spain.*
[2]*Dipartimento di Fisica e Astronomia 'G. Galilei', University of Padova, Vicolo dell'Osservatorio 3, I-35122 Padova, Italy.*
[3]*Instituto de Cerámica y Vidrio, CSIC, C/ Kelsen 5, Campus Cantoblanco, 28049 Madrid, Spain.*
[4]*Université Cote d'Azur, Observatoire de la Cote d'Azur, CNRS, Laboratoire Lagrange UMR7293, Nice, France.*
[5]*INAF Astrophysical Observatory of Torino, Via Osservatorio 20, I-10025 Pino Torinese (TO), Italy.*
[*]*corresponding author's e-mail: elisa.frattin@unipd.it*

Polarimetric observations of dust clouds are a powerful tool in planetary science. They allow to investigate the nature and properties of solar system bodies and planetary systems in different stages of development, e.g. asteroids, comets and protoplanetary disks. For example, the relations among the polarization curve parameters and the asteroids spectral behaviour help to refine their taxonomic classification [1, 2] and are useful to identify, among asteroids, some having a possible cometary origin [3]. In order to exploit this wealth of information, we need to experimentally characterize the polarimetric curves of different materials. Physical properties of the dust, such as their refractive index, size, composition, porosity and surface structure define their capacity to scatter the light. The CODULAB facility is specifically set to measure and study the scattering matrix as a function of the scattering angle of clouds of randomly oriented cosmic dust analogues [4]. In this work, we present the experimental phase function and the degree of linear polarization of micron-sized samples and mm-sized grains of two types of material, olivine and spinel. In particular, olivine is an extensively diffuse silicate in asteroids and comets and spinel is a magnesium/aluminium mineral characteristic component of the unusual class of presumably ancient Barbarian asteroids (which includes also a couple of dynamical families) and an important component of Calcium Aluminium-rich Inclusions (CAI) found in primitive meteorites [5, 6]. We study the effect of the size on the scattering matrix elements, especially on the degree of linear polarization curve. The measurements have been obtained at 514 nm for the micron-sized samples and at 520 for the mm-sized grains. The scattering angle covers the range from 3° to 177°. We find that the behaviour of the polarization curve parameters (e.g. inversion angle, maximum and minimum of polarization) is strongly dependent on particle size.

References

[1] Belskaya I.N. et al., *Refining the asteroid taxonomy by polarimetric observations.* ICARUS, Vol. 284, pp. 30-42, 2017.
[2] López-Sisterna C. et al., *Polarimetric survey of main-belt asteroids. VII. New results for 82 main-belt objects.* A&A, Vol. 626, A42, 2019.
[3] Cellino A. et al., *Unusual polarimetric properties of (101955) Bennu: similarities with F-class asteroids and cometary bodies.* MNRAS, Vol.481, pp.L49-L53, 2018.
[4] Muñoz O. et al., *Experimental determination of scattering matrices of dust particles at visible wavelengths: The IAA light scattering apparatus.* JQSRT, Vol. 111, 187–196, 2009.
[5] Cellino A. et al., *A successful search for hidden Barbarians in the Watsonia asteroid family.* MNRAS, Vol. 439, L75-L79, 2014.
[6] Devogèle M. et al., *New polarimetric and spectroscopic evidence of anomalous enrichment in spinel-bearing calcium-aluminium-rich inclusions among L-type asteroids.* ICARUS, Vol. 304, pp. 31-57. 2018.

Scattering simulation of generalized Bessel beams by arbitrary particles

S. A. Glukhova[1,2*] and M. A. Yurkin[1,2]

[1]*Voevodsky Institute of Chemical Kinetics and Combustion, SB RAS, Institutskaya 3, 630090 Novosibirsk, Russia*
[2]*Novosibirsk State University, Pirogova 2, 630090 Novosibirsk, Russia*
[*]*corresponding author's e-mail: stefgluhova@gmail.com*

Introduction

Bessel beams are at the frontier of different types of structured light with orbital angular momentum. These beams have numerous applications in such fields as optical manipulation (tweezing), material proceeding, imaging, etc. In many physical problems it is important to take into account the scattering of Bessel beams, which is much better studied for particles with simple symmetries than for arbitrary ones. Moreover, there are a variety of existing types of Bessel beams that have been barely named [1], with neither a complete picture nor clear relations between them. In this regard, this work has two goals: the classification of various types of high-order vector Bessel beams and the development of capability to simulate scattering of any such beam by an arbitrary particle using the discrete dipole approximation.

Results

Vector Bessel beams can be presented in several different forms or types. These types differ by their polarizations, field, and energy configurations. Among them are beams with circularly symmetric energy density (CS type), with transverse electric and magnetic fields – TE and TM types, respectively, and LE and LM – beams with linear polarizations of electric and magnetic fields, respectively. In order to classify them, we developed a new description of various polarizations through the 2x2 matrix **M**, associated with the transverse Hertz vector potentials. This approach clarifies the relations between all Bessel beam types and their polarizations. Also, within this framework, we managed to relate beams of different orders using the rotation and duality operators, which action corresponds to simple transformations of the matrix **M**. We have implemented all standard Bessel beam types as well as a generalized Bessel beam specified by a matrix **M** (4 complex values) in ADDA package [2]. We successfully validated this implementation against the reference results of GLMT for spheres [3]. Currently, it is available at a separate fork of ADDA: https://github.com/stefaniagl/adda.

In conclusion, now it is easy for anyone to simulate the scattering of various Bessel beams by particles with arbitrary shape and internal structure. The obtained theoretical results clarify the general picture and relations between various types of Bessel beams. Similar considerations can potentially be applied to other complex light beams.

References

[1] J. J. Wang, T. Wriedt, J. A. Lock, and Y. C. Jiao, *General description of transverse mode Bessel beams and construction of basis Bessel fields*, J. Quant. Spectrosc. Radiat. Transf., 195:8–17, 2017.
[2] M. A. Yurkin and A. G. Hoekstra, *The discrete-dipole-approximation code ADDA: capabilities and known limitations*, J. Quant. Spectrosc. Radiat. Transf., 112:2234–2247, 2011.
[3] Z. Chen, Y. Han, Z. Cui, and X. Shi, *Scattering of a zero-order Bessel beam by a concentric sphere*, J. Opt., 16:055701, 2014.

The Umov effect in dust aggregates: Dependence on porosity

Himadri S. Das[a,*], and Ayesha M. Mazarbhuiya[a]

[a]*Department of Physics, Assam University, Silchar 788011, India*

[*]*Presenting author (hsdas13@gmail.com)*

The *Umov effect* [1] is an inverse correlation between the reflectivity (or geometric albedo) of an object and the degree of linear polarization of light scattered by it. In this work, three different types of fractal aggregates (BA, BAM1, and BAM2) having the same characteristic radius and varying porosity are considered to study the effect of porosity on geometric albedo (*A*) and the maximum value of the positive polarization (*Pmax*). The porosity of BA, BAM1, and BAM2 is taken to be 0.87, 0.74, and 0.64, respectively. Using the multisphere T-matrix code (MSTM), *Pmax* and *A* are calculated for three different aggregated structures with silicate composition and are plotted against each other in logarithmic scale to visualize the *Umov effect*. The plot shows a linear correlation between them where *Pmax* decreases significantly with an increase of *A*. It is observed that the decrease of porosity shows a decrease in *Pmax* and an increase in *A*. The present study shows that the porosity of the aggregates plays a major role in the *Pmax versus A* diagram.

References

[1] Umov, N. A., 1905: Chromatische depolarisation durch lichtzerstreung. *Phis. Zeits.* **6**, 674–676.

Preferred mode of presentation: **Oral**

Optical trapping, manipulation, and characterization of cosmic dust particles

A. Magazzù[1,*], D. Bronte Ciriza[1], P. Polimeno[1,2], A. Musolino[3], M. G. Donato[1], A. Foti[1], P. G. Gucciardi[1], M. A. Iatì[1], R. Saija[2], L. Folco[3,4], A. Rotundi[5], and O. M. Maragò[1,*]

[1]*CNR-IPCF, Istituto per i Processi Chimico-Fisici, Messina, Italy*
[2]*Dipartimento MIFT, Università di Messina, Italy*
[3] *Dipartimento di Scienze della Terra, Università di Pisa, Pisa, Italy*
[4] *CISUP, Centro per l'Integrazione della Strumentazione dell'Università di Pisa, Pisa, Italy*
[5] *Dipartimento di Scienze e Tecnologie, Universit`a di Napoli "Parthenope", Napoli, Italy*
[*]*magazzu@ipcf.cnr.it, onofrio.marago@cnr.it, webpage: spacetweezers.org*

We investigated cosmic dust samples from different meteorites by Optical Tweezers (OT) and Raman Tweezers(RT) [1, 2]. The scattered light by the trapped dust particle is analysed by a photo-detector providing information about optical forces on the trapped particle [1, 2]. This provided more accurate information to theoretical models for the calculation of radiation pressure for a variety of complex particles of astrophysical interest. Furthermore, by RT it was possible to identify minerals and organic composition of micron-sized individual meteorites fragments, having a better sight on the bench work where H_2 molecules and simple organic compounds, carbon monoxide and ammonia are produced [3]. We discuss the Raman spectra of single 3D-trapped fragments of the lunar meteorite DEW 12007, comparing the Raman peaks of our samples obtained by RT with the Raman spectra of the components of DEW 12007 found in literature [4]. The agreements of our result with the literature documents the high potential and applicability of our high-resolution spectroscopic technique for the non-destructive and contactless analyses of planetary materials [5-7]. Our results open medium term new perspectives for the investigation, in controlled laboratory conditions, of extra-terrestrial particles collected in space and brought back to Earth by space probes (e.g. from Mars, Moon, asteroids, comets) and by balloon born instruments. On a longer term frame, our efforts are addressed to space tweezers development for planetary space mission in situ applications.

We acknowledge funding from the agreement ASI-INAF n.2018-16-HH.0, project "SPACE Tweezers" and from the MSCA ITN (ETN) project "Active Matter".

References

[1] P. H. Jones, O. M. Maragò, and G. Volpe. *Optical tweezers: Principles and applications.* CUP, Cambridge, 2015
[2] P. Polimeno, A. Magazzù, M. A. Iati, F. Patti, R. Saija, C. Degli Esposti Boschi, M. G. Donato, P. G. Gucciardi, P. H. Jones, G. Volpe, and O. M. Maragò. *Optical tweezers and their applications.* JQSRT, 218, 131–150, 2018.
[3] T. J. Millar. *Dust and chemistry in astronomy.* Routledge, 2019.
[4] A. Collareta, M. D'Orazio, M. Gemelli, A. Pack, and L. Folco. *High crustal diversity preserved in thelunar meteorite mount dewitt 12007 (victoria land, antarctica)*. Meteorit. Planet. Sci.,51, 351–371, 2016.
[5] Z. Gong, Y.-L. Pan, G. Videen, C. Wang, *Optical trapping and manipulation of single particles in air: principles, technical details, and applications*. JQSRT 214, 94–119, 2018.
[6] H. Alali, Z. Gong, G. Videen, Y.-L. Pan, O. Muñoz, C. Wang. *Laser spectroscopic characterization of single extraterrestrial dust particles using optical trapping-cavity ringdown and raman spectroscopy*. JQSRT 255, 107249, 2020.
[7] P. Polimeno, A. Magazzù, M. A. Iatì, R. Saija, L. Folco, D. Bronte Ciriza, M. D. Donato, A. Foti, P. G. Gucciardi, A. Saidi, C. Cecchi-Pestellini, A. Jimenez Escobar, E. Ammannito, G. Sindoni, I. Bertini, V. Della Corte, L. Inno, A. Ciaravella, A. Rotundi, O. M. Maragò, (Space tweezers collaboration*). Optical tweezers in a dusty universe*, EPJ Plus 136, art. 339, 2021.

A Correlation-based Inversion Method for Aerosol Property Retrieval from AirMSPI and AERONET Measurements

F. Xu[1,*], T. Huang[1], D.J. Diner[2], L. Gao[1], C. Flynn[1], J. Redemann[1], and O. Dubovik[3]

[1]*School of Meteorology, The University of Oklahoma, Norman, USA*
[2]*Jet Propulsion Laboratory, California Institute of Technology, Pasadena, USA*
[3]*Université de Lille, CNRS, UMR 8518 - LOA - Laboratoire d'Optique Atmosphérique, Lille, France*

[*]*e-mail: fengxu@ou.edu*

Abstract

Aerosols present high spatial and temporal variations at global scale. At regional scale, however, such variations are associated with a finite number of prevailing aerosol types. This results in a correlation of aerosol properties that can be observed and captured by a set of dominating principal components (PC). We developed a correlation-based inversion method for aerosol property (CIMAP) retrieval [1]. Algorithm tests were performed to retrieve some airborne polarimetric measurements acquired by JPL's Airborne Multi-angle SpectroPolarimetric Imager (AirMSPI [3]) during multiple field campaigns [1], and some ground-based radiometric measurements of sky radiances and optical depths acquired by Aerosol Robotic Network (AERONET [2]) over regions including California, Beijing, and southern Africa where different types of aerosols prevail [4]. The retrieval is informed by an *a priori* PC analysis of aerosol climatology over the targeted area. PC weights and PC vector components are then adjusted during the retrieval optimization. The smoothness constraints on spatial and/or spectral variations of aerosol abundance and properties [5] are imposed on the PC quantities [1]. By using a small number of PCs, CIMAP significantly improves the efficiency of inverse and forward modeling. CIMAP retrievals are compared to the AERONET operational products, including aerosol optical depth, single scattering albedo, Ångström exponent, real and imaginary parts of the complex refractive index of aerosols, and effective radii of fine and coarse mode aerosols. The differences for all geophysical variables are found within the uncertainties of these AERONET products [6]. Given its gain of retrieval efficiency and retain of accuracy, CIMAP is promising to process a large volume of satellite data. In addition, we are interfacing CIMAP with chemical transport model or aerosol reanalysis products (such as those from ECMWF/MERRA2) to initialize *a priori* sets of PCs. This will potentially compensate for the insufficient information carried by measurements alone to resolve a large set of unknowns such as aerosol species properties, its chemical composition, etc.

References

[1] Xu F, Diner DJ, Dubovik O, and Schechner Y. A *correlated multi-pixel inversion approach for aerosol remote sensing*. Remote Sens. 11, 746 (2019).

[2] Holben B, Eck TF, Slutsker I, Tanré D, Buis JP, Setzer A, et al. *AERONET-A federated instrument network and data archive for aerosol Characterization*. Remote Sens. Environ. 66, 1-16 (1998).

[3] Diner DJ, Xu F, Garay MJ, Martonchik JV, Rheingans BE, Geier S, et al. *The Airborne Multiangle SpectroPolarimetric Imager (AirMSPI): a new tool for aerosol and cloud remote sensing*, Atmos. Meas. Tech. 6, 2007–2025 (2013).

[4] Huang T, Xu F, Gao L, Flynn C, and Dubovik. O. *A correlation-based inversion method for aerosol property (CIMAP) retrieval from AERONET Measurements*. J. Quant. Spectrosc. Radiat. Transfer. *under review*.

[5] Dubovik O, Herman M, Holdak A, Lapyonok T, Tanré D, Deuzé JL, et al. *Statistically optimized inversion algorithm for enhanced retrieval of aerosol properties from spectral multi-angle polarimetric satellite observations*. Atmos. Meas. Tech. 4, 975–1018 (2011).

[6] Dubovik O, Smirnov A, Holben BN, King MD, Kaufman YJ, Eck TF, et al. *Accuracy assessments of aerosol optical properties retrieved from Aerosol Robotic Network (AERONET) Sun and sky radiance measurements*. J. Geophys. Res. Atmos. 105, 9791-806 (2000).

Accelerating multi-angle polarimetric aerosol and ocean color retrievals for NASA's PACE mission

Meng Gao[1,2,*], Bryan A. Franz[1] , Kirk Knobelspiesse[1], Peng-Wang Zhai[3], Vanderlei Martins[3], Sharon Burton[4], Brian Cairns[5], Richard Ferrare[4], Joel Gales[1,6], Otto Hasekamp[7], Yongxiang Hu[4], Amir Ibrahim[1,2], Brent McBride[2,3], Anin Puthukkudy[3], P. Jeremy Werdell[1], and Xiaoguang Xu[3]

[1]*NASA Goddard Space Flight Center, Code 616, Greenbelt, Maryland 20771, USA*
[2]*Science Systems and Applications, Inc., Greenbelt, MD, USA*
[3]*JCET/Physics Department, University of Maryland, Baltimore County, Baltimore, MD 21250, USA*
[4]*MS 475 NASA Langley Research Center, Hampton, VA 23681-2199, USA*
[5]*NASA Goddard Institute for Space Studies, New York, NY 10025, USA*
[6]*Science Applications International Corp., Greenbelt, MD, USA*
[7]*Netherlands Institute for Space Research (SRON, NWO-I), Utrecht, The Netherlands*
**corresponding author's e-mail: meng.gao@nasa.gov*

The NASA Plankton, Aerosol, Cloud, ocean Ecosystem (PACE) mission is designed to observe the global ocean and atmosphere and provide extended data records of ocean ecology, biogeochemistry, atmospheric aerosols and clouds [1]. The instruments on PACE inlcude a hyperspectral Ocean Color Instrument (OCI) and two Multi-Angle Polarimeters (MAP): the UMBC Hyper-Angular Rainbow Polarimeter (HARP2) and the SRON Spectro-Polarimeter for Planetary EXploration one (SPEXone). To harvest the rich information content measured by these MAPs, an efficient aerosol and ocean color retrieval algorithm was developed by the PACE Project Science and Science Data Segments (SDS) teams in collaboration with the PACE Science and Applications Team (SAT) and instrument teams[2]. The algorithm, called FastMAPOL, is based on a coupled atmosphere and ocean radiative transfer forward model. To achieve high accuracy and speed for operational processing, deep learning techniques were incoporated into the development of the forward model, Jacobian matrix, and atmospheric correction procedures. The retrieval uncertainties of aerosol optical and microphysical properties are evaluated with respect to various aerosol loadings and ocean surface properties. The impacts of the aerosol properties on water leaving reflectance retrieval are also evaluated. Data products produced from this algorithm from AirHARP measurements during the ACEPOL field campaign had acceptable errors compared with HSRL and AERONET data products [3]. The algorithm and associated experience will be useful for efficient processing the large volume of polarimetric data acquired by PACE and other future Earth observing satellite missions with similar capabilities.

References:

[1] Werdell, P. J., Behrenfeld, M. J., Bontempi, P. S., Boss, E., Cairns, B., Davis, G. T., Franz, B. A., Gliese, U. B., Gorman, E. T.,Hasekamp, O., Knobelspiesse, K. D., Mannino, A., Martins, J. V., McClain, C. R., Meister, G., and Remer, L. A.: The Plankton, Aerosol, Cloud, Ocean Ecosystem Mission: Status, Science, Advances, Bulletin of the American Meteorological Society, 100, 1775– 1794, https://doi.org/10.1175/BAMS-D-18-0056.1, 2019.

[2] Gao, M., Franz, B. A., Knobelspiesse, K., Zhai, P.-W., Martins, V., Burton, S., Cairns, B., Ferrare, R., Gales, J., Hasekamp, O., Hu, Y., Ibrahim, A., McBride, B., Puthukkudy, A., Werdell, P. J., and Xu, X.: Efficient multi-angle polarimetric inversion of aerosols and ocean color powered by a deep neural network forward model, Atmos. Meas. Tech. Discuss. [preprint], https://doi.org/10.5194/amt-2020-507, accepted, 2021

[3] NASA Open Data Portal: https://data.nasa.gov/Earth-Science/FastMAPOL_ACEPOL_AIRHARP_L2/8b9y-7rgh.

Light scattering by packed media formed by Gaussian particles: modeling surfaces of icy satellites of Saturn.

Ludmilla Kolokolova[1], Dmitry Petrov[2], Gen Ito[3], Karly Pitman[4]

[1]*University of Maryland, College Park, MD, USA*
[2]*Crimean Astrophysical Observatory of Russian Academy of Science, Crimea*
[3]*CNRS/Université de Lorraine, Vandoeuvre-lés-Nancy, France*
[4]*Space Science Institute, Boulder, Colorado, USA*
[*]*corresponding author's e-mail: lkolokol@umd.edu*

Abstract

We use the radiative transfer theory with the static structure factor correction for studying densely packed media, consisting of irregular particles presented as Gaussian random particles of different type and size. We provide an example application of this approach simulating the spectra acquired by the Cassini Visual and Infrared Mapping Spectrometer (VIMS) instrument for the icy satellites of Saturn. The results of our simulations show that the surfaces of Saturnian satellites consist of solid non-spherical icy particles of radius 1-2 micron.

We use a development of the radiative transfer theory with the static structure factor correction to study the densely packed media formed by irregularly shaped particles. This approach, developed by Mishchenko [1] for spherical particles as units of media, has been recently updated to treat particles as clusters of spheres [2,3]. In this study we modeled particles as random Gaussian particles [4] having different roughness ratio and irregularity. We calculated the single-scattering characteristics by the Sh(shape)-matrix method [5]. Being based on the T-matrix technique, this approach separates the shape-dependent factors from those size- and refractive-index-dependent. The Sh-matrix approach was found very convenient to consider light scattering by Gaussian particles, i.e., the particles created by disturbing a sphere of a given radius such that the sphere radii become randomly lognormally distributed. Two radial distances relate to one another through correlation angle; by changing correlation angle from 0 to 90º we can model particles from spheres to a random complex shape. The other parameter defining the shape of a Gaussian particle is its roughness ratio that is 100%·(max(R)-min(R))/mean(R), where $R = R(\theta,\varphi)$ is the particle radius in a spherical coordinate system.

Combining the model of Gaussian particles with static-structure-factor corrected radiative transfer theory, we modeled the spectra acquired by Cassini VIMS for several icy satellites of Saturn. We examined a large number of radii of particles in submicron and micron ranges and Gaussian particles at correlation angles 7° and 20° and roughness ratios from 60% to 100%. The best fit to the VIMS spectra was achieved for the medium of porosity 90% and for Gaussian particles having radius 1- 2 micron, correlation angle $\gamma = 7°$, and roughness ratio 80%.

References

[1] Michael I. Mishchenko, *Asymmetry parameters of the phase function for densely packed scattering grains*. J. Quant. Spectrosc. Radiat. Transfer 52.1: 95-110, 1994.

[2] G. Ito, M. I. Mishchenko, and T.D. Glotch *Radiative-transfer modeling of spectra of planetary regoliths using cluster-based dense packing modifications*. J. Geophys. Res.: Planets, 123.5: 1203-1220, 2018.

[3] L. Kolokolova, G. Ito, K. Pitman, K. McMichael, K., and N. Reui *Spectral Modeling Using Radiative Transfer Theory with Packing Density Correction: Demonstration for Saturnian Icy Satellites.* Planet. Sci. J. 1.3: 74–78, 2020.

[4] Karri Muinonen, *Light scattering by Gaussian random particles: Rayleigh and Rayleigh-Gans approximations*. J. Quant. Spectrosc. Radiat. Transfer 55.5: 603-613, 1996.

[5] D. Petrov, Y. Shkuratov, and G. Videen, *Electromagnetic wave scattering from particles of arbitrary shapes.* J. Quant. Spectrosc. Radiat. Transfer 112.11: 1636-1645, 2011.

Numerical results for polarized light scattering in a spherical atmosphere

S. Korkin[1,*], E.-S. Yang[2], R. Spurr[3], C. Emde[4], N. Krotkov[5], A. Vasilkov[2], and A. Lyapustin[5]

[1]*Universities Space Research Association GESTAR, Columbia, MD, USA.*
[2]*Science Systems and Applications Inc., Lanham, MD, USA.*
[3]*RT Solutions Inc., Cambridge, MA, USA.*
[4]*Meteorological Institute, Ludwig-Maximilians-University, Germany.*
[5]*NASA Goddard Space Flight Center, Greenbelt, MD, USA*
[*]*corresponding author's e-mail: sergey.v.korkin@nasa.gov*

Back in the 1990's, Michael Mishchenko extended the invariant imbedding method to include polarization and developed a vector (polarized) Radiative Transfer (RT) code. Using this code, he published accurate numerical results for the angular distribution of polarized light reflected from a plane-parallel Rayleigh scattering atmosphere with exponentially varying gaseous absorber [1]. Mishchenko also demonstrated the importance of polarization in radiance calculations for Rayleigh-scattering atmosphere [2]. These results have become benchmarks for vector RT codes.

In this work we extend Michael's results [1] to include curvature (sphericity) of the Earth atmosphere. We pursue two specific goals: a) to provide benchmarks for the validation of existing and future spherical RT codes (especially those using approximations), and b) to better understand the influence of atmospheric curvature on the signal of a spaceborne polarimeter. To achieve these goals, we use two state-of-the art RT codes: libRadtran's MYSTIC (Monte Carlo) model [3] and the VLIDORT (discrete ordinates) code [4]. MYSTIC simulates light scattering in a true-spherical atmosphere; multi-point spherical corrections in VLIDORT deliver reasonable approximations to spherical-medium scattering.

Using MYSTIC and VLIDORT, we report numerical results for polarized light reflected from the top of a Rayleigh scattering spherical atmosphere with height-dependent single scattering albedo, over a black surface, separately for single and multiple scattering, for two optical thickness values, namely, 0.25–where the effect of atmospheric curvature is pronounced [5], and 1 – where the radiance error from the neglect of polarization reaches its maximum [2]. This work continues Michael's, and our own [5], efforts on the publication of benchmark results for RT numerical simulations.

References

[1] M. I. Mishchenko *The fast invariant imbedding method for polarized light: Computational aspects and numerical results for Rayleigh scattering*. J. Quant. Spectrosc. Radiat. Transfer, 43:163-171, 1990.

[2] M. I. Mishchenko, A. A. Lacis, and L. D. *Travis Errors induced by the neglect of polarization in radiance calculations for Rayleigh-scattering atmospheres.* J. Quant. Spectrosc. Radiat. Transfer, 51:491-510, 1994.

[3] C. Emde, R. Buras-Schnell, A. Kylling, B. Mayer, J. Gasteiger, U. Hamann, J. Kylling, B. Richter, C. Pause, T. Dowling, and L. Bugliaro *The libRadtran software package for radiative transfer calculations (version 2.0.1)*. Geosci. Model Dev., 9:1647-1672, 2016 (note: v.2.0.4 is the latest).

[4] R. Spurr, and M. Christi *The LIDORT and VLIDORT linearized scalar and vector discrete ordinate radiative transfer models: updates in the last 10 years*. In: A. Kokhanovsky (Ed.), Springer series in light scattering, 1-62, 2019.

[5] S. Korkin, Y. Eun-Su, R. Spurr, C. Emde, N. Krotkov, A. Vasilkov, D. Haffner, J. Mok, and A. Lyapustin *Revised and extended benchmark results for Rayleigh scattering of sunlight in spherical atmospheres*. J. Quant. Spectrosc. Radiat. Transfer, 254:107181, 2020.

Characterization of a single sphere using amplitude and phase Fourier spectrum of its light-scattering profile

Andrey V. Romanov[1,2*] and Maxim A. Yurkin[1,2]

[1] *Voevodsky Institute of Chemical Kinetics and Combustion SB RAS, Institutskaya Str. 3, 630090, Novosibirsk, Russia*
[2] *Novosibirsk State University, Pirogova Str. 2, 630090, Novosibirsk, Russia*
[*] *corresponding author's e-mail: avm.romanov@gmail.com*

Measuring light scattering of single particles is one of the most promising approaches to their non-invasive characterization, since the corresponding inverse problem is usually well posed. Along with the technical aspects, the solution of such inverse light-scattering problems is of great complexity [1]. One of the possible approaches is the compression of information in the measured light-scattering profiles or patterns (LSP) into several parameters that determine the model characteristics of the particle under study. Such methods usually possess advantages of high-speed performance and the robustness with respect to diverse distortions contributed both by experiment and by the particle model imperfection. Several recent examples include spectral methods for determining the size and refractive index of spheres [2,3] and for non-sphericity estimation [4].

In particular, an accurate and robust sphere characterization was based on extraction of two parameters from the Fourier spectrum of the one-dimensional LSP: the main peak position and the zero-frequency amplitude, which highly correlated with the size and refractive index, respectively [2]. However, the zero-frequency amplitude has one-to-one (monotonous) correspondence with the refractive index, only for relatively low values of the latter. Thus, it cannot be used for a common task of characterization of polystyrene beads in a liquid.

Analyzing the Rayleigh-Gans-Debye and Wentzel–Kramers–Brillouin approximations, we obtained an analytical representation of the refractive index influence on the Fourier phase spectrum of the LSP. The obtained results confirmed the linear dependence of the spectrum phase on the refractive index m at the first-order approximation in powers of $(m-1)$, previously observed in the rigorous Lorentz-Mie theory. Based on this general theory, we developed a specific characterization method for characterization of polystyrene beads from the LSP measured with the scanning flow cytometer. This fast method uses two spectral parameters: the position of the main peak and the phase value at that point. The details of its performance on both synthetic and real experimental data will be reported at the conference.

References

[1] A. V. Romanov, and M. A. Yurkin *Single-particle characterization by elastic light scattering.* Laser & Photon. Rev; 15:2000368, 2021.
[2] A. V. Romanov, A. I. Konokhova, E. S. Yastrebova, K. V. Gilev, D. I. Strokotov, A. V. Chernyshev, V. P. Maltsev and M. A. Yurkin *Spectral solution of the inverse Mie problem.* J. Quant. Spectrosc. Radiat. Transfer, 200:280–294, 2017.
[3] A. I. Konokhova, E. S. Yastrebova, D. I. Strokotov, A. V. Chernyshev, A. A. Karpenko and V. P. Maltsev *Ultimate peculiarity in angular spectrum enhances the parametric solution of the inverse Mie problem.* J. Quant. Spectrosc. Radiat. Transfer, 235:204–208, 2019.
[4] A. V. Romanov, A. I. Konokhova, E. S. Yastrebova, K. V. Gilev, D. I. Strokotov, V. P. Maltsev and M. A. Yurkin *Sensitive detection and estimation of particle non-sphericity from the complex Fourier spectrum of its light-scattering profile.* J. Quant. Spectrosc. Radiat. Transfer, 235:317–331, 2019

Light scattering by fractal agglomerated debris particles model

Dmitry Petrov, Elena Zhuzhulina

Crimean Astrophysical Observatory of Russian Academy of Science, Crimea
**corresponding author's e-mail: dvp@craocrimea.ru*

Abstract

Measurements of the of comet 67P/Churyumov–Gerasimenko environment by the Rosetta have shown, that cometary dust particles have a very complex structure. Most of cometary particles are found to be aggregates with hierarchical structure [1]. That is, the particles are represented by a collection of smaller particles. It is highly likely that hierarchical aggregates are a widespread kind of natural dust particles. Large number of different hierarchical aggregates was developed [2]. On the other hand, both the Rosetta and Stardust missions have shown the presence of compact particles with low porosity [3]. Computer simulation of light scattering by solid cometary particles in the form of agglomerated debris particles by [4-6] has shown that the solid compact particles dramatically affect on light scattering. Halder & Ganesh [7] developed a model of heterogeneous dust particles, having two levels of hierarchy: solid core is surrounded by fluffy aggregates of small particles. We suggest a slightly different model that allows one to fractalize an agglomerate debris particle. It combines the presence of both larger and smaller debris. By changing the parameters of the model, you can achieve a different ratio between them, making the particle more compact or, on the contrary, more fluffy, as shown in Fig.1. Such model can be useful in computer simulation of light scattering by real objects both for DDA and Multi-Sphere T-Matrix method.

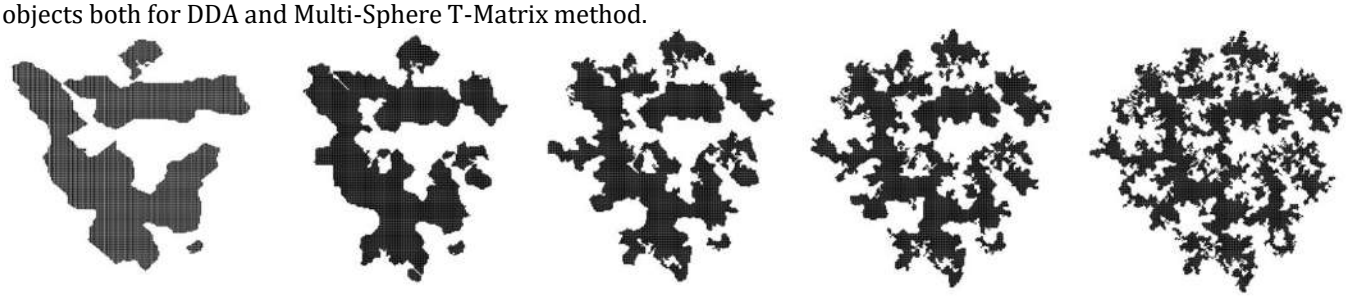

Figure 1: Examples of fractal agglomerated debris particles model

References

[1] Bentley M.S., Schmied R., Mannel T., Torkar K., Jeszenszky H., Romstedt J., et al. *Aggregate dust particles at comet 67P/Churyumov–Gerasimenko.* Nature, 537(7618):73–5, 2016.

[2] Kolokolova L., Nagdimunov L., Mackowski D. *Light scattering by hierarchical aggregates*. J. Quant. Spectrosc. Radiat. Transfer. 204: 138-143, 2018.

[3] Güttler C., Mannel T., Rotundi A., Merouane S., Fulle M., Bockelée-Morvan D., et al. *Synthesis of the morphological description of cometary dust at comet 67P/Churyumov-Gerasimenko*. Astronomy & Astrophysics, 630, 2019.

[4] Zubko E., Muinonen K., Videen G., Kiselev N. N. *Dust in Comet C/1975 V1 (West).* MNRAS, 440, 2928, 2014.

[5] Zubko E., Videen G., Hines D.C., Shkuratov Y. *The positive-polarization of cometary comae*. Planetary and Space Science, 123, 63, 2016.

[6] Zubko E., Videen G., Arnold J. A., MacCall B., Weinberger A. J., Kim S.S. *On the Small Contribution of Supermicron Dust Particles to Light Scattering by Comets*. The Astrophysical Journal, 895, 110, 2020.

[7] Halder, P., Ganesh, S. *Modelling heterogeneous dust particles: an application to cometary polarization.* MNRAS, 501, 1766–1781, 2021.

Machine learning to enhance the calculation of optical forces in the geometrical optics approximation

David Bronte Ciriza[1,*], Alessandro Magazzù[1], Agnese Callegari[2], Maria A. Iatì[1], Giovanni Volpe[2], and Onofrio M. Maragò[1,*]

[1]*CNR-IPCF, Istituto per i Processi Chimico-Fisici, V. le F. Stagno D'Alcontres 37, I-98158 Messina, Italy.*
[2]*Institutionen för Fysik, Göteborgs Universitet, I-41296 Göteborg, Sweden.*
[*]*brontecir@ipcf.cnr.it, onofrio.marago@cnr.it*

Abstract

Since the pioneering work by Ashkin in the 1970's [1], optical forces have played a fundamental role in fields like biology, nanotechnology, or atomic physics. In all these fields, numerical simulations are of great help for validating theories, for the planning of experiments, and in the interpretation of the results. However, the calculation of the forces is computationally expensive and prohibitively slow for numerical simulations when the forces need to be calculated many times in a sequential way. Recently, machine learning has been demonstrated to be a promising approach to improve the speed of these calculations and therefore, to expand the applicability of numerical simulations for experimental design and analysis [2].

In this work we show that machine learning can be used to improve not only the speed but also the accuracy of the force calculation in the geometrical optics regime, valid when the particles are significantly bigger than the wavelength of the incident light. This is first demonstrated for the case of a spherical particle with 3 degrees of freedom and later expanded to 9 degrees of freedom by including all the relevant parameters involved in the optical forces calculation. Machine learning is proved as a compact, accurate, and fast approach for optical forces calculation and presents a tool that can be used to study systems that, due to computation limitations, were out of the scope of the traditional ray optics approach.

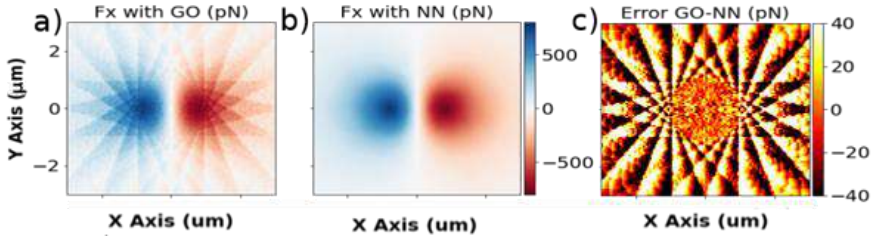

Figure 1: Comparison between the optical forces calculated with the geometrical optics approach (a) and the neural network (b) for the case of 3 degrees of freedom. (c) shows the difference between both calculations.

We acknowledge financial contribution from the MSCA-ITN-ETN project ActiveMatter sponsored by the European Commission (Horizon 2020, Project Number 812780) and from the agreement ASI-INAF n.2018-16-HH.0, project "SPACE Tweezers".

References

[1] A. Ashkin, "Acceleration and trapping of particles by radiation pressure," Phys. Rev. Lett. **24**, 156 (1970).

[2] I. C. D. Lenton, G. Volpe, A. B. Stilgoe, T. A. Nieminen, and H. Rubinsztein-Dunlop, "Machine learning reveals complex behaviours in optically trapped particles," Mach. Learn. Sci. Technol. **1**, 45009 (2020).

Optimization of the discrete-dipole approximation for large optically soft particles

Konstantin G. Inzhevatkin[1,2,*] and Maxim A. Yurkin[1,2]

[1]*Voevodsky Institute of Chemical Kinetics and Combustion, SB RAS, Institutskaya str. 3, 630090 Novosibirsk, Russia*
[2]*Novosibirsk State University, Pirogova 2, 630090 Novosibirsk, Russia*
[*]*k.inzhevatkin@yandex.ru*

Background

The discrete dipole approximation method (DDA) solves the direct light scattering problem, i.e. calculates the light scattering pattern (LSP) given the parameters of the particle (scatterer) and the incident wave [1]. The drawback of the DDA is the significant computational time. Moreover, a large number of launches with different scatterer parameters are often required. The latter is relevant in solving inverse problems (characterization of single particle by LSP), when a previously calculated database of LSPs (up to a million elements) is used. In biological applications of the DDA, we usually deal with large optically soft particles i.e. $|m-1| \ll 1$ and $x \gg 1$, where m – relative refractive index, $x = kR$ – size parameter, k is the wave vector, R is the (effective) radius of the particle. In this regard, the task of optimizing the DDA for such particles is relevant. The most time-consuming and resource-intensive part of DDA is the solution of a system of linear equations. This time depends on the initial electric field inside the particle (first guess in the iterative solver). Thus, it is important to have as accurate guess as possible, at least among those obtainable with little extra calculations.

Results

To solve this problem, we propose a modified Wentzel-Kramers-Brillouin approximation (WKBr). The original WKB takes into account the phase shift of the incident wave in a particle [2,3]. The WKBr accounts also for the refraction at the boundary. In this work, we showed that the WKB eliminates the error of order $x(m-1)$ in the internal field, and WKBr – all errors of order x (with any dependence on m). Our theoretical and numerical analysis uncovers the scaling of various optical phenomena (refraction, reflection, ray focusing) with m and x, which supports the design of the WKBr (leaving only the significant and easy to implement corrections). Refining the internal electric field, we also considered the problem of the additional phase $\pi/2$ at the passage of a focal line [4]. Simulation results for spheres shows that the WKBr both improves the accuracy of the internal fields and accelerates the DDA simulation. In some cases, such as a sphere with $x = 250$ and $m = 1.1$, the DDA iterative solver converges to the relative residual of 10^{-3} only when the WKB or WKBr are used as a first guess. Moreover, the WKBr is significantly superior to the WKB in this case.

References

[1] M.A. Yurkin, A.G. Hoekstra *The discrete dipole approximation: An overview and recent developments.* J. Quant. Spectrosc. Radiat. Transfer, 106:558-89–52, 2007.
[2] V.N. Lopatin, N.V. Shepelevich *Consequences of the integral wave equation in the Wentzel-Kramers–Brillouin approximation.* Opt. Spectrosc, 81:103-6, 1996.
[3] J.D. Klett, R.A. Sutherland *Approximate methods for modeling the scattering properties of nonspherical particles: evaluation of the Wentzel-Kramers-Brillouin method.* Appl. Opt, 31:373-86, 1992.
[4] H.C. van de Hulst. *Light Scattering by Small Particles*. Dover, New York, 1981.

Recent progress in studying polarization of the Jupiter's satellite Europa

N. Kiselev[1,*], K. Muinonen[2,3], L. Kolokolova[4], V. Rosenbush[5], A. Savushkin[1], N. Karpov[6]

[1]*Crimean Astrophysical Observatory, Nauchny, Crimea*
[2] *Department of Physics, University of Helsinki, Helsinki, Finland*
[3]*Finnish Geospatial Research Institute, Masala, Finland*
[4]*University of Maryland, USA*
[5]*Astronomical Observatory of Taras Shevchenko National University of Kyiv, Kyiv, Ukraine*
[6]*ICAMER, Peak Terskol Observatory, Ukraine*
[*]*corresponding author's e-mail: kiselevnn42@gmail.com*

Abstract

At small phase angles the negative branch of polarization (NBP) can have different shape and polarization values for different composition of the surfaces. For rocky surfaces, it has a parabolic shape with a minimum around 10 deg. and inversion point (the angle where polarization changes from negative to positive) around ~20 deg. However, for icy surfaces (satellites of giant planets, cometary nuclei, and TNOs), the NBP becomes very asymmetric, and its minimum shifts to smaller phase angles. The cause of this has been attributed to Coherent Backscattering Effect (CBE), which is known to be very sensitive to the size of particles and porosity of the medium. Recently we have been able to accurately determine the NBP of Jovian satellite Europa. It appeared that Europa's NBP is not bimodal with a deep and narrow and broad and shallow overlapping NPBs [1], but has a single very sharp minimum at phase angle <0.4 deg. and inversion point at ~ 6 deg (Fig. 1, left panel). Such NBP is evidently formed by CBE. We studied wavelength dependence of the Europa's NBP to better characterize the CBE (Fig. 1, right panel). Using the modeling technique [2] we estimated the size of icy particles ~20 micron and porosity ~70%.

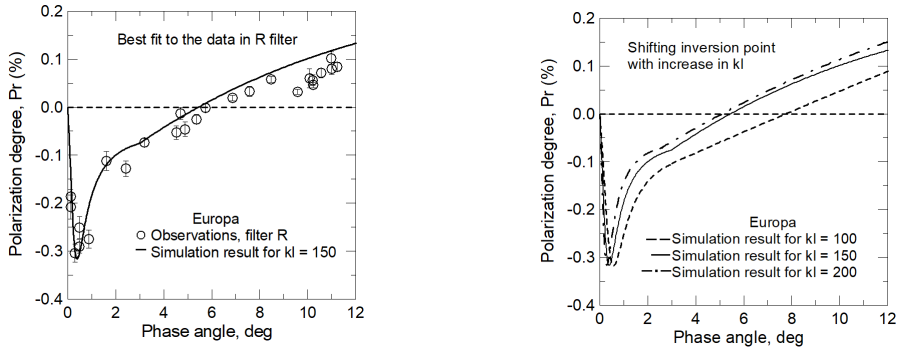

Figure 1: Europa's phase-angle polarization dependence in the R filter (observations - open circles, left panel,) and their the RT-CB modeling (lines for different free path length kl ~ 1/wavelength)- left and right panels)).

References

[1] Rosenbush, V., Kiselev, N., Afanasiev, V. *Icy moons of the outer planets.* In:Polarimetry of Stars and Planetary Systems. (Eds. L. Kolokolova, J. Hough, A-Ch. Levasseur-Regourd), Cambridge University Press, Cambridge, 340-359. 2015.

[2] Muinonen, K., Penttilä, A., and Videen. *Multiple scattering of light in particulateplanetary media*. In:Polarimetry of Stars and Planetary Systems. (Eds. L. Kolokolova, J. Hough, A-Ch. Levasseur-Regourd), Cambridge University Press, Cambridge, 117-129. 2015.

Inverse Design of Metasurface Based on Neural Network

Liu Yang[1], Renxian Li[1,2,*], and Shu Zhang[1]

[1]*School of Physics and Optoelectronic Engineering, Xidian University, Xi'an 710071, China*
[2]*Collaborative Innovation Center of Information Sensing and Understanding, Xidian University, Xi'an 710071, China*
[*]*corresponding author's e-mail: rxli@mail.xidian.edu.cn (R. Li).*

Abstract

Metasurface is a kind of artificial material, which has attracted much attention because of its flexible optical manipulation in subwavelength propagation distance. The traditional design is to use the iterative calculation method, combined with FEM or FDTD to accurately predict the spectral characteristics and functions of the metasurface, then to prepare the metasurface nanostructure according to the model. The process of calculation and design is complex, and a group of discrete elements need to be obtained by calculating the phase amplitude change of the radiation field in the whole parameter space, which will take a long time. What's more, its shape is relatively regular and the ability to control the beam is limited. As an important branch of machine learning algorithm, the neural network is a kind of multi-level characterization of learning technology, which can find and classify the characterization automatically from the original data, and use a large number of cascade transformation through the nonlinear combination of neurons to learn complex functions in a data-driven way in order to establish input-output data mapping [1]. At present, it has attracted the attention of materials science, particle physics and other relevant fields. The overall idea of the inverse design for the metarsurface based on the neural network is to train it, and when a set of required optical responses are input, the trained generation network will quickly calculate the requirements of the target phase and output a metasurface overall structure with input optical characteristics [2]. Compared with the previous method, there is no need to calculate each local element separately and then carry out complex layout design [3].The efficiency is significantly improved. It is also of great significance to realize the metasurface structure of irregular shape and the function of spatial optical control.

References

[1] Jiang J , Fan J A. *Global optimization of dielectric metasurfaces using a physics-driven neural network.* Nano Letters, 2019.
[2] Zhaocheng, Liu, Dayu, et al. *Generative Model for the Inverse Design of Metasurfaces..* Nano letters, 2018.
[3] Wei M , Cheng F , Liu Y . *Deep-Learning Enabled On-Demand Design of Chiral Metamaterials..* Acs Nano, 2018:acsnano.8b03569-.

Measuring the contribution of structure to light extinction by aggregates

L. Cremonesi[1,2,*], M.A.C. Potenza[2], F. Ferri[3], and A. Parola[4]

[1] *Earth and Environmental Sciences Dept., University Milano-Bicocca, 20126 Milan, Italy*
[2] *Physics Dept., Università degli Studi di Milano, 20133 Milan, Italy*
[3] *Science and High Technology Dept. and To.Sca.Lab, Università degli Studi dell'Insubria, 22100, Como, Italy*
[4] *Science and High Technology Dept., Università degli Studi dell'Insubria, 22100, Como, Italy*
[*] *corresponding author's e-mail: llorenc.cremonesi@unimib.it*

Abstract

We collected experimental evidence of the effect of the internal structure of inhomogeneous particles, such as colloidal fractal aggregates, on their radiative properties. An approximate analytical model for the forward scattering amplitude, $S(0)$, as well as the extinction cross section is derived in terms of the structure and form factors [2]. The interest for such characteristics lies in their direct bearing on determining the asymmetry parameter and single scattering albedo. Experimental results and Discrete Dipole Approximation simulations are in good agreement with expectations, whereas they both differ considerably from the mean field approximation [1]. Similarly, the spectral trend of the extinction cross section is reasonably described in terms of the three parameters that characterize the fractal morphology [3]. Conversely, preliminary experimental and numerical results on absorbing fractal aggregates suggest that the absorption cross section is far less sensitive to the internal structure of the particle as compared to dielectric scatters.

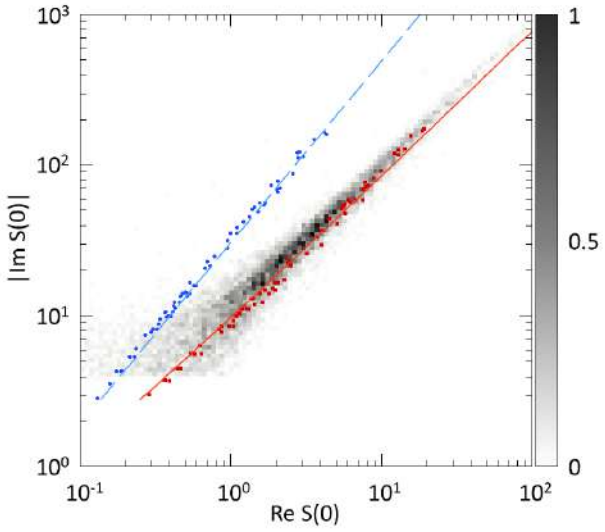

Figure 1: Measurements of the forward scattering amplitude, $S(0)$, from colloidal fractal aggregates compared to simulations (red) and equivalent Lorentz-Lorenz spheres (blue). The analytical models are shown as a solid line of the corresponding colour.

References

[1] Hendrik C. van de Hulst. *Light scattering by small particles.*. Courier Corporation, 1981.
[2] L. Cremonesi, C. Minnai, F. Ferri, A. Parola, B. Paroli,T. Sanvito, and M.A.C. Potenza *Light extinction and scattering from aggregates composed of submicron particles.* J. Nanoparticle Res., 22(11): 1-17, 2020.
[3] C. M. Sorensen *Light scattering by fractal aggregates: a review.* Aerosol Sci. Technol. 35(2): 648-687, 2001.

Cloud scattering property parameterizations and their applications in remote sensing and GCM

Bingqi Yi[1,2,*]

[1]*School of Atmospheric Sciences and Guangdong Province Key Laboratory for Climate Change and Natural Disaster Studies, Sun Yat-sen University, Guangzhou, China*
[2]*Southern Marine Science and Engineering Guangdong Laboratory (Zhuhai), Zhuhai, China*
[*]*corresponding author's e-mail: yibq@mail.sysu.edu.cn*

Abstract

In this paper, we focus on the parameterizations of scattering properties of clouds and their downstream applications in remote sensing and global climate model. Clouds can be classified into ice, liquid water, and mixed-phase clouds according to the phase of water in clouds. Compared with the liquid water cloud, the optical properties of ice and mixed-phase clouds are much more complex and depend on various factors. We developed parameterization schemes of scattering properties of various cloud particle models with considerations of different factors, and applied them in fast radiative transfer models for remote sensing studies [1,2] and general circulation models for climate simulations [3]. It is evident to find that consistent cloud scattering property parameterization for forward radiative transfer calculation and for retrieval purposes is needed to reduce further uncertainties. Different ice cloud optical property parameterization schemes are found to perturb the top of the atmosphere irradiance and significantly influence the regional surface temperature simulation. It is concluded that a unified cloud scattering property parameterization is needed for both remote sensing and climate simulation purposes.

References

[1] B. Yi, P. Yang, Q. Liu, P. van Delst, S. Boukabara, and F. Weng. *Improvements on the ice cloud modeling capabilities of the Community Radiative Transfer Model*. J. Geophys. Res. Atmos., 121:13577-13590, 2016.
[2] B. Yi, S. Ding, and L. Bi. *Impacts of cloud scattering properties on FY-3D HIRAS simulations*, J. Quant. Spectros. Rad. Trans., 246, 106902, 2020.
[3] B. Yi. *Diverse cloud radiative effects and global surface temperature simulations induced by different ice cloud optical property parameterizations*. submitted to npj Climate and Atmos., 2021.

Polarization dependencies based on DBCP V2.0

O. Shubina[1,*]

[1] *Main astronomical observatory of National academy of sciences of Ukraine, 27 Akademika Zabolotnoho str., 03143, Kyiv, Ukraine*
[*] *corresponding author's e-mail: olena.shubina.sci@gmail.com*

Polarimetric methods are effective to determine the physical properties of comets. Comparison observations with results of theoretical modeling and laboratory measurements follows us to determine the most likely composition, structure, and some other characteristics of comet dust envelopment. For such comparison, however, we must have sufficiently complete phase-angel dependence curves of polarization in a wide range of phase angles and wavelengths. Unfortunately, it is impossible to get the phase-angle dependence of polarization for a particular comet in a wide range of phase angles, with few exceptions. In this case one can use the average phase-angle dependence that formed based on observations of various comets. This approach allows us to get the average polarization parameters for different groups of comets according to their dynamic characteristics, and to provide some comets with unique individual characteristics of polarized light. In our study, we used the second version of the database of comet polarimetry [1] that covers ranges of phase angles, helio- and geocentric distances 0.0–122.1°, 0.0–7.01 au and 0.01–6.52 au, respectively. We analyzed the phase-angle dependence of the degree of linear polarization of comets, as a function of wavelength filter used, heliocentric and geocentric distance, dynamic characteristics and other parameters. It allowed to select comets and to find the connection of physical properties of dust with dynamical characteristics of comets and, therefore, with places of comet formation in the Solar system or evolutionary features of different groups of comets.

References

[1] N. Kiselev, O. Shubina, S. Velichko, K. Jockers, V. Rosenbush, and S. Kikuchi (eds.) *Compilation of Comet Polarimetry from Published and Unpublished Sources*, urn:nasa:pds:compil-comet:polarimetry::1.0, NASA Planetary Data System, 2017.

New practical approach to light scattering by spheroids with a use of the spheroidal basis

V.B. Il'in[1,2,3,*], D.G. Turichina[1], and V.G. Farafonov[2]

[1] *St.Petersburg University, St.Petersburg, Russia*
[2] *St.Petersburg University of Aerospace Instrumentation, St.Petersburg, Russia*
[3] *Pulkovo Astronomical Observatory, St.Petersburg, Russia*
[*] *corresponding author's e-mail: v.b.ilin@spbu.ru*

Some applications still need an exact solution to light scattering problem for large non-spherical scatterers. The Mie theory using the spherical basis provides such solution for very large spheres if one overcomes a couple of numerical obstacles. The next step could be the application of the separation of variables method with the spheroidal basis to spheroids. However, the problem becomes more complicated (because of not complete separation of variables in the boundary conditions) and there appears a difficult task of calculations of the spheroidal functions of complex arguments (because of eigenvalue branching).

We describe several steps made by us to develop a very accurate contemporary code to treat light scattering by large spheroids and to present its results in a convenient form.

Spheroidal functions

Among several routines developed during the last decade to compute the spheroidal functions and their first derivatives we selected those recently created by van Buren [1]. Our thorough testing has shown that these Fortran 90 routines greatly exceed similar ones when one treat dielectric materials (the imagine part of the refractive index $k <\sim 0.05$). For prolate and oblate spheroids with the aspect ratio $a/b < 30$ van Buren's routines give the function values with accuracy at the level of about 10^{-20} for the diffraction parameters $x_{\rm V}$ as large as 100.

T-matrix transformations

Following [2], we use the EBCM method with the spheroidal basis $\vec{M}^{\vec{z}}$, $\vec{M}^{\vec{r}}$ to solve the light scattering problem for a homogeneous spheroid and to calculate the corresponding spheroidal T-matrix $T_{\rm sph}$.

This matrix is transformed into the T-matrix T_{s1} for the spherical basis $\vec{M}^{\vec{z}}$, $\vec{M}^{\vec{r}}$. Then the matrix T_{s1} is converted into the usual T-matrix appeared in the case of the standard spherical basis $\vec{M}^{\vec{r}}$, $\vec{N}^{\vec{r}}$. So far, such transformation has been done just from the spheroidal basis $\vec{M}^{\vec{r}}$, $\vec{N}^{\vec{r}}$ to the corresponding spheroidal one in [3].

We incorporate the derived spherical T-matrix in the free pyhton/C++ package CosTuuM that computes the optical properties of spheroid ensembles with given orientation, alignment and shape distributions and makes task-based parallelization [4].

Our approach limitations

We find that our code written in Fortran 90 is able to very accurately calculate the optical properties of homogeneous prolate and oblate spheroids as large as $x_{\rm a} = 2\pi a/\lambda \approx 250-300$, where a is the major semi-axis and λ the wavelength. The particles can have as large aspect ratio as 30 or more, but their refractive index should be rather dielectric ($k < 0.05$). The limiting value of $x_{\rm a}$ is determined by the used memory volume of 8 Gb, and we investigate different ways to make this restriction weaker. We are also going to involve some other routines to calculate the spheroidal functions that would better perform for larger k (i.e. more absorbing materials).

References

[1] L.A. van Buren. *Calculation of oblate spheroidal wave functions with complex argument.* arXiv preprint math/2009.01618, 2020.
[2] V.G. Farafonov, and N.V. Voshchinnikov. *Light scattering by a multilayered spheroidal particle.* Appl. Opt., 51:1586–1597, 2012.
[3] M.F. Schulz, K. Stamnes, and J. Stamnes. *Scattering of electromagnetic waves by spheroidal particles: a novel approach exploiting the T matrix computed in spheroidal coordinates.* Appl. Opt., 37:7875–7896, 1998.
[4] B. Vandenbroucke, M. Baes, and P. Camps. *CosTuuM: polarized thermal dust emission by magnetically oriented spheroidal grains.* Astron. J., 160:55, 2020.

Dual-beam optical trapping and optical manipulation of gain-assisted plasmonic/dielectric nanoshells

P. Polimeno[1,2,*], F. Patti[1,2], M. Infusino[3], J. Sánchez[3], M. A. Iatì[2], R. Saija[1], G. Volpe[4], O. M. Maragò[2], and A. Veltri[3]

[1] *Dipartimento di Scienze Matematiche e Informatiche, Scienze Fisiche e Scienze della Terra, Università degli Studi di Messina, I-98166, Messina, Italy*
[2] *CNR-IPCF, Istituto per i Processi Chimico-Fisici, I-98158, Messina, Italy*
[3] *Colegio de Ciencias e Ingenieria, Universidad San Francisco de Quito, Quito 170901, Ecuador*
[4] *Institutionen för Fysik, Göteborgs Universitet, I-41296 Göteborg, Sweden*
[*] *corresponding author's e-mail: polimenop@unime.it*

Various types of nanostructures can be manipulated by properly focused light [1–3]. A wide variety of dielectric, metal, and/or biological particles from the nano- to the microscale can be trapped, pushed, or binded thanks to Optical Tweezers (OT) directly in liquid, air or vacuum environment [4]. In their standard configuration, OT consist of a single laser beam generally focused by a high numerical aperture (NA) objective to a diffraction-limited spot [1,2]. Thus, a nanoparticle can be trapped near the focal point by optical forces associated with the high intensity gradients surrounding the focal region [1, 2]. However, for typical incident laser powers, the scattering force and the thermal fluctuations can prevent the optical trapping for small nanoparticles [4]. The use of two counter-propagating beams can avoid the counterproductive effects of scattering forces [1]. These stationary traps are based on the use of low NA lenses and allow trapping of nanoparticles with reduced incident power in a focal region that is wider than for standard optical tweezers [5]. With linearly polarized light, a standing wave trap is formed and many equilibrium positions are generated by the maximum intensity peaks that form along the beam axis [6]. Therefore, through such configuration, we study theoretically the optomechanics of dyed dielectric/metallic nanoshells [7–9]. We also investigate theoretically the stability configurations and particle dynamics in the trap by means of Brownian dynamics simulations [10]. For a more complete analysis we consider also that metal nanoparticles act as local heat sources when illuminated by electromagnetic fields [11, 12]. Therefore, we study the heat effect delivered by the nanoshell under the focused light irradiation.

References

[1] A. Ashkin *Acceleration and Trapping of Particles by Radiation Pressure* Phys. Rev. Lett., 24:156, 1970.
[2] P. H. Jones, O. M. Maragò, G. Volpe. *Optical Tweezers: Principles and Applications.* Cambridge, UK: Cambridge University Press, 2015.
[3] P. Polimeno, A. Magazzù, M. A. Iatì, F. Patti, R. Saija, C. Degli Esposti Boschi, M. G. Donato, P. G. Gucciardi, P. H. Jones, G. Volpe, O. M. Maragò *Optical Tweezers and their Applications* J. Quant. Spectrosc. Radiat. Transf., 218: 131-150, 2018.
[4] O. M. Maragò, P. H. Jones, P. G. Gucciardi, G. Volpe, A. C. Ferrari *Optical Trapping and Manipulation of Nanostructures* Nat. Nanotechnol., 8:807–819, 2013.
[5] O. Brzobohatý, M. Šiler, J. Trojek, L. Chvátal, V. Karásek, A. Paták, Z. Pokorná, F. Mika, P. Zemánek *Three-dimensional Optical Trapping of a Plasmonic Nanoparticle using Low Numerical Aperture Optical Tweezers* Sci. Rep., 5:8106, 2015.
[6] P. Zemánek, A. Jonáš, M. Liška *Simplified Description of Optical Forces Acting on a Nanoparticle in the Gaussian Standing Wave* J. Opt. Soc. Am. A, 19:1025–1034, 2002.
[7] P. Polimeno, F. Patti, M. Infusino, J. Sánchez, M. A. Iatì, R. Saija, G. Volpe, O. M. Maragò, A. Veltri *Gain-Assisted Optomechanical Position Locking of Metal/Dielectric Nanoshells in Optical Potentials* ACS Photonics, 7:1262–1270, 2020.
[8] A. Veltri, A. Chipouline, A. Aradian *Multipolar, Time-dynamical Model for the Loss Compensation and Lasing of a Spherical Plasmonic Nanoparticle Spaser Immersed in an Active Gain Medium* Sci. Rep., 6:33018, 2016.
[9] A. Veltri, A. Aradian *Optical Response of a Metallic Nanoparticle Immersed in a Medium with Optical Gain* Phys. Rev. B, 85:115429, 2012.
[10] G. Volpe, G. Volpe *Simulation of a Brownian Particle in an Optical Trap* Am. J. Phys., 81:224–230, 2013.
[11] G. Baffou *Thermoplasmonic in Heating Metal Nanoparticles Using Light* World Scientific, 2017.
[12] R. Gillibert, F. Colas, M. L. de La Chapelle, P. G. Gucciardi *Heat Dissipation of Metal Nanoparticles in the Dipole Approximation* Plasmonics, 15:1001–1005, 2020.

Aperture polarimetry of comets

E. Zhuzhulina[a,*], N. Kiselev[a], N. Karpov[b], A. Savushkin[a], D. Petrov[a]

[a]*Crimean Astrophysical Observatory of Russian Academy of Science (CrAO RAS), Crimea*
[b]*Terskol Branch of Institute of Astronomy of the Russian Academy of sciences (INASAN), Russia*

[*]*corresponding author's e-mail: zhuzhulina.alena@yandex.ru*

Polarimetry is an effective method for studying the physical properties of small bodies in the solar system. Currently, two methods are used to study the polarization of comets - aperture and panoramic polarimetry.

In 2018, new two-channel photoelectric polarimeter named N.M. Shakhovskoy was constructed at the Crimean Astrophysical Observatory (CrAO). This made it possible to significantly expand the range of observed comets (up to 15 magnitude) and to increase the accuracy of the results. Between 2018 and 2021, polarimetric observations of 18 comets (8 short-period and 10 for long-period) were carried out in CrAO and at Terskol observatory.

The integral luminosity of comets was in the range of 10–15 magnitude, and the range of phase angles was from 1.4° to 103°. For many comets, the data of polarimetric observations were obtained for the first time. Observations were carried out in UBVRI filters and in narrow-band comet filters. Figure 1 shows synthetic phase curves of observed comets in filters I, V and R.

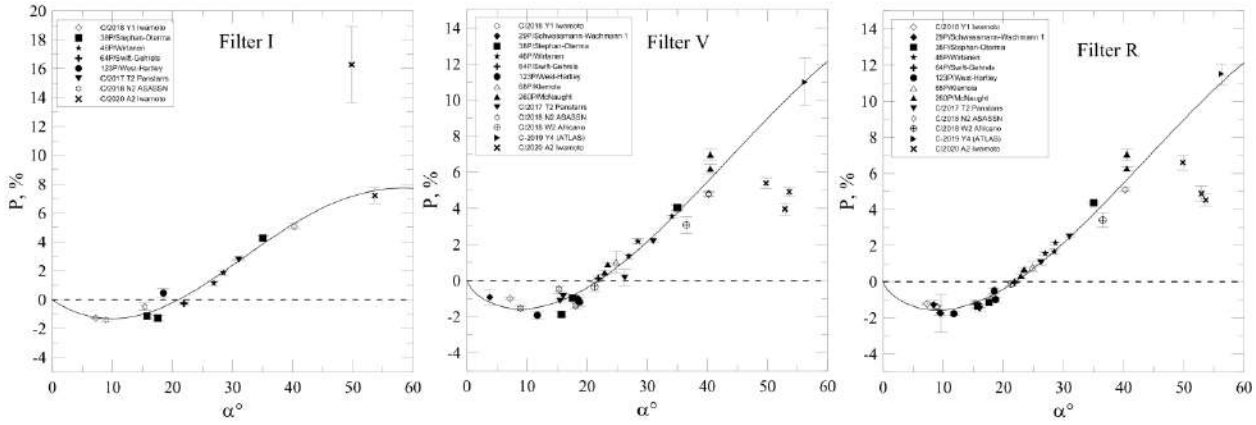

Figure 1: Synthetic phase curves of observed comets in filters I, V and R.

The polarization phase dependences of the 18 comets are constructed. A comparison between the synthetic phase dependence of the cometary polarization and the data of the polarimetric database of comets has been done.

Observational data can be used as a basis for interpretation using various computational techniques, among which the T-matrix method occupies an important place, an incredibly efficient software implementation of which was developed by M. Mishchenko.

Polarimetric remote sensing of the atmosphere in the UV-VIS spectrum: Modeling scattering and absorption by Brown Carbon

J. Chowdhary[1,2,*], H. Moosmüller[3], G. Schuster[4], L. Liu[1,2], K. Tsigaridis[1,2], M. Ottaviani[2,5], and S. Stamnes[4]

[1]*Columbia University, New York, NY, USA*
[2]*NASA Goddard Institute for Space Studies, New York, NY, USA*
[3]*Desert Research Institute, Reno, NV, USA*
[4]*NASA Langley Research Center, Hampton, VA, USA*
[5]*Terra Research Inc, Hoboken, NJ, USA*
[*]*corresponding author's e-mail: jacek.chowdhary@nasa.gov*

The NASA Aerosol Plankton, Aerosol, Cloud, ocean Ecosystem (PACE) mission, scheduled for launch in 2023, will carry two instruments that measure UV radiance emerging from the top of the atmosphere (TOA): the Ocean Color Instrument (OCI) and the Spectro-Polarimeter for Planetary Exploration (SPEXone) instrument. OCI will provide single-view, hyperspectral radiometric data with a spectral resolution of 5 nm, whereas SPEXone will provide multiangle, multispectral polarimetric data with a degree of linear polarization accuracy of 0.3% [1]. Together, these instruments will be the most advanced in NASA's history for the combined observation of ocean color and atmospheric aerosols in the UV, and they will therefore provide unprecedented research opportunities for the ocean color and atmospheric aerosol communities. In particular, UV observations are best suited to constrain Colored Dissolved Organic Matter (CDOM) in the ocean, and Brown Carbon (BrC) aerosols in the atmosphere. However, both CDOM and BrC exhibit very similar absorption spectra in the UV-VIS; hence, care must be taken in accurately modeling these spectra for analyses of OCI and SPEXone measurements [2,3]. In this talk, we focus on modeling variations in the scattering and absorption properties of BrC in the UV-VIS, and on the impact of those variations on TOA total and polarized multiangle radiances.

References

[1] Werdell, P.J., M.J. Behrenfeld, P.S. Bontempi, E. Boss, B. Cairns, G.T. Davis, B.A. Franz, U.B. Gliese, E.T. Gorman, O. Hasekamp, K.D. Knobelspiesse, A. Mannino, J.V. Martins, C.R. McClain, G. Meister, and L.A. Remer, 2019: The Plankton, Aerosol, Cloud, ocean Ecosystem (PACE) mission: Status, science, advances. *Bull. Amer. Meteor. Soc.*, **100**, no. 9, 1775-1794, doi:10.1175/BAMS-D-18-0056.1.

[2] Chowdhary, J., P.-W. Zhai, E. Boss, H. Dierssen, R. Frouin, A. Ibrahim, Z. Lee, L.A. Remer, M. Twardowski, F. Xu, X. Zhang, M. Ottaviani, W.R. Espinosa, and D. Ramon, 2019: Modeling atmosphere-ocean radiative transfer: A PACE mission perspective. *Front. Earth Sci.*, **7**, 100, doi:10.3389/feart.2019.00100.

[3] Frouin, R.J., B.A. Franz, A. Ibrahim, K. Knobelspiesse, Z. Ahmad, B. Cairns, J. Chowdhary, H.M. Dierssen, J. Tan, O. Dubovik, X. Huang, A.B. Davis, O. Kalashnikova, D.R. Thompson, L.A. Remer, E. Boss, O. Coddington, P.-Y. Deschamps, B.-C. Gao, L. Gross, O. Hasekamp, A. Omar, B. Pelletier, D. Ramon, F. Steinmetz, and P.-W. Zhai, 2019: Atmospheric correction of satellite ocean-color imagery during the PACE Era. *Front. Earth Sci.*, **7**, 145, doi:10.3389/feart.2019.00145.

A laboratory Pi-polarimeter to evaluate light scattering by complex-shaped particles at near and exact backscattering: mineral dust, soot aggregates, core-shell organic sulfates

A. Miffre[1,*] D. Cholleton[1] and P. Rairoux[1]

[1] *Institute of Light and Matter, Lyon University, F-69622, Villeurbanne, France*
[*] *corresponding author's e-mail: alain.miffre@univ-lyon1.fr*

While mineral dust and soot particles are known to contribute to the Earth's radiative budget by scattering and absorption, no analytical solution of the Maxwell's equations exists for such complex-shaped particles, presenting a highly irregular shape, sometimes with sharp edges and surface roughness as for mineral dust or fractal aggregates as for soot particles [1]. Hence, despite major recent advances in both numerical and laboratory fields, light scattering by such complex-shaped particles is difficult to quantify and the phase matrix can only be obtained in limited scattering regions, from 3° to 177°, as underscored in [2]. Interpolations to the 180°-backscattering angle are then to be discussed for such irregularly-shaped particles, as recently underlined [2,3]. This requires to increase the scattering angle range accessible to laboratory light scattering experiments, to cover the gap from 177° up the 180°-backscattering angle.

In this context, a controlled laboratory experiment has been built and operated which complements existing laboratory experimental set-ups by providing precise evaluation of the scattering matrix elements of mineral dust, from 176.0 to 180.0° scattering angle with a 0.4° step [4]. Interestingly, T-matrix numerical simulations agree with our laboratory polarimeter, showing the applicability of the spheroidal model to describe light scattering by mineral dust also at near and exact backscattering angles. Besides, our laboratory Pi-polarimeter also provides accurate evaluations of F_{22}/F_{11} at the strict lidar backscattering of Pi at UV and VIS-wavelengths simultaneously, which may be used in 2λ-polarization lidar applications. Hence, for the first time, the particles depolarization ratio of freshly-emitted soot aggregates could be evaluated in laboratory [5]. Various mineral dust samples have also been studied. Moreover, within the sensitivity and accuracy of our laboratory Pi-polarimeter, we could reveal a net decrease in light backscattering by the sulfate aerosol in the presence of organic compounds, giving rise to core-shell structures [6]. For the involved organics are among the most important secondary organic aerosol precursors in the atmosphere, this laboratory finding may be key for quantifying the direct radiative forcing of sulfates in the presence of organic compounds, thus more clearly resolving the impact of such aerosol particles on the Earth's climate.

References

[1] Michael I. Mishchenko. *Electromagnetic Scattering by Particles and Particle Groups. An Introduction*. Cambridge University Press, Cambridge, 2014.
[2] Huang X, G. Kattawar, P. Yang, K.N. Liou, J. Quant. Spectrosc. Radiat. Transfer, 151:97-109, 2015.
[3] Videen G , E. Zubko, J.A. Arnold, N. McCall, AJ. Weinberger, Y. Shkuratov, O. Munoz., J. Quant. Spectrosc. Radiat. Transfer, 211:123-128, 2018.
[4] Miffre, A., Cholleton, D., and P. Rairoux, J. Quant. Spectrosc. Radiat. Transfer, 222:45-59, 2019.
[5] Paulien, L., R. Ceolato, F. Foissard, P. Rairoux and A. Miffre, (UV, VIS) Laboratory evaluation of the lidar depolarization ratio of freshly emitted soot aggregates from pool fire in ambient air at exact backscattering angle, J. Quant. Spectrosc. Radiat. Transfer, 260:107451, 2021.
[6] Dubois, C., D. Cholleton, R. Gemayel, Y. Chen, J.D. Surratt, C. George, P. Rairoux, A. Miffre and M. Riva, Decrease in sulfate aerosol light backscattering due to reactive uptake of epoxydiols, Phys. Chem. Chem. Phys, 23:5927-5935, 2021.

Laboratory evaluation of the scattering matrix of complex-shaped ragweed pollen particles at near and exact backscattering

A. Miffre[1,*] D. Cholleton[1], E. Bialic[2], A. Dumas[2], P. Kaluzny[2], and P. Rairoux[1]

[1] *Institute of Light and Matter, Lyon University, F-69622, Villeurbanne, France*
[2] *Tera-sensor, Rousset, France*
[*] *corresponding author's e-mail: alain.miffre@univ-lyon1.fr*

While pollen particles are impacting human health through allergies and expected to play a more significant role on the Earth's climate in the forthcoming decades, ragweed pollen particles are seldom studied in the literature, except the contribution by Berg and Videen [1]. One possible explanation is that there is no analytical solution of the Maxwell's equations exists for such large size and complex-shaped particles [2]. Indeed, microscopic images of ragweed pollen exhibit a near but non-spherical overall shape, due to regular spikes and holes and a whole diameter of about 20 µm [3], which are, to our knowledge, beyond the reach of numerically exact light-scattering methods. Controlled laboratory experiments are highly desirable in this context.

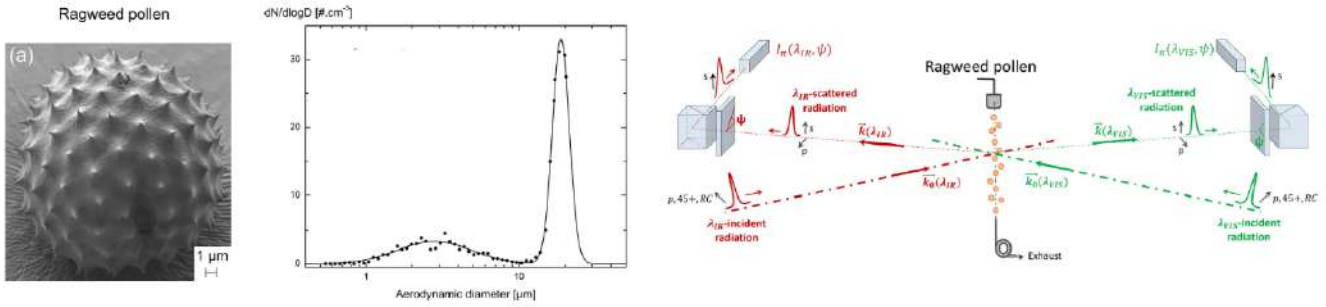

Figure 1: Ragweed pollen microscopic image (overall shape but regular spikes and one hole), size distribution and controlled-laboratory light-scattering experiment for retrieving the ragweed pollen scattering matrix [3].

This contribution is dedicated to laboratory light scattering measurements on ragweed pollens particles embedded in ambient air. The non-spherical complex shape of ragweed pollen is accounted for by applying the scattering matrix formalism [2] with a laboratory polarimeter operating at two wavelengths simultaneously (532 and 1064 nm) [3] and several scattering angles, ranging from 176 to 180°. Interestingly, our laboratory experiment exhibits sufficient sensitivity and accuracy to reveal the spectral dependence of the scattering matrix elements of ragweed pollen [3]. We believe this contribution may interest researchers working on light-scattering numerical models as well as experimentalists, working in the atmospheric lidar and biological communities.

References

[1] Berg, MJ , G. Videen, J. Quant. Spectrosc. Radiat. Transfer, 112: 1776-1783, 2011.
[2] Michael I. Mishchenko. *Electromagnetic Scattering by Particles and Particle Groups. An Introduction*. Cambridge University Press, Cambridge, 2014.
[3] Cholleton, D., E. Bialic, A. Dumas, P. Kaluzny, P. Rairoux, A. Miffre, J. Quant. Spectrosc. Radiat. Transfer, 254: 107223, 2020.

Polarization lidar: Investigating the dependence of Backscattering Ångström exponents with the particles size, shape and complex refractive index

A. Miffre[1,*] D. Cholleton[1] and P. Rairoux[1]

[1] *Institute of Light and Matter, Lyon University, F-69622, Villeurbanne, France*
[*] *corresponding author's e-mail: alain.miffre@univ-lyon1.fr*

In 1 929, while studying the ability of light scattering to reveal the size of atmospheric dust, A. Ångström published a paper [1] where he introduced a quantity that he called *a* and noted that "*the larger the particles, the smaller was the value found for a*." Today, the particles backscattering Ångström exponent BAE_p, i.e., the value of *a* in the backward scattering direction, is considered as a qualitative particle size indicator and remotely evaluated every day from atmospheric multi-wavelength lidar instruments [2]. However, according to the light scattering theory [3], particles backscattering Ångström exponents, which describe the wavelength dependence of lidar particles optical backscatter (β_p) between wavelength pair (λ_1, λ_2), depend on the particle size, shape, and complex refractive index. This dependence is however implicit and hence difficult to handle.

In this contribution, we investigate the dependence of backscattering Ångström exponents with the particles size, shape and complex refractive index [4]. The basic idea is to revisit backscattering Ångström exponents by taking benefit from light polarization. Where previous interpretation of Ångström exponent was that of a particle size indicator, using light polarization, we investigate the Ångström exponent dependence on the particle shape, by separately retrieving the backscattering Ångström exponent of the spherical (*s*) and non-spherical (*ns*) particles contained in an atmospheric particle mixture (*p*) = {*s*, *ns*}. As an output, analytical solutions of the Maxwell's equations (Lorenz–Mie theory, spheroidal model) are then applied to investigate the Ångström exponent dependence on the particle size and complex refractive index for each assigned shape. Interestingly, such lidar-retrieved vertical profiles of backscattering Ångström exponents specific to *s*- and *ns*-particles can be used by the lidar remote sensing community in complement to existing inversion algorithms, to improve the accuracy of the retrievals, by reducing the range of involved particle sizes and complex refractive indices, and this for both *s* and *ns* particle shapes [4]. An example of application of this new methodology is proposed on a case study dedicated to the lidar remote sensing observation of a nucleation event promoted by mineral dust [5].

References

[1] Ångström, A., Geografiska Annaler 11, 156, 1929.
[2] Haarig, M., A. Ansmann, H. Baars, C. Jimenez, I. Veselovskii, R.Engelmann, and D. Althausen, Atmos. Chem. Phys. 18: 11847, 2018.
[3] Michael I. Mishchenko. *Electromagnetic Scattering by Particles and Particle Groups. An Introduction*. Cambridge University Press, Cambridge, 2014.
[4] Miffre A., D. Cholleton and P. Rairoux, 2020: Opt. Lett., 45:1084-1087, 2020.
[5] Miffre A, D Cholleton, T. Mehri and P Rairoux, Rem. Sensing, 11(15), 1761, 2019.

Application of relationship between reflectivity and lidar depolarizaition ratio. AERONET data case.

K. Shmirko[1,2*], V. Lisitsa[1,2], E. Zubko[2], and A. Pavlov[1]

[1] *Institute of Automation and Control Processes FEB RAS*
[2] *Far Eastern Federal University*
[*] *e-mail: shmirko.konstantin@gmail.com*

May 1, 2021

The Umov law describes qualitatively an inverse correlation between the reflectivity of a target surface and the maximum value of the linear polarization that initially unpolarized incident light acquires when scattered from that surface. In the article [1] we found that the logarithm of the geometric albedo $\log(A)$ of polydispersions of agglomerated debris particles approximately correlates with their lidar linear or circular depolarization ratios, μ_L. In the analysis for the simplicity we assume that agglomerated debris particles obey a power-law size distribution $N(r) \sim r^{-n}$.

But the power-law size distribution is the simplification, that didn't reprsent important features of aerosol distribution. Of the various mathematical functions that have been proposed, the log-normal distribution [2] often provides a good fit and is regularly used in atmospheric applications. In most cases this distribution have two modes.

In our analysis we use AERONET INVERSION PRODUCT V3 dataset for the period from 2004 to 2020 for Ussuriisk station. All the data from AERONET passed to a procedure, that for every row calculates geometric albedo taking into account spheroidal shape of a particles. Spheroids mixture is defined by [3]. In out study total aerosol concentration is calculated as $N_{tot} = N_s + N_{ns} = f \cdot N_{tot} + (1 - f) \cdot N_{tot}$ where f - spheroid fraction, N_s - number concentration of spherical particles, N_{ns} - of nonspherical ones.

In the article [1] we found that $\log A = a \cdot \mu_l + c$ (model 2). In this paper for the case of bimodal lognormal disrtibution the equation $\log A = a \cdot \mu_l + b \cdot mr + c$ (model 1) has better fit of experimental data. Here a, b, c - fiting parameters.

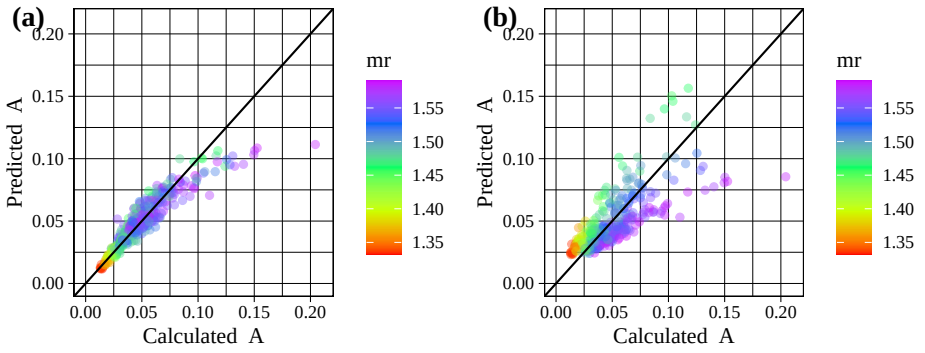

Figure 1: Sun photometer data. Bimodal size distribution. Sphericity less than 5%. a) model 1, b) model 2

On the figure 1 scattering diagrams shows quality of model 1 and model 2 for real data. For model 1 we achieve $R^2 = 0.91$ and for model 2 $R^2 = 0.61$. We also found that regression equations are applicable for data with amount of spherical particles less than 15%.

References

[1] Evgenij Zubko, Konstantin Shmirko, Andrey Pavlov, Wenbo Sun, Gorden Videen, Yongxiang Hu, Snorre Stamnes, Ali Omar, Rosemary Baize, Patrick McCormick, Robert Loughman, Jessica Arnold, and Gregory Schuster *Active remote sensing of atmospheric dust using relationships between their depolarization ratios and reflectivity.* Optics Letters, doi:10.1364/OL.426584, 2021.

[2] Aitchison, J., and J. A. C. Brown. 1957. *The Lognormal Distribution.* Cambridge University Press, Cambridge 1957

[3] Dubovik, O. and Sinyuk, A. and Lapyonok, T. and Holben, B. N. and Mishchenko, M. and Yang, P. and Eck, T. F. and Volten, H. and Muñoz, O. and Veihelmann, B. and van der Zande, W. J. and Leon, J.-F. and Sorokin, M. and Slutsker, I. *Application of spheroid models to account for aerosol particle nonsphericity in remote sensing of desert dust.* J. Geophys. Res., 111, 2006.

Shining from all sides: orientation-averaged optical properties of nanoparticle assemblies

Atefeh Fazel-Najafabadi[1,2], Sebastian Schuster[1,2], and Baptiste Auguié[1,2,*]

[1] *School of Chemical and Physical Sciences, Victoria University of Wellington, New Zealand*
[2] *The MacDiarmid Institute for Advanced Materials and Nanotechnology, Wellington, New Zealand*
[*] *Presenting and corresponding author:* baptiste.auguie@vuw.ac.nz

Nanoparticles can substantially affect the absorption of light in materials, raising considerable interest for such diverse applications as light-harvesting in solar cells, photothermal therapy, or surface-enhanced optical spectroscopies [1]. With advances in nanotechnology and synthesis, artificial nanostructures have been proposed that combine a number of nanoparticles into rigid aggregates with well-defined positions and orientations in space, such as oligomers [2] or helices, for example. The optical properties of such nano-aggregates can reveal a complex interplay between the individual nanoparticles' response, and collective multiple-scattering interactions that depend crucially on the relative positions and orientations of neighbouring particles. Often such particles aggregate are synthesised and/or used in solution, and consequently are randomly oriented.

The superposition T-matrix framework is a powerful method for the theoretical description of light scattering by such aggregates; it enables fast and accurate computations of far-field cross-sections as well as near fields. A particular strength of the method lies in the prediction of orientation-averaged quantities: the T-matrix captures the optical response of the particles independently of the incident field, and the properties of vector spherical harmonics used to describe incident and scattered fields enable the derivation of analytical formulas for orientation-averaged optical properties. This powerful formalism enables benchmark calculations for various quantities of interest, which include orientation-averaged extinction, scattering and absorption [3, 4], circular dichroism [5], but also near-field intensity [6], and more recently the local degree of optical chirality [7, 8]. Although analytical, the orientation-averaged expressions can become quite involved, and their evaluation is not necessarily faster than performing purely numerical orientation-averaging by simulating the optical properties for a discrete number of incidence directions, with a numerical quadrature [9, 10].

We will discuss a comparison of different numerical quadrature methods and their application in orientation-averaging of optical properties – both in the far-field and in the near-field. Specifically, we have implemented several schemes of spherical cubature, including Gauss-Legendre, Fibonacci, Lebedev, Spherical Designs, and Quasi-Monte Carlo; their relative strengths or drawbacks are first illustrated on toy problems such as standard integrands and combinations of spherical harmonics, followed by realistic light scattering problems of varying degree of difficulty. We use the analytical results as a benchmark for accuracy, and compare the convergence rate of the different methods with increasing number of incidence angles. The results are also of interest in the theoretical modelling of nanoparticle assemblies using other numerical methods, where the computation of orientation-averaged quantities must be done numerically without analytical results to use as a benchmark.

References

[1] L. Novotny and B. Hecht, *Principles of nano-optics*. Cambridge Univ, 2006.
[2] M. Hentschel, D. Dregely, R. Vogelgesang, H. Giessen, and N. Liu, "Plasmonic oligomers: The role of individual particles in collective behavior," *ACS Nano*, vol. 5, pp. 2042–2050, 03 2011.
[3] M. Mishchenko, "Extinction of light by randomly-oriented non-spherical grains," *Astrophysics and space science*, vol. 164, no. 1, pp. 1–13, 1990.
[4] N. G. Khlebtsov, "Orientational averaging of light-scattering observables in the T-matrix approach," *Applied Optics*, vol. 31, no. 25, pp. 5359–5365, 1992.
[5] R. N. S. Suryadharma and C. Rockstuhl, "Predicting Observable Quantities of Self-Assembled Metamaterials from the T-Matrix of Its Constituting Meta-Atoms," *Materials*, vol. 11, p. 213, 1 2018.
[6] J.-C. Auger and B. Stout, "Local field intensity in aggregates illuminated by diffuse light: T matrix approach," *Applied Optics*, vol. 47, pp. 2897–2905, 6 2008.
[7] Y. Tang and A. E. Cohen, "Optical chirality and its interaction with matter," *Physical Review Letters*, vol. 104, p. 163901, 4 2010.
[8] A. Fazel-Najafabadi, S. Schuster, and B. Auguié, "Orientation averaging of optical chirality near nanoparticles and aggregates," *Phys. Rev. B*, vol. 103, p. 115405, 2021.
[9] A. Penttilä and K. Lumme, "Optimal cubature on the sphere and other orientation averaging schemes," *Journal of Quantitative Spectroscopy and Radiative Transfer*, vol. 112, no. 11, pp. 1741–1746, 2011.
[10] Y. Okada, "Efficient numerical orientation averaging of light scattering properties with a quasi-Monte-Carlo method," *Journal of Quantitative Spectroscopy and Radiative Transfer*, vol. 109, no. 9, pp. 1719–1742, 2008.

The use of Debye's series and a ray-tracing technique to study near-backscattering polarization of coated particles

Meng Li [1] and Lei Bi [1,*]

[1] *Key Laboratory of Geoscience Big Data and Deep Resource of Zhejiang Province, School of Earth Sciences, Zhejiang University, Hangzhou, 310027, China.*

[*] *corresponding author's e-mail: bilei@zju.edu.cn*

Abstract

Inhomogeneous particles with a core-mantle structure can be frequently observed in the atmosphere. For example, sea salt aerosols may contain solid cores as the ambient humidity decreases to a certain threshold [1]. This feature is common for hygroscopic aerosols which uptake water vapor in the atmosphere to form a water coating. In this study, we systematically examined the optical properties of inhomogeneous coated particles. In particular, we focused on studying how the near-backscattering polarization change with the particle inhomogeneity and size, because near-backscattering signals could be observed by a passive polarimetry instrument aboard on a satellite.

In our simulations, we used the Lorenz-Mie theory and the invariant imbedding T-matrix method [2,3] to compute the optical properties of homogeneous and inhomogeneous spheres, respectively. We found that the inhomogeneous sphere causes a negative extreme of $-P_{12}/P_{11}$ at the scattering angle between 170°–175°, but the homogeneous sphere model has no this optical phenomenon. Next, the physical mechanism of the near-backscattering polarization was explored by using Debye' series and a ray tracing technique, following the theoretical formalisms given in [4]. Physically, the negative extreme of $-P_{12}/P_{11}$ was found to stem from the incident rays passing through the core of coated sphere and undergoing one internal reflection upon the host particle interface. The reflection angle involved in the internal reflection was found to be close to the Brewster's angle. Finally, the polarized radiance on the top of atmosphere (TOA) was simulated by using an adding-doubling radiative transfer method [5]. According to our theoretical simulations, the negative extreme of near-backscattering $-P_{12}/P_{11}$ could cause observable negative polarized radiance at the scattering angle between 170°–175°, which was further confirmed by analyzing the PARASOL (Polarization and Anisotropy of Reflectances for Atmospheric Science coupled with Observations from a Lidar) observational data for sea salt aerosols. The implications for this study for accurate radiative transfer and relevant remote sensing studies will be discussed.

References

[1] J. Zeng et al *Sea salt deliquescence and crystallization in atmosphere: An in situ investigation using x-ray phase contrast imaging.* Surf. Interface Anal., 45:930–936, 2013.

[2] L. Bi, P. Yang, G. W. Kattawar, and M. I. Mishchenko *Efficient implementation of the invariant imbedding T-matrix method and the separation of variables method applied to large nonspherical inhomogeneous particles.* J. Quant. Spectrosc. Radiat. Transf, 116:169–183, 2013.

[3] L. Bi and P. Yang *Accurate simulation of the optical properties of atmospheric ice crystals with the invariant imbedding T-matrix method*. J. Quant. Spectrosc. Radiat. Transf, 146:158–174, 2014.

[4] P. Laven and J. A. Lock *Understanding light scattering by a coated sphere Part 1: Theoretical considerations*. J. Opt. Soc. Am. A, 29:1498, 2012.

[5] X. Huang, P. Yang, G. Kattawar, and K. N. Liou *Effect of mineral dust aerosol aspect ratio on polarized reflectance*. J. Quant. Spectrosc. Radiat. Transf, 151:97–109, 2015.

Negative Polarization in Comet 29P/Schwassmann–Wachmann

A. Kochergin[1,2,*], E. Zubko[3], E. Chornaya[1,2], M. Zheltobryukhov[2], G. Videen[3,4], G. Kornienko[2], S.S. Kim[3,5]

[1]*School of Natural Sciences, Far Eastern Federal University, Russia*
[2]*Institute of Applied Astronomy of RAS, Russia*
[3]*Humanitas College, Kyung Hee University, South Korea*
[4]*Space Science Institute, 4750 Walnut Street, Boulder Suite 205, CO 80301, USA*
[5]*Department of Astronomy and Space Science, Kyung Hee University, South Korea*
[*]*corresponding author's e-mail: kochergin.av@outlook.com*

Introduction and Observations

Comet 29P/Schwassmann–Wachmann holds a special place among other small bodies in the Solar System, as the comet has remained continuously active for nearly a century, since its discovery in 1927 [1]. Its suggests it is a member of the Jupiter-Family Comets (JFC); whereas, the 29P/S-W nucleus is giant compared to other JFCs, having a diameter of ~60 km (e.g., [1] for review). We conducted observations of the comet during five nights between February 3 and 10, 2021, using the *RC500* telescope (D = 0.5 m; F = 4 m) at the Ussuriysk Astrophysical Observatory, a division of the Institute of Applied Astronomy of RAS. This telescope is equipped with a CMOS detector *ZWO ASI 6200 pro* (resolution – 9576 × 6388, size of pixel – 3.76 μm) that is used in the 2 × 2 binning mode. We monitored the degree of linear polarization in Comet 29P/S–W with the broadband R filter of the Bessell photometric system (efficient wavelength λ_{eff} = 0.64 μm and FWHM = 0.16 μm), which is a glass analog of the Cousins R filter devised for CCD detectors. Reduction of observations is similar to what was previously used in polarimetric studies of other comets (e.g., [2]). We calculate the degree of linear polarization using an aperture centered at the 29P/S-W nucleus and having radii of ρ = 10,000 km and ρ = 27,000 km. This is the first monitoring of the polarization in Comet 29P/S-W during a period of its quiescent activity.

Results

The degree of linear polarization $P_Q = -Q/I$, where I and Q are the Stokes parameters, appears to have negative sign on all five epochs. It is worth noting that during our observations, the phase angle of 29P/S-W remained nearly constant at α ≈ 9.5°, where the negative polarization in other comets attains its minimum value (e.g., [3] for review). Over the course of our observations, the polarization remained nearly constant, P_Q ≈–2.1%. It is worth noting that the negative polarization has several immediate implications. First of all, it reveals a negligible contribution of the gaseous emissions in the light-scattering response from Comet 29P/S-W [3]. Our modeling of the negative polarization using agglomerated debris particles also constrains the material absorption of the cometary dust. In at least one type of particles, the imaginary part of refractive index should be less than 0.1 [4].

References

[1] R Miles et al. *Anatomy of outbursts and quiescent activity of Comet 29P/Schwassmann–Wachmann*. Icarus, 272:327–355, 2016.
[2] E. Chornaya et al. *Imaging polarimetry and photometry of comet 21P/Giacobini Zinner*. Icarus, 337:113471, 2020.
[3] E. Zubko et al. *The positive-polarization of cometary comae*. Planet. Space Sci., 123:63-76, 2016.
[4] E. Zubko et al. *Evaluating the carbon depletion found by the Stardust mission in Comet 81P/Wild 2*. Astron. Astrophys., 544:L8, 2012.

Airy theory revisited with VCRM and physical optics

C. Zhang[1], C. Rozé[1], and K. F. Ren[1*]

[1] *UMR 6614/CORIA, CNRS - Université et INSA de Rouen, Avenue de l'Université BP 12, 76801 St-Etienne du Rouvray, France*
[*] *corresponding author's e-mail: fang.ren@coria.fr*

Abstract

Airy published a paper in 1838 to remedy the problem of the infinite intensity in the rainbow angles of a spherical droplet predicted by the geometrical optics (GO) [1]. His theory has been studied by mathematicians and physicists since then from different points of view [2]. Airy theory predicts the main and secondary peak positions and amplitudes as function of the refractive index and the particle size. Therefore, it is still largely used in the optical particle measurement though it is known that its precision is limited compared to the rigorous theories [3].

In this communication, the Airy theory is revisited with the Vectorial Complex Ray model (VCRM) [4] and the physical optics (PO). Two key points are examined: The first is that the cubic phase function in Airy theory is obtained from the relation in the vicinity of the rainbow angles, but this is extended to infinity in the integration. The second is the assumption of constant amplitude of the emergent rays, which is not true because the amplitude varies due to the convergence and divergence of the wave on the curved surface of the particle.

We follow the idea of Airy, but the phase and the amplitude of the emergent rays are calculated in the framework of VCRM [4] with rigorous geometry. Figure 1 (a) shows that the phase on the virtual line v given by the cubic function of Airy [2] (red line with circles) is in good agreement with that calculated by VCRM (green line with diamants) around $v = 0$ (corresponding to the geometrical rainbow angle) but differs more and more when the point is far from 0. The variation of the amplitude is also significant, from about 0.1 to 0.35 for v in the range [-20,20].

The physical optics is then applied to calculate the scattered intensity according to the phase and the amplitude calculated by VCRM. Figure 1 (b) shows that the intensity predicted by our method (VCRM+PO) is in very good agreement with Debye theory (rigorous) while Airy peaks differ from Debye theory more and more with increase of the scattering angle and GO predict an infinite intensity in the rainbow angle ($\sim 138°$).

Furthermore, our method can be applied directly to particles of arbitrary shape with smooth surface.

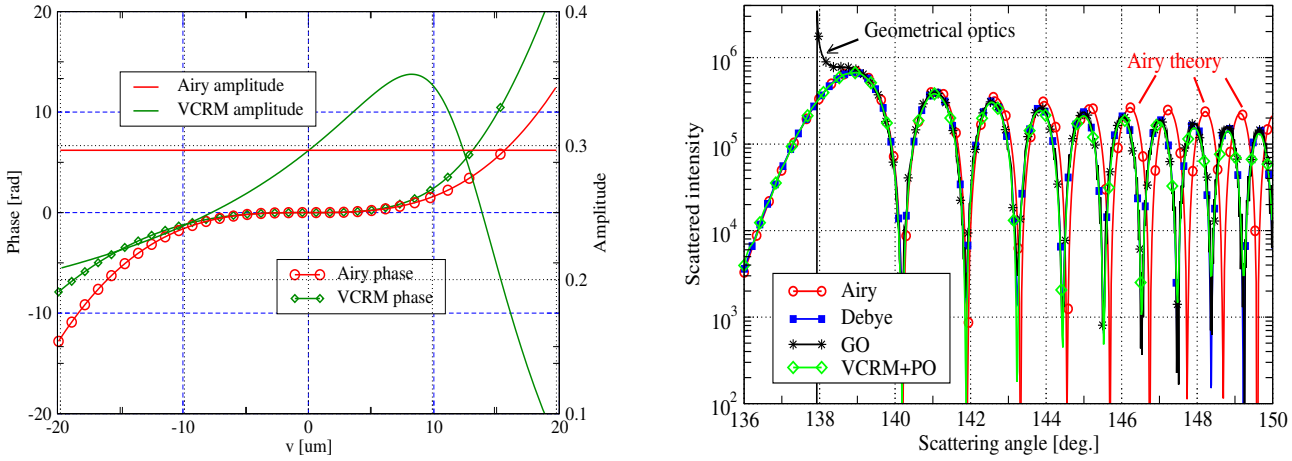

(a) Phase and amplitude on the virtual line.

(b) Scattering diagrams near the rainbow angle.

Figure 1: A plane wave of wavelength $\lambda = 0.6328$ μm is scattered by a spherical droplet of radius $a = 100$ μm and refractive index $m = 1.333$ for the order of ray $p = 2$. The incident wave is polarized perpendicularly to scattering plane.

References

[1] G. B. Airy, *On the intensity of light in the neighbourhood of a caustic*, Trans. Cambridge Phil. Soc., 6(:397-402, 1838

[2] H.C. van de Hulst, *Light scattering by small particles, Chap. 13.* Courier Corporation, 1981.

[3] E. Hovenac and J. Lock, *Assessing the contributions of surface waves and complex rays to far-field Mie scattering by use of the Debye series.* JOSA A, 9(5):781–795, 1992.

[4] K. F. Ren, F. Onofri, C. Rozé and T. Girasole, *Vectorial complex ray model and application to two-dimensional scattering of plane wave by a spheroidal particle.* Opt. Lett., 36(3):370–372, 2011.

Scattering of Non-paraxial Airy beam by the dielectric Ellipsoid particle based on T-matrix

Shu Zhang[1], Bing Wei[1], Qun Wei[1], Renxian Li[1,2,*], and Ningning Song[1]

[1] *School of Physics and Optoelectronic Engineering, Xidian University, Xi'an 710071, China*
[2] *Collaborative Innovation Center of Information Sensing and Understanding, Xidian University, Xi'an 710071, China*
[*] *corresponding author's e-mail: rxli@mail.xidian.edu.cn*

Abstract

According to relationship of momentum and angular momentum flux, it is possible for the optical forces and optical torques to trap the particle, realize micromanipulation [2] and binding [3]. Airy beam as one of the optical tweezer light sources, has great potential applications in particle manipulation [4], and handling along curved trajectories [5], with its special characteristic of auto-accelerating and auto-bending. The scattering of Airy beam is the basis of optical force and torque by Airy beam.

It is interesting to study the Airy beam scattering by the ellipsoid particle, including the distribution of scattering intensities, with the influence of transverse scale parameter and lobe width. The generalized Lorenz-Mie theory [1] (GLMT) is suitable for arbitrary illumination to the calculation of optical tweezer. However, the theory of GLMT is rigorous to homogeneous isotropic spheres. It is unavoidable for the optical tweezers to study the other particle shapes in daily research. Limited to the particle shapes, it is right for T-matrix [6] description of scattering, depending on the particle properties – the composition, size, shape, and direction of the particle, independent of the incident field. For any particular particle, the T-matrix needs to be computed only once, and can be repeated with the matrix for subsequent studies, which reduces the number of double counting.

Further, the present solution can be used to calculate the optical radiation force and torque, which is of great importance in particle transport and rotation.

References

[1] Gouesbet G, Gréhan G. *Generalized lorenz-mie theories* . Berlin: Springer, 2011.
[2] Gréhan G, Ren K F, Gouesbet G, et al. *Evaluation of a particle sizing technique based on laser sheets*. J. Particle & particle systems characterization, 1994, 11(1): 101-106.
[3] Rockstuhl C, Herzig H P. *Rigorous diffraction theory applied to the analysis of the optical force on elliptical nano-and micro-cylinders*. J. Journal of Optics A: Pure and Applied Optics, 2004, 6(10): 921.
[4] Baumgartl J, Mazilu M, Dholakia K. *Optically mediated particle clearing using Airy wavepackets*. J. Nature photonics, 2008, 2(11): 675-678.
[5] Siviloglou G A, Broky J, Dogariu A, et al *Observation of accelerating Airy beams*. J. Physical Review Letters, 2007, 99(21): 213901.
[6] Nieminen T A, Rubinsztein-Dunlop H, Heckenberg N R. *Calculation of the T-matrix: general considerations and application of the point-matching method*. J. Quant. Spectrosc. Radiat. Transfer, 2003, 79: 1019-1029.

A study of ultrahigh polarization of the active NEA asteroid (3200) Phaethon: observations and modeling

V. Rosenbush[1,2,*], N. Kiselev[3], D. Petrov[3], and V. Afanasiev[4]

[1]*Astronomical Observatory of Taras Shevchenko National University of Kyiv, Kyiv, Ukraine*
[2]*Main Astronomical Observatory of the National Academy of Sciences of Ukraine, Kyiv, Ukraine*
[3] *Crimean Astrophysical Observatory, Nauchnij, Crimea*
[4] *Special Astrophysical Observatory of the RAS, Nizhnij Arkhyz, Russia*
[*]*corresponding author's e-mail: vera.rosenbush@gmail.com*

Potentially hazardous asteroid (3200) Phaethon, discovered on October 11, 1983 by NASA's Infrared Astronomical Satellite, is a one of the most enigmatic objects among the known asteroids. It is classified as an asteroid but dynamically it associated with the Geminid meteoroid stream and, hence, its source, implying significant mass loss during its previous perihelion passages. Due to a very low perihelion (q = 0.14 au), Phaethon is not only a near-Earth asteroid (NEA) but also a near-Sun asteroid. Observations around perihelion in 2009 and 2012 obtained by the Solar and Terrestrial Relations Observatory revealed its strong brightening and a comet-like tail. This may suggest that Phaethon is an extinct or dormant comet, sometimes called a rock comet [1].

We present all available polarimetric data for asteroid Phaethon obtained in 2016–2020 with the B, V, R, and I filters. We observed asteroid Phaethon during its closest approach to the Earth on December 16, 2017 (the geocentric distance was 0.0768 au), when the phase angle (α) changed from 19.2° to 134.9° and on October 16, 2020 at α = 52.2°. The CCD spectropolarimetry and imaging polarimetry were performed at the 6-m telescope of the SAO RAS. Aperture polarimetry and photometry were carried out at the 2.6-m and 1.25-m of the CrAO.

From our and all available in the literature data, we obtained the phase-angle dependence of polarization for Phaethon and found that the maximum of linear polarization degree in the V+R bands is P_{max} = (45 ± 1)% at phase angle α_{max} = (124.0 ± 0.4)°. However, the polarization of the asteroid measured in the 2016 apparition by Ito et al. [2] at the large phase angles significantly differs from the data derived in 2017 at corresponding angles, up to 50% at α=106.5° in the R filter. A very high polarization at large phase angles indicates that geometric albedo of the object should be low. Actually, using dependence polarimetric slope–albedo, we found geometric albedo of asteroid Phaethon to be p_v = 0.061 ± 0.002. The obtained value of the geometric albedo is a much smaller than that derived from IR observations.

To calculate the scattering properties of dust particles on the Phaethon's surface, the Sh-matrix method was used [3]. A mixture of silicate forsterite particles and amorphous carbon particles was adopted as a substance model. Conjugated Random Gaussian particles were used as a model of irregular particles [4]. The main feature of these particles is the presence of both large-scale and small-scale surface roughness. The parameters of the scattering particles, such as the size distribution and the carbon/silicates ratio were selected in such a way as to best approximate the observational data. The obtained results of observations and their simulation will be presented.

References

[1] D. Jewitt, and J. Li, *Activity in Geminid parent (3200) Phaethon*. Astron. J., 140:1519–1527, 2010.
[2] T. Ito, M. Ishiguro, T. Arai et al. *Extremely strong polarization of an active asteroid (3200) Phaethon*. Nature Comm. 9:1-8, 2018.
[3] D. Petrov, Yu. Shkuratov, and G. Videen. *Light scattering by arbitrary shaped particles with rough surfaces: Sh-matrices approach*. J. Quant. Spectrosc. Radiat. Transfer, 113:2406-2418, 2012.
[4] D. V. Petrov, and N. N. Kiselev. *Conjugated Gaussian Random particle model and its applications for interpreting cometary polarimetric observations*. Sol. Syst. Res. 53:294–305, 2019.

Principal Component Analysis for the simultaneous characterisation of size and refractive index of dispersed particles in a fluid

D. Marwick[1,2,*], R. Poolman[1], and M. Mazilu[2]

[1]*Malvern Panalytical, Enigma Business Park, Grovewood Road, Malvern, WR14 1XZ*
[2]*School of Physics and Astronomy, University of St Andrews, St Andrews, KY16 9SS*
[*]*corresponding author's e-mail: dm271@st-andrews.ac.uk*

Laser diffraction is a measurement technique that is widely used to determine the size distribution of particles suspended in a fluid. This technique measures the scattering that occurs as a laser beam passes through a sample of these suspended particles. The angular intensity distribution of the scattered light is used along with modelled Mie scattering distributions to calculate the size of the particles in the sample.

Laser diffraction is used across many industries due to the speed, accuracy and reproducibility of the technique. However, the accuracy of the particle size determined by laser diffraction is dependent on many factors including the accuracy to which the particle refractive index is known. For many applications, particularly those where new materials are being developed, the refractive index of the measured particles is not well understood and is often estimated. In these cases, errors in the particle refractive index will lead to errors in the calculated particle size.

The objective of this work is to develop a new method to simultaneously extract the size and refractive index of a particle ensemble based on a single laser diffraction measurement. The method uses principal component analysis (PCA) to compare a measured angular intensity distribution with a training matrix of known scattering distributions. We have demonstrated a method to derive accurate size as well as complex refractive index and polydispersity properties from a modelled scattering distribution generated using the characteristics of a commercially available laser diffraction instrument.

How do cloud images form? → 2 intertwined diffusion processes

A. B. Davis, [1,*] L. Forster, [1,2] D. J. Diner, [1] and B. Mayer[2]

[1]*Jet Propulsion Laboratory, California Institute of Technology, Pasadena, California, USA*
[2]*Meteorological Institute, Ludwig-Maximilians-Universität, Munich, Germany*
[*]*corresponding author's e-mail: Anthony.B.Davis@jpl.nasa.gov*

Computed cloud tomography (CCT) is a promising new approach in remote sensing of large vertically-developed clouds using space-based imaging sensors with pixel scales in the 100s of meters. Prime examples are the Multi-angle Imaging Spectro-Radiometer (MISR) and the MODerate-resolution Imaging Spectrometer (MODIS), both on NASA's flagship Terra satellite. Current operational cloud property retrievals in the solar spectrum, which are grounded in 1D radiative transfer (RT) predictions for reflected radiation emanating from a single pixel and view angle at just two wavelengths. In sharp contrast, CCT embraces the 3D nature of real clouds and exploits collocated multi-spectral/multi-angle/multi-pixel data to recover volumetric information. However, CCT has been demonstrated so far only for rather small clouds using airborne sensors with ~20 m pixels [1].

A first step in the right direction was recently taken by Forster et al. [2] who defined the "veiled core" (VC) of large opaque clouds as the optically deep-enough region where detailed 3D structure of the cloud has negligible impact on the multi-angle/multi-spectral images as long as the mean VC extinction coefficient and any significant cloud-scale gradient are preserved. Quantitatively, the difference between radiance fields escaping the clouds is commensurate with sensor noise when said clouds differ only in the small-scale distribution of extinction inside their VCs.

An important corollary for the large and ill-posed CCT inverse problem is that the only unknowns of interest for the whole VC are its mean extinction coefficient and any potential cloud-scale vertical trend in that property. Another ramification for CCT algorithms currently under development for space-based sensor data is that the forward 3D RT model driving the inversion may be vastly simplified in the VC to gain efficiency. We explore here that possibility, assuming radiative diffusion as the simplified RT for the VC. On the way, we describe the relevant RT physics that unfold in the VC and in the outer shell (OS) of the cloud, where detailed spatial structure does matter for image formation. This includes control by the VC of the cloud-scale contrast between the brightness of illuminated and shaded cloud sides, as well as the gradual blurring of spatial structure via directional diffusion with increasing optical distance into the OS.

Transport space is a merger of 3D physical space and 2D direction space. Cloud image formation thus involves two radiative diffusion processes (i.e., random walks): one in each of these sub-spaces, depending on the prevailing transport regime [3]. Fortunately for the future of CCT, and of passive cloud remote sensing in general, there is a clear spatial separation: asymptotic limit of radiative diffusion in the VC, and standard RT with multiple scattering in the OS. A hybrid forward model for CCT will make use of this fact of life in cloud image formation.

References

[1] A. Levis, Y. Y. Schechner, A. Aides, and A. B. Davis. *Airborne three-dimensional cloud tomography*. 2015 IEEE International Conference on Computer Vision (ICCV), 3379-3387, https://doi.org/10.1109/ICCV.2015.386, 2015.

[2] L. Forster, A. B. Davis, D. J. Diner, and B. Mayer. *Toward cloud tomography from space using MISR and MODIS: Locating the "veiled core" in opaque convective clouds*. J. Atmos. Sci., 78:155-166, https://doi.org/10.1175/JAS-D-19-0262.1, 2021.

[3] A. B. Davis, L. Forster, D. J. Diner, and B. Mayer. *Toward cloud tomography from space using MISR and MODIS: The physics of image formation for opaque convective clouds*. J. Atmos. Sci. (in preparation), https://arxiv.org/abs/2011.14537, 2021.

Polarization constraints on core-mantle interstellar dust grains

P. Polimeno[1,2], M.A. Iatì[2,*] R. Saija[1,2], and C. Cecchi-Pestellini[3]

[1]*Dipartimento di Scienze Matematiche e Informatiche, Scienze Fisiche e Scienze della Terra, Università degli Studi di Messina, Italy*
[2]*CNR-IPCF, Istituto per i Processi Chimico-Fisici, Messina, Italy*
[3]*INAF-Osservatorio Astronomico di Palermo, Italy*

[*] *mariaantonia.iati@cnr.it*

The 3.4 μm feature and its implications for the nature of carbon dust

The structure of interstellar dust grains and whether the carbon and the silicate components are separated or not is still a much-debated issue [1]. The core-mantle model, a silicate core covered by a carbon shell, has been challenged by the spectropolarimetric observations of the feature at 3.4 μm. Such absorption feature, observed in the diffuse interstellar medium, is commonly attributed to the C-H stretching mode in aliphatic hydrocarbons residing in some components of interstellar dust. Chiar et al. [2] found that this feature is negligibly polarized for a line of sight toward the Galactic Center. Such evidence, together with the observation of a strong polarization in the silicate feature at 9.7 μm along the same sightline, suggests that carbon and silicate grains are separate components. In this picture the silicate grains appear to be non-spherical and aligned so as to originate the observed strong polarization feature at 9.7 μm, while the carbon grains should not be aligned to explain the non-detection of polarization in the 3.4 μm feature. This last assumption for a separate carbon component is reasonable due to the carbon diamagnetic nature which does not favor alignment.

Are silicate and carbon necessarily separate components of interstellar dust? Should we definitely rule out the core-mantle dust model? We investigate the problem using a wide range of silicate-carbon core-mantle grain models, comparing the computed polarization of the 3.4 μm feature with the observational upper limit.

Additional information

The layered grains have been modelled as central spherical silicate cores covered by two carbon mantles, an inner sp^2 carbon layer and an outer sp^3 layer [3]. Such stratified spheres have been aggregated in composite (compact or fluffy) and partially aligned structures. Their extinction and polarization properties have been computed through the Transition matrix method [4].

References

[1] Qi Li, S. L. Liang and A. Li *Spectropolarimetric constraints on the nature of interstellar grains.* Mon. Not. R. Astron. Soc. L, 440:56-60, 2014
[2] J. E. Chiar, A. J. Adamson, D. C. B. Whittet, et al. *Spectropolarimetry of the 3.4 μm feature in the diffuse ISM toward the Galactic Center quintuplet cluster*. Astrophys. J., 651:268-271, 2006
[3] M. A. Iatì, R. Saija, F. Borghese, P. Denti, C. Cecchi-Pestellini, and D. A. Williams *Stratified dust grains in the interstellar medium – I. An accurate computational method for calculating their optical properties.* Mon. Not. R. Astron. Soc., 384:591-598, 2008
[4] F. Borghese, P. Denti and R. Saija. *Scattering by model non-spherical particles.* 2nd edn. Springer, 2007

FORMA and BEFORE: expanding applications of optical tweezers

L. Pérez García[1,*], M.Selin[1], A. Magazzù[2], G.Volpe[3], A. V.Arzola[4], I. Pérez Castillo[5], and G.Volpe[1]

[1] *Department of Physics, University of Gothenburg, Gothenburg, Sweden*
[2] *CNR-IPCF, Istituto Processi Chimico-Fisici, V.le F. Stagno D'Alcontres 37, 98158 Messina, Italy,*
[3] *Department of Chemistry, University College London, 20 Gordon Street, London WC1H 0AJ, UK*
[4] *Instituto de Física, Universidad Nacional Autónoma de México, Cd. de México, C.P. 04510, México*
[5] *Departamento de Física, Universidad Autónoma Metropolitana Iztapalapa, San Rafael Atlixco 186, Ciudad de México 09340, México*
[*] *corresponding author's e-mail: laura.perez.garcia@physics.gu.se*

Force reconstruction via Maximum Likelihood estimator

We recently introduced force reconstruction via maximum-likelihood-estimator analysis (FORMA) to calculate the stiffness of a trap κ acting on a Brownian particle by analyzing its trajectory displacements. FORMA exploits the linear relationship between the time series of the position of a Brownian particle x_n and drag forces $f_n = \gamma \frac{\Delta x_n}{\Delta t_n}$ at instant n.

$$f_n = -\kappa x_n + \sigma w_n$$

Where $\sigma = \sqrt{\frac{2D\gamma^2}{\Delta t}}$ and w_n is a random Gaussian number with zero mean and unit variance. We apply a maximum likelihood estimator to obtain the most probable values of the stiffness κ^*, obtaining $\kappa^* = -\frac{\sum_n x_n f_n}{\sum_n x_n^2}$.Which can also be interpreted as a linear fit where κ^* is the slope of the linear fit to the data pairs $\{\mathbf{x}, \mathbf{f}\}$ and σ is related with the dispersion of the data.

FORMA has proven to be faster, more precise, more accurate, and ten-fold less data-intensive than the previous well-established methods. Furthermore, with FORMA, we have characterized the force field's conservative and non-conservative components, which was not feasible with previous methods. Another key advantage of FORMA is that its application does not depend on the fine-tuning of a fitting parameter, which is the case of autocorrelation function method and power spectrum density method [1].

Using Bayesian inference

In the context of inference statistics, FORMA uses a linear non-Bayesian approach to estimate the properties of the force field and the diffusive properties of the particle. Recently, we have developed a method that uses Bayesian inference to expand and generalize FORMA.

With Bayesian Force Reconstruction (BEFORE), we have derived formulas for the posterior distribution for a set of parameters $\{D, \gamma, \kappa\}$ denoted by θ, also called a model. The posterior distribution $P(\theta|x, f)$ gives us the probability that a model θ explains the data-set provided by the vector pair $\{\mathbf{x}, \mathbf{f}\}$.

$$P(\theta|x, f) = \frac{\mathcal{L}(f|x, \theta)P_0(\theta)}{\int \mathrm{d}\theta' \mathcal{L}(f|x, \theta')P_0(\theta')} \tag{1}$$

Using more informative priors, BEFORE can provide reasonable estimates of the parameters even when little data is available; it can also be generalized to more than one dimension and be used for time series with any time interval Δt.

Both FORMA and BEFORE represent an approach for calibration of optical tweezers using statistical inference techniques.Their advantages become relevant whenever we have few data points, out of equilibrium systems, non-conservative forces, underdamped regime, or inhomogeneous time sampling. All these advantages will allow expanding experiments towards more complex scenarios such as biological systems, time-varying conditions, and active baths [2].

References

[1] Laura Pérez García et al. "High-performance reconstruction of microscopic force fields from Brownian trajectories" in *Nature Communications*, Vol. 9, 5166, (2018).

[2] Jan Gieseler et al."Optical Tweezers-from calibration o applications: atutorial" in *Adv. Opt. and Photon.*, 13, 74-241(2021)

Laboratory microwave analog measurements and simulations of dust in planet-forming disks

Vanesa Tobon Valencia[1,*], François Ménard[2], Jean-Michel Geffrin[1], Jean-Baptiste Renard[3], Hervé Tortel[1], Pascal Rannou[4], Christelle Eyraud[1], Julien Milli[2], Amélie Litman[1].

[1] *Aix Marseille Univ, CNRS, Centrale Marseille, Institut Fresnel, Marseille, France*
[2]*Univ. Grenoble Alpes, CNRS, IPAG, F-38000 Grenoble, France*
[3]*LPC2E, CNRS - Université d'Orléans - CNES, Orléans, France*
[4]*GSMA - Université de Reims, Reims, France*
[*]*corresponding author's e-mail: vanesa.tobon-valencia@fresnel.fr*

The microwave analogy is a well known method relying on the Scale Invariance Rule (SIR) that has been used to measure the scattering properties of objects that would otherwise be difficult to manipulate individually [1]. The SIR states that the scattering properties of analog particles measured at a different wavelength are equivalent to those of the original particles of the same shape, as long as the refractive index and the size-to-wavelength ratio are conserved. Over the years, our group at Fresnel Institute in Marseille has been studying a variety of analogs: from microorganisms [2] and trees [3] to asteroids [4]. In this presentation we will be focusing on dust found in the Solar System and in planet-forming disks, the ultimate goal being to provide direct observational constraints on the first phases of planet assembly, when tiny solid particles start to grow to form larger bodies. We have, for now, considered two types of particles: fractal-like aggregates and compact particles with rough surfaces [5]. These particles were produced by additive manufacturing where the possibility to control their shape, structure, and refractive index is unique and a definite advantage over other measurement methods. In this talk, we will summarize our first results on these protoplanetary dust analogs. We will detail how they are produced, what are the measurement conditions and the scattering results. In particular, the phase function and degree of linear polarization of these analogs will be presented, i.e., the elements S_{11} and $-S_{12}/S_{11}$ of the Mueller matrix respectively. An example of particles to be discussed is presented in figure 1. These measurements are compared to our numerical model [2] to validate the method and highlight their distinctive features, the ultimate goal being to retrieve the particles' properties like the surface roughness, fractal dimension (D_f), porosity and others. These results are the first laboratory measurements of protoplanetary dust disks analogs with controlled structures using the microwave analogy.

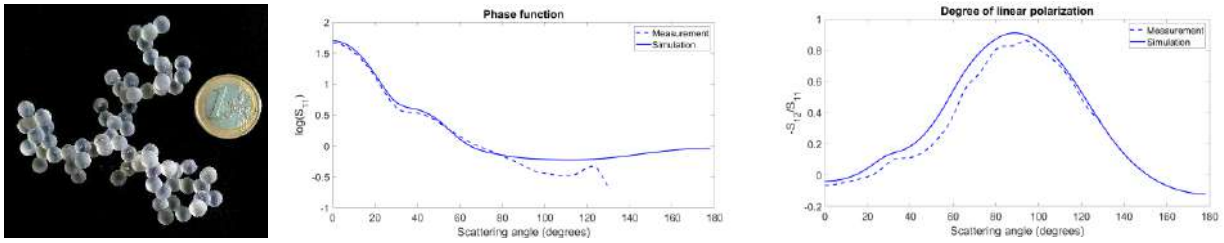

Figure 1: Scattering results of a printed aggregate with a D_f=1.7 and size parameter of the monomer of 0.6.

References

[1] J. M. Greenberg, et al. J Appl Phys, 1961, 32, pp. 233–242. https://doi.org/10.1063/1.1735984
[2] H. Saleh, et al. J Quant Spectrosc Radiat Transf, 2017, 196, pp.1–9. https://doi.org/10.1016/j.jqsrt.2017.03.024
[3] L. Hettak, et al. IEEE Geoscience and Remote Sensing Letters, 2020, 17 (6), pp.933. https://hal.sorbonne-universite.fr/hal-02474268
[4] C. Eyraud, et al. Astron Astrophys, 2020, 643, A68.. https://doi.org/10.1051/0004-6361/202038510
[5] J. B. Renard, et al. *Number of independent measurements required to obtain reliable mean scattering properties of irregular particles having a small size parameter, using microwave analogy measurements*. J Quant Spectrosc Radiat Transf (Accepted)

On the tomography of irregular rough particles using interferometric particle imaging

B. Delestre[1], A. Abad[1], M. Talbi[1], M. Fromager[2] and M. Brunel[1,*]

[1]UMR CNRS 6614 CORIA, Avenue de l'Université, BP 12, 76801 St-Etienne du Rouvray Cedex, France
[2]UMR CNRS 6252 CIMAP, 6 Bd Maréchal Juin, F-14050 Caen Cedex, France
[*]corresponding author's e-mail: marc.brunel@coria.fr

Introduction

The tomography of irregularly-shaped particles in a flow is particularly interesting in many domains. A single-shot technique that could tend to real-time analysis would be very attractive. Interferometric rough particle imaging, which consists in analyzing the speckle patterns generated by particles under laser illumination, is a promising candidate.

Results

In this study, the possibility to perform the tomography of irregularily-shaped translucent rough particles using multi-views interferometric particle imaging is investigated [1]. Combining three perpendicular angles of views, as illustrated on figure 1(a), we reconstruct the 3D-shape of particles from their three speckle patterns. The individual 2D-reconstructions are done for each view using the error-reduction algorithm [2]. The principle is tested numerically and confirmed experimentally by analysing sets of three interferometric images of "programmed" particles generated by a digital micromirrors device (DMD) [3]. Figure 1(b) shows an example of 2D-projection of a 3D-dendrite like particle reconstructed from three speckle-like interferometric images.

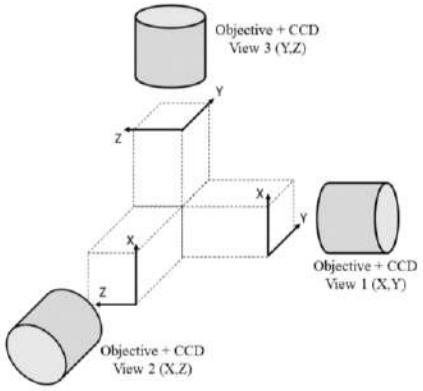

(a)

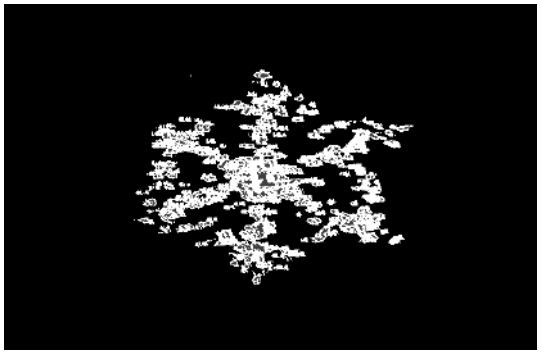

(b)

Figure 1: Multi-views interferometric particle imaging set-up (a) and projection of a reconstructed dendrite-particle (b)

References

[1] M. Talbi, G. Gréhan and M. Brunel *Interferometric particle imaging of ice particles using a multi-view optical system*. Appl. Opt. 57:6188-6197, 2018.

[2] R. Fienup, T.R. Crimmins and W. Holsztynski, *Reconstruction of the support of an object fro the support of its autocorrelation*. J. Opt. Soc. Am. 7:3-13, 1982.

[3] M. Fromager, K. Aït Ameur, and M. Brunel *Digital micromirror device as programmable rough particle in interferometric particle imaging.* Appl. Opt. 56:3594-3598, 2017.

Effect of scattering angle on Earth reflectance

Alexander Marshak[1*], Alfonso Delgado-Bonal[1,2] and Yuri Knyazikhin[3]

[1]*NASA/Goddard Space Flight Center, Greenbelt, MD, USA*
[2]*GESTAR/USRA, Greenbelt, MD, USA*
[3]*Earth and Environment Department, Boston University, Boston, MA, USA*
[*]*corresponding author's e-mail: Alexander.Marshak@nasa.gov*

Abstract

After March 2020 the range of scattering angle for DSCOVR EPIC (Earth Polychromatic Imaging Camera) has been substantially increased towards backscattering reaching 178 degrees. This provides a unique opportunity to observe correlation of reflectance with scattering angle. The dependence of reflection of scattering angle is shown separately for ocean and land areas, for cloudy and clear pixels, while cloudy pixels are also separated to liquid and ice clouds. A strong increase of reflectance towards back-scattering direction observed for all wavelengths. The spectral signature of the dependence indicates the strongest increase at near IR (780 nm) where contribution from vegetation dominates.

Light scattering in airborne ice crystals

Jarmo Moilanen[1,2,3*], Maria Gritsevich[1,2], and Marko Riikonen[3]

[1] *Finnish Geospatial Research Institute (FGI), Geodeetinrinne 2, Masala, Finland*
[2] *University of Helsinki, Faculty of Science, Gustav Hällströmin katu 2, Helsinki, Finland*
[3] *Ursa Astronomical Association, Helsinki, Finland*
[*] *corresponding author's e-mail: jarmo.moilanen@nls.fi*

Atmospheric halos are a light scattering phenomenon caused by airborne ice crystals in the atmosphere [1, 2, 3, and 4]. Halos can be seen by naked eye. They provide information to the observer on what kind of ice crystals are present in the sky during a halo display. Nearly 120 different identifiable halo forms are known today. Most known halos are made by crystals of hexagonal water ice (I_h). A combination of ice crystals' shape, their orientation, and light's ray paths through the crystals dictates what halos will be created. Some of the documented halos cannot be explained by using common hexagonal ice crystals. Abnormal crystal shape, crystals of cubic ice (I_c) or crystals of other minerals may be needed to explain these exotic halos [5, 6]. Halos can be seen also in the atmospheres of other planets providing insight of the airborne ice crystals or crystals of other minerals [7, 8].

In this presentation, we summarize current knowledge of atmospheric halos. We show which halo forms cannot be explained by ordinary hexagonal ice crystals and why. We also present some modern photographic technics applied recently to enhance documentation of halo displays.

Figure 1. A halo display in Kirkkonummi, Finland in 3rd May 2021.

References

[1] R. Greenler, 1980: *Rainbows, Halos and Glories*. Cambridge University Press, UK.
[2] W. Tape. 1994: *Atmospheric Halos*. Antarctic Research Series, Volume 64, AGU, Washington, D.C., USA.
[3] W. Tape and J. Moilanen, 2006: *Atmospheric Halos and the Search for Angle X*. AGU, Washington, D.C., USA.
[4] M. Riikonen, 2011: *Halot: Jääkidepilvien valoilmiöt*. A book (in Finnish, English translation available from the author). Ursa Astronomical Association, Helsinki, Finland.
[5] M. Riikonen., M. Sillanpää, L. Virta, D. Sullivan, J. Moilanen, and I. Luukkonen, 2000: *Halo observations provide evidence of airborne cubic ice in the Earth's atmosphere*. Applied Optics, 38, 6080-6085.
[6] N.A. Lefaudeux., 2011: *Crystals of hexagonal ice with (2 0 -2 3) Miller index faces explain exotic arcs in the Lascar halo display*. Applied Optics, 50, F121-F128.
[7] L. Cowley and M. Schroeder, 1999: *Forecasting Martian Halos*, Sky & Telescope, Dec '99, pp. 60-64.
[8] G.P. Können, 2006: *A halo on Mars*. Weather, 61, pp. 171-172, UK.

On the Simulation of the Absorbance of Ag-Au Alloyed Nanoparticles

A. Saidi[1,*], R. Saija[1,*], M. Santoro[1], E. Fazio[1], F. Neri[1], M. Tommasini[2], and P.M Ossi[3]

[1]*Dipartimento di Scienze Matematiche e Informatiche, Scienze Fisiche e Scienze della Terra, Universita' degli Studi di Messina, 98166 Messina, Italy*
[2]*Dipartimento di Chimica, Materiali e Ingegneria Chimica "G. Natta", Politecnico di Milano, 20133 Milano, Italy*
[3]*Dipartimento di Energia, Politecnico di Milano, 20133 Milano, Italy*
[*]*corresponding author's e-mail: asaidi@unime.it,rsaija@unime.it*

Abstract

Over the past twenty years, the study of plasmonic nanostructures has involved a large scientific community since their optical properties have proven to be of interest for their wide field of application that ranges from nanomedicine to nanotechnology [1,2]. Recently, considerable attention was paid to the properties of silver-gold alloy nanostructures suitable for many applications where individual metals do not have the desired characteristics [3]. Currently, the production, manipulation, and experimental characterization of these structures are carried out with state-of-the-art methodologies able to highlight all the potential applications [4,5]. From the theoretical point of view, despite the use of validated theoretical methods based on first-principle approaches, the simulated optical properties are susceptible to the choice of dielectric function model. For this reason, with the help of experimental measurements conducted in a controlled way and within the framework of the T matrix approach [6], this research carried out a theoretical study using the dielectric functions proposed in the literature identifying the reason why some of these models fail to describe the actual optical properties of alloy nanoparticles [7].

References

[1] G. Chen, I. Roy, C. Yang, and P. N. Prasad. *Nanochemistry and Nanomedicine for Nanoparticle-based Diagnostics and Therapy.* Chem. Rev. 2016, 116, 5, 2826–2885, 2016.

[2] M. Mesch, B. Metzger, M. Hentschel, and H. Giessen. *Nonlinear Plasmonic Sensing.* Nano letters 16.5: 3155-3159, 2016.

[3] C. Gong, A. Kaplan, Z. A. Benson, D. R. Baker, J. P. McClure, A. R. Rocha, and M. S. Leite. *Band Structure Engineering: Band Structure Engineering by Alloying for Photonics (Advanced Optical Materials 17/2018).* Advanced Optical Materials, 6(17), 1870066, 2018.

[4] V. Amendola and M. Meneghetti.
Laser ablation synthesis in solution and size manipulation of noble metal nanoparticles. Phys. Chem. Chem. Phys. 11, 3805-3821, 2009.

[5] G. Compagnini, E. Messina, O. Puglisi and V. Nicolosi. *Laser synthesis of Au/Ag colloidal nano-alloys: Optical properties, structure and composition.* Appl. Surf. Sci., 254, 1007-1011, 2007.

[6] F. Borghese, P. Denti, and R. Saija. *Scattering from model nonspherical particles: theory and applications to environmental physics.* Springer Science & Business Media, 2007.

[7] E. Fazio, R. Saija, M. Santoro, A. Saidi, F. Neri, M. Tommasini, and P. M. Ossi. *On the Optical Properties of Ag–Au Colloidal Alloys Pulsed Laser Ablated in Liquid: Experiments and Theory.* The Journal of Physical Chemistry C 124 (45), 24930-24939, 2020.

Retrieval of aerosol single scattering albedo from a combination of satellite and surface visibility measurements

Yueming Dong[1] and Jing Li[1,*]

[1]*Department of Atmospheric and Oceanic Sciences, School of Physics, Peking University, Beijing 100871, China*
[*]*corresponding author's e-mail: jing-li@pku.edu.cn*

Abstract

Aerosol single scattering albedo (SSA) measures the ratio of scattering to extinction, which is critical in determining aerosol radiative effect. However, spaceborne SSA retrieval is restricted by comprehensive monitoring requirements of both direct solar radiance and scattered sky radiance. Most existing passive satellite sensors such as MODIS and VIIRS only provide the measurements of reflected solar radiation at the top of the atmosphere (TOA), which are sensitive to both aerosol optical depth (AOD) and SSA. Current AOD products are commonly derived from satellites on the basis of assumed SSA. On the other hand, it would be possible to retrieve SSA using satellite measurements with known AOD. In this study, a machine learning approach is developed for the retrieval of SSA using joint visibility and satellite measurements. With meteorological and ancillary information, surface visibility can be converted to column AOD. Therefore, combining these variables representing AOD with MODIS measured TOA apparent reflectance, we retrieve SSA at over 2000 stations worldwide. The results show a great consistency with AERONET retrieved SSA. We also applied our method to surface PM2.5 measurements and obtained satisfactory results. Our work generates a global aerosol SSA dataset with extensive coverage over land, which can be used for the estimation of aerosol radiative forcing and the validation of climate models.

References

[1] K. H. Lee, Z. Li, M. S. Wong, J. Xin, Y. Wang, W. M. Hao and F. Zhao. *Aerosol single scattering albedo estimated across China from a combination of ground and satellite measurements*. J. Geophys. Res., 112: D22S15, 2007.

[2] J. Wei, W. Huang, Z. Li, W. Xue, Y. Peng, L. Sun and M. Cribb. *Estimating 1-km-resolution PM2.5 concentrations across China using the space-time random forest approach*. Remote SENS. ENVIRON., 231:111221, 2019.

[3] Y. Dong, and J. Li. *A machine learning approach to retrieve aerosol single scattering albedo using joint satellite and surface visibility measurements*. AGU Fall Meeting 2020. Online. 1-17 December 2020.

Light Scattering by Large Raindrops: Simulation with the Vectorial Complex Ray Model

Qingwei DUAN[1,2], Xiang'e HAN[1,*] and Kuan Fang REN[2,*]

[1]*School of Physics and Optoelectronic Engineering, Xidian University, Xi'an 710071, China*
[2]*CORIA-UMR 6614-Normandie Université, CNRS-Université et INSA de Rouen, 76800 Saint-Etienne du Rouvray, France*
[*]*corresponding author's e-mail: xehan@mail.xidian.edu.cn, fang.ren@coria.fr*

This communication presents our recent progress on the three-dimensional (3D) light scattering by raindrops of large size and complex morphological characteristics. The equal-volume radii of the non-spherical raindrops in nature usually range from hundreds of microns to several millimeters [1], much greater than the wavelength of light. Since the conventional numerical methods (T-matrix, FDTD or DDA) [2] are limited to small particles, there is still no satisfying solution to the light scattering of non-spherical raindrops. As an advanced ray model of light, the vectorial complex ray model (VCRM) [3] integrated the local wavefront curvatures as new properties of a light ray, thereby allowing to predict the coarse and fine scattering patterns of large non-spherical particles [4]. The implementation of VCRM for 3D scattering (VCRM3D) has been achieved recently [5], opening up perspectives for simulating and understanding the 3D scattering of large particles of any smooth surface. Here presents the application of VCRM3D to the non-spherical raindrops in nature, and reveals their scattering patterns in 3D space.

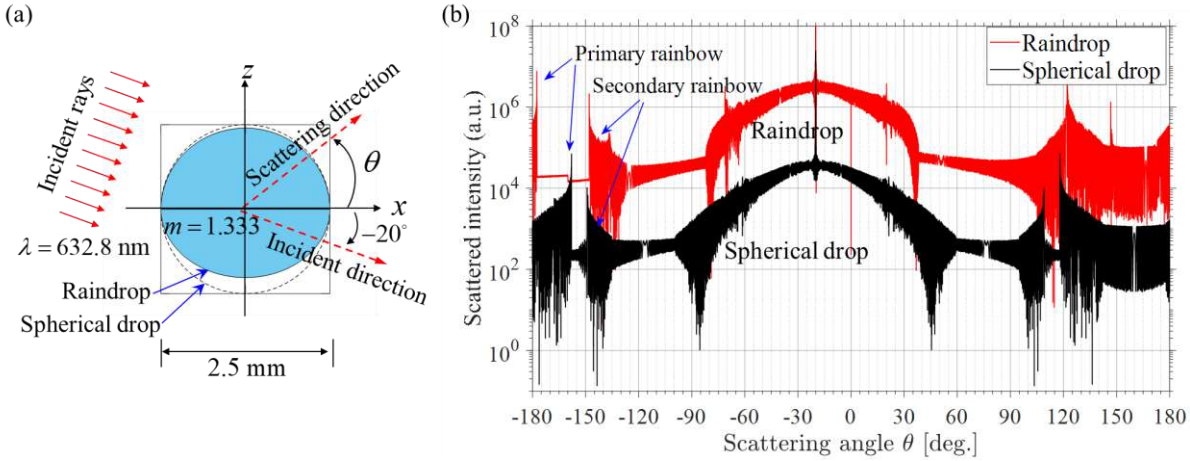

Figure 1: (a) Model of a large raindrop of diameter 2.5 mm. Equivalent spherical drop is outlined by the dotted line. (b) Comparison between the scattering diagrams of the spherical drop and the non-spherical raindrop (offset by 10^2) in the symmetry *xz* plane. The full 3D scattering patterns are in progress and to be presented in the conference.

References

[1] K.V. Beard, C. Chuang, J. Atmos. Sci. 44 (11):1509–1524, 1987.
[2] M.I. Mishchenko, J.W. Hovenier, L.D. Travis (Eds.), Light Scattering by Nonspherical Particles: Theory, Measurements, and Applications, Academic Press, San Diego, 2000.
[3] K.F. Ren, F. Onofri, C. Rozé, T. Girasole, Opt. Lett. 36 (3):370–372, 2011.
[4] F. Onofri, K.F. Ren, M. Sentis, Q. Gaubert, C. Pelcé, Opt. Express 23 (12):15768–15773, 2015.
[5] Q.W. Duan, F. Onofri, X.E. Han and K.F. Ren, Generalized rainbow patterns of oblate drops simulated by a ray model in three dimensions, in submission, 2021

A light scattering view of magnetic polariton in gratings

Hangjie Li[1,2] , Junming Zhao[1,2*] and Linhua Liu[3]

[1] *School of Energy Science and Engineering, Harbin Institute of Technology, Harbin 150001, China*
[2] *Key Laboratory of Aerospace Thermophysics, Ministry of Industry and Information Technology, Harbin 150001, China*
[3] *School of Energy and Power Engineering, Shandong University, Qingdao 266237, China*
[*] *corresponding author's e-mail: jmzhao@hit.edu.cn*

ABSTRACT

Magnetic polariton (MP) is a significant resonance mode in tailoring the surface radiative properties within nano/micro-structured metamaterials. One salient feature of MP is its localized property as compared to the surface plasmon/phonon polariton (SPP). The MP structure in a grating can be considered as an isolated unit as indicated by the LC circuit model [1]. The neighboring structures has a weak effect on the properties of the MP, as long as their separation distance is large enough. In this work, we present a 'particle' view of the MP structure based on the localized property of the MP structure. The common concepts in light scattering such as scattering cross-section and absorption cross-section are defined to describe the properties of MP in gratings. The MP scattering cross-section and absorption cross-section in example gratings are calculated and the geometric effects on their scattering characteristics are analyzed. The results show that the absorption cross-section of the MP in deep grating remains unchanged when the period is large enough, supporting the isolated 'particle' view of the structure. When the grating period, i.e., the distance between the slits in the deep grating is small, the dependent scattering effect appears, which will influence the MP resonance frequency. The MP will also interact with the SPP in gratings which cause the shift of resonance frequency and the scattering properties. The absorption cross-section of a MP structure is demonstrated to be a good measure of the light absorption performance of the single structure (e.g., a slit), and gives a measure of the 'optical' size of the MP structure. The new view of MP and related concept presented in this study may facilitate the understanding and design of photonic metamaterial structures based on MP.

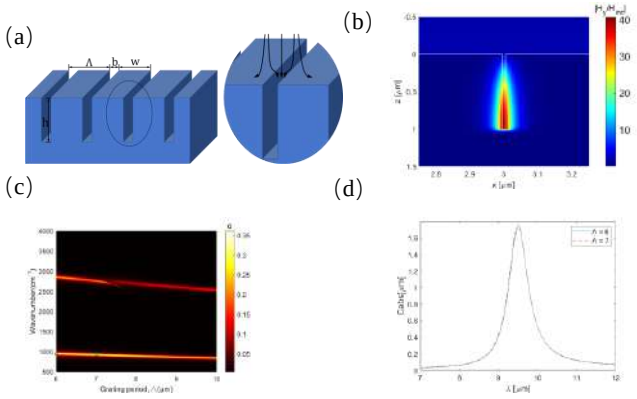

Figure 1: (a)Schematic of the 1D metallic grating with a period Λ, height or depth h, ridge width w, and trench width b and light scattering of MP structures. (b) The magnetic field distribution in the Ag grating with Λ=6μm, b=0.01μm and h=1μm at resonance frequency. (c) Contour plot of the normal absorptance in terms of the wavenumber and period for Ag gratings with b=0.01μm and h=1μm. (d) Absorption cross section spectra at normal incidence of TM wave with Λ=6μm and 7μm.

References

[1] L. P. Wang and Z. M. Zhang , "Resonance transmission or absorption in deep gratings explained by magnetic polaritons" , Applied Physics Letters 95, 111904 (2009)

Convection-type heat transfer behavior in the asymmetric nanoparticle chains via thermal photons

Minggang Luo[1,2], Junming Zhao[1,2,*], and Linhua Liu[3]

[1]*School of Energy Science and Engineering, Harbin Institute of Technology, 92 West Street, Harbin 150001, China*
[2]*Key Laboratory of Aerospace Thermophysics, Ministry of Industry and Information Technology, Harbin 150001, China*
[3]*School of Energy and Power Engineering, Shandong University, Qingdao 266237, China*
[*]*corresponding author's e-mail: jmzhao@hit.edu.cn*

Abstract

Near-field radiative heat transfer (NFRHT) in nanostructure networks recently attracts a lot of research interests for both fundamental and applicative reasons. When separation between nanostructures is comparable to or less than the characteristic thermal wavelength, the near-field effects become important and the radiative heat flux can exceed the Planckian blackbody limit by several orders of magnitudes. In the nanoparticle networks, nanoparticles usually lie in the near field of each other, which results in the significant multiple scattering of the thermally excited electromagnetic waves, namely many-body interaction (MBI). The complex MBI significantly affects the heat transfer behavior inside the networks composed of many nanoparticles. In literature, heat superdiffusion was demonstrated in the linear ordered chain with strong MBI due to near-field interaction from the point view of continuum. However, few results on heat transfer behavior in the asymmetric chains have ever been reported at continuum scale, of which the reason is that no continuum-scale theoretical framework for heat transfer in asymmetric structures has been developed yet. It is still unclear how MBI affects heat transfer in such asymmetric nanoparticle chains. Our recent work provides a normal diffusion theory (governing equation see below) starting from the fluctuational electrodynamics applicable for investigating heat transfer in the asymmetric structures due to near-field interaction [1], where the effective thermal conductivity (ETC) and asymmetrical photonic heat transfer coefficient (APHTC) are defined to characterize the diffusion-type and convection-type heat transfer process via thermal photons, respectively. In this work, heat transfer in asymmetric nanoparticle chains is investigated by means of the normal diffusion theory. Effect of the asymmetry of structure on NFRHT is analyzed. The spatial distributions (profiles) of temperature and heat transfer coefficients (i.e., ETC and APHTC) along the chain are also analyzed. For heat transfer in asymmetric nanoparticle chains via thermal photons, in addition to the heat diffusion process, the convection-type heat transfer process caused by the asymmetry of the structure also exists. Heat transfer in the asymmetric chain has an obvious preferential direction, which is due to the existence of the convection-type heat transfer process via thermal photons. In the considered asymmetric nanoparticle chains, the spatial variation of nanoparticle packed density is obvious, which results in the spatial-dependent heat transfer coefficients. Magnitude of both ETC and APHTC for the position with densely packed nanoparticles is much larger than that of the position with loosely packed nanoparticles. The sign of APHTC means for the preferential direction of heat transfer. For the asymmetric chain where nanoparticles packs densely at the left hand side and packs loosely at the right hand side, the sign of the APHTC is '-' meaning for the heat tranfer preferential direction from left to right. It is also noted that temperature gradient along the asymmetric chain varies from position to position and increases with decreasing the effective thermal conductivity. This work may help for micro-nanoscale heat management and understanding of the heat transfer in asymmetric particulate system via near-field thermal photons.

$$\underbrace{\mathbf{h}_{\mathrm{loc}} \cdot \nabla T}_{\mathbf{h}_{\mathrm{loc}}\text{: APHTC}} + \underbrace{\nabla \cdot (\mathbf{K}_{\mathrm{loc}} \cdot \nabla T)}_{\mathbf{K}_{\mathrm{loc}}\text{: ETC}} + S = \frac{\mathrm{d}E}{\mathrm{d}t}, \tag{1}$$

References

[1] M. G. Luo, J. M. Zhao, L. H. Liu. *Normal heat diffusion in many-body system via thermal photons.* 2020, arXiv: 2011.07588.

Nonlinear light scattering by particulate matter: a model based on RGD approximation

Ankur Gogoi[1,*], Guan-Yu Zhuo[2], Biswa Jyoti Sharma[3] and Gazi A Ahmed[4]

[1]*Department of Physics, Jagannath Barooah College, Jorhat 785001, Assam*
[2]*Institute of New Drug Development, China Medical University, No. 91, Hsueh-Shih Rd., Taichung 40402, Taiwan*
[3]*Department of Computer Science, Jagannath Barooah College, Jorhat 785001, Assam*
[4]*Department of Physics, Tezpur University, Tezpur 784028, Assam*
[*]*corresponding author's e-mail: ankurgogoi@gmail.com*

Abstract

In this work, we report the extension of Rayleigh-Gans-Debye (RGD) approximation to calculate the nonlinear light scattering properties of particulate matter. In this model, the scattered field amplitudes are calculated by using the nonlinear susceptibility which is determined from molecular hyperpolarizability and particle surface susceptibility. The results of the nonlinear light scattering properties of monodisperse or polydisperse particles, having sizes within RGD limit and calculated as a function of scattering angle, will be presented.

References

[1] de Beer, A.G. and Roke, S., 2010: Obtaining molecular orientation from second harmonic and sum frequency scattering experiments in water: Angular distribution and polarization dependence. *The Journal of chemical physics*, **132(23)**, 234702.
[2] de Beer, A.G. and Roke, S., 2007: Sum frequency generation scattering from the interface of an isotropic particle: Geometrical and chiral effects. *Physical Review B*, **75(24)**, p.245438.
[3] Braun, B., Dorgan, J.R. and Chandler, J.P., 2008: Cellulosic nanowhiskers. Theory and application of light scattering from polydisperse spheroids in the Rayleigh– Gans– Debye regime. *Biomacromolecules*, **9(4)**, 1255-1263.
[4] Dadap, J.I., Shan, J., Eisenthal, K.B. and Heinz, T.F., 1999: Second-harmonic Rayleigh scattering from a sphere of centrosymmetric material. *Physical Review Letters*, **83(20)**, 4045-4048.

Brownian dynamics simulations of sphere clusters in complex optical beams

J. Fung[1,*]

[1] *Ithaca College*
[*] *corresponding author's e-mail: jfung@ithaca.edu*

Abstract

Simulations of the behavior of particles in complex optical fields can lead to practical applications such as predicting how the particles can be manipulated with optical tweezers. Particles in complex optical fields can also exhibit rich physical phenomena, such as photokinetic effects, arising from the interplay between deterministic electromagnetic forces and torques and stochastic thermal fluctuations. Performing such simulations is challenging for wavelength-sized particles since the simulations must account for the details of how the particles scatter light. Here, we discuss recent progress in simulating the motion of wavelength-sized sphere clusters in complex optical fields using Brownian dynamics [1].

Our simulations account for the exact electromagnetic forces and torques on the clusters. Specifically, we use a point-matching technique to calculate the vector spherical wave function (VSWF) expansions of arbitrary optical fields including focused Gaussian beams and Laguerre-Gaussian beams [2]. We then determine the electromagnetic forces and torques on the clusters from T-matrix computations of how they scatter those optical fields [3]. In addition, our simulations account for anisotropic hydrodynamic and stochastic forces on the sphere clusters. We generate trajectories that track the position and orientation of the clusters in three dimensions.

Using our simulations, we explore phenomena such as the photokinetic rotation of optically-trapped two-sphere clusters in elliptically-polarized Gaussian beams which carry spin angular momentum. We consider how the rotation depends on the particle size and beam power. We also simulate the motion of clusters in Laguerre-Gaussian beams that carry orbital angular momentum. Finally, we examine the trapping equilibria of highly asymmetric clusters like the one shown in Fig. 1.

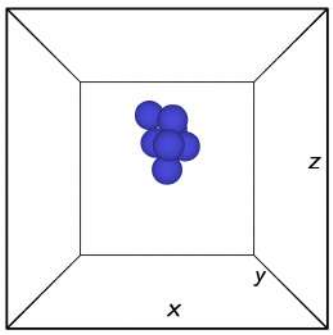

Figure 1: Snapshot rendered from a simulated trajectory of an optically-trapped 7-sphere cluster in water. The 1064-nm-wavelength, 5 mW, horizontally-polarized beam propagates in the $+z$ direction and is focused at the center of the box by a 1.2 NA objective lens. The spheres have a radius of 0.4 µm and a refractive index of 1.45.

References

[1] W. Vigilante, O. Lopez, and J. Fung *Brownian dynamics simulations of sphere clusters in optical tweezers.* Opt. Express, 28:36131-36146, 2020.

[2] T. A. Nieminen, H. Rubinsztein-Dunlop, and N. R. Heckenberg *Multipole expansion of strongly focussed laser beams.* J. Quant. Spectrosc. Radiat. Transfer, 79-80:1005-1017, 2003.

[3] D. W. Mackowski and M. I. Mishchenko *Calculation of the T matrix and the scattering matrix for ensembles of spheres.* J. Opt. Soc. Am. A, 13:2266-2278, 1996.

Linearization of single scattering properties with respect to refractive indices, size parameters, and aspect ratios

B. Sun[1,*], C. Gao[1], and D. Liang[1]

[1]*Department of Atmospheric and Oceanic Sciences, Fudan University, Shanghai, 200438, China*
[*]*corresponding author's e-mail: bingqsun@fudan.edu.cn*

Light scattering properties of a single particle include its differential scattering properties represented by a scattering phase matrix and its integrated scattering properties such as extinction, absorption, and scattering cross-sections, and asymmetry factor. Input parameters for a single scattering are refractive indices, size parameters, and aspect ratios. Sensitivity of scattering properties are reflected by its linearization and especially important in the retrieval of particle microphysical properties. Consequently, the derivatives (or linearization) of light scattering properties with respect to the input parameters are obtained in this study using the invariant-imbedding T-matrix method [1] and physical-geometric optics methods. The sensitivities associated with linearized parameters are shown and their preliminary applications are also discussed.

References

[1] B. Sun, C. Gao, L. Bi, and R. Spurr. *Analytical Jacobians of single scattering optical properties using the invariant imbedding T-matrix method*. Opt. Express, 29: 9635-9669, 2021.

On the application of scattering matrix measurements to detection and identification of major types of airborne aerosol particles: volcanic ash, desert dust and pollen

Juan Carlos Gómez Martín[1*], Daniel Guirado[1], Elisa Frattin[2], Maria Bermudez-Edo[3], Paloma Cariñanos Gonzalez[4,5], Francisco José Olmo Reyes[5,6], Timo Nousiainen[7], Pedro J. Gutiérrez[1], Fernando Moreno[1], Olga Muñoz[1*].

[1] *Instituto de Astrofísica de Andalucía (IAA-CSIC), Granada, Spain*
[2] *Department of physics and Astronomy "Galileo Galilei", University of Padova, Padova, Italy.*
[3] *Departamento de Lenguajes y Sistemas Informáticos, Escuela Técnica Superior de Ingenierías Informática y de Telecomunicación, Universidad de Granada, Granada, Spain*
[4] *Departamento de Botánica, Facultad de Farmacia, Universidad de Granada, Granada, Spain*
[5] *IISTA-CEAMA, Andalusian Institute for Earth System Research, Universidad de Granada, Granada, Spain*
[6] *Departamento de Física Aplicada, Facultad de Ciencias, Universidad de Granada, Granada, Spain*
[7] *Finnish Meteorological Institute, Helsinki, Finland*
[*] *corresponding author's e-mail: jcgomez@iaa.es, olga@iaa.es*

Abstract

Atmospheric aerosols play key roles in climate and have important impacts on human activities and health. Hence, much scientific effort has been directed towards developing methods of improved detection and discrimination of different types of aerosols. Among these, light scattering-based detection of aerosol offers several advantages including applications in both in situ and remote sensing devices, bulk detection and multi-angle and multi-wavelength measurements. In this work, new scattering matrix measurements for two samples of airborne desert dust collected at Spain and China are reported, showing that these samples have very similar scattering properties. Such remarkable similarity between samples collected in different parts of the world has also been previously observed in the case of volcanic ashes [1,2]. Thus, the average extrapolated scattering matrices of airborne desert dust and of volcanic ash at two wavelengths have been calculated and compared (Figure 1) with the aim of finding criteria to distinguish these two types of aerosol in atmospheric observations. Additionally, the scattering matrix of cypress pollen has been measured and extrapolated to explore differences with mineral dust that can be exploited in atmospheric detection.

Field measurements of the backscattering linear and circular depolarization ratios have been used to obtain information about non-sphericity and discrimination between fine and coarse aerosol [3–5]. However, the average backscattering linear depolarization ratio for the three types of aerosols considered in this work in the visible spectral range is $\delta_L(180°) = 0.40 \pm 0.05$. This indicates that $\delta_L(180°)$ is not very informative about the nature of irregular aerosol particles, e.g. composition or morphology. By contrast, measurements of scattering matrix elements or depolarization ratios at different scattering angles may provide information about the structural differences of particles, and in particular may enable to differentiate airborne volcanic ash from desert dust, which otherwise are very similar in terms of size and optical constants. Cluster analysis of the scattering matrices obtained in this work together with those included in the Granada-Amsterdam light scattering database [6] indicates that measurements of two or three matrix elements at two or three scattering angles are enough to classify these samples. Compact aggregate particles with round but uneven surfaces at the micron scale and below (desert dust) show consistently lower $F_{22}(\theta)/F_{11}(\theta)$ and $F_{44}(\theta)/F_{11}(\theta)$ than compact particles with smoother surfaces (volcanic ash). Cypress pollen shows a characteristic $F_{12}(\theta)/F_{11}(\theta)$ curve very different from polydisperse irregular mineral dust. Field and remote sensing instruments based on the measurement of light scattering characteristics of aerosol particles could extract more information if modifications are introduced to perform concurrent measurements of the phase curves of several scattering matrix elements or depolarization ratios.

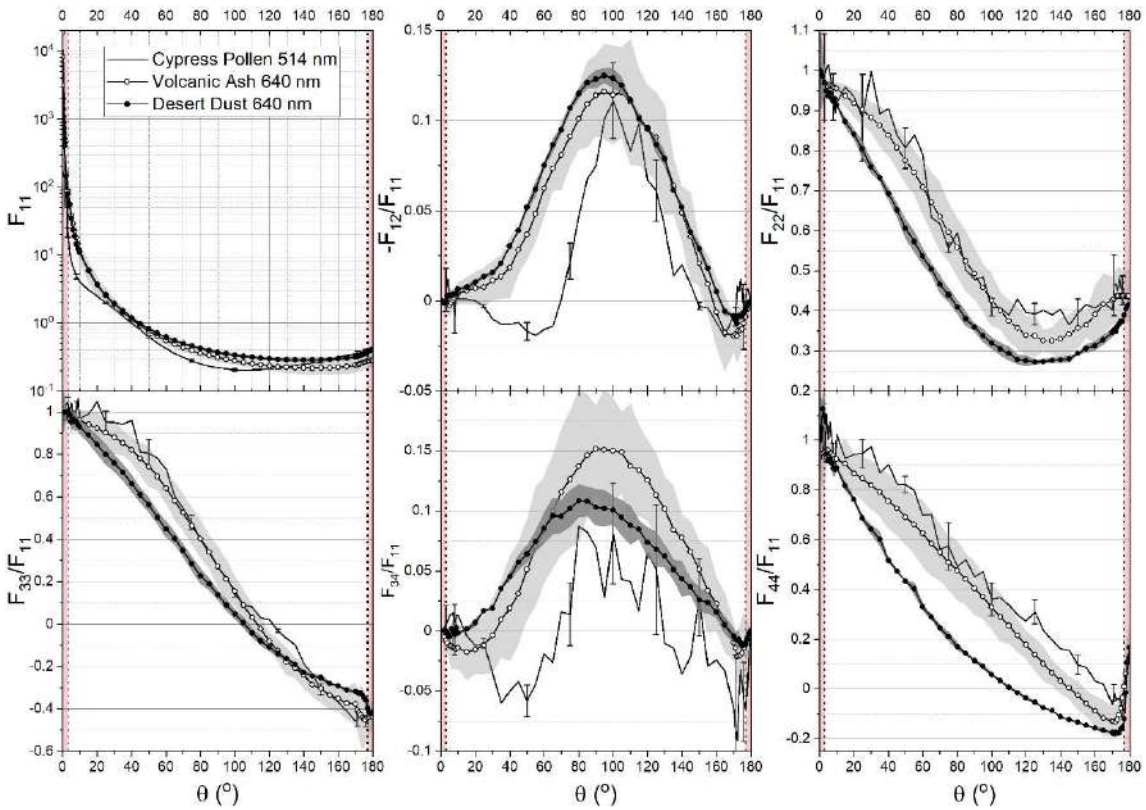

Figure 1: Non-zero average scattering matrix elements in the red (632.8 nm - 647 nm) of clouds of randomly oriented airborne natural aerosol samples collected outdoors: volcanic ash (empty circles) and desert dust (full circles). The grey shaded areas enveloping each averaged curve indicate the range of the data entering the averages. The scattering matrix elements of cypress pollen measured in the green (514 nm) are also shown (solid lines), with error bars indicating experimental uncertainty (shown every five angles for clarity). The shaded red regions indicate the scattering angle ranges where measurements could not be carried out and the curves have been extrapolated to 0° and 180°.

References

[1] Muñoz O, Volten H, Hovenier JW, Veihelmann B, van der Zande WJ, Waters LBFM, et al. Scattering matrices of volcanic ash particles of Mount St. Helens, Redoubt, and Mount Spurr Volcanoes. J Geophys Res Atmos 2004;109. https://doi.org/10.1029/2004jd004684.

[2] Merikallio S, Muñoz O, Sundström A-M, Virtanen TH, Horttanainen M, Leeuw G de, et al. Optical modeling of volcanic ash particles using ellipsoids. J Geophys Res Atmos 2015;120:4102–16. https://doi.org/10.1002/2014jd022792.

[3] Sassen K. Polarization in Lidar. Lidar, Springer-Verlag; 2006, p. 19–42. https://doi.org/10.1007/0-387-25101-4_2.

[4] Järvinen E, Kemppinen O, Nousiainen T, Kociok T, Möhler O, Leisner T, et al. Laboratory investigations of mineral dust near-backscattering depolarization ratios. J Quant Spectrosc Radiat Transf 2016;178:192–208. https://doi.org/https://doi.org/10.1016/j.jqsrt.2016.02.003.

[5] Bohlmann S, Shang X, Giannakaki E, Filioglou M, Saarto A, Romakkaniemi S, et al. Detection and characterization of birch pollen in the atmosphere using a multiwavelength Raman polarization lidar and Hirst-type pollen sampler in Finland. Atmos Chem Phys 2019;19:14559–69. https://doi.org/10.5194/acp-19-14559-2019.

[6] Guirado D, Muñoz O, Gómez Martín J, Volten H, Moreno F. Granada-Amsterdam Light Scattering Database. ELS-XIX, 2021.

On the application of scattering matrix measurements to detection and identification of major types of airborne aerosol particles: volcanic ash, desert dust and pollen

Juan Carlos Gómez Martín[1*], Daniel Guirado[1], Elisa Frattin[2], Maria Bermudez-Edo[3], Paloma Cariñanos Gonzalez[4,5], Francisco José Olmo Reyes[5,6], Timo Nousiainen[7], Pedro J. Gutiérrez[1], Fernando Moreno[1], Olga Muñoz[1*].

[1] *Instituto de Astrofísica de Andalucía (IAA-CSIC), Granada, Spain*
[2] *Department of physics and Astronomy "Galileo Galilei", University of Padova, Padova, Italy.*
[3] *Departamento de Lenguajes y Sistemas Informáticos, Escuela Técnica Superior de Ingenierías Informática y de Telecomunicación, Universidad de Granada, Granada, Spain*
[4] *Departamento de Botánica, Facultad de Farmacia, Universidad de Granada, Granada, Spain*
[5] *IISTA-CEAMA, Andalusian Institute for Earth System Research, Universidad de Granada, Spain*
[6] *Departamento de Física Aplicada, Facultad de Ciencias, Universidad de Granada, Granada, Spain*
[7] *Finnish Meteorological Institute, Helsinki, Finland*
[*] *corresponding author's e-mail: jcgomez@iaa.es, olga@iaa.es*

Abstract

Atmospheric aerosols play key roles in climate and have important impacts on human activities and health. Hence, much scientific effort has been directed towards developing methods of improved detection and discrimination of different types of aerosols. Among these, light scattering-based detection of aerosol offers several advantages including applications in both in situ and remote sensing devices, bulk detection and multi-angle and multi-wavelength measurements. In this work, new scattering matrix measurements for two samples of airborne desert dust collected at Spain and China are reported, showing that these samples have very similar scattering properties. Such remarkable similarity between samples collected in different parts of the world has also been previously observed in the case of volcanic ashes. Thus, the average extrapolated scattering matrices of airborne desert dust and of volcanic ash at two wavelengths have been calculated and compared with the aim of finding criteria to distinguish these two types of aerosol in atmospheric observations. Additionally, the scattering matrix of cypress pollen has been measured and extrapolated to explore differences with mineral dust that can be exploited in atmospheric detection.

Field measurements of the backscattering linear and circular depolarization ratios have been used to obtain information about non-sphericity and discrimination between fine and coarse aerosol. However, the average backscattering linear depolarization ratio for the three types of aerosols considered in this work in the visible spectral range is $\delta_L(180°) = 0.40 \pm 0.05$. This indicates that $\delta_L(180°)$ is not very informative about the nature of irregular aerosol particles, e.g. composition or morphology. By contrast, measurements of scattering matrix elements or depolarization ratios at different scattering angles may provide information about the structural differences of particles, and in particular may enable to differentiate airborne volcanic ash from desert dust, which otherwise are very similar in terms of size and optical constants. Cluster analysis of the scattering matrices obtained in this work together with those included in the Granada-Amsterdam light scattering database indicates that measurements of two or three matrix elements at two or three scattering angles are enough to classify these samples. Compact aggregate particles with round but uneven surfaces at the micron scale and below (desert dust) show consistently lower $F_{22}(\theta)/F_{11}(\theta)$ and $F_{44}(\theta)/F_{11}(\theta)$ than compact particles with smoother surfaces (volcanic ash). Cypress pollen shows a characteristic $F_{12}(\theta)/F_{11}(\theta)$ curve very different from polydisperse irregular mineral dust. Field and remote sensing instruments based on the measurement of light scattering characteristics of aerosol particles could extract more information if modifications are introduced to perform concurrent measurements of the phase curves of several scattering matrix elements or depolarization ratios.

Radar polarimetric analysis of bistatic Mini-RF observations of Mare Imbrium, Censorinus, and Aristarchus regions

A. K. Virkki[1,*], D. T. Blewett[2], and G. W. Patterson[2]

[1] *University of Helsinki*
[2] *Johns Hopkins Applied Physics Laboratory*
[*] *corresponding author's e-mail: anne.virkki@helsinki.fi*

Abstract

Planetary radar is a powerful tool for the research of planetary objects, moons, and small bodies of the Solar System providing observational data at much longer wavelengths than optical. We present a comparative polarimetric analysis of three lunar crater regions observed using bistatic radar: transmitting using the Arecibo Observatory S-band (2380 MHz, 12.6 cm) planetary radar system and receiving using the Lunar Reconnaissance Orbiter's Mini-RF instrument during the Third and Fourth Extended Science Missions. The selected regions include craters close to Mare Imbrium, the Censorinus crater, and the Aristarchus crater (with Aristarchus plateau). The Mini-RF data were processed into four 100-m/pixel maps, one for each Stokes vector element. Using the Stokes element maps, we derived various polarimetric parameters, including the linear and circular polarization ratios, the preferential ellipticity and orientation of the polarization ellipse, and *m-chi* decomposition, as introduced to lunar radar analysis by Raney et al. [1], which provides information of the relative size-frequency distributions of wavelength-scale (or larger) and sub-wavelength-scale particles in specific regions. Often primarily circular-polarization ratio is used for analyzing the lunar radar maps; however, we performed comparative analysis of each polarization property listed above as a tool to analyze the crater region structures as imaged using the Mini-RF instrument. With support from modeling work (*e.g.*, [2]), we evaluate the features around the craters and how the radar scattering varies between the crater floors, around the crater rims, and regions further away from the craters to improve our understanding of radar scattering by the Moon and in general for comparative studies to other planetary and small bodies of the Solar System. As an example, we observed a linear-polarization banding phenomenon [3] in the Mare Imbrium region.

References

[1] R. K. Raney, J. T. S. Cahill, G. W. Patterson, and D. B. J. Bussey *The m-chi decomposition of hybrid dual-polarimetric radar data with application to lunar craters*, Journal of Geophysical Research, 117, E00H21, 2012.

[2] A. K. Virkki and S. S. Bhiravarasu *Modeling Radar Albedos of Laboratory-Characterized Particles: Application to the Lunar Surface*, Journal of Geophysical Research: Planets, 124(11): 3025-3040, 2019.

[3] L. M. Carter, B. A. Campbell, C. D. Neish, M. C. Nolan, G. W. Patterson, J. R. Jensen, and D. B. J. Bussey *A Comparison of Radar Polarimetry Data of the Moon From the LRO Mini-RF Instrument and Earth-Based Systems*, IEEE Transactions on Geoscience and Remote Sensing, 55(4): 1915-1927, 2017.

Spectropolarimetry of planet Earth

C.Emde[1,4,*], M. Sterzik[2], M.Manev[1], and S. Bagnulo[3]

[1] *Meteorological Institute, Ludwig-Maximilians-University (LMU), Theresienstr. 37, D-80333 Munich, Germany*
[2] *European Southern Observatory, Karl-Schwarzschild-Str. 2, D-85748 Garching, Germany*
[3] *Armagh Observatory & Planetarium, College Hill, Armagh BT61 9DG, UK*
[4] *German Aerospace Center (DLR), Oberpfaffenhofen, Germany*
[*] *corresponding author's e-mail: claudia.emde@lmu.de*

Earthshine, i.e. sun-light reflected from Earth towards the Moon and back-reflected from the lunar surface to Earth, can be observed by ground-based astrophysical facilities such as the Very Large Telescope (VLT), corresponding to observations of planet Earth from afar.

We observed polarimetric spectra in the visible spectral range from 430-920 nm using FORS2 at VLT for phase angles (Sun-Earth-Moon angle) in the range from 33° to 136°, including the maximum polarization for Rayleigh scattering at 90° and also the cloudbow at about 40° [2,3]. Another feature is the sun-glint, which is visible at times, when a large part of the Pacific ocean is illuminated.

We use the three-dimensional fully-spherical Monte Carlo model MYSTIC [4, 5] to simulate and analyze the observations, trying to include planet Earth as realistic as possible [1]. Land-surfaces are modeled as Lambertian surfaces with albedos taken from MODIS satellite observations. The sea-surface is modeled as a polarized bidirectional reflectance distribution function (BPDF). Three-dimensional cloud data (liquid and ice water) is taken from the ECMWF weather forecast model, corresponding to the time of the observation. The simulations generally match well the observations and we can clearly identify biosignatures such as liquid water (sun-glint), cloud water (cloudbow) and oxygen via the O2A-band. The cloudbow observations even allow to retrieve Earth-averaged microphysical cloud properties, i.e. refractive index, effective droplet size and cloud optical thickness.

We conclude that observations of polarimetric spectra and phase curves of planets beyond the Solar System would be very useful to characterize their atmospheres and surfaces.

References

[1] C. Emde, R. Buras, M. Sterzik, and S. Bagnulo. *Influence of aerosols, clouds, and sunglint on polarization spectra of Earthshine*. Astron. Astrophys., 605(A2), 2017
[2] M. F. Sterzik, S. Bagnulo, D. M. Stam, C. Emde, and M. Manev. *Spectral and temporal variability of Earth observed in polarization*. Astron. Astrophys., 622:A41, 2019.
[3] M.F. Sterzik, S. Bagnulo, C. Emde, and M. Manev. *The cloudbow of planet Earth observed in polarisation*. Astron. Astrophys., 639:A89, 2020.
[4] B. Mayer. *Radiative transfer in the cloudy atmosphere*. European Physical Journal Conferences, 1:75-99, 2009
[5] C. Emde, R. Buras, B. Mayer, and M. Blumthaler. *The impact of aerosols on polarized sky radiance: model development, validation, and applications*. Atmos. Chem. Phys., 10(2):383-396, 2010.

Radiative transfer for coupled atmosphere and ocean systems in ultraviolet: challenges and applications

P. Zhai[1,*], P. J. Werdell[2], B. Franz[2], I. Amir[2], M. Gao[2], Y. Hu[3], and J. Chowdhary[4]

[1]*Physics Department. UMBC*
[2]*NASA Goddard Space Flight Center*
[3]*NASA Langley Research Center*
[4]*NASA Goddard Institute for Space Studies*
[*]*corresponding author's e-mail: pwzhai@umbc.edu*

Radiative transfer theory models the spatial, directional, spectral, and polarization distribution of light field in turbid media. In coupled atmosphere and ocean systems, radiative transfer models have great applications in aerosol and ocean color remote sensing and simulating the radiative forcing and photosynthetically available radiation, etc.[1,2]. In recent years, radiative transfer modeling in the ultraviolet (UV) spectral region has becoming more and more important due to its applications in the atmospheric correction for ocean color remote sensing. In particular, both brown carbon aerosols and colored dissolved organic matter (CDOM) in ocean waters show similar enhanced absorption features, which makes it difficult to separate the signals from these components [3,4]. Radiative transfer simulation faces great challenges in the UV. First of all, the absorption coefficients by pure sea water shows large uncertainties in this spectral range [5]. In addition, the absorption properties of phytoplankton particles have not been characterized well [5]. In this paper we will report a number of new results of radiative transfer simulation in the UV for coupled atmosphere and ocean systems, which include the variation of the reflectance at the top of the atmosphere due to the uncertainty of the pure ocean water absorptions and the impacts of the different CDOM absorption models. In addition, we will also cover the contribution of inelastic scattering to the reflectances for sensors in the atmosphere in the UV, which is of importance for aerosol and ocean color remote sensing in the UV.

References

[1] Zhai, P., Hu, Y., Trepte, C. R., Lucker, P. L. (2009). A vector radiative transfer model for coupled atmosphere and ocean systems based on successive order of scattering method. *Optics express, 17*(4), 2057-2079.
[2] Zhai, P., Hu, Y., Chowdhary, J., Trepte, C. R., Lucker, P. L., Josset, D. B. (2010). A vector radiative transfer model for coupled atmosphere and ocean systems with a rough interface. Journal of Quantitative Spectroscopy and Radiative Transfer, 111(7), 1025-1040.
[3] Frouin R. et al. (2019). Atmospheric Correction of Satellite Ocean-Color Imagery During the PACE Era. Frontiers in Earth Science, 7, 145.
[4] Chowdhary, J., Zhai, P., Boss, E., Dierssen, H., Frouin, R., Ibrahim, A., Lee, Z., Remer, L. A., Twardowski, M., Xu, F., Zhang, X., Ottaviani, M., Espinosa, W. R., Ramon, D. (2019). Modeling Atmosphere-Ocean Radiative Transfer: A PACE Mission Perspective. *Frontiers In Earth Science, 7*, 1-53.
[5] IOCCG Protocol Series (2018). Inherent Optical Property Measurements and Protocols: Absorption Coefficient, Neeley, A. R. and Mannino, A. (eds.), IOCCG Ocean Optics and Biogeochemistry Protocols for Satellite Ocean Colour Sensor Validation, Volume 1.0, IOCCG, Dartmouth, NS, Canada.

Light backscattering from large clusters of densely packed irregular particles

Y. Grynko[1,*], Y. Shkuratov[2], and J. Förstner[1]

[1]*Department of Theoretical Electrical Engineering, Paderborn University, Warburger Str. 100, 33102 Paderborn, Germany*
[2]*Institute of Astronomy of Kharkiv National University, Sumska Str. 35, 61022 Kharkiv, Ukraine*
[*]*corresponding author's e-mail: yevgen.grynko@upb.de*

Numerical simulations of light backscattering from powder-like surfaces require methods that allow description of arbitrary geometries of individual scatterers and their dense placement. Here, we apply a model that represents a realistic structure of powder samples. Using the Discontinuous Galerkin Time Domain method [1] we solve a light scattering problem for clusters of hundreds to thousands of random irregular particles [2] packed with a packing density of ρ = 0.5 (Figure 1a). The material is non-absorbing and the complex refractive index is m = 1.5 + 0i which implies an important role of multiple scattering. The results of simulations show that diffuse scattering is significantly reduced in such systems and light transport follows propagation channels that are determined by the particle size and topology of the medium. This kind of localization produces coherent backscattering intensity surge and an enhanced negative polarization branch if compared to lower density samples.

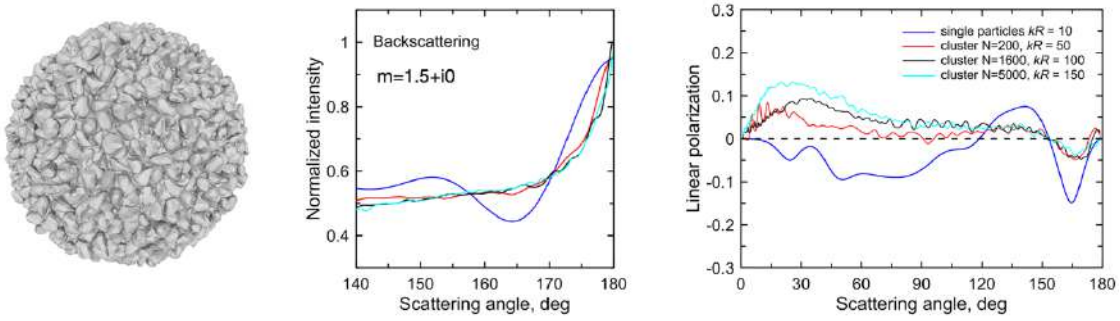

Figure 1: Sample of a dense cluster of N=5000 particles with packing density ρ = 0.5 (a) and intensity (b) and linear polarization (c) scattering angle curves for single random irregular particles with size parameter kR_c = 10 and clusters with sizes kR = 50, 100 and 150.

References

[1] J. S. Hesthaven, T. Warburton, *Nodal High-Order Methods on Unstructured Grids: I. Time-Domain Solution of Maxwell's Equations*, Journal of Computational Physics, 186:186-221, 2002.

[2] Y. Grynko, Y. Shkuratov, and J. Förstner, *Intensity surge and negative polarization of light from compact irregular particles*, Optics letters, 43:3562-3565, 2018.

Optically induced aggregation by radiation pressure of gold nanorods on graphene for SERS detection of biomolecules

A. Foti[1,*], M.G. Donato[1], O.M. Maragò[1], and P.G. Gucciardi[1]

[1]*CNR-IPCF, Istituto per i Processi Chimico-Fisici, V.le F. Stagno D'Alcontres 37, I-98158, Messina, Italy*
[*]*corresponding author's e-mail: antonino.foti@cnr.it*

Radiation pressure can be used to push gold nanorods and create plasmonic aggregates for Surface-Enhanced Raman Spectroscopy (SERS) in liquid [1-2]. The nature of the substrate where the aggregation takes place plays a role in the process [3]. Here gold nanorods aggregation is carried out on multilayered graphene creating hybrid SERS-active surfaces for ultrasensitive detection of bovine serum albumin (BSA). The aggregation kinetics is studied as a function of the irradiation time [4]. We observe that optical aggregation on graphene is 3.5 times slower compared to glass, while no stable aggregation is obtained on gold. We attribute the differences to the destabilization effect of the standing wave produced on the metallic substrates, due to their higher reflectivity, and to the reduced thermophoretic effects, related to the higher heat dissipation [4]. Despite the slowdown of the aggregation kinetics, the usage of graphene as substrate offers manifold benefits: an almost negligible fluorescence background when using near-infrared light (785 nm), the absence of thermal absorption as well as the possibility to easily functionalize the surface to enhance the affinity with the analytes. Our results enlarge the spectrum of materials that can be used for optical aggregation and SERS detection of biomolecules, highlighting the importance of controlling the physical properties of the surfaces.

We acknowledge financial contribution from the agreement ASI-INAF n. 2018-16-HH.0, project "SPACE Tweezers" and the MSCA ITN (ETN) project "Active Matter".

References

[1] B. Fazio, C. D'Andrea, A. Foti, E. Messina, A. Irrera, M. G. Donato, V. Villari, N. Micali, O. M. Maragò, and P. G. Gucciardi, *SERS detection of Biomolecules at Physiological pH via aggregation of Gold Nanorods mediated by Optical Forces and Plasmonic Heating*, Sci. Rep. 6, 26952, 2016.

[2] A. Foti, C. D'Andrea, V. Villari, N. Micali, M. G. Donato, B. Fazio, O. M. Maragò, R. Gillibert, M. Lamy de la Chapelle, and P. G. Gucciardi, *Optical aggregation of gold nanoparticles for SERS detection of proteins and toxins in liquid environment: Towards ultrasensitive and selective detection*, Materials 11, 440, 2018.

[3] M. G. Donato, V. P. Rajamanickam, A. Foti, P. G. Gucciardi, C. Liberale, and O. M. Maragò, *Optical force decoration of 3D microstructures with plasmonic particles*, Opt. Lett. 43, 5170, 2018.

[4] A. Foti, M. G. Donato, O. M. Maragò, and, P. G. Gucciardi, *Optically induced aggregation by radiation pressure of gold nanorods on graphene for SERS detection of biomolecules*, Eur. Phys. J. Plus, 136, 30, 2021.

On the Interference of Incident and Scattered Fields in Generalized Lorenz-Mie Theory

J. Gienger[1,*]

[1] *Physikalisch-Technische Bundesanstalt (PTB), Abbestraße 2–12, 10587 Berlin, Germany*
[*] *corresponding author's e-mail: jonas.gienger@ptb.de*

Generalized Lorenz-Mie Theory (GLMT) describes the scattering of a Gaussian beam by a single sphere. A Gaussian beam can be characterized by its wavenumber $k = 2\pi/\lambda$, its waist radius w_0 and its waist center $\boldsymbol{r}_0 = (x_0, y_0, z_0)^T$. To lowest order ("order L approximation") in the dimensionless waist parameter $s = 1/(k\,w_0)$ the Cartesian components of the electric field read [1]

$$\boldsymbol{E}^{\mathrm{inc}}(\boldsymbol{r}) = \begin{pmatrix} 1 \\ 0 \\ -2Q\,s\,\frac{x-x_0}{w_0} \end{pmatrix} E_0 \Psi_0 \mathrm{e}^{-\mathrm{i}k\,(z-z_0)}, \text{ with } \Psi_0 = \mathrm{i}Q\,\exp\left(-\mathrm{i}Q\,\frac{(x-x_0)^2+(y-y_0)^2}{w_0^2}\right),\ Q = \frac{1}{\mathrm{i}+2s\,\frac{z-z_0}{w_0}}. \quad (1)$$

At the so-called "order L^- approximation" this is further simplified by $E_z^{\mathrm{inc}} = 0$.

The total electric field $\boldsymbol{E}^{\mathrm{tot}} = \boldsymbol{E}^{\mathrm{inc}} + \boldsymbol{E}^{\mathrm{sca}}$ is composed of an incident and a scattered wave. Analogous to standard (plane wave) Lorenz-Mie Theory (LMT), in GLMT, one uses series expansions of the fields, which in regular vector spherical wave functions (VSWFs) $\boldsymbol{M}_{mn}^{(1)}$, $\boldsymbol{N}_{mn}^{(1)}$ and irregular (outgoing) VSWFs $\boldsymbol{M}_{mn}^{(4)}$, $\boldsymbol{N}_{mn}^{(4)}$ can be written as [2]

$$\begin{Bmatrix} \boldsymbol{E}^{\mathrm{inc}}(\boldsymbol{r}) \\ \boldsymbol{E}^{\mathrm{sca}}(\boldsymbol{r}) \end{Bmatrix} = E_0 \sum_{n=1}^{\infty}\sum_{m=-n}^{n} (-\mathrm{i})^{n+1}\frac{2n+1}{n(n+1)}(-1)^{m+\frac{m-|m|}{2}}\frac{(n-m)!}{(n-|m|)!}\begin{Bmatrix} -\mathrm{i}g_{n,\mathrm{TE}}^m \boldsymbol{M}_{mn}^{(1)}(k\boldsymbol{r}) + g_{n,\mathrm{TM}}^m \boldsymbol{N}_{mn}^{(1)}(k\boldsymbol{r}) \\ \mathrm{i}b_n\, g_{n,\mathrm{TE}}^m \boldsymbol{M}_{mn}^{(4)}(k\boldsymbol{r}) - a_n\, g_{n,\mathrm{TM}}^m \boldsymbol{N}_{mn}^{(4)}(k\boldsymbol{r}) \end{Bmatrix}. \quad (2)$$

I. e., an $\mathrm{e}^{\mathrm{i}\omega t}$ time dependence is assumed for all fields. The sphere's scattering coefficients a_n, b_n are identical to those in LMT. In addition, the GLMT features *beam shape coefficients* (BSCs) $g_{n,\mathrm{TM}}^m, g_{n,\mathrm{TE}}^m$ describing the incident field $\boldsymbol{E}^{\mathrm{inc}}$. For Gaussian beams computing the BSCs such that $\boldsymbol{E}^{\mathrm{inc}}$ in Eq. (2) represents Eq. (1) is a non-trivial task for which multiple methods can be used [1], including the so-called *localized approximation* (LA) providing a heuristic, approximate analytical expression and a numerically inexpensive tool for computing the BSCs.

The far field limit ($r \to \infty$) of $\boldsymbol{E}^{\mathrm{sca}}$ is an outgoing spherical wave with direction-dependent amplitude

$$\boldsymbol{E}^{\mathrm{sca}}(r,\vartheta,\varphi) \sim \boldsymbol{E}_\infty^{\mathrm{sca}}(\vartheta,\varphi)\,\frac{\mathrm{e}^{-\mathrm{i}k\,r}}{k\,r}. \quad (3)$$

In LMT, the far-field behavior of $\boldsymbol{E}^{\mathrm{inc}}$ would correspond to a δ-distribution-like behavior at $\vartheta = 0, \pi$, due to the exactly-defined direction of propagation of a plane wave. In GLMT however, due to the divergence of a focused beam, $\boldsymbol{E}^{\mathrm{inc}}$ is nonzero for $\vartheta \neq 0, \pi$ as $r \to \infty$ and contains both outgoing and incoming wave components. Hence, interference between $\boldsymbol{E}^{\mathrm{inc}}$ and $\boldsymbol{E}^{\mathrm{sca}}$ occurs at finite (typically small) angles ϑ (or $\pi - \vartheta$) even in the far-field limit.

When evaluating the equations for a given scattering problem, $\boldsymbol{E}^{\mathrm{sca}}$ is computed from Eq. (2) or the corresponding $r \to \infty$ limit. Computing the total fields $\boldsymbol{E}^{\mathrm{tot}} = \boldsymbol{E}^{\mathrm{inc}} + \boldsymbol{E}^{\mathrm{sca}}$ can be done with one of two approaches: (a) Using $\boldsymbol{E}^{\mathrm{inc}}$ from Eq. (1), or (b) using $\boldsymbol{E}^{\mathrm{inc}}$ from Eq. (2). Supposedly the two are equivalent at least within the order L/L^- approximation and the intensities $I^{\mathrm{inc}} \propto |\boldsymbol{E}^{\mathrm{inc}}|^2$ associated with either description are indeed virtually identical for reasonably small s. However, significantly different numerical results are obtained with the two methods for $\boldsymbol{E}^{\mathrm{tot}}$. Obviously, they cannot both be physically correct. In this talk we will discuss the cause of this and explain which method for the numerical computation of such interference effects is consistent with physical intuition.

References

[1] Gérard Gouesbet and Gérard Gréhan. *Generalized Lorenz-Mie Theories*. Springer, 2nd edition, 2017.
[2] Gérard Gouesbet. T-matrix formulation and generalized Lorenz–Mie theories in spherical coordinates. *Optics Communications*, 283(4):517–521, 2010.

Negative polarization at backscattering from clusters of absorbing irregular particles: numerical simulations

S. Alhaddad*, Y. Grynko , and J. Förstner

Department of Theoretical Electrical Engineering, Paderborn University, Germany
**corresponding author's e-mail: samer.alhaddad@uni-paderborn.de*

Introduction

Optical opposition phenomena like backscattering intensity surge and negative polarization (NP) are often observed for surfaces that are formed by densely packed randomly shaped mineral particles. Their parameters such as the intensity peak width and the depth and inversion angle of the NP branch depend on the physical properties of the scatterers and the topology of the upper surface layer. Hence, this dependence can be utilized in the data retrieval in remote sensing applications. Approximate numerical models like clusters of very small spheres or hybrid geometric/wave optics schemes are usually used in the study of these phenomena, but due to their limitations they do not provide insightful explanation of their origin and of negative polarization in particular. Therefore we follow a full wave optics approach in this work.

Model description and results

We apply the Discontinuous Galerkin Time Domain (DGTD) [1] method and densely packed Gaussian random field shapes [2] to solve a full wave optics problem for dense agglomerates of irregular absorbing particles larger than the wavelength. With the refractive index of material m=1.5 - i0.3 and the size parameter of the constituents kr=30 this reproduces typical conditions in low-albedo surfaces with minimum multiple scattering. Our results show that single scattering by isolated particles with high absorption does not produce NP at all. Basic double scattering in compact two-particles structures shows very little or no sign of the effect. At the same time agglomerates of three, four and more particles are able to reproduce NP in the same extent as very large monolayers and thick slabs of hundreds of particles. Thus, we deduce that the NP branch is formed by double scattering if sufficient geometry variation is provided by the random structure of the scatterer. Furthermore, the study of NP properties for large systems in the case of high absorption can be reduced to simulation of clusters of a few particles.

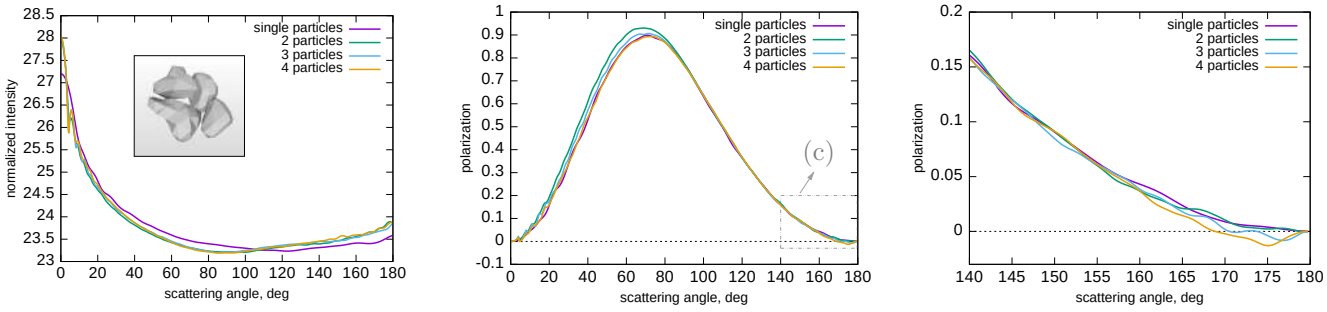

(a) (b) (c)

Figure 1: Normalized intensity (a) and linear polarization (b,c) of scattered light calculated for single irregular particles and agglomerates of two, three and four particles. The size parameter of constituents is kr=30 and the refractive index is m=1.5 - i0.3.

References

[1] J. S. Hesthaven and T. Warburton *Nodal Discontinuous Galerkin Methods*. Springer New York, 2008.
[2] Y. Grynko, Y. Shkuratov, and J. Förstner *Light backscattering from large clusters of densely packed irregular particles*. J. Quant. Spectrosc. Radiat. Transfer, 255:107234, 2020.

Optical forces in front of epsilon-near-zero metamaterials

Maria G. Donato[1,*], Y. Kiasat[2], M. El Kabbash[3,4], T. Letsou[4], M. Hinczewski[4], R. Saija[1,5], O. M. Maragò[1], G. Strangi[4,6,7], and N. Engheta[2]

[1] *CNR-IPCF, Istituto per i Processi Chimico-Fisici, Messina, I-98158, Italy*
[2] *Univ. Penn., Elect Syst Engn Dept, Philadelphia, PA 19104 USA*
[3] *Univ Rochester, Inst Opt, Rochester, NY 14627 USA*
[4] *Case Western Reserve Univ, Dept Phys, Cleveland, OH 44106 USA*
[5] *Dip. di Scienze Matematiche e Informatiche, Scienze Fisiche e Scienze della Terra, Univ. Messina, Messina I - 98166, Italy*
[6] *Univ Calabria, CNR Nanotec, Arcavacata Di Rende, Italy*
[7] *Univ Calabria, Dept Phys, Arcavacata Di Rende, Italy*
[*] *corresponding author's e-mail: maria.donato@cnr.it*

Abstract

In optical tweezers [1, 2] micro- or nano-particles can be used as extremely sensitive probes of force fields in front of surfaces. This approach allows force sensing in the femtoNewton range, with a spatial resolution controlled by the size of the trapped probe [3]. Recently, it has been suggested that near-field repulsive forces are expected on a radiating dipole in front of epsilon-near-zero (ENZ) metamaterials [4]. In this work, we look at the general features of optical forces exerted on nanoparticles in front of an ENZ surface using different approaches: dipole approximation, finite elements calculations, and T-matrix modeling in combination with the evaluation of forces by the integration of Maxwell stress tensor. In addition, we describe the role of realistic layered materials that for specific wavelength range behaves as ENZ surfaces. Finally, we discuss the role of composition and shape of the trapped particle by studying optical forces on core-shell SiO_2-Ag spheres, Janus nanoparticles, and Ag ellipsoids. The results of this theoretical study may guide the experimental observation of this near-field force in front of properly designed metamaterials surfaces.

References

[1] A. Ashkin *Acceleration and trapping of particles by radiation pressure.* Phys. Rev. Lett. 24:156-159, 1970
[2] P. H. Jones, O. M. Maragò, G. Volpe *Optical Tweezers - Principles and Applications.* Cambridge University Press, Cambridge, 2015
[3] R. Desgarceaux, Z. Santybayeva, E. Battistella, A. L. Nord, C. Braun-Breton, M. Abkarian, O. M. Maragò, B. Charlot, and F. Pedaci *High-resolution photonic force microscopy based on sharp nanofabricated tips.* Nano Letters, 20:4249-4255, 2020.
[4] F. J. Rodríguez-Fortuño, A. Vakil, and N. Engheta *Electric levitation using ε-near-zero metamaterials.* Phys. Rev. Lett. 112:033902, 2014.

Retrieving dust properties of debris disks

J. A. Arnold[1,*], A. J. Weinberger[2], G. Videen[1,3], E. Zubko[4]

[1]Army Research Laboratory, 2800 Powder Mill Rd. Adelphi, MD 20783, USA
[2]Department of Terrestrial Magnetism, Carnegie Institution for Science, 5421 Broad Branch Rd. Washington, DC 20015, USA
[3]Space Science Institute, 4750 Walnut Street, Boulder Suite 205, CO 80301, USA
[4]Kyung Hee University, 1732, Deogyeong-daero, Giheung-gu, Yongin-si, Gyeonggi-do 17104, Republic of Korea

[*]Presenting author (jessy.arnold@gmail.com)

Debris disks are dusty circumstellar disks analogous to our solar system's Kuiper belt, asteroid belt, and zodiacal cloud [1]. The dust in these disks is produced by the destruction of comets, asteroids, and protoplanets. Understanding the composition of the material within these extrasolar systems may provide insight into the planet formation process, especially in cases where the star also hosts planets. For example, AU Microscopii (AU Mic) hosts both a debris disk and a Neptune-sized exoplanet [2].

As debris disks are typically too cold to produce key identifying silicate spectral features in thermal emission near 10 μm [3], scattered light observations in the VNIR wavelength range are important for making compositional determinations. To these observations we need to model the light scattering properties of the constituent dust, which depend on grain composition, size, and structure. Often these models assume compact, spherical particles [e.g. 4], although other grain shapes such as ellipsoids and distributed hollow spheres have been considered [e.g. 5].

Here we present a model that uses the discrete dipole approximation (DDA) method [6,7] to calculate scattering efficiencies for realistic grain shapes [7]. To apply these calculations to debris disk spectra we generate a lookup table of the scattering properties as a function of grain size and refractive index. We then use a Markov chain Monte Carlo (MCMC) model [8] to fit the scattered light spectra using these lookup tables.

Composition is parameterized as the volume fraction of each component based on the wavelength-dependent complex refractive index and includes astronomical silicate, amorphous carbon, water ice, tholin, and metallic iron. The disk is modeled in 3D, then projected in 2-D so that spectra generated from a given set of parameters can be extracted and compared to the measured flux ratio from telescopic data.

References

[1] Hughes A. M., Duchene G., and Matthews B. C. (2018) *An. Rev. A&A.,* 56, 541–591.
[2] Plavchan P. et al (2020) *Nature*, 582, 7813, 497–500
[3] Matthews B. C., Krivov A. V., Wyatt M. C., et al. (2014) *Protostars & Planets VI*, 25 p.
[4] Kruegel E. and Siebenmorgen R. (1994) *A&A*, 288, 929–941.
[5] Min M., Hovenier J. W., de Koter A. (2005) *A&A*, 404, 35–46.
[6] Draine B. T. and Flatau P. J. (1994) *J. Opt. Soc. Am. A*, 11, 1491–1499.
[7] Zubko E., Petrov D., Shkuratov Y. et al. (2005) *Appl. Opt.*, 44, 30.
[8] Foreman-Mackey D. et al. (2013) *PASP*, 125, 925.

A numerically stable T-matrix algorithm

Stuart C. Hawkins[1,*] and M. Ganesh[2]

[1] *Department of Mathematics and Statistics, Macquarie University, Sydney, NSW 2109, Australia*
[2] *Department of Applied Mathematics and Statistics, Colorado School of Mines, Golden, Colorado*
[*] *corresponding author's e-mail: stuart.hawkins@mq.edu.au*

Abstract

The T-matrix is an important tool for scattering simulations and is widely used in many applications including atmospheric science, meteorology, oceanography, and biology. The T-matrix was conceived a half century ago and was computed using the null field method or extended boundary condition method (EBCM) [4]. However it is well known that the EBCM is numerically unstable for particles that deviate significantly from a sphere. Related methods involving point matching have similar stability issues.

An extensive literature has been devoted to modifying the EBCM to overcome numerical stability issues, for example by exploiting knowledge of the scatterer shape [2,3,5], or using extended precision arithmetic [1]. However, the EBCM is not intrinsic to the T-matrix and in this talk we describe a completely different approach that is numerically stable for all scatterers. The key to our method is calculating the T-matrix in the far field instead of on the scatterer surface.

We describe a recently developed object oriented Matlab toolbox implementing our method. Using the toolbox we demonstrate the enhanced numerical stability of our method for scattering by geometries with large aspect ratios and large size parameters.

References

[1] M. I. Mishchenko and L. D. Travis. T-matrix computations of light scattering by large spheroidal particles. *Opt. Commun.*, 109:16–21, 1994.
[2] A. Sarkissian, C. F. Gaumond, and L. R. Dragonette. T-matrix implementation of forward scattering from rigid structures. *J. Acoust. Soc. Am.*, 94:3448–3453, 1993.
[3] W. R. C. Somerville, B. Auguié, and E. C. Le Ru. Severe loss of precision in calculations of T-matrix integrals. *J Quant Spectrosc Radiat Transfer*, 113:524–535, 2012.
[4] P. C. Waterman. Matrix formulation of electromagnetic scattering. *Proc. IEEE*, 53:805–812, 1965.
[5] P. C. Waterman. The T-matrix revisited. *J. Opt. Soc. Am. A*, 24:2257–2267, 2007.

Two Decades of Ground-based Multisensor AOD Measurements at US Continental Site: Acquisition and Merger

E. Kassianov[1,*], G. Gibler[1], E. Cromwell[1], J. Monroe[2,3,6], L.D. Riihimaki[4,5], C. Flynn[6], J. Barnard[7], J.J. Michalsky[8], G. Hodges[4,5], Y. Shi[1], J.M. Comstock[1]

[1] *Pacific Northwest National Laboratory, USA*
[2] *Cooperative Institute for Mesoscale Meteorological Studies (CIMMS), USA*
[3] *NOAA National Severe Storms Laboratory, USA*
[4] *Cooperative Institute for Research in Environmental Science (CIRES), USA*
[5] *NOAA Global Monitoring Laboratory, USA*
[6] *University of Oklahoma, USA*
[7] *University of Nevada Reno, USA*
[8] *NOAA Global Monitoring Laboratory, USA*
[*] *corresponding author's e-mail: Evgueni.Kassianov@pnnl.gov*

Abstract

Long-term records of aerosol optical depth (AOD) with high quality, suitable temporal continuity and spatial coverage are of immense interest to climate-related research activities. Both satellite- and ground-based measurements of AOD are typically provided by instruments with different designs, and distinct data acquisition and processing schemes. Thus, the corresponding AOD records likely have different accuracy, spatial coverage, and temporal resolution. Several studies have been focused on the synergy of multi-sensor satellite AOD products. Here we combine multi-year (1997-2018) AOD records available from four collocated ground-based instruments deployed at the mid-continental Southern Great Plains (SGP) Central Facility supported by the U.S. Department of Energy Atmospheric Radiation Measurement (ARM) Program. We demonstrate how to minimize drawbacks (patchy spots) and to maintain benefits (high quality) of these records. Our demonstration finds a combined AOD obtained at two wavelengths (500 and 870 nm), with high temporal resolution (1-min), and provides the user with an estimate of the AOD uncertainty. Finally, we highlight expected applications of the merged dataset and its future extensions.

Granada-Amsterdam Light Scattering Database

D. Guirado[1,*], O. Muñoz[1], H. Volten[2], J.C. Gómez Martín[1], and F. Moreno[1]

[1] *Instituto de Astrofísica de Andalucía, CSIC, Granada, Spain*
[2] *National Institute for Public Health and the Environment (RIVM), Bilthoven, The Netherlands*
[*] *corresponding author's e-mail: dani@iaa.es*

Abstract

A new light scattering web database is presented, including measurements of scattering matrices produced by both the Light Scattering Laboratory at the Vrije Universiteit [1, 2], and the Cosmic Dust Laboratory at the Instituto de Astrofísica de Andalucía - CSIC [3]. Measurements of scattering matrices for each sample of dust particles with astrophysical interest, plus some other samples, are freely available. Some more information on the samples is included, such as for instance, measurements of size distributions, SEM images, and synthetic matrices for the whole range $[0, 180]deg.$ of the scattering angle.

Samples from Amsterdam and Granada are not separated anymore within this database, as they were in a previous version [4].

The main menu is a quite simple panel of six self-explanatory boxes (see Fig. 1).

Figure 1: Main menu of the Granada-Amsterdam light-scattering database.

In the "List of All Samples" sub-menu, a quick reference table containing all measurements in Amsterdam and Granada and some basic information on them is presented, so readers can decide whether or not they are interested in a certain sample. By clicking on the selected sample, we move to the corresponding place of that sample in the "Samples Categories" sub-menu. All measurements and details on that sample can be found there.

References

[1] O. Muñoz, H. Volten, J.F. de Haan, W. Vassen, and J.W. Hovenier. *Experimental determination of scattering matrices of olivine and Allende meteorite particles.* Astron. Astrophys, 360: 777788, 2000.

[2] H. Volten, O. Muñoz, E. Rol, J.F. de Haan, W. Vassen, and J.W. Hovenier. *Scattering matrices of mineral aerosol particles at 441.6 nm and 632.8 nm.* J. Geoph. Research, 106, No. D15:17,375-17,401, 2001.

[3] O. Muñoz, F. Moreno, D. Guirado, J.L. Ramos, A. López, F. Girela, J.M. Jerónimo, L.P. Costillo, and I. Bustamante. *Experimental determination of scattering matrices of dust particles at visible wavelengths: The IAA light scattering apparatus.* J. Quant. Spectrosc. Radiat. Transfer, 111:187-196, 2010.

[4] O. Muñoz, F. Moreno, D. Guirado, D.D. Dabrowska, H. Volten, and J.W. Hovenier. *The AmsterdamGranada Light Scattering Database.* J. Quant. Spectrosc. Radiat. Transfer, 113:565-574, 2012.

Lidar multiple scattering by soot fractal aggregates

L.Paulien[1,2,*], R.Ceolato[1], F.Enguehard[3], L.Soucasse[2], A.Soufiani[2]

[1]*ONERA, The French Aerospace Lab, Toulouse FR 31055, France*
[2]*Laboratoire EM2C, CentraleSupélec, Université Paris-Saclay, Gif-sur-Yvette FR 91192, France*
[3] *Institut PPrime, CNRS, Université de Poitiers, ISAE-ENSMA, Futuroscope, Chasseneuil FR 86962, France*
[*]*corresponding author's e-mail: lucas.paulien@onera.fr*

Introduction

Smoke particles are a product of the combustion of organic compound. Shortly after the combustion process, smoke particles exhibit a fractal-like morphology, and are formed of clustered primary particles called monomers [1]. Smoke particles are found to induce a positive radiative forcing through both direct and indirect effects (*e.g.* increase in cloud lifetime, role as cloud condensation nuclei) [2][3]. Still, the evaluation of these particles radiative forcing remains subject to uncertainties. These uncertainties are partly engendered by these particles morphological and composition complexity, which are also subject to changes during their atmospheric lifetime. To further evaluate their contribution to the radiative budget, the measurement of their micro-physical properties at each steps of their lifetime is needed. Lidar are remote-sensing instruments able to retrieve some of these properties (*e.g.* particle number concentration, particle type). Nevertheless, several factors such as the multiple scattering can induce uncertainties in the retrieval of these micro-physical properties. The effect of multiple scattering on the lidar measurements acquired on smoke plumes remains mostly unknown.

Modelling of multiply scattered polarized lidar signal

In this study, the fractal aggregate model is used to describe the soot particles morphology. The radiative properties of these particles are computed using the Multiple-Sphere T-matrix Method. In order to simulate a polarized lidar signal, a simulation code based on the Monte-Carlo method has been developed. The scattering medium is modelled with a gaussian particle number concentration profile and using the previously computed radiative properties. Several cases are computed at three different wavelengths (*i.e.* 355nm, 532 nm and 1064 nm) and two different field of view (*i.e.* 0.5 mrad and 5 mrad).

We study the variation of the multiple scattering fraction (MSF) and of the linear depolarization ratio (LDR) according to the cloud optical depth and to the integrated attenuated backscattering. We find an increase of both MSF and LDR at larger optical depth, integrated attenuated backscatter and field of view.

References

[1] Forrest, S. R., & Witten Jr, T. A. (1979). Long-range correlations in smoke-particle aggregates. *Journal of Physics A: Mathematical and General*, *12*(5), L109.

[2] Myhre, G., D. Shindell, F.-M. Bréon, W. Collins, J. Fuglestvedt, J. Huang, D. Koch, J.-F. Lamarque, D. Lee, B. Mendoza, T. Nakajima, A. Robock, G. Stephens, T. Takemura and H. Zhang, 2013: Anthropogenic and Natural Radiative Forcing. In: *Climate Change 2013: The Physical Science Basis. Contribution of Working Group I to the Fifth Assessment Report of the Intergovernmental Panel on Climate Change* [Stocker, T.F., D. Qin, G.-K. Plattner, M. Tignor, S.K. Allen, J. Boschung, A. Nauels, Y. Xia, V. Bex and P.M. Midgley (eds.)]. Cambridge University Press, Cambridge, United Kingdom and New York, NY, USA, pp. 659–740, doi:10.1017/ CBO9781107415324.018.

[3] Kärcher, B. (2018). Formation and radiative forcing of contrail cirrus. *Nature communications*, *9*(1), 1-17.

Simulating nanoparticles interaction with an electron beam using the discrete dipole approximation

A.A. Kichigin[1,2*] and M.A. Yurkin[1,2]

[1]*Voevodsky Institute of Chemical Kinetics and Combustion, SB RAS, Institutskaya 3, 630090 Novosibirsk, Russia*
[2]*Novosibirsk State University, Pirogova 2, 630090 Novosibirsk, Russia*
[*]*corresponding author's e-mail: alkichigin@gmail.com*

Introduction

Studying the optical properties of plasmonic nanoparticles, scientists conduct experiments in which the nanoparticle is scanned by an electron beam [1]. The main advantage of an electron beam over optical methods (limited by the diffraction limit) is that it allows one to localize plasmon resonances on the surface of a nanoparticle with the accuracy of at least 1 nm. When scanning a nanoparticle, fast electrons lose energy (electron energy loss spectroscopy – EELS), and the particle emits light (cathodoluminescence – CL). As a result of the experiment, EELS and CL spectra are obtained for each position of the beam on the particle cross-section.

To correctly interpret the data obtained in the experiment, it is necessary to numerically simulate the experiment. The existing theory covers only the case of interaction of a particle and an electron in a vacuum - when there nothing else present. But in reality, the particle is placed on a substrate (or inside a substrate) to resist gravity and collisions with fast electrons.

Results

In this work, the volume-integral formulation of Maxwell's equations in terms of the Green's tensor was used [2]. As a result, we obtained a generalized solution for interaction of a particle and electron in an arbitrary (including absorbing) infinite host medium, including the case of Cherenkov radiation. This solution was not known previously, but its limiting case of vacuum matches the previously known theory.

The expressions obtained with this solution for simulating the EELS and CL were implemented in the open-source software ADDA (currently available in a separate fork – https://github.com/alkichigin/adda), based on the discrete dipole approximation [3]. The simulation results for spheres in a vacuum showed agreement with the exact reference solution (Lorentz-Mie theory). Moreover, the simulated spectrum for a silver sphere in a non-absorbing medium (SiNx plate, speed of light 0.55c, where c is the speed of light in vacuum) matched the experimental one, where electrons had the 120 keV energy (the corresponding speed is 0.59c – Cherenkov radiation case). This and other results will be demonstrated at the conference.

[1] F. J. García de Abajo, 'Optical excitations in electron microscopy', *Rev. Mod. Phys.*, vol. 82, no. 1, pp. 209–275, Feb. 2010, doi: 10.1103/RevModPhys.82.209.
[2] M. A. Yurkin and M. I. Mishchenko, 'Volume integral equation for electromagnetic scattering: Rigorous derivation and analysis for a set of multilayered particles with piecewise-smooth boundaries in a passive host medium', *Phys. Rev. A*, vol. 97, no. 4, p. 043824, Apr. 2018, doi: 10.1103/PhysRevA.97.043824.
[3] M. A. Yurkin and A. G. Hoekstra, 'The discrete dipole approximation: an overview and recent developments', *J. Quant. Spectrosc. Radiat. Transf.*, vol. 106, no. 1–3, pp. 558–589, 2007, doi: 10.1016/j.jqsrt.2007.01.034.

Electromagnetic scattering by a three-dimensional object composed of an orthorhombic dielectric-magnetic medium with magnetoelectric gyrotropy

Hamad M. Alkhoori[1,*]

[1] *United Arab Emirates University*
[*] *corresponding author's e-mail: hamad.alkhoori@uaeu.ac.ae*

Abstract

This work investigates electromagnetic scattering by a three-dimensional object composed of an orthorhombic dielectric-magnetic medium with magnetoelectric gyrotropy using the extended boundary condition method (EBCM) [1,2]. Known vector spherical wave functions were used to represent the fields in the surrounding space. After deriving closed-form expressions of the vector spherical wave functions for the chosen medium (available in coordinate-free form but not in closed-form [3]), the internal fields were represented as superpositions of those vector spherical wave functions. Application of the Ewald–Oseen extinction theorem and the Huygens principle then yielded a transition matrix to relate the unknown scattered field coefficients to the known incident field coefficients.

Numerical results were obtained for scattering of a plane wave by an ellipsoid composed of the chosen medium. The scattering, absorption, and extinction efficiencies were calculated thereby in relation to: (i) the shape of the object, (ii) the constitutive-anisotropy parameters of the permittivity and permeability dyadics, (iii) the magnetoelectric-gyrotropy vector, and (iv) the orientation of the constitutive principal axes with respect to the shape principal axes.

A study on the shape of the object and the constitutive-anisotropy parameters revealed that the total scattering efficiency can be smaller than the absorption efficiency for some configurations of the incident plane wave but not necessarily for others. The shape of the object has a stronger influence on the total scattering efficiency than on the absorption efficiency. Even though the ellipsoid is not necessarily a body of revolution, it is anisotropic, and it is not impedance matched to free space, the backscattering efficiency can be minuscule but the forward-scattering efficiency is not.

The effects of the magnetoelectric-gyrotropy vector can be envisioned in that both the total scattering and forward-scattering efficiencies are maximum when the plane wave is incident in a direction coparallel (but not antiparallel) to the magnetoelectric-gyrotropy vector, and the backscattering efficiency is minimum when the magnetoelectric-gyrotropy vector is parallel to the incidence direction. The total scattering and forward-scattering efficiencies are maximum when the incidence direction is parallel to the largest semi-axis of the ellipsoid if the incidence direction is coparallel (but not antiparallel) to the magnetoelectric-gyrotropy vector. From these results, I concluded that Lorentz nonreciprocity in an object is intimately connected to the shape of that object in affecting the scattered field.

The orientation of the constitutive principal axes with respect to the shape principal axes has a noticeable effect on the total scattering and absorption efficiencies as the electrical size increases. Furthermore, the polarization state of the incident plane wave has a more visible effect on the total scattering and absorption efficiencies for ellipsoids compared to spheres.

As an application that involves the chosen medium of this work, I determined sufficient conditions for zero backscattering from an object composed of the chosen medium and suspended in an isotropic dielectric-magnetic medium with magnetoelectric gyrotropy by an analysis of the transition matrix. The elements of the transition matrix must satisfy certain conditions for zero backscattering. Numerical results obtained thereby showed that the sufficient set of three zero-backscattering conditions are as follows: (i) The object is a body of revolution with the incident plane wave propagating along the axis of revolution. (ii) The impedances of both mediums are equal. (iii) The magnetoelectric-gyrotropy vectors of both mediums are aligned along the axis of revolution, whether or not both magnetoelectric-gyrotropy vectors are co-parallel.

References

[1] P. C. Waterman *Matrix formulation of electromagnetic scattering.* Proc. IEEE, 53: 805-812, 1965.

[2] A. Lakhtakia, "The Ewald–Oseen extinction theorem and the extended boundary condition method," in *The World of Applied Electromagnetics*, A. Lakhtakia and C. M. Furse, eds., Springer, 2018.

[3] A. Lakhtakia and T. G. Mackay, *Vector spherical wavefunctions for orthorhombic dielectric-magnetic material with gyrotropic-like magnetoelectric properties.* J. Opt. (India), 41: 201–213, 2012.

IPRT polarized radiative transfer model intercomparison project - Three-dimensional test cases

C.Emde[1,7,*], V. Barlakas[2,8], C. Cornet[3], F. Evans[4], Z. Wang[5], L. C.-Labonnote[4], A. Macke[2], B. Mayer[1], and M. Wendisch[6]

[1]*Meteorological Institute, Ludwig-Maximilians-University (LMU), Theresienstr. 37, D-80333 Munich, Germany*
[2]*Leibniz Institute for Tropospheric Research, Permoserstr. 15, Leipzig, Germany*
[3]*Laboratoire d'Optique Atmosphérique, Université Lille, France*
[4]*University of Colorado, Boulder, CO 80309, USA*
[5]*Nanjing University of Information Science and Technology, China*
[6]*Leipzig Institute for Meteorology, University of Leipzig, Stephanstr. 3, Leipzig, Germany*
[7]*German Aerospace Center (DLR), Oberpfaffenhofen, Germany*
[8]*Chalmers University of Technology, Gothenburg, Sweden*
[*]*corresponding author's e-mail: claudia.emde@lmu.de*

Initially unpolarized solar radiation becomes polarized by scattering in the Earth's atmosphere. Each atmospheric constituent, e.g., molecules, cloud droplets, and ice crystals, produces a characteristic polarization signal, thus spectro-polarimetric measurements are frequently employed for remote sensing of aerosol and cloud properties.

Retrieval algorithms require efficient radiative transfer models and commonly the plane-parallel approximation is applied. For remote sensing applications, the radiance is considered constant over the instantaneous field-of-view of the instrument and each sensor element is treated independently in plane-parallel approximation, neglecting horizontal radiation transport between adjacent pixels. In order to estimate the errors due to the IPA approximation, three-dimensional (3D) vector radiative transfer models are required.

So far, only a few such models exist. Therefore, the International Polarized Radiative Transfer (IPRT) working group of the International Radiation Commission (IRC) has initiated a model intercomparison project in order to provide benchmark results for polarized radiative transfer. The group has first performed an intercomparison for one-dimensional (1D) multi-layer test cases [2]. The second the intercomparison shown in this presentation is for 2D and 3D test cases [1]: a step cloud, a cubic cloud, and a more realistic scenario including a 3D cloud field generated by a Large Eddy Simulation model and typical background aerosols.

All commonly established benchmark results for 3D polarized radiative transfer are available at the IPRT website (`http://www.meteo.physik.uni-muenchen.de/~iprt`).

References

[1] C. Emde, V. Barlakas, C. Cornet, F. Evans, Z. Wang, L. C.-Labonotte, A. Macke, B. Mayer, and M. Wendisch. *IPRT polarized radiative transfer model intercomparison project – Three-dimensional test cases (phase B).* J. Quant. Spectrosc. Radiat. Transfer, 209:19-44, 2018

[2] C. Emde, V. Barlakas, C. Cornet, F. Evans, S. Korkin, Y. Ota, L. C.-Labonnote, A. Lyapustin, A. Macke, B. Mayer, and M. Wendisch. *IPRT polarized radiative transfer model intercomparison project – Phase A.* J. Quant. Spectrosc. Radiat. Transfer, 164(0):8-36, 2015.

CBFM on Adaptive Mesh for Efficient Calculation of Scattering by Complex-Shaped Mixed-Phase Hydrometeors

I. Fenni[1,2,*], K-S. Kuo[3] and H. Roussel[4]

[1] *JIFRESSE, University of California Los Angeles, USA*
[2] *Jet Propulsion Laboratory, California Institute of Technology, Los Angeles, USA*
[3] *Earth System Science Interdisciplinary Center, University of Maryland, College Park, USA*
[4] Sorbonne Université, Laboratoire Génie électrique et électronique de Paris, France
[*] *corresponding author's e-mail: ines.fenni@jpl.nasa.gov*

We have developed a 3D full-wave model for scattering from complex-shaped particles (MIDAS), to overcome the computational efficiency issues plaguing the Discrete Dipole Approximation (DDA)-based codes [1-3]. Our goal is to provide the precipitation retrieval community with an efficient tool to mitigate the uncertainty on the physical and single scattering properties (SSPs) of ice and mixed-phase hydrometeors, representing today a great challenge for the passive and active microwave remote sensing of precipitations. The main concept in MIDAS (MoM Integral-equation Decomposition for Arbitrarily-shaped Scatterers) is the use of a direct solver-based domain-decomposition method, namely the Characteristic Basis Function Method (CBFM), in the context of volume integral equation method (VIEM) to efficiently compute orientation-averaged SSPs of realistic precipitation particles. The VIEM is solved by mean of a Method of Moments (MoM) with piecewise constant basis functions. Then, the application of the CBFM significantly reduces the numerical size, and thus the computational cost of the original EM problem, particularly when dealing with a large number of target orientations (or equivalently incident directions).

We have recently adapted and applied our model to the calculation of EM scattering by inhomogeneous hydrometeors and started implementing a non-uniform mesh according to the dielectric properties composing the simulated particle. The goal is to efficiently and accurately calculate the SSPs of mixed-phase hydrometeors, such as melting and rimed snow particles, characterized by high dielectric contrast between the water and ice portions. Ensuring that MIDAS provides accurate SSPs of mixed-phase ice/water particle, at a reasonable calculation cost, is of high importance to the precipitation retrieval community, knowing that the current DDA-based codes, such as DDSCAT [2], are particularly vulnerable and computationally very intensive when applied to scatterers with high dielectric constants, because of their use of iterative solvers.

When MIDAS and DDSCAT are applied to a (30% water, 70% ice) snow aggregate of equivalent radius a_p=1.36 mm and maximum diameter d_{max}=8.2 mm with a dielectric constant of the water $m_w = 2.8 + j2.1e^{-3}$ at $f = 94$ GHz and $m_w = 4 + j2.1e^{-3}$ at $f = 35.5$ GHz, the two codes yield identical results at $f = 94$ GHz in 9min 18sec with MIDAS and 18min 51sec with DDSCAT. At $f = 35.5$ GHz, MIDAS spends even less time as its performance depends only on the numerical size of the problem. On the other hand, the iterative solver struggles to converge because of the higher value of m_w and DDSCAT fails to provide a result before hitting the calculation time wall of 8 days. This promising primary result suggests that our model can outperform the iterative solver-based DDA implementations, in terms of cpu time, when dealing with large mixed-phase water/ice particle, and this even when considering only one single target orientation.

References

[1] I. Fenni, Z.S. Haddad, H. Roussel, K.S. Kuo and R. Mittra, 2017. A computationally efficient 3-D full-wave model for coherent EM scattering from complex-geometry hydrometeors based on MoM/CBFM-enhanced algorithm. IEEE Transactions on Geoscience and Remote Sensing, 56(5), pp.2674-2688.

[2] B.T. Draine, P.J. Flatau, 1994. Discrete-dipole approximation for scattering calculations. Josa a, 11(4), pp.1491-1499

[3] M. A. Yurkin, A.G. Hoekstra, 2007. The discrete dipole approximation: an overview and recent developments. Journal of Quantitative Spectroscopy and Radiative Transfer, 106(1-3), pp.558-589

The ScattPort story

Thomas Wriedt[1,*]

[1]*Leibniz-Institut für Werkstofforientierte Technologien – IWT, University of Bremen, Badgasteiner Str. 3, 28359 Bremen, Germany*
[*]*corresponding author's e-mail: thw@iwt.uni-bremen.de*

Astract

In this presentation the history and the concept of the ScattPort web site will be presented. ScattPort started as a list of available computer programs but later turned into an information portal for the light scattering community.

History of ScattPort

The start of ScattPort dated back to 1994, when I distributed the Fortran Mie code by Wiscombe to a group of German scientists who had meet to discuss problems with Mie scattering programs. As they did not know Wiscombe's code I started a web page with a list of available programs. This page can still be found on ScattPort and it has also be published in an article [1]. At that time this list was the web page with the most hits on the server of the faculty. This made clear that there was a high demand for such kind of information. We erected a more professional web site with more information of computer programs suitable to compute light scattering by particles. See Fig. 1.

To have an even more professional web site we managed to obtain funding by the German Research Foundation DFG within a program to develop information portals for scientists [1, 2] and in this way ScattPort started.

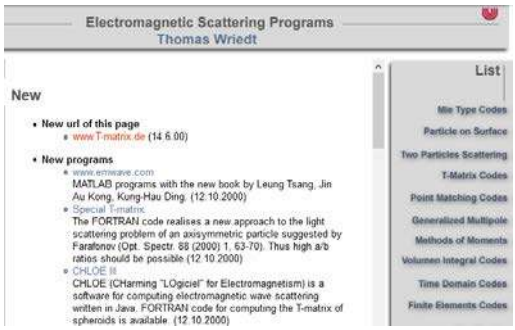

Figure 1: Screenshot of www.T-matrix.de in 2000.

References

[1] T. Wriedt T *Available electromagnetic-scattering programs*. IEEE Antennas Propag. Mag. 36:36:61–63, 1994.

[2] T. Wriedt and J. Hellmers *New Scattering information portal for the light-scattering community*. Journal of Quantitative Spectroscopy & Radiative Transfer 109:1536-1542, 2008.

[3] J. Hellmers and T. Wriedt *New approaches for a light scattering Internet information portal and categorization schemes for light scattering software*. Journal of Quantitative Spectroscopy & Radiative Transfer 110:1511-1517, 2009.

Inverse Scattering of a Dielectric Cone Based on Neural Network

Jiarui Liang[a],Renxian Li[a], Chunbo Liu[a]

[a]*School of Physics and Optoelectronic Engineering, Xidian University, Xi'an 710071, China*

[*]*Presenting author (jrliang@stu.xidian.edu.cn)*

Inverse scattering is the inverse problem of partial differential equations. It is based on the known incident waves and the measured external scattered field of the scatterer to study the scatterer's physical characteristics, such as the size, position, dielectric constant, conductivity, etc. Inverse scattering theory is widely used in remote sensing, geophysical survey, biomedical engineering and other fields. The non-linearity and ill-posedness of the inverse scattering problem make the inverse scattering research very difficult. The strong learning ability and non-linear mapping ability of neural network is suitable for the study of non-linear problems. [1,2]

This paper discusses the application of neural network to the problem of electromagnetic inverse scattering of dielectric cone in free-space. The work of this paper is to determine the number of neurons in the input layer by the set number of receiving points of the scattered field, and use the scattered field as the input; the physical characteristics of the corresponding dielectric cone as the output; the activation function of the hidden layer neurons uses Sigmoid function. The neural network is trained and learned using known scattered field data samples to determine the weights and thresholds of the neurons in each layer, thereby establishes neural network model. After inputting new scattered field data, the physical properties of the media cone are inverted.[3]

References

[1] Qinghe Zhang,Appllication research of machine learning methods in electromagnetic inverse scattering problems[in Chinese],SCIENCE PRESS,2019.

[2] Longdao Xu, Physics dictionary [in Chinese],SCIENCE PRESS,2004.

[3] Hamid A K, AlSunaidi M. Inverse scattering by dielectric circular cylindrical scatterers using a neural network approach[C]. Antennas and Propagation Society International Symposium 1997. Digest. IEEE, 1997, 4: 2278-2281.

Resonance force of a spherical particle illuminated by an Airy light-sheet

Wenze Zhuang[1], Renxian Li[1,2,*], Ningning Song[1] and Jiarui Liang[1]

[1]*School of Physics and Optoelectronic Engineering, Xidian University, Xi'an 710071, China*
[2]*Collaborative Innovation Center of Information Sensing and Understanding, Xidian University, Xi'an 710071, China*
[*]*corresponding author's e-mail: rxli@mail.xidian.edu.cn*

With the development of laser technology, the micromanipulation of neutral particles can be realized by radiation force. Micromanipulation is an emerging branch of science and technology, can be divided into light binding, light trapping, light attract- ion, and micromanipulation technology has been applied to physics, biomedicine, nanotechnology and other fields, with a wide range of development space. [1]

The optical force is calculated by Maxwell stress tensor using generalized Lorenz-Mie theory (GLMT), and the resonance force on a small sphere (ethanol Mie particle) induced by an Airy light-sheet is studied by resonance and background separation methods. The transverse resonance force and longitudinal resonance force of the sphere are calculated, and the influences of the radius of the sphere and the parameters of the Airy light-sheet (Airy wavenumber, transverse scale, attenuation coefficient, and so on.) on the resonance force are discussed. [2,3]

This paper will play an important role in the further application of optical force, and then promote the development of micro-control technology.

References

[1] Ashkin A . Optical Trapping and Manipulation of Neutral Particles Using Lasers[J]. Proceedings of the National Academy of Sciences of the United States of America, 1997, 94(10):4853-4860.
[2] Lin Z, Guo X, Tu J, et al. Acoustic non-diffracting Airy beam[J]. Journal of Applied Physics, 2015, 117(10):1499.
[3] F.G. Mitri, Appl. Phys. Lett. 110, 091104 (2017).

A scattering-based effective-medium model for dense suspensions of large tenuous particles and its application to the diagnosis of diseases of the blood

Alexander Nahmad-Rohen[1,*] and Augusto García-Valenzuela[1]

[1]*Instituto de Ciencias Aplicadas y Tecnología (ICAT), Universidad Nacional Autónoma de México (UNAM), Mexico*
[*]*corresponding author's e-mail: alexander.nahmad@icat.unam.mx*

Abstract

Complex materials —that is, those which are heterogeneous on optical scales— interact with light in complicated ways, making their optical study difficult. However, effective-medium theories, such as the Maxwell-Garnett [1] and Clausius-Mossotti [2] models, allow for fairly simple calculation of average properties, such as the effective-refractive index (which correctly describes the transmission and extinction of the coherent component of light in the complex medium [3]). These average properties depend on the various parameters that describe a complex medium, such as the volume fractions, shapes and optical properties of its constituents. Therefore, by measuring the effective refractive index, for example, of a complex material one can infer the values of said parameters and learn something about the material in question. The optical study of complex materials has many applications, such as quality control in manufacturing processes, ecological analysis of satellite images, meteorological studies and noninvasive medical diagnosis.

One of the better-known effective-medium models is that of H C van de Hulst [4]. While its traditional derivations [4–6] seem to imply that the model is only valid for very dilute suspensions and/or when the point of observation is in the far field of the medium in question, this is not, in fact, always the case, as I will show.

I will present scattering-based effective-medium models for two types of suspensions of large tenuous particles which adequately model different kinds of biological tissue [7, 8]. Both models ultimately lead to the van de Hulst formula for the effective refractive index of the suspension without invoking the usual dilute-suspension or far-field arguments, proving that the formula is valid even for dense suspensions of particles on the condition that the particles be large and tenuous.

I will also derive two corrections to the van de Hulst formula. These corrections arise naturally from the derivations I will present of the formula. I will show that they are small in the case of human whole blood [7].

Finally, I will discuss how the formula can be applied to the diagnosis of diseases that affect blood [9], using sickle-cell anaemia and spherocytosis as examples.

References

[1] Sihvola A H (1999): *Electromagnetic mixing formulas and applications*, IEEE, section 3.1
[2] Priou A (1992): *Dielectric properties of heterogeneous materials*, Elsevier Science Publishing, 104–107
[3] Foldy L L (1945): *The multiple scattering of waves*, Physical Review 67, 107–119
[4] van de Hulst H C (1981): *Light scattering by small particles*, Dover, 28–36, 105–106, 172–175
[5] Bohren C F & Huffman D R (1983): *Absorption and scattering of light by small particles*, Wiley, 77–78, 83–101
[6] Barrera R G, Reyes-Coronado A & García-Valenzuela A (2007): *Nonlocal nature of the electrodynamic response of colloidal systems*, Physical Review B 75, 184202
[7] Nahmad-Rohen A & García-Valenzuela A (2021): *Unambiguous derivation of the effective refractive index of biological suspensions and an extension to dense tissue such as blood*, Journal of the Optical Society of America A 38, 775–783
[8] Xu M & Alfano R R (2005): *Fractal mechanisms of light scattering in biological tissue and cells*, Optics Letters 30, 3051–3053
[9] Nahmad-Rohen A, Contreras-Tello H, Morales-Luna G & García-Valenzuela A (2016): *On the effective refractive index of blood*, Physica Scripta 91, 015503

Extinction of an infinite circular cylinder in absorbing media

Shangyu Zhang[1,2], Wenjie Zhang[1,2], Jian Dong[1,2], and Linhua Liu[1,2,*]

[1] *School of Energy and Power Engineering, Shandong University, Jinan 250061, China*

[2] *Optics & Thermal Radiation Research Center, Shandong University, Qingdao 266237, China*

[*] *corresponding author's e-mail: liulinhua@sdu.edu.cn*

Abstract

Conventional far-field electromagnetic scattering theory (EST) applies only to a particle immersed in a *transparent host* medium, where the optical cross sections can be derived by integrating the total Poynting vector on the conceptual spherical surface (CSS) in a far-field region. Extension of the conventional EST to an *absorbing host* medium has attracted much research attention and has suffered some controversies (see Ref. [1] and references therein). The main controversy stems from the desire to extend the CSS method to absorbing host media, which leads to the optical cross sections of the particle depending on the radius of the conceptual sphere. The resolution is to model theoretically the readings of a specific detector (SD) of electromagnetic energy, which is presented by Mishchenko *et al* [1]. Until now, the generalized EST of a sphere in the absorbing host has been extensively studied using SD method, however, the EST of *an infinite cylinder in absorbing host media* has not been studied so far. As a fundamental problem, extinction of the infinite cylinder embedded in the absorbing host is studied in this paper. The generalized extinction efficiencies (EE) per unit length cylinder under *normally* incident *p*- and *s*- polarized lights are derived in the framework of SD method, which can reduce to the conventional equations if the host medium is transparent. For large cylinders, the increasing absorption of the host medium leads to an increasing amplitude of interference oscillation and the emergence of negative extinction, which is similar to those of spheres and has been interpreted in Ref. [2]. For small cylinders in a weak absorbing host medium, we present theoretically the conditions of the emerging negative extinction and quantitatively analyze the differences of EE in absorbing host media to that in the non-absorbing counterpart. It is found that the ratio of EE depends only on the ratios of the imaginary part of host medium's refraction index (RI) and the cylinder's complex RI to the real part of host medium's RI. The conclusions are verified with a specific case of a Ge cylinder in polyethylene (PE), of which the complex RI can be found in Ref. [3].

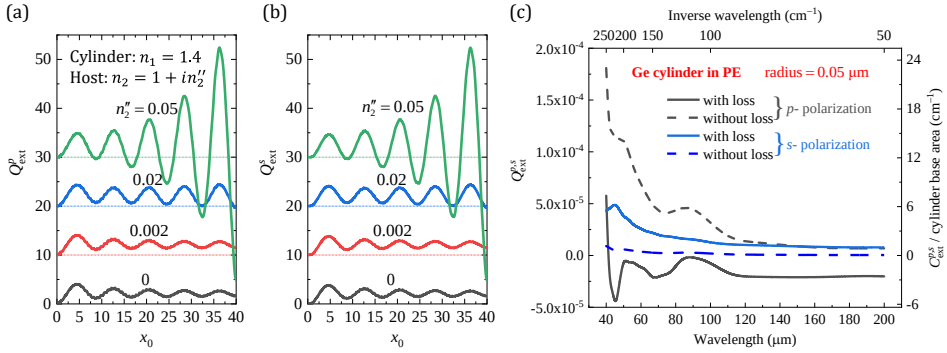

Figure 1: (a)-(b): $Q_{\text{ext}}^{p,s}$ versus vacuum size parameter x_0 for (a) *p*- polarization and (b) *s*- polarization with the cylinder's refraction index 1.4 and the host medium's refraction index $1 + in_2''$. (c): $Q_{\text{ext}}^{p,s}$ of a Ge cylinder in polyethylene (PE) considering the PE's absorption and neglecting the absorption with the radius of cylinder 0.05 μm.

References

[1] M. I. Mishchenko, and P. Yang. *Far-field Lorenz–Mie scattering in an absorbing host medium: Theoretical formalism and FORTRAN program*. J. Quant. Spectrosc. Radiat. Transfer, 205:241–252, 2018.

[2] M. I. Mishchenko, G. Videen, and P. Yang. *Extinction by a homogeneous spherical particle in an absorbing medium.* Opt. Lett. 42:4873–4876, 2017.

[3] D. R. Smith, and E. V. Loewenstein. *Optical constants of far infrared materials. 3: plastics.* Appl. Opt. 14(6):1335–1341, 1975.

Significance of refractive index in light scattering measurements with allusion to biological particles

Sanchita Roy*,1, Jamil Hussain[1], Semima Sultana Khanam[1] and Showhil Noorani[1]

[1] *Department of Physics, School of Applied Sciences, University of Science and Technology, Meghalaya, District- Ri Bhoi, 793101, Meghalaya, India.*

e-mail: rsanchita1@gmail.com

Abstract

Light scattering is an important optical diagnostic tool. The investigations carried out with this technique is used in multidisciplinary areas. It has proven to be a non-invasive and non-destructive tool for morphological characterization of diverse particulate matter especially biological particles. One must address the concept of refractive index of the particulate matter precisely, while carrying out investigations or analyses using light scattering tool. Usually refractive index effects are most pronounced when particles are spherical, transparent, refractive index of the particle is close the wavelength of the light source used and also the medium of suspension. Keeping these points in view, it must be noted that the dependency of light scattering studies on refractive index plays a vital role. As such, proper interpretation of light scattering results to quantify morphological characterization of biological particles like bacterial cells and viruses can be validated by proper information of refractive index. Many researchers reported information about quantification of size and shape of biological particle using light scattering tool but refractive index parameter was either chosen as a median value of similar biological cells or taken as a standard value adopted from other researchers. Mostly refractive index of all viruses are taken as 1.06 for visible range and for most bacterial cells it lies in the range of 1.36 to 1.39, imaginary component being taken as zero. Since refractive index is frequency dependent so inclusion of correct value of refractive indices can only give correct interpretation of light scattering signatures. In the present work, we have extensively explored light scattering investigations that were carried out on some biological particles and arrived at a conclusion that we need a strong analysis on inclusion of proper refractive index for elucidation of light scattering studies, either experimental or modelling. This point is otherwise not conceptualised in many works which were reported earlier and until recent times. We mainly took an attempt to find the significance of refractive index in light scattering measurements with reference to biological particles like *E.coli*, *S. aureus*, *Corona virus* etc.

References

[1] Dmitry Petrov. *Photopolarimetrical properties of coronavirus model particles: Spike proteins number influence,* J. Quant. Spectrosc. Radiat. Transfer, 248:107005, 2020.

[2] M. I. Mishchenko, L. D. Travis, A. A. Lacis, *Absorption and Emission of Light by small particles*, Cambridge University Press, 2002.

[3] W M Balch, J Vaughn, J Novotny, DT Drapeau, R Vaillancourt, J Lapierre, A Ashe, *Light scattering by viral suspensions*, Limnol Oceanogr., 45(2):492–8, 2000.

[4] G. Wang, A. Chakrabarti, and C. M. Sorensen, *Effect of the imaginary part of the refractive index on light scattering by spheres,* J. Opt. Soc. Am. A, 32, 1231-1235,2015.

Significance of refractive index in light scattering measurements with allusion to biological particles

Sanchita Roy*,1, Jamil Hussain[1], Semima Sultana Khanam[1] and Showhil Noorani[1]

[1] *Department of Physics, School of Applied Sciences, University of Science and Technology, Meghalaya, District- Ri Bhoi, 793101, Meghalaya, India.*

e-mail: rsanchita1@gmail.com

Abstract

Light scattering is an important optical diagnostic tool. The investigations carried out with this technique is used in multidisciplinary areas. It has proven to be a non-invasive and non-destructive tool for morphological characterization of diverse particulate matter especially biological particles. One must address the concept of refractive index of the particulate matter precisely, while carrying out investigations or analyses using light scattering tool. Usually refractive index effects are most pronounced when particles are spherical, transparent, refractive index of the particle is close the wavelength of the light source used and also the medium of suspension. Keeping these points in view, it must be noted that the dependency of light scattering studies on refractive index plays a vital role. As such, proper interpretation of light scattering results to quantify morphological characterization of biological particles like bacterial cells and viruses can be validated by proper information of refractive index. Many researchers reported information about quantification of size and shape of biological particle using light scattering tool but refractive index parameter was either chosen as a median value of similar biological cells or taken as a standard value adopted from other researchers. Mostly refractive index of all viruses are taken as 1.06 for visible range and for most bacterial cells it lies in the range of 1.36 to 1.39, imaginary component being taken as zero. Since refractive index is frequency dependent so inclusion of correct value of refractive indices can only give correct interpretation of light scattering signatures. In the present work, we have extensively explored light scattering investigations that were carried out on some biological particles and arrived at a conclusion that we need a strong analysis on inclusion of proper refractive index for elucidation of light scattering studies, either experimental or modelling. This point is otherwise not conceptualised in many works which were reported earlier and until recent times. We mainly took an attempt to find the significance of refractive index in light scattering measurements with reference to biological particles like *E.coli*, *S. aureus*, *Corona virus* etc.

References

[1] Dmitry Petrov. *Photopolarimetrical properties of coronavirus model particles: Spike proteins number influence,* J. Quant. Spectrosc. Radiat. Transfer, 248:107005, 2020.

[2] M. I. Mishchenko, L. D. Travis, A. A. Lacis, *Absorption and Emission of Light by small particles*, Cambridge University Press, 2002.

[3] W M Balch, J Vaughn, J Novotny, DT Drapeau, R Vaillancourt, J Lapierre, A Ashe, *Light scattering by viral suspensions*, Limnol Oceanogr., 45(2):492–8, 2000.

[4] G. Wang, A. Chakrabarti, and C. M. Sorensen, *Effect of the imaginary part of the refractive index on light scattering by spheres,* J. Opt. Soc. Am. A, 32, 1231-1235,2015.

Light scattering by large nonspherical particles within the physical optics method

Alexander V. Konoshonkin[a,b,*], Natalia V. Kustova[a], Victor A. Shishko[a], Dmitriy N. Timofeev[a], Ilya V. Tkachev[a,b] and Anatoli G. Borovoi[a]

[a]*V. E. Zuev Institute of Atmospheric Optics, SB RAS, Academician Zuev Sq. 1, 634055 Tomsk, Russia*
[b]*National Research Tomsk State University, Lenina Ave. 36, 634050 Tomsk, Russia*

[*]*Presenting author (sasha_tvo@iao.ru)*

The light scattering problem by large nonspherical particles such as Earth and cosmic dust particles, atmospheric ice crystals of cirrus clouds has not been satisfactory solved yet. This solution is mainly required for interpreting the polarimetric and lidar observations. Some success was achieved only in solving the problem of light scattering for Earth's dust aerosol. Since large dust particles quickly settle in the atmosphere, for dust particles observed in nature with sizes less than 10 microns the rigorous methods such as the DDA, FDTD, PSDT and II-TM were used[1]. However, cosmic dust can be significantly larger and for it, as well as for atmospheric ice particles reaching sizes of 10,000 microns, the rigorous methods are not applicable. For this case, they are forced to use approximate methods, such as geometrical and physical optics[2].

This report presents the capabilities of the physical optics method for solving the light scattering problem for large nonspherical particles, such as dust particles and atmospheric ice crystals. It is shown that the solution obtained by this method is in good agreement with rigorous numerical methods. It is also shown that the physical optics method managed to calculate the light scattering by such large non-spherical particles with moderate requirement to computational resources[3].

References

[1] Mishchenko, M.I., Hovenier, J.W., Travis, L.D, 2000: *Light scattering by nonspherical particles: theory, measurements, and applications*. San Diego: Academic Press, 690 p.

[2] Liou, K.-N., Yang, P., 2016: *Light Scattering by Ice Crystals: Fundamentals and Applications*. Cambridge University Press, Cambridge, UK, 460 p.

Preferred mode of presentation: Oral

Lattice Kerker effect in arrays of Al nanoparticles

A. S. Kostyukov[1,*], A. E. Ershov[1,2], V. S. Gerasimov[1,2], R. G. Bikbaev[1,3], I. L. Rasskazov[4], I. L. Isaev[2], P. N. Semina[1], V. I. Zakomirnyi[1,2], S. P. Polyutov[1], and S. V. Karpov[1,3]

[1] *Siberian Federal University, Krasnoyarsk, 660041, Russia*
[2] *Institute of Computational Modelling of the Siberian Branch of the Russian Academy of Sciences, Krasnoyarsk, 660036, Russia*
[3] *L. V. Kirensky Institute of Physics, Federal Research Center KSC SB RAS, Krasnoyarsk, 660036, Russia*
[4] *The Institute of Optics, University of Rochester, Rochester, New York 14627, USA*
[*] *corresponding author's e-mail: askostyukov@sfu-kras.ru*

In this report we demonstrate the lattice Kerker effect in plasmonic periodic rectangular arrays of spherical Al nanoparticles.

We show that a complete suppression of the backscattering can be tuned within the UV and visible spectral ranges by varying geometry of arrays (see fig. 1a), i.e., radius 1c of NPs and the distance between them. The plasmonic lattice Kerker effect is based on the interference suppression of dominant ED radiation (with negligible MQ impact) by the cumulative contribution of the fields produced by MD and EQ that is introduced in classical electrodynamics. High absorption and strong electric field localization are observed at the frequency that corresponds to the lattice Kerker effect.

This effect is clearly visible in Fig. 1(b), which shows the phases of the reflected wave created by individual multipoles. It can be seen from this figure that at $\lambda = 420$ nm, phases of the ED and MQ are close to zero while the phases of the EQ and MD are near to π. This means that the multipoles are in antiphase and destructively interfere with each other at the wavelength of the Kerker effect. It should be noted that this condition is not fulfilled near the $[1;0]$ RA.

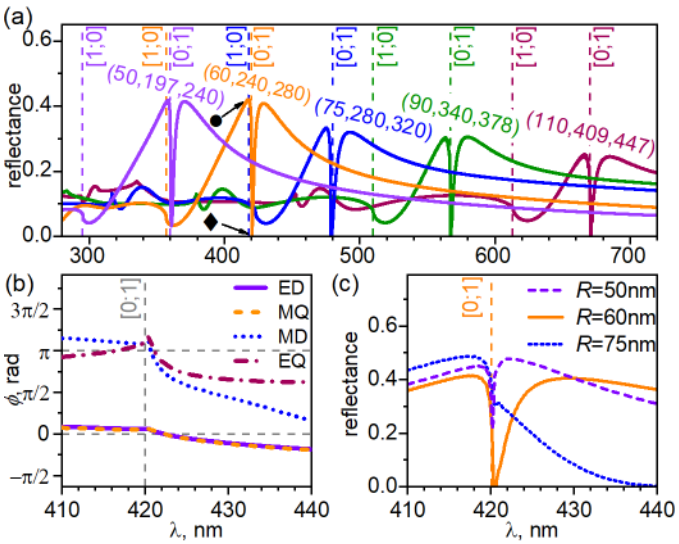

Figure 1: (a) Reflectance for arrays with different geometrical parameters (R, h_x, h_y) as marked in the legend. Vertical dashed lines show respective spectral positions of $[1;0]$ and $[0;1]$ RAs for each array. (b) Multipole decomposition of the phase of the reflection amplitude for NPs array with $(60, 240, 280)$ nm [cf. orange line in (a)]. Notice the $\Delta\phi = \pi$ phase difference between EQ and MD contributions on one hand, and ED and MQ counterparts on the other hand, at $\lambda = \sqrt{\varepsilon_h} h_y$, the wavelength of the lattice Kerker effect. (c) Reflectance for arrays with different NP radii R and fixed $h_x = 240$ nm, $h_y = 280$ nm.

Utilization of aluminum completely eliminates spectral restrictions and makes it possible to create conditions for the manifestation of the Kerker effect both in the entire visible and in the long-wavelength range of the UV spectrum.

The research was supported by the Ministry of Science and High Education of Russian Federation (Project No. FSRZ-2020-0008), and was funded by RFBR, Krasnoyarsk Territory and Krasnoyarsk Regional Fund of Science, project number 20-42-240003.

Direct testing of polarized radiative transfer Monte Carlo codes

J. Freimanis[1,*] and R. Peženkovs[1]

[1] *Engineering Research Institute "Ventspils International Radio Astronomy Centre" of Ventspils University of Applied Sciences*
[*] *corresponding author's e-mail: jurisf@venta.lv*

Monte Carlo versus integral equations

We have created a polarized radiative transfer (PRT) Monte Carlo code named *Ventspils RTMC*. It is suitable for continuum PRT modelling in medium of arbitrary configuration and morphology, but on condition that the medium is isotropic, and the extinction is characterized by scalar matrix. Our main interest is the modelling of PRT inside specific astrophysical objects, namely, post-asymptotic giant branch (post-AGB) objects [1] having the star surrounded by extensive gas-dust envelope of complicated shape and morphology. It is believed that such stars are in transition stage to planetary nebulae nuclei. The most intriguing question is how the initially spherical star encounters very asymmetrical mass loss; this asymmetry appears in peculiar (often bipolar) shapes of both the dusty envelope of the post-AGB object and (later) the newly created planetary nebula. Some spatially resolved post-AGB objects exhibit very high linear polarization degree (up to 80 percent) distributed unevenly over the image of the dust envelope.

For at least 10 years, there exists a PRT code RADMC-3D created by C.Dullemond and many collaborators; its last, the most advanced version is Release 2.0 [2]. Similarly to *Ventspils RTMC*, RADMC-3D is limited to statistically isotropic dusty medium and scalar extinction matrix as well, but its advanced data input system allows for multiwavelength RT calculations both in continuum and spectral lines, and it is capable to calculate the temperature and thermal radiation of dust. RADMC-3D has been widely used by many authors for modelling astrophysical objects, but surprisingly in most cases it was done fully neglecting polarization.

There exist a lot of PRT codes based on Monte Carlo method, and their correctness is often tested by mutual comparison of their results. Several Monte Carlo codes were tested in [3] against some type of benchmark solutions but the method of creating these benchmark solutions is not clearly explained even in their reference [4]; RADMC-3D was not considered.

We tested both *Ventspils RTMC* and RADMC-3D in case of physically simple problem: homogeneous isotropic spherical medium of finite radius is scattering according to Rayleigh's law, with concentric spherical star of finite radius inside it. The star is homogeneous over its surface, and it emits isotropic unpolarized radiation. This simple case allowed us to write down linear Fredholm integral equations for the components of the vectorial source function, and we created the computer code for their solution.

Comparison of the images of such a model onto virtual CCD matrix of virtual telescope proved that all three codes – *Ventspils RTMC*, RADMC-3D and numerical solution of integral equations – give compatible results at least for optical radius of the medium being from 0.1 to 10, and single scattering albedo from 0.4664 to 1.0.

References

[1] Hans-Peter Gail, Erwin Sedlmayr. *Physics and Chemistry of Circumstellar Dust Shells*. Cambridge University Press, New York, USA, 2014.
[2] Cornelis Dullemond. *radmc3d. Release 2.0*. https://www.ita.uni-heidelberg.de/ dullemond/software/radmc-3d/, August 29, 2020.
[3] K. D. Gordon et al. *TRUST. I. A 3D externally illuminated slab benchmark for dust radiative transfer*. Astronomy and Astrophysics, 603:A114, 2017.
[4] https://ipag.osug.fr/RT13//RTTRUST/concept.php

Observing charging events on optically trapped particles

Isaac C.D. Lenton* and Scott R. Waitukaitis

Institute of Science and Technology Austria, Am Campus 1, 3400 Klosterneuburg, Austria
**corresponding author's e-mail: isaac.lenton@ist.ac.at*

Since Millikan's famous oil drop experiment, where oil droplets were observed to have discrete charges, there have been multiple experiments revealing not only the discrete nature of particle charging but also how particle charge evolves over time [1, 2]. Particle charge and charging dynamics has implications for particle cohesion and repulsion, important for many fields including tribocharging, atmospherics, aerosols and pharmaceuticals. There are many open questions about the mechanism causing particles to become charged and how the charge evolves over time [3], for example: What are the species responsible for the particle's charge? What role does humidity, or the concentration of mobile ions in the surrounding medium, have in charging dynamics? And, how does a charged particle deplete available ions?

Our group is interested in tackling some of these questions with experiments that span multiple length scales. We are currently building experiments to investigate contact electrification and charging dynamics at the cm-scale, mm-scale, and µm-scale. In this talk I will describe our optical tweezers experiment to probe the importance of humidity on the charging dynamics of microscopic particles.

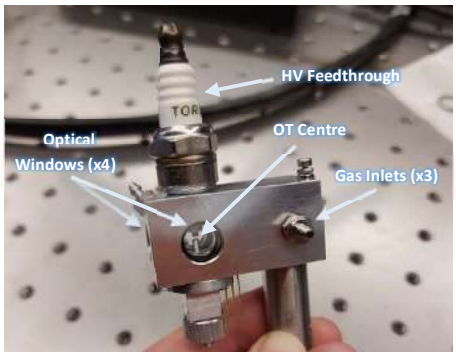

Figure: Photo of our sample chamber mid-assembly.

Specifically, we will use counter propagating optical tweezers (OT) to study how the charge on a microscopic particle evolves over time. OT have previously been used to observe individual charging events in liquid [1] and vacuum [2]. Our system aims to study charging dynamics in air: built around a humidity-controlled chamber (see Figure) with two electrodes positioned near the trap center to apply (up to) a 5MV/m AC electric field across the sample. To stabilize the particle and measure the charge, a quadrant photo-detector monitors light scattered perpendicular to the OT axis. In this configuration, the scattered light provides information about how far the particle is from the OT equilibrium, giving insight into the non-optical forces acting on the particle. Using OT to study this system may introduce additional complications: although our chosen wavelength shouldn't directly cause photo-electric discharge, we cannot yet rule out other multi-photon processes [4]. At high humidity, changes in surface charge/conductivity may also have interesting consequences on the interaction between the particle and the optical/electric field. In this talk, I will discuss what we have learnt so far about this system.

References

[1] Filip Beunis, Filip Strubbe, Kristiaan Neyts, and Dmitri Petrov. Beyond Millikan: The Dynamics of Charging Events on Individual Colloidal Particles. Phys. Rev. Lett. 108, 016101 (2012)

[2] David C. Moore, Alexander D. Rider, and Giorgio Gratta. Search for Millicharged Particles Using Optically Levitated Microspheres. Phys. Rev. Lett. 113, 251801 (2014)

[3] Daniel J. Lacks & Troy Shinbrot. Long-standing and unresolved issues in triboelectric charging. Nature Reviews Chemistry. 3, 465–476 (2019).

[4] A. Ashkin and J. M. Dziedzic. Observation of a New Nonlinear Photoelectric Effect Using Optical Levitation. Phys. Rev. Lett. 36, 267 (1976)

Depolarization and lidar ratio observations in Saharan dust at 355, 532, and 1064 nm

Moritz Haarig[1,*], Ronny Engelmann[1], Albert Ansmann[1], Holger Baars[1], Martin Radenz[1], Dietrich Althausen[1], and Ulla Wandinger[1]

[1]*Leibniz Institute for Tropospheric Research, Leipzig, Germany*
[*]*corresponding author's e-mail: haarig@tropos.de*

Measuring the spectral slope (355, 532, and 1064 nm) of the particle linear depolarization ratio and the lidar ratio at the same time provides valuable information of the particle's properties such as shape, size and absorption. Especially for non-spherical dust particles.

For the first time, it was possible to use a Raman lidar to measure the depolarization ratio and the lidar ratio at 1064 nm in a dust plume. The rotational Raman technique [1] was used to derive the extinction coefficient and the lidar ratio at 1064 nm in the Raman lidar BERTHA [2]. The nighttime measurements of two Saharan dust events over Leipzig, Germany, on 22 February and 3 March 2021 could be used to derive the so called full 3+3+3 data set (3 backscatter coefficients, 3 extinction coefficients, 3 depolarization ratios). The results of the first very strong Saharan dust outbreak (8 km thick!) could be compared to AERONET retrieved depolarization and lidar ratios. The results are presented in the figures below. Although AERONET results indicate a broader range, the general tendency of the lidar ratio at 1064 nm agrees quite well. The lidar ratio was previously compared between AERONET and lidar [3,4], but until now, lidar ratios could not be measured at 1064 nm with a lidar.

The results are quite new and the discussion will be extended in the presentation at the ELS conference.

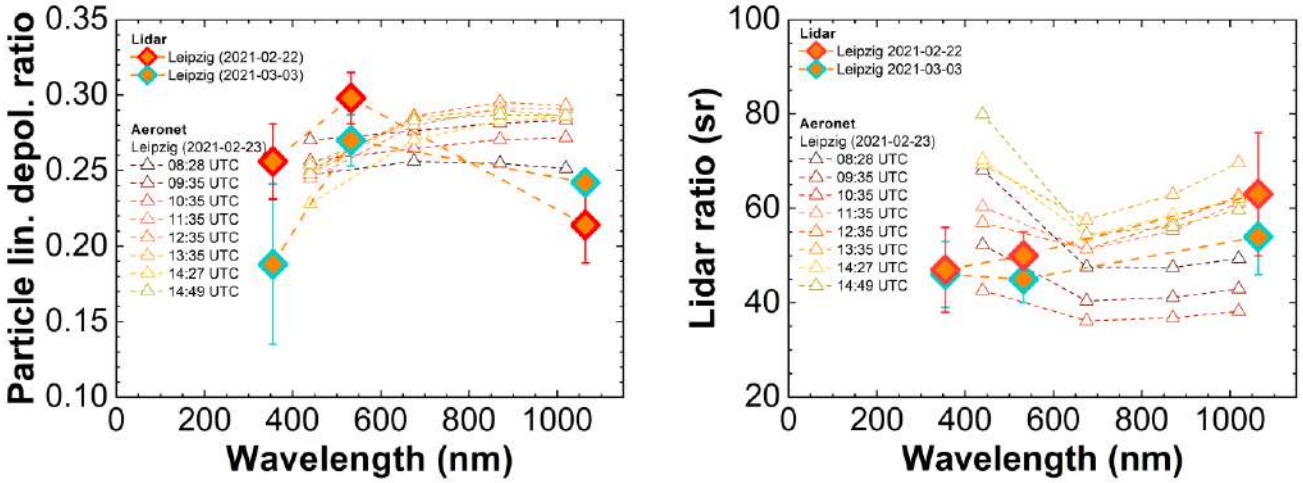

Figure 1: Spectral slope of the particle linear depolarization ratio (left) and lidar ratio (right) of Saharan dust measured with lidar on 22 February and 3 March 2021 over Leipzig compared to the AERONET results of the same dust plume on 23 February 2021.

References

[1] Haarig, M., Engelmann, R., Ansmann, A., Veselovskii, I., Whiteman, D. N., and Althausen, D.: 1064 nm rotational Raman lidar for particle extinction and lidar-ratio profiling: cirrus case study, Atmospheric Measurement Techniques, 9, 4269–4278, https://doi.org/10.5194/amt-9-4269-2016, 2016.

[2] Haarig, M., Ansmann, A., Althausen, D., Klepel, A., Groß, S., Freudenthaler, V., Toledano, C., Mamouri, R.-E., Farrell, D. A., Prescod, D. A., Marinou, E., Burton, S. P., Gasteiger, J., Engelmann, R., and Baars, H.: Triple-wavelength depolarization-ratio profiling of Saharan dust over Barbados during SALTRACE in 2013 and 2014, Atmos. Chem. Phys., 17, 10767–10794, https://doi.org/10.5194/acp-17-10767-2017, 2017.

[3] Tesche, M., Ansmann, A., Müller, D., Althausen, D., Mattis, I., Heese, B., Freudenthaler, V., Wiegner, M., Esselborn, M., Pisani, G., and Knippertz, P.: Vertical profiling of Saharan dust with Raman lidars and airborne HSRL in southern Morocco during SAMUM, Tellus B, 85 61, 144–164, https://doi.org/10.1111/j.1600-0889.2008.00390.x, 2009.

[4] Shin, S.-K., Tesche, M., Kim, K., Kezoudi, M., Tatarov, B., Müller, D., and Noh, Y.: On the spectral depolarisation and lidar ratio of mineral dust provided in the AERONET version 3 inversion product, Atmospheric Chemistry and Physics, 18, 12 735–12 746, https://doi.org/10.5194/acp-18-12735-2018, 2018.

Impacts of laser beam divergence on lidar multiple scattering polarization returns from water clouds

Zhen Wang[1,*] and Jingxin Zhang[1] and Haiyang Gao[1]

[1]*Key Laboratory for Aerosol-Cloud-Precipitation of China Meteorological Administration, School of Atmospheric Physics, Nanjing University of Information Science and Technology, Nanjing 210044, China*

[*]*corresponding author's e-mail: intersharp@126.com*

Theoretically, laser beam divergence can redistribute multiple scattering lights by spreading laser illumination and thus alter lidar polarization measurements. To study multiple scattering effects of laser divergence on lidar polarization signals, we apply the Monte Carlo polarized radiative transfer model MSCART to simulate lidar Stokes vector signals from a uniform water cloud with and without taking account of laser divergences. The comparison analysis shows that for lidar receiver footprints with roughly the same sizes of the multiple scattering regimes, laser divergence has almost no effect on ground-based lidar signals, but can have significantly large and much complex polarization effects on spaceborne lidar signals. An increase in laser divergence on one hand can greatly enhance spaceborne lidar multiple scattering depolarization when the divergence is larger than the FOV, and on the other hand can also weaken it slightly when the divergence less than the FOV. The weakest multiple scattering depolarization occurs at the divergence equal to the FOV. Furthermore, laser divergence can significantly reduce the sensitivity of FOV-resolved polarization measurement of spaceborne lidar to non-diagonal elements of phase matrix and make the measurement at different receiving polar angles only sensitive to diagonal elements of phase matrix at almost the same scattering angles. The spaceborne MFOV and CCD polarized lidar thus might not provide more information about phase matrix than the single FOV lidar does.

References

[1] Zhen Wang, Jingxin Zhang, Haiyang Gao. *Impacts of laser beam divergence on lidar multiple scattering polarization returns from water clouds*. J. Quant. Spectrosc. Radiat. Transfer, 268:107618, 2021.

[2] Jingxin Zhang, Zhen Wang, Feng Zhang, Haiyang Gao, Jinhu Wang, Shengcheng Cui. *A novel multiple small-angle scattering framework for interpreting anisotropic polarization pattern of lidar returns from water clouds*. J. Quant. Spectrosc. Radiat. Transfer, 242:106794, 2020.

Mapping Colloidal Ellipsoids with A Rotatable Stage via Scattering Morphology Resolved Total Internal Reflection Microscopy (SMR-TIRM)

Jiarui Yan[1] and Christopher Wirth[2,*]

[1]*Chemical and Biomedical Engineering, Cleveland State University, 2121 Euclid Ave, Cleveland, Ohio, USA 44115*
[2]*Chemical and Biomolecular Engineering Department, Case Western Reserve University, 2102 Adelbert Road, Cleveland, Ohio USA 44106*
[*]*corresponding author's e-mail: clw22@case.edu*

Anisotropic colloidal particles could be widely found in products like paints, liquid crystals, and drug delivery systems. Although the colloidal interactions are between particles are in ~kT scale, they could still dictate the performance and properties of the product. To measure such small forces in a more accurate way, our lab is currently working on the development of Scattering Morphology Resolved Total Internal Reflection Microscopy (SMR-TIRM), which is a variant of TIRM.**Error! Reference source not found.** This technique intends to utilize the scattering morphology and the integrated intensity for measuring the orientation and position of the anisotropic colloidal particles. Herein, we present a novel method of mapping the scattering morphology from ellipsoidal colloids with a rotatable stage. Specifically, the morphologies would be collected as a function of the azimuthal angles, incident beam polarization, and the aspect ratio of ellipsoidal colloids. A custom-made truncated hemisphere prism was set to be stationary on the central axis of a rotatable stage. Meanwhile, a laser was coupled on the stage such that the incident beam could go over all the azimuthal angles. The microfluidic cell contains deposited ellipsoidal colloids in the electrolyte was placed on the top of the prism with refractive index matching oil in between. We tuned the azimuthal angle for every 10° and use a camera to capture the light scattering images from above accordingly. Besides, ellipsoidal colloids with two different aspect ratios would be conducted to justify our hypothesis from the previous publication, meaning the experimental results of ellipsoidal colloids scattered evanescent waves with morphologies would be directly used to compare with the simulation results we reported.**Error! Reference source not found.** The work summarized herein would significantly supplement our understanding of scattering morphologies from ellipsoidal colloids.

References

[1] Rashidi, A., Domínguez-Medina, S., Yan, J., Efremenko, D. S., Vasilyeva, A. A., Doicu, A., ... & Wirth, C. L. (2020). Developing Scattering Morphology Resolved Total Internal Reflection Microscopy (SMR-TIRM) for Orientation Detection of Colloidal Ellipsoids. Langmuir, 36(43), 13041-13050.

Development of Jacobian Computational Capability in Vector Radiative Transfer Model

J. Ding* and P. Yang

Department of Atmospheric Sciences, Texas A&M University, 3150 TAMU, College Station, TX 77843, USA
**corresponding author's e-mail: njudjc@tamu.edu*

Abstract

Clouds and aerosols in the atmosphere, and oceanic particles scatter, absorb and polarize incident solar radiation and earth thermal emission. The observational radiometric and polarimetric signal can be inverted to obtain the optical and microphysical properties of the clouds, aerosols and hydrosols via remote sensing retrieval algorithms and data assimilation systems. A vector radiative transfer model and associated Jacobian computational model are indispensable modules in these algorithms and systems.

We develop a Jacobian computational model for the Texas A&M University vector radiative transfer model (TAMU-VRTM) [1], which is based on a two-component [2] (small-angle approximation and adding-doubling) method. The Jacobian computational model calculates derivatives of the full Stokes vector with respect to almost all model input. Both tangent linear and adjoint models are available. The derivatives of the Stokes vector can be seamlessly incorporated into a retrieval algorithm or data assimilation system to compute the Jacobian matrix that relates polarimetric observation and to be retrieved atmospheric and oceanic properties such as optical depth and sea surface wind speed.

Additional information

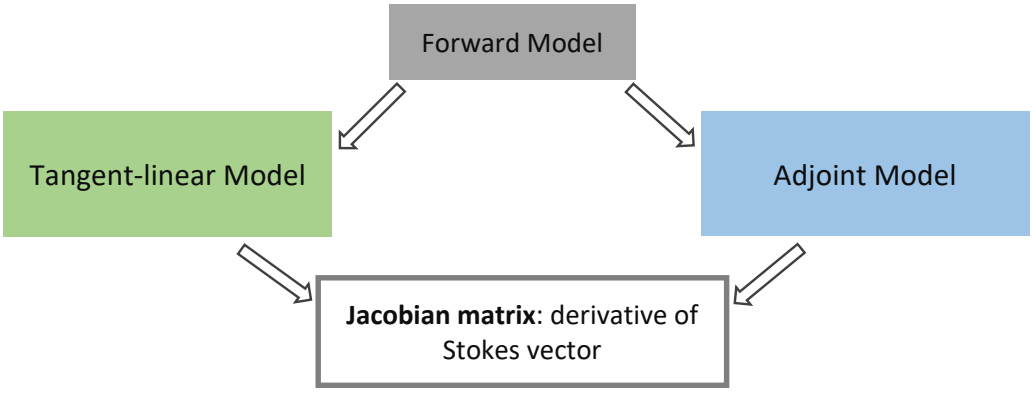

Figure 1: Schematic of TAMU-VRTM Jacobian computational model.

References

[1] J. Ding, P. Yang, M. D. King, S. Platnick, X. Liu, K. G. Meyer, and C. Wang *A fast vector radiative transfer model for the atmosphere-ocean coupled system.* J. Quant. Spectrosc. Radiat. Transfer, 239:106667, 2019.

[2] B. Sun, G. W. Kattawar, P. Yang, and E. Mlawer *An improved small-angle approximation for forward scattering and its use in a fast two-component radiative transfer method*. J. Atmos. Sci. 74:1959-1987, 2017.

Modelling of Corona virus using light scattering

Sanchita Roy*,1, Rajmukut Talukdar[1], Murshida Zannat[1] and Rokkime Marak[1]

[1] *Department of Physics, School of Applied Sciences, University of Science and Technology, Meghalaya, District- Ri Bhoi, 793101, Meghalaya, India.*

[*] *e-mail: rsanchita1@gmail.com*

Abstract

Investigation and studies of Corona virus is a burning topic in present times. The undesirable wide spread of Human Corona virus has caused pandemic since year 2020 as declared by WHO. It has caused threat to the human civilization around the globe. Researchers around the world are working extensively to find a solution of this pathogen. Modelling of biological particles using light scattering technique is an interesting and useful approach when real experimentation under laboratory conditions is not feasible. Powerful algorithm serves as a potential tool for characterization and analyses of the particles under investigation. Morphological characterization by using light scattering tool for biological particles like bacterial cells and viral suspensions has been carried out by many researchers successfully and reported over decades. This technique is widely used because it is a non-destructive means of characterization. However, some pathogenic strains require strict safety laboratory conditions for investigations to restrict pathogenic spread in the environment, so it may not be possible to conduct experimentations under ordinary laboratory conditions. The biological particles can get destroyed when bio-chemical procedures are followed for experimentation and analysis. Thus, simulation or modelling using standard and acceptable code is an alternative way for characterization of such particles. In this work, we took an attempt to simulate the light scattering from Coronavirus model using modified version of a novel Monte Carlo code based on Mie theory. We used different images of Corona virus and modelled it by incorporating the size distribution function wherever necessary. The scattering profile which also includes contribution from the protein spikes present in each cell is presented and justified. Main challenge lies in inclusion of the spike heads of the Corona virus. Our primary step was to acquire information about the first two elements of Mueller matrix. The investigations indicate that the presence of spikes gives a significant scattering profile and how inclusion or exclusion of spikes contribute to the uniqueness of profile.

References

[1] Dmitry Petrov. *Photopolarimetrical properties of coronavirus model particles: Spike proteins number influence,* J. Quant. Spectrosc. Radiat. Transfer, 248:107005, 2020.

[2] S.Roy, et al. Study of ZnO nanoparticles: Antibacterial property and light depolarization property using light scattering tool, J. Quant. Spectrosc. Radiat. Transfer, 118, 8-13, 2013.

[3] S. Roy and G. A Ahmed,. Monte Carlo simulation of light scattering from size distributed sub-micron spherical CdS particles in a volume element, *Optik-Int. J. Light Electron Opt.* , **122**, 1000 - 1004, 2011

[4] M. I. Mishchenko, L. D. Travis, A. A. Lacis, *Absorption and Emission of Light by small particles*, Cambridge University Press, 2002.

Vector Spherical Harmonics Expansion Truncation in the Invariant Imbedding T-matrix Method

Y. Zhang[1], J. Ding[1], R. L. Panetta[1,2], and P. Yang[1,*]

[1]*Department of Atmospheric Sciences, Texas A&M University, College Station, TX 77843, USA*
[2]*Department of Mathematics, Texas A&M University, College Station, TX 77843, USA*
[*]*pyang@tamu.edu*

Abstract

The invariant-imbedded T-Matrix (II-TM) method is a powerful numerical method developed for single scattering property computations of dielectric particles in recent years [1-2]. The II-TM transition matrix (T-matrix) has infinite dimensions, but must be truncated in practice [3-5]. The accuracy and efficiency of the II-TM computation is directly linked to the truncated dimension of the transition matrix, which is equal to the number of vector spherical harmonics expansion terms. To minimize computation time and maximize accuracy while retrieving atmospheric cloud and aerosol properties based on large-volume satellite data, we perform comprehensive numerical experiments to develop a suitable convergence criterion for the II-TM relative error. With the new convergence criterion, we proceed to develop an empirical formula that correlates the truncation number of the T-matrix with basic particle properties including size parameter, refractive index and aspect ratio. We then validate this formula for various nonspherical ice and dust particles with complicated geometries [6].

References

[1] B. R. Johnson *Invariant imbedding T-matrix approach to electromagnetic scattering*. Appl. Opt., 27(23):4861-73, 1988.

[2] L. Bi, P. Yang, G. W. Kattawar, and M. I. Mishchenko *Efficient implementation of the invariant imbedding T-matrix method and the separation of variables method applied to large nonspherical inhomogeneous particles.* J. Quant. Spectrosc. Radiat. Transfer, 116:169-83, 2013.

[3] W. J. Wiscombe *Improved Mie scattering algorithms*. Appl. Opt., 19(9):1505-09, 1980.

[4] Michael I. Mishchenko, Larry D. Travis, and Andrew A. Lacis. *Scattering, Absorption, and Emission of Light by Small Particles*. Cambridge University Press, Cambridge, 2002.

[5] S. Zhai, R. L. Panetta, and P. Yang. *Improvements in the computational efficiency and convergence of the invariant imbedding T-Matrix method for spheroids and hexagonal prisms*. Opt. Expr., 27(20):A1441-A57, 2019.

[6] P. Yang, L. Bi, B. A. Baum, K-N. Liou, G. W. Kattawar, M. I. Mishchenko, et al. *Spectrally consistent scattering, absorption, and polarization properties of atmospheric ice crystals at wavelengths from 0.2 to 100 μm*. J. Atmos. Sci., 70(1):330-47, 2013.

Edge Effect Correction to the Physical Geometric Optics Method Using the Debye Series for Super-spheroid Non-spherical Particles

N. Okeudo[1,*], J. Ding[1], P. Yang[1], and R. Saravanan[1]

[1] *Department of Atmospheric Sciences, Texas A&M University, College Station, Texas 77843, USA*
[*] *Corresponding author: nnokeudo@tamu.edu*

Abstract

Accurate quantification of the radiative effects of non-spherical particles on the energy budget requires a better characterization of their light scattering and absorption properties. A recent study has shown that super-spheroids have the potential to provide good estimates of the optical properties of natural non-spherical particles [2], [4]. It is possible to model the single scattering properties of all sizes of non-spherical atmospheric particles by combining the numerically exact invariant imbedded T-matrix (II-TM) method and the approximate physical geometric optics method (PGOM) [5], although II-TM cannot be applied to very large size particles due to the huge computational burden, and PGOM cannot be applied to very small size particles due to limitations of the geometric optics approximation [5]. In addition, PGOM does not include the edge effect contributions to extinction and absorption efficiencies. Unfortunately, we only know the edge efficiency for spheres [3] and spheroids [1]. In this study, we will develop a formula for the edge effect efficiency of super-spheroids. Then, we apply the edge effect correction formula for super-spheroids and shape properties to calculate the edge efficiency for arbitrary non-spherical particles. We will add the edge effect correction formula to PGOM in the hopes of improving the accuracy of the extinction and absorption efficiency in PGOM for moderate size parameters.

References

[1]. L. Bi, and P. Yang *High-frequency extinction efficiencies of spheroids: Rigorous T-matrix solutions and semi-empirical approximations*. Opt. Expr., 22:10270-10293, 2014.
[2]. W. Lin, L. Bi, and O. Dubovik *Assessing superspheroids in modeling the scattering matrices of dust aerosols*. J. Geophys. Res. Atmos., 123:13-917, 2020.
[3]. H. M. Nussenzveig, and W. J. Wiscombe *Efficiency factors in Mie scattering*. Phys. Rev. Lett. 45:1490, 1980.
[4]. L.-H. Sun, L. Bi, and B. Yi *The Use of Superspheroids as Surrogates for Modeling Electromagnetic Wave Scattering by Ice Crystals.* Remote Sens., 13:1733, 2021.
[5]. P. Yang, J. Ding, R. L. Panetta, K. N. Liou, G. W. Kattawar, and M. I. Mishchenko *On the convergence of numerical computations for both exact and approximate solutions for electromagnetic scattering by nonspherical dielectric particles*, PIER, 164:27–61, 2019.

Assessing surface albedo biases over the ocean in the Community Earth System Model (CESM)

J. Wei[1,*], P. Yang[2]

[1]*Department of Oceanography, Texas A&M University, College Station, TX, USA*
[2]*Department of Atmospheric Sciences, Texas A&M University, College Station, TX, USA*
[*]*corresponding author's e-mail: anser@tamu.edu*

Abstract

Understanding electromagnetic energy exchange between the atmosphere and the ocean, especially in the solar spectrum, is of primary importance in enhancing our ability to determine the radiative energy budget of the Earth. However, most global climate models (GCMs) still assume a 'static' ocean surface in the shortwave (SW) radiation scheme of their atmosphere models (i.e., no interactions between the physical and oceanic biogeochemical systems). In addition, the ocean surface albedo (OSA) calculation isn't generally partitioned into direct and diffuse portions that always equal each other. This study assesses both direct and diffuse OSA parameterizations in UV-VIS and NIR bands through simulations from the Community Earth System Model (CESM), version 2.1.3 [1], and compares simulations with results from a validated OSA computational scheme that is developed with appropriate treatment of the ocean surface chlorophyll concentration-based inherent optical properties (IOPs) of the water column [2]. We also evaluate the influence of chlorophyll concentration on OSA. The OSA biases are larger over ocean regions where chlorophyll concentration is high. Those biases appear more significant in UV-VIS bands instead of NIR due to the higher sensitivity to light attenuation by seawater in UV-VIS bands. Therefore, inclusion of the chlorophyll concentration in OSA parameterization may permit a more complete delineation of the process of electromagnetic interaction at the air-sea interface. The more realistic OSA computational scheme is intended to be used mainly in general circulation models (GCMs).

References

[1] G. Danabasoglu, J. F. Lamarque, J. Bacmeister, D. A. Bailey, A. K. DuVivier, J. Edwards, ..., and W. G. Strand *The community earth system model version 2 (CESM2)*. J. Adv. Model. Earth. Sy, 12(2): 1-35, 2020.

[2] J. Wei, T. Ren, P. Yang, S. F. DiMarco, and E. Mlawer *An improved ocean surface albedo computational scheme: Structure and Performance*. J. Geophys. Res. Oceans, under review, 2021.

Performance of cloud 3D solvers in anvil-like ice cloud shortwave radiation closure at the top of the atmosphere over the equatorial western Pacific Ocean

T. Ren[1]*, P. Yang[1], and J. Wei[2]

[1] *Department of Atmospheric Sciences, Texas A&M University, College Station, TX, USA.*
[2] *Department of Oceanography, Texas A&M University, College Station, TX, USA.*
[*] *corresponding author's e-mail: tr7585@tamu.edu*

Abstract

The resolution of general circulation models has become increasingly finer, making the horizontal homogeneity assumption of cloud fields in conventional radiation parameterization schemes problematic. By assuming optically thin and thick cloudy regions, the Tripleclouds solver [1] was developed for computationally efficient cloud horizontal inhomogeneity treatment. In addition, through linearization of the horizontal radiation exchange rate between two optically distinct regions, a computationally efficient horizontal radiation flux treatment, the Speedy Algorithm for Radiative Transfer through Cloud Sides (SPARTACUS), was introduced [2]. Both the Tripleclouds and SPARTACUS solvers are included in the European Centre for Medium-Range Weather Forecasts (ECMWF) radiation scheme *ecRad*. However, the Tripleclouds and SPARTACUS solvers have not been extensively evaluated using passive sensor retrievals of cloud properties, where cloud vertical structures are unknown. This study collocates Aqua Moderate Resolution Imaging Spectroradiometer (MODIS) Collection 6 Level 2 1×1 km^2 pixels with Clouds and the Earth's Radiant Energy System (CERES) near-nadir footprints (or Fields-of-View) in July 2008 over the equatorial Pacific Ocean region. The *ecRad* 1.4.0 scheme is used to perform radiation calculations for individual selected CERES anvil-like ice cloud footprints with input cloud parameters from MODIS retrievals. The calculations are performed three times with the conventional homogeneous, Tripleclouds, and SPARTACUS solvers, respectively, for a comparison. The resultant upward shortwave radiation fluxes at the top of the atmosphere are compared with the CERES unfiltered counterparts. The homogeneous, Tripleclouds, and SPARTACUS radiation fluxes show mean absolute percentage errors (MAPEs) of 13.61%, 11.87%, and 11.77%, respectively. We also calculate the cloud top height gradient along the horizontal direction of incident sunlight at each MODIS pixel within every selected CERES footprint. The standard deviation of cloud top height gradients within every CERES footprint is named directional heterogeneity index (DHI) in this study. SPARTACUS significantly outperforms Tripleclouds mostly when DHI is small but the fractional standard deviation of cloud optical thickness [3] is large. In other words, the SPARTACUS solver shows best performance when cloud optical thickness shows strong spatial variations but cloud top height is relatively homogeneous. The result suggests that some metric of cloud top height spatial variation—such as DHI—may be used to modify the cloud perimeter length in the uppermost cloud layer, when passive-sensor-based cloud retrievals are used to drive SPARTACUS. Further, the sensitivities of the selected *ecRad* solvers to cloud overlapping assumptions and cloud particle size vertical variations are tested.

References

[1] J. K. Shonk, and R. J. Hogan. *Tripleclouds: An efficient method for representing horizontal cloud inhomogeneity in 1D radiation schemes by using three regions at each height*. J. Climate, 21:2352-70, 2008.

[2] R. J. Hogan, S. A. Schäfer, C. Klinger, J. C. Chiu, and B. Mayer. *Representing 3-D cloud radiation effects in two-stream schemes: 2. Matrix formulation and broadband evaluation*. J. Geophys. Res.-Atmos., 121:8583-99, 2016.

[3] L. Liang, L. Di Girolamo, and S. Platnick. *View-angle consistency in reflectance, optical thickness and spherical albedo of marine water-clouds over the northeastern Pacific through MISR-MODIS fusion*. Geophys. Res. Lett., 36, 2009.

Light scattering by space debris. Experiments, modelling, and space applications

J. Peltoniemi[1,*], M. Gritsevich[1,2], and et al[1,2]

[1] *Finnish Geospatial Research Institute FGI, 02431 Masala, Finland*
[2] *Second affiliation*
[*] *corresponding author's e-mail: jouni.peltoniemi@nls.fi*

Space debris

The modern society utilises space-based infrastructures for a large number of tasks. However, the quickly increasing number of space debris threatens to damage the satellites and in the worst case scenario to make the space totally unusable. There are over one million objects in orbit sufficient to kill a satellite, but below current observation threshold. It is thus very necessary to develop new detection, manipulation, and protection techniques. We contribute to this emerging field by developing physical light scattering models and experiments.

Experiments

We have built a novel laboratory setup to measure the scattering from space debris analogues in the size range 1-10 cm. The sensor can move in freely programmable path around the scatterer and the target can be rotated along one axis. The configuration can be easily modified for various purposes. Almost full Muller matrix can be retrieved in a spectral range of 400–2400 nm.

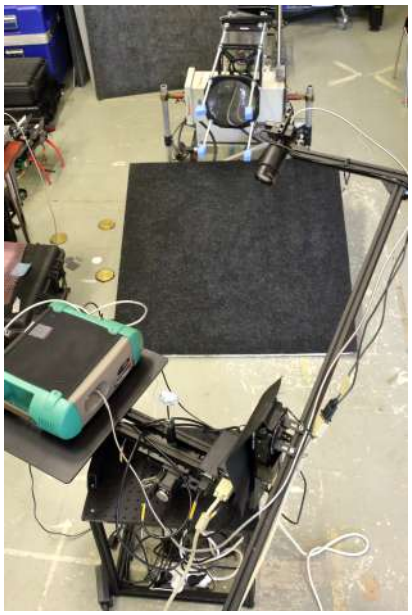

Figure 1: FGI's new laboratory setup to measure the light scattering

Model

Based on recent studies [1–3], most dominant space particles in the range 0.1 – 10 mm are CFRP flakes and bent metal pieces from collisions and explosions, peeled off paint flakes, carbon fibre needles from micro particle collision ejecta, and meteoroidal background. We model these objects as rough ellipsoids, cylinders, or small aggregates of such, with Fresnel reflection and refraction from the surface, and internal diffuse scattering from voids and contaminants. We compute the scattering using Monte Carlo ray-tracing [4].

We are currently validating the model against experiments.

Conclusions

The model is being applied for laser momentum transfer deflection studies [5] and for developing orbital and terrestrial observations. The light scattering experiments can be used to validate models and to study even rather complex objects. More realistic analogue samples are being researched and collected.

References

[1] *MASTER*. Published: \emph https://sdup.esoc.esa.int/master/.

[2] S. Allen and N. Fitz-Coy. DebriSat fragment characterization: Quality assurance. *Journal of Space Safety Engineering*, 7(3):235–241, Sept. 2020.

[3] P. H. Krisko, M. Horstman, and M. L. Fudge. SOCIT4 collisional-breakup test data analysis: With shape and materials characterization. *Adv. Space Res.*, 41(7):1138–1146, 2008.

[4] J. I. Peltoniemi, M. Gritsevich, J. Markkanen, T. Hakala, J. Suomalainen, N. Zubko, O. Wilkman, and K. Muinonen. A COMPOSITE MODEL FOR REFLECTANCE AND POLARISATION OF LIGHT FROM GRANULATE MATERIALS. *ISPRS Annals of Photogrammetry, Remote Sensing and Spatial Information Sciences*, V-1-2020:375–382, 2020.

[5] J. I. Peltoniemi, O. Wilkman, M. Gritsevich, M. Poutanen, A. Raja-Halli, J. Näränen, T. Flohrer, and A. D. Mira. Steering reflective space debris using polarised lasers. *Advances in Space Research*, Jan. 2021.

Impacts of pixel down-sampling on GOES-16 ABI ice cloud retrievals

D. Li*, M. Saito and P. Yang

Department of Atmospheric Sciences, Texas A&M University, 3150 TAMU, College Station, TX 77843, USA
**corresponding author's e-mail: lidc@tamu.edu*

Abstract

Variations of the microphysical and optical properties of ice clouds affect the Earth's radiation budget on various temporal and regional scales. Geostationary satellites play a vital role in monitoring these ice cloud optical and microphysical characteristics. In particular, Advanced Baseline imager (ABI) observations from the Geostationary Operational Environment Satellite-16 (GOES-16) provide an unprecedented opportunity to access radiative signals spanning from visible and near-infrared (VIS–NIR) to thermal infrared (TIR) bands with high temporal (30 seconds to 10 minutes) and spectral (0.5 km to 2 km) resolutions. Ice cloud properties with high spatiotemporal resolution can be inferred from GOES-16 ABI top of atmosphere (TOA) solar reflectances in the visible band (band 2) and near-IR bands (band 3 & 5) using the Nakajima-King method [1]. However, the resolution of TOA reflectance data is 0.5 km for the visible band, 1 km for the near-IR bands and 2km for other bands. It is necessary to have the same 2 km resolution for each band, which will improve computational efficiency in the retrieval process, as it reduces the number of pixels.

The two methods for pixel down-scaling from 0.5–1 km to 2 km are sub-sampling, and averaging the surrounding pixels [2]. Although the first method is more efficient and straightforward than the second one, this could lead to systematic biases depending on horizontal scales of clouds. For instance, a spatial scale of some clouds might be as small as a 0.5-1 km pixel, and their contribution could be simply omitted by using the first method. Therefore, we evaluate the impacts of these down-sampling techniques on the GOES-16 ABI observational signals with 2 km resolution as well as on the ice cloud property retrievals for various cloud types classified based on the International Satellite Cloud Climatology Project (ISCCP) cloud classification diagram.

References

[1] T. Nakajima, and M. D. King *Determination of the optical-thickness and effective particle radius of clouds from reflected solar-radiation measurements. Part I: Theory.* J. Atmos. Sci. 47, 1878–1893, 1990.

[2] T. J. Schmit, M. M. Gunshor, G. Fu, T. Rink, K. Bah, and W. Wolf *GOES-R Advanced Baseline Imager (ABI) algorithm theoretical basis document for cloud and moisture imagery product. Version 2.3.* NOAA NESDIS STAR, 62, 2010.

Physical optics beam tracer models for smooth and rough non-spherical particles

E. Hesse[1,*], L. C. Taylor[1] and E. R. Mathen[1]

[1]*University of Hertfordshire, AL10 9AB, UK.*

[*]*e.hesse@herts.ac.uk*

Abstract

Imaging methods are widely used for particle characterisation, however for small particles optical aberrations and constrained depth of field restrict the quality of the information obtainable. Such constraints do not apply to instruments such as the Aerosol Ice Interface Transition Spectrometer (AIITS) [1], which acquire far field scattering patterns. Obtaining quantitative morphological data by inversion of the patterns can be very challenging. Therefore, the creation of databases of two-dimensional (2D) scattering patterns of known particle morphologies is extremely useful for particle characterization. Exact methods such as T-matrix [2] and semi-exact methods like the finite difference time domain (FDTD) method [3] and the discrete dipole approximation (DDA) [4] can be used for computations of light-scattering properties for non-axisymmetric particles. Approximate methods, such as the geometric optics approximation or physical optics [5,6,7] have to be used for scatterers much larger than the wavelength of radiation.

Here we present two beam tracer methods, a fast one suitable for facetted objects [8] and a beam tracer method using very fine beamlets, suitable for particles with complex shapes and/or surface roughness. For the two methods we show comparisons with DDA computations by A. Penttilä and T. Nousiainen [9] for hexagonal prisms with smooth and rough surfaces, respectively. Particle models with Gaussian random surfaces were obtained using the method developed by C T. Collier [9]. The beam tracer models have been applied for interpretation of AIITS scattering images during the NERC and NASA Co-ordinated Airborne Studies in the Tropics and Airborne Tropical Tropopause Experiment [10].

References

[1] E. Hirst, C Stopford, P. H. Kaye, R. S. Greenaway and J D Dorsey. *The Aerosol Ice Interface Transition Spectrometer – A new particle phase.* ATTREX Science Meeting. Boulder, United States. 30 September 2013.

[2] M. I. Mishchenko, N. T. Zakharova, N. G. Khlebtsov, T. Wriedt, G. Videen. *Comprehensive thematic T-matrix reference database: a 2013–2014 update*. J Quant Spectrosc Radiat Transf 2014;146:349–54 .

[3] P. Yang, K. N. Liou. In: M. I. Mishchenko, J. W. Hovenier, L. D. Travis, editors. *Light scattering by nonspherical particles.* New York: Academic Press; 1999. p. 173–221 .

[4] M. A. Yurkin, A. G. Hoekstra. *The discrete-dipole-approximation code ADDA: capabilities and known limitations*. J Quant Spectrosc Radiat Transf 2011;112:2234–47

[5] P. Yang and K. Liou. Geometric-optics-integral-equation method for light scattering by nonspheric ice crystals. *Applied Optics,* vol. 35, no. 33, pp. 6568-6584, 1996.

[6] A. V. Konoshonkin, N. V. Kustova and A. G. Borovoi, Y. Grynko, J. Förster. *Light scattering by ice crystals of cirrus clouds: comparison of the physical optics methods*. J Quant Spectrosc Radiat Transf 2016; 54-67.

[7] E. Hesse, L. Taylor, C. T. Collier, A. Penttilä, T. Nousiainen, Z. Ulanowski. *Discussion of a physical optics method & its application to absorbing smooth and slightly rough hexagonal prisms.* J Quant Spectrosc Radiat Transf 2018; 12-23.

[8] L. C. Taylor. *A Beam Tracing Model for Electromagnetic Scattering by Atmospheric Ice Crystals*, PhD thesis, University of Hertfordshire, 2016.

[9] C. T. Collier, E. Hesse, L. Taylor, Z. Ulanowski, A. Penttilä, T. Nousiainen*. Effects of surface roughness with two scales on light scattering by hexagonal ice crystals large compared to the wavelength: DDA results.* J Quant Spectrosc Radiat Transf 2016;182:225–39.

[10] E. R. Mathen, E. Hesse, A. J. Baran. *Analysis and Modelling of TTL ice crystals based on in-situ measurement of scattering patterns*. 19th Electromagnetic and Light Scattering Conference. Online. 12-16 July 2021.

Improved Ice Particle Backscattering Computations from a Newly Developed Single-Scattering Database

J. Coy[1*], M. Saito[1], J. Ding[1], and P. Yang[1]

[1]*Texas A&M University, Department of Atmospheric Sciences*
[*]*corresponding author's e-mail: jcoy93@email.tamu.edu*

Abstract

New ice cloud single-scattering databases are frequently being developed or improved to better represent the properties of actual ice clouds in downstream applications. Computational methods have also been developed to accurately calculate the single-scattering properties of ice particles, especially for moderate and large size parameters. The Improved Geometric Optics Method (IGOM) is based on mapping of the conventional ray-tracing method result, which is most accurate for large size parameters and is also computationally efficient [1]. For shortwave, non-absorptive wavelengths, IGOM falls short of providing accurate backscattering calculations in terms of the phase matrix for moderate size parameters. The Physical Geometric Optics Model (PGOM) is based on mapping the equivalent tangential electric and magnetic currents on a particle surface to the far field via an exact electromagnetic relationship [2]. The PGOM is more computationally demanding than IGOM, but is more accurate for moderate size parameters, and especially improves backscattering in the phase matrix. For this presentation, we develop a two-habit model (THM) single-scattering database comprised of a 60-partiicle ensemble of distorted columns (small sizes) and a 20-particle ensemble of distorted 20-column aggregates (large sizes). We utilize the Invariant Imbedding T-Matrix (IITM) method [3] for small size parameters and IGOM for moderate and large size parameters. We then replace the backscattering region of the IGOM phase matrix calculations with truncated PGOM calculations to both improve the backscattering accuracy and reduce computation time. For downstream lidar calculations we will focus on 355, 532, and 1064 nm wavelengths and compare the results with the THM developed by Loeb et al. 2018 [4].

Improved Backscattering Calculations of the PGOM

Figure 1 shows the THM P11 component of the phase matrix at 532 nm and particle size of 100 μm calculated by IGOM (blue line) and IGOM with PGOM backscattering (red line). PGOM provides a higher backscattering magnitude than IGOM, which will result in more accurate downstream lidar-based calculations.

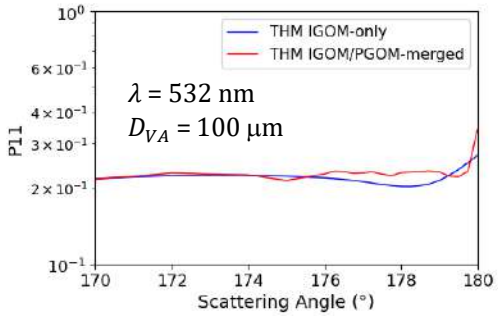

Figure 1: THM P11 component of phase matrix calculated at a wavelength of 532 nm and volume-projected area particle equivalent diameter (D_{VA}) of 100 μm, using IGOM and PGOM computation methods.

References

[1] Cai, Q., and K. N. Liou. *Polarized light scattering by hexagonal ice crystals: Theory.* Appl. Opt., 21:3569-3580, 1982.
[2] Yang, P., and K. N. Liou. *Geometric-optics-integral-equation method for light scattering by non-spherical ice particles*. Appl. Opt., 35:6568-6584, 1996.
[3] L. Bi, and P. Yang. *Accurate simulation of the optical properties of atmospheric ice crystals with invariant imbedding T-matrix method.* J. Quant. Radiat. Transfer, 138:17-35, 2014.
[4] N. G. Loeb, P. Yang, F. G. Rose, G. Hong, S. S. Mack, P. Minnis, S. Kato, S. H. Ham, W. L. Smith, S. Hioki, and G. Tang. *Impact of Ice Cloud Microphysics on Satellite Cloud Retrievals and Broadband Flux Radiative Transfer Model Calculations*. J. Clim., 31:1851-1864, 2018.

Assessing AVIRIS and HySICS visible and near-infrared reflected radiance sensitivities and uncertainties for cirrus cloud retrievals

J. Mast* and P. Yang

Texas A&M University
**corresponding author's e-mail: jcmast@tamu.edu*

Ice cloud microphysical and optical properties (i.e., effective radius and optical depth) are among the most uncertain components in our understanding of cloud-climate forcings and feedbacks. Reduction in cloud feedback uncertainty is recommended as a *most important* endeavor by the decadal survey [1]. Hyperspectral measurements of clouds are important due to the potential for abundant information content in a multitude of channels. We investigate the potential of a pair of reflective solar hyperspectral imagers for cirrus cloud microphysical retrievals. In this presentation, we present results from sensitivity studies (cloud optical depth, effective particle size, and crystal habit uncertainty) and uncertainty studies (temperature and water vapor vertical profile uncertainties and instrument uncertainties). These studies are performed over a range of cloud optical depths, effective particle sizes, cloud heights, and solar zenith angles. We model their measured radiances using the Line-by-Line Radiative Transfer Model (LBLRTM) [2] to calculate gas optical depths followed by the Discrete Ordinate Radiative Transfer Model (DISORT) [3] scattering calculations. The Airborne Visible InfraRed Imaging Spectrometer (AVIRIS) [4] is an aircraft mounted instrument with a spectral coverage of 400-nm to 2500-nm with a 10-nm resolution. The Hyperspectral Imager for Climate Science (HySICS) [5] is the imaging spectrometer developed for the future CLARREO-Pathfinder mission [6]. HySICS has a spectral coverage of 350-nm to 2300-nm with a 6-nm spectral resolution and a planned systematic uncertainty of 0.3%.

References

[1] National Academies of Science and Medicine. *Thriving on Our Changing Planet: A Decadal Strategy for Earth Observation from Space*. The National Academies Press., Washington, DC, 2018

[2] S. A. Clough, and coauthors, *Atmospheric radiative transfer modeling: A summary of the AER codes*, J. Quant. Spectrosc. Radiat. Transfer, 91: 233-244, 2005.

[3] K. Stamnes, SC. Tsay, W. Wiscombe and K. Jayaweera, *Numerically stable algorithm for discrete-ordinate-method radiative transfer in multiple scattering and emitting layered media*, Appl. Opt., 27(12): 2502–2509, 1988

[4] R. O. Green, and coauthors, *Imaging spectroscopy and the Airborne Visible/Infrared Imaging Spectrometer (AVIRIS)*. Remote Sens. Environ., 65(3): 227-248, 1998

[5] G. Kopp, and coauthors, *Radiometric flight results from the HyperSpectral Imager for Climate Science (HySICS)*. Geosci. Instrum. Method. Data Syst., 6: 169–191, 2017

[6] Y. Shea, and coauthors, *CLARREO-Pathfinder: Mission overview and current status*. IEEE International Geosciences and Remote Sensing Symposium, Virtual, 26 September – 2 October, 2020

TAMUdust2020: A comprehensive database of the single-scattering properties of irregular dust aerosols

M. Saito[1,*] and P. Yang[1]

[1]*Department of Atmospheric Sciences, Texas A&M University, College Station, TX*
[*]*corresponding author's e-mail: masa.saito@tamu.edu*

Abstract

Mineral dust aerosol plays a complex role in the Earth's energy budget through scattering and absorbing radiation in the atmosphere. The optical properties of mineral dust aerosols differ among regions and environmental conditions due to various mineralogical compositions (i.e., the complex refractive index), sizes, and particle shapes. In particular, mineral dust particle shapes are exclusively nonspherical. Although previous studies partly incorporate the aspheric characteristics into dust optical property models using a spheroidal or ellipsoidal model, microscopic images have confirmed that a simple spheroid/ellipsoid is not always suitable to represent the dust aerosol particles. As a result, radiative transfer simulations as well as retrieved properties obtained by remote sensing techniques involving mineral dust particles could have systematic biases. There is a pressing need to develop improved and more realistic mineral dust optical property models.

We will introduce a recently developed comprehensive database of the single-scattering properties of irregular dust aerosol particles (called the TAMUdust2020 database) for various remote sensing applications involving passive and active sensor observations [1]. The TAMUdust2020 database incorporates a realistic irregular particle shape ensemble model that mimics morphological characteristics of airborne mineral dust particles. The single-scattering properties of these particles are computed with state-of-the-art light scattering computational techniques. Comparisons of the scattering properties between laboratory measurements and the TAMUdust2020 database show reasonable consistency. We also use the computed dust aerosol scattering properties to simulate various spaceborne satellite data, including multiangle polarimetric observations, thermal infrared observations, and lidar observations. The TAMUdust2020 database is publicly available [2].

References

[1] M. Saito, P. Yang, J. Ding, and X. Liu *A comprehensive database of the optical properties of irregular aerosol particles for radiative transfer simulations.* J. Atmos. Sci., in press.

[2] http://doi.org/10.5281/zenodo.4711247

Modeling the single-scattering properties of roughened ice crystals

M. Saito[1,*] and P. Yang[1]

[1]*Department of Atmospheric Sciences, Texas A&M University, College Station, TX*
[*]*corresponding author's e-mail: masa.saito@tamu.edu*

Abstract

Incorporating effects of ice crystal surface roughness is essential for radiative transfer simulations involving ice clouds, as roughness dramatically alters the angular distributions of the phase matrix, or the electromagnetic wave scattered by an ice crystal. As the size parameter of ice crystals is generally large in the shortwave domain, the scattering computations are often performed using the geometric optics principle. Historically, an *idealized* roughness effect is implemented into conventional geometric-optics methods by randomly tilting the local surface of an ice crystal when solving the Fresnel equation for each ray of light [1,2]. This approach has been widely used for radiative transfer simulations involving ice crystals because the optical property models of roughened ice crystals greatly improve the ice cloud property retrievals.

Recent advances in light scattering computational capabilities achieve almost identical consistency in the single-scattering properties between the rigorous Invariant-Imbedding T-matrix Method (IITM) [3] and approximate methods based on the geometric optics principle for ice crystals with a smoothed particle surface with size parameters as small as 150 [4], which confirms the applicability of the geometric optics approximations limited to these sizes or larger. However, there are still a number of outstanding questions remaining, such as 1) *Is the size limit of the geometric optics method applicable to roughened ice crystals as well?* 2) *How much more accurate is an idealized roughness model compared to a geometrically roughened ice crystal counterpart?*

To address these questions, we use IITM to simulate the single-scattering properties of geometrically roughened ice crystals with size parameters up to 250, and compare the results to the counterparts based on geometric-optics methods. This presentation will discuss the quantitative impacts of the degree of surface roughness on the single-scattering properties of ice crystals as well as remaining issues.

References

[1] A. Macke, J. Mueller, and E. Raschke *Single scattering properties of atmospheric ice crystals*. J. Atmos. Sci., 53:2813–2825, 1996.

[2] P. Yang, and K. N. Liou *Single-scattering properties of complex ice crystals in terrestrial atmosphere*. Contrib. Atmos. Phys., 71:223–248, 2008.

[3] L. Bi, and P. Yang *Accurate simulation of the optical properties of atmospheric ice crystals with the invariant imbedding T-matrix method,* J. Quant. Spectro. Radiat. Trans., 138:17–35, 2014.

[4] P. Yang, J. Ding, R. L. Panetta, K. N. Liou, G. W. Kattawar, and M. I. Mishchenko *On the convergence of numerical computations for both exact and approximate solutions for electromagnetic scattering by nonspherical dielectric particles*, PIER, 164:27–61, 2019.

Retrieval of aerosol water fraction and dry size distribution using multi-angle polarimetry

B. van Diedenhoven[1*], O. P. Hasekamp[1], S. Stamnes[2], B. Cairns[3]

[1]*SRON Netherlands Institute for Space Research*
[2]*NASA Langley*
[3]*NASA Goddard Institute for Space Studies*

[*]*corresponding author's e-mail: b.van.diedenhoven@sron.nl*

Depending on the environmental humidity and their hygroscopicity, aerosols may absorb water causing their size to increase. Consequently, aerosol optical depth may increase in the relatively humid environments close to clouds, which complicates the interpretation of observed correlations between aerosol optical depth and cloud properties. In addition, methods that use satellite-retrieved aerosol size distributions to estimate the fraction of aerosol acting as cloud condensation nuclei may be substantially biased when ignoring such aerosol-swelling. It has been shown that different soluble mixtures have very similar real refractive indices for a given volume fraction of water, even if the dry refractive indices vary substantially. Hence, aerosol refractive index that is retrieved simultaneously with aerosol number and ambient size may be used to infer the volume fraction of absorbed water, as well as the aerosol dry size distribution. The SPEXone instrument that will be launched on board of NASA's PACE satellite is expected to deliver accurate retrievals of aerosol number, size and complex refractive index, allowing the volume fraction of water and dry size distribution to be inferred. In this presentation we will show some preliminary results of a project to determine the accuracy of this approach to infer aerosol water fraction and dry size distribution. For this, we will use simulated measurements based on output from an atmospheric model, as well as observations of the airborne Research Scanning Polarimeter along with collocated in situ measurements that provide constraints on the dependence of aerosol scattering on humidity.

We will do this making use of the accurate retrievals of the Real part of the Refractice Index (RRI), which will be retrieved from SPEXone with unprecedented accuracy30. We will follow the approach of Schuster et al.17, who has shown that different soluble mixtures (e.g. with sea salt, ammonium nitrate or ammonium sulphate) have very similar RRI for a given volume fraction of water (fw), even if the dry refractive indices may vary

between 1.49-1.55. For these mixtures, fw can be accurately determined (5-10%) by assuming an average refractive index for the dry

aerosol component (say 1.52) and by computing the refractive index for the humidified aerosol using partial molar refraction17,18. Using

some assumptions, the approach can be extended to mixtures including insoluble aerosols, but given that we can use the retrieved

fraction of spheres to select scenes dominated by soluble aerosols, our baseline is to apply the approach for soluble particles. Having the

volume of water, it is straightforward17 to translate the 'wet' to the 'dry' aerosol size distribution. With the aerosol dry size distribution,

we expect that the CCN column can be more accurately derived because variation in the number of aerosol particles with wet radius > rlim

(0.15μm) is to some extend still affected by variation in water uptake (for constant number of CCN), while this is not the case if a cut-off

radius for dry particles is defined. This will be mainly important for the CCN-CF and LWP relationships. Also, the cut-off radius for dry

particles can be more accurately compared to the cut-off radius for CCN particles found in field experiments6. For the dry size distribution,

we have to define a new optimal size cut-off value rlim . We will do this in the same manner as in HGQ2019 choosing rlim that maximizes

susceptibility for Nd. We will do this separately for the synthetic data and real measurements to be not too dependent on the model

assumptions used to create the synthetic data set

References

[1] Michael I. Mishchenko. *Electromagnetic Scattering by Particles and Particle Groups. An Introduction*. Cambridge University Press, Cambridge, 2014.

[2] M. I. Mishchenko, N. T. Zakharova, N. G. Khlebtsov, G. Videen, and T. Wriedt *Comprehensive thematic T-matrix reference database: a 2015-2017 update*. J. Quant. Spectrosc. Radiat. Transfer, 202:240-246, 2017.

[3] J. M. Dlugach, and M. I. Mishchenko. *Multiple scattering of polarized light by particles in an absorbing host medium*. 18th Electromagnetic and Light Scattering Conference. Hangzhou, China. 10-14 June 2019.

Optical pulling force on a magneto-dielectric Mie sphere illuminated by a linearly-polarized Airy light-sheet

Ningning Song[1] , Bing Wei[1,2], Renxian Li[1,2*], Shuhong Gong[1,2], Shu Zhang[1], and Bojian Wei[1]

[1]*School of Physics and Optoelectronic Engineering, Xidian University, Xi'an 710071, China*
[2]*Collaborative Innovation Center of Information Sensing and Understanding, Xidian University, Xi'an 710071, China*

[*]*corresponding author's e-mail: rxli@xidian.edu.cn*

The specific structure beam has been widely applied in the realm of optical manipulation of particles. The crucial technology of optical manipulation of micro-nano particles is the specific excellent light field. In recent years, some specific structural beams having limited-diffracting characteristics have been developed, including Bessel and Airy beams, which are excellent light sources for the optical manipulation system. The Airy beam, as an important non-diffracting beam, involves the properties of self-acceleration [1], self-healing [2], and non-diffraction [3], which can transport particles along a parabola trajectory. The Airy light-sheet is equivalent to a two-dimensional state of the three-dimensional Airy beam in space, at the same time it retains all the Airy beam's properties. Besides, the Airy light-sheet has been applied in particle sizing, laser microsurgery, and light-sheet microscopy. Pulling a particle illuminated by a structural beam is a topic of importance in particle manipulation. It is found that pulling force will occur when an Airy light-sheet illuminates a dielectric sphere. Due to the self-bending characteristics of the Airy light sheet, a particle can be pulled along a curved track. Magneto-dielectric sphere has unique scattering characteristics that the backscattering or forward scattering field of the magneto-dielectric sphere can be enhanced or suppressed according to the refractive index of the sphere and its size relative to the incident radiation wavelength. The optical force can be predicted by this unique scattering characteristic, which is of significance in the emergent technologies for particle manipulation. To our knowledge, the optical force of an Airy light-sheet acting on a magneto-dielectric Mie sphere has not been published.

The purpose of this work is to rigorously examine the optical pulling force on the magneto-dielectric Mie sphere of arbitrary size in the field of a linearly-polarized Airy light-sheet based on the generalized Lorenz-Mie theory (GLMT) [4]. The influence of the dimensionless transverse scale, attenuation parameter, and the polarization of the Airy light-sheet will be discussed and the effect of varying the size parameter ka of the sphere will be also studied.

References

[1] M. I. Mishchenko, N. T. Zakharova, N. G. Khlebtsov, G. Videen, and T. Wriedt *Comprehensive thematic T-matrix reference database: a 2015-2017 update*. J. Quant. Spectrosc. Radiat. Transfer, 202:240-246, 2017.

[2] G. A. Siviloglou, J. Broky, and A. Dogariu *Observation of Accelerating Airy Beams.* J. Physical Review Letters, 99(21):213901, 2007.

[3] J. Broky, G. A. Siviloglou, and A. Dogariu *Self-healing properties of optical Airy beams.* J. Optics Express, 16(17):12880-91, 2008.

[4] I. Dolev, T. Ellenbogen, and N. Voloch-Bloch. *Control of free space propagation of Airy beams generated by quadratic nonlinear photonic crystals.* J. Applied Physics Letters, 95(20):201112, 2009.

[5] G. Gouesbet , G. Grehan. *A generalized Lorenz-Mie theory*. J. Journal of Optics, 13:97-103, 1982.

Optical pulling force on a magneto-dielectric Mie sphere illuminated by a linearly-polarized Airy light-sheet

Ningning Song[1] , Bing Wei[1,2], Renxian Li[1,2*], Shuhong Gong[1,2], Shu Zhang[1], and Bojian Wei[1]

[1]*School of Physics and Optoelectronic Engineering, Xidian University, Xi'an 710071, China*
[2]*Collaborative Innovation Center of Information Sensing and Understanding, Xidian University, Xi'an 710071, China*

[*]*corresponding author's e-mail: rxli@xidian.edu.cn*

The specific structure beam has been widely applied in the realm of optical manipulation of particles. The crucial technology of optical manipulation of micro-nano particles is the specific excellent light field. In recent years, some specific structural beams having limited-diffracting characteristics have been developed, including Bessel and Airy beams, which are excellent light sources for the optical manipulation system. The Airy beam, as an important non-diffracting beam, involves the properties of self-acceleration [1], self-healing [2], and non-diffraction [3], which can transport particles along a parabola trajectory. The Airy light-sheet is equivalent to a two-dimensional state of the three-dimensional Airy beam in space, at the same time it retains all the Airy beam's properties. Besides, the Airy light-sheet has been applied in particle sizing, laser microsurgery, and light-sheet microscopy. Pulling a particle illuminated by a structural beam is a topic of importance in particle manipulation. It is found that pulling force will occur when an Airy light-sheet illuminates a dielectric sphere. Due to the self-bending characteristics of the Airy light sheet, a particle can be pulled along a curved track. Magneto-dielectric sphere has unique scattering characteristics that the backscattering or forward scattering field of the magneto-dielectric sphere can be enhanced or suppressed according to the refractive index of the sphere and its size relative to the incident radiation wavelength. The optical force can be predicted by this unique scattering characteristic, which is of significance in the emergent technologies for particle manipulation. To our knowledge, the optical force of an Airy light-sheet acting on a magneto-dielectric Mie sphere has not been published.

The purpose of this work is to rigorously examine the optical pulling force on the magneto-dielectric Mie sphere of arbitrary size in the field of a linearly-polarized Airy light-sheet based on the generalized Lorenz-Mie theory (GLMT) [4]. The influence of the dimensionless transverse scale, attenuation parameter, and the polarization of the Airy light-sheet will be discussed and the effect of varying the size parameter ka of the sphere will be also studied.

References

[1] M. I. Mishchenko, N. T. Zakharova, N. G. Khlebtsov, G. Videen, and T. Wriedt *Comprehensive thematic T-matrix reference database: a 2015-2017 update*. J. Quant. Spectrosc. Radiat. Transfer, 202:240-246, 2017.

[2] G. A. Siviloglou, J. Broky, and A. Dogariu *Observation of Accelerating Airy Beams.* J. Physical Review Letters, 99(21):213901, 2007.

[3] J. Broky, G. A. Siviloglou, and A. Dogariu *Self-healing properties of optical Airy beams.* J. Optics Express, 16(17):12880-91, 2008.

[4] I. Dolev, T. Ellenbogen, and N. Voloch-Bloch. *Control of free space propagation of Airy beams generated by quadratic nonlinear photonic crystals.* J. Applied Physics Letters, 95(20):201112, 2009.

[5] G. Gouesbet , G. Grehan. *A generalized Lorenz-Mie theory*. J. Journal of Optics, 13:97-103, 1982.

Measurement of droplets with nanoparticles using two wavelength extinction rainbow refractometry

Can Li[1, 2, *], Qimeng Lv[2], Xuecheng Wu[2] and Yingchun Wu[2]

[1]*National Key Laboratory of Transient Physics, Nanjing University of Science and Technology, Nanjing 210094, China*
[2]*State Key Lab of Clean Energy Utilization, Zhejiang University, Hangzhou 310027, China*

[*]*Presenting author (lican@njust.edu.cn)*

Characterization of droplets with nanoparticles (inclusions) is nowadays of great academic interest and has wide applications, for instance nanofluid fuel, paint, coating, surface patterning, particle deposition [1, 2]. Reported here is an investigation to simultaneously measure the liquid phase parameters (droplet size, liquid refractive index) and solid phase parameters (averaged inclusion size and concentration) of a droplet with nanoparticles using rainbow refractometry with two incident wavelengths.

In this work, a piezoelectric monodisperse droplet generator [3] generates a stream of distilled water droplets with a size of 120-150 μm. Polystyrene particles with a diameter of 200 and 500 nm are dispersed in the water with different concentrations (0%, 0.1%, 0.2% and 0.3%) by controlled dilution. Measurement signals, recorded by a color camera, are separated by the two wavelengths according to the wavelength response characteristics of the camera. As the extinction factor is the moronic function of specific inclusion size, the concentration and averaged size of inclusions can be estimated from the intensity extinction ratio of the rainbow peak of the two wavelength rainbow signal [4, 5]. Experimental size measurement results are also compared with the SEM results.

References

[1] Zhong X, Crivoi A, Duan F. *Sessile nanofluid droplet drying*. Advances in colloid and interface science. 217:13-30, 2015.
[2] Li L, Tropea C. *Measurement of the colloidal particle concentration and size within a drop using the time-shift technique*. Journal of Quantitative Spectroscopy and Radiative Transfer. 263:107548, 2021.
[3] Berglund RN, Liu BY. *Generation of monodisperse aerosol standards*. Environmental Science & Technology. 7:147-53, 1973.
[4] Li C, Wu Y, Wu X, Tropea C. *Simultaneous measurement of refractive index, diameter and colloid concentration of a droplet using rainbow refractometry*. Journal of Quantitative Spectroscopy and Radiative Transfer. 245:106834, 2020.
[5] Li C, Wu X, Cao J, Chen L, Gréhan G, Cen K. *Application of rainbow refractometry for measurement of droplets with solid inclusions*. Optics & Laser Technology. 98:354-62, 2018.

Preferred mode of presentation: Oral

Spectral albedo of polluted snow layers

A. Kokhanovsky[1], B. Di Mauro [2], R. Garzonio[3], and R. Colombo[3]

[1]Telespazio Belgium, Darmstadt, Germany

[2]Institute of Polar Sciences, National Research Council of Italy, Venice, Italy

[3]Earth and Environmental Sciences Department, University of Milano – Bicocca, Milan, Italy

*corresponding author's e-mail: a.kokhanovsky@vitrocisetbelgium.com

Snow is composed of irregularly shaped large ice grains with a relatively high packing density. The optical thickness of snow layers is very high and in most of cases a snow surface can be considered as a semi-infinite medium as far as snow optics is of concern [1]. The local optical properties of snow layers are usually derived in the framework of geometrical optics in the assumption of various shape and size distributions of randomly oriented ice crystals. In this work, we present results of experimental measurements of polluted snow spectral albedo under solar light illumination at a site in Italian Alps. The pollution is due to the Saharan dust deposited at the snow surface. We have found that the measured snow spectral albedo can be modelled using just three parameters – effective absorption length (EAL) and two parameters to characterize the dust absorption coefficient (dust effective concentration, dust absorption Angström parameter). In the case of clean snow, spectral albedo can be characterized by just one parameter (EAL), which is proportional to the snow grain size. The effective absorption length does not depend on the wavelength in the visible and near – infrared regions of the electromagnetic spectrum and can be determined from the albedo measurements at a single wavelength (say, at 865 or 1020nm). Therefore, the effective absorption length determines the clean snow spectral albedo and can be used for the snow characterization using ground, airborne and satellite observations of snow cover. In the case of polluted snow, the three parameters can be determined using the measurements at multiple wavelengths in combination with optimal estimation or least square techniques. Alternatively, the measurements at three spectral channels in combination with the asymptotic radiative transfer theory can be used for the analytical determination of three spectral invariants discussed above. In particular, the measurements at 410, 500, and 865nm can be used. The accuracy of the technique is demonstrated in Fig.1. The additional data sets should be tested to extend the proposed theory at different snow conditions and dust types.

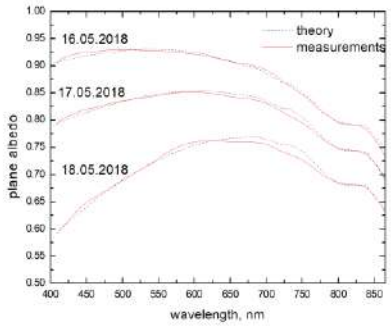

Figure 1: The measured (red solid lines) and calculated (black dash lines) plane albedo of polluted snow. The solar zenith angles were in the range 24-27 degrees.

References

[1] M. I. Mishchenko, J. M. Dlugach, J. Chowdhary, and N. T. Zakharova, Polarized bidirectional reflectance of optically thick sparse particulate layers: an efficient numerically exact radiative-transfer solution. J. Quant. Spectrosc. Radiat. Transfer, 156: 97-108, 2015.

Assessing light absorbing aerosol optical properties and radiative forcing by combining laboratory results, satellite data, and numerical models

Yuan Wang[1,*], Chao Liu[2], Jianfei Peng[3], Renyi Zhang[3], Yuk L. Yung[1]

[1]*California Institute of Technology*
[2]*Nanjing University of Information Science and Technology*
[3]*Texas A&M University*
[*]*corresponding author's e-mail: yuan.wang@caltech.edu*

Abstract

Light absorbing aerosols (LAC) exert profound impacts on air quality and climate because of its high absorption cross-section over a broad range of electromagnetic spectra, but the current results on absorbing and scattering capability of LAC particles during atmospheric aging remain conflicting. Here, we quantified the aging and variation in the optical properties of black carbon (BC) particles under ambient conditions in Beijing, China, and Houston, United States, using a novel environmental chamber, an radiation transfer model, as well as a global aerosol-climate model. BC aging exhibits two distinct stages, i.e., initial transformation from a fractal to spherical morphology with little absorption variation and subsequent growth of fully compact particles with a large absorption enhancement. Tropospheric Monitoring Instrument (TROPOMI) aerosol layer height and aerosol index are analyzed to character LAC from space. We capitalize those direct observations to calibrate a key parameter associated with BC lifetime and physical properties in a global climate model, NCAR CESM. Our findings indicate that BC under polluted urban environments could play an essential role in pollution development and contribute importantly to large positive radiative forcing. The variation in direct radiative forcing is dependent on the rate and timescale of BC aging, with a clear distinction between urban cities in developed and developing countries, i.e., a higher climatic impact in more polluted environments. We suggest that mediation in BC emissions achieves a co-benefit in simultaneously controlling air pollution and protecting climate, especially for developing countries.

References

[1] Wang, Y., P. Ma, J. Peng, R. Zhang, J.H. Jiang, R. Easter and Y. Yung, "Constraining Aging Processes of Black Carbon in the Community Atmosphere Model Using Environmental Chamber Measurements", J. Adv. Model. Earth Syst. 10(10), 2514-2526 (2018).

[2] Peng, J., M. Hu, S. Guo, Z. Du, J. Zheng, D. Shang, M. Zamora, L. Zeng, M. Shao, Y. Wu, J. Zheng, Y. Wang, C. Glen, D. Collins, M.J. Molina, R. Zhang, "Markedly enhanced direct radiative forcing of black carbon particles under polluted urban environments", Proc. Natl Acad. Sci. USA, 113(16), 4266-4271 (2016).

[3] Wang, Y., A. Khalizov, M. Levy, R. Zhang, "New Directions: Light Absorbing Aerosols and Their Atmospheric Impacts", Atmos. Environ., 81, 713-715 (2013).

Professor Kuo-Nan Liou's contributions to Light Scattering, Radiative Transfer, and Remote Sensing

P. Yang[1,*], Y. Gu[2], and Q. Fu[3]

[1]*Department of Atmospheric Sciences, Texas A&M University, College Station, TX 77843, USA*
[2]*Joint Institute for Regional Earth System Science and Engineering/Department of Atmospheric and Oceanic Sciences, University of California, Los Angeles; Los Angeles, CA 90095 USA*
[3]*Department of Atmospheric Sciences, University of Washington, Seattle, WA 98195, USA*

[*]*corresponding author's e-mail: pyang@tamu.edu*

Prof. Kuo-Nan Liou's scientific accomplishments and Services to the Science Conmmunity

Prof. Kuo-Nan Liou, one of the greatest atmospheric physicists of the last half century, passed away on 20 March 2021. He was a *Distinguished Professor* in the Department of Atmospheric and Oceanic Sciences at the University of California, Los Angeles (UCLA), and the founding director of UCLA's Joint Institute for Regional Earth System Science and Engineering (JIFRESSE). Before joining UCLA, he was a professor at the University of Utah for 22 years.

Prof. Liou made seminal contributions to atmospheric and climate science in many areas, particularly in atmospheric radiation and light scattering. He moved the field of atmospheric radiation forward with a quantum leap through his work on the theory of radiative transfer and light scattering, the investigation of radiative forcing effects of clouds and aerosols, and the development of methods for inferring atmospheric and surface parameters by means of remote sensing. Prof. Liou was actively engaged in services to the science community throughout his career. He served on numerous national and international committees. To list a few, he served as Chair of Section 12, Special Fields and Interdisciplinary Engineering, National Academy of Engineering (2008-2010), Chair of the AGU Atmospheric Sciences Section Fellows Committee (2013-2014), Chair of the AGU Roger Revelle Medal Committee (2017-2020), Chair of the 1986 International Radiation Symposium, Chair of the AMS Committee on Atmospheric Radiation (1982-1984), and Chair-Elect of the AMS Atmospheric Research Awards Committee (2021-2022). Although Prof. Liou always had a very busy schedule, he often reviewed manuscripts for a number of journals and research proposals for funding agencies. Moreover, he served as an editor for the *Journal of the Atmospheric Sciences* (1999-2005), a Guest Editor for Special Volume on Clouds and Radiation, *Journal of Geophysical Research* (1987), a Review Editor for the Intergovernmental Panel on Climate Change (IPCC) Report (1998-1999), and an Associate Editor for *Journal of Quantitative Spectroscopy and Radiative Transfer* (2011-2021). As tribute to Prof. Liou, this presentation will summarize his groundbreaking scientific accomplishments, contributions to education, and voluminous service to the science community.

Additional information

Figure 1: Professor Kuo-Nan Liou, 1943-2021.